Microalgae as a novel production platform for antibacterial proteins

Laura Stoffels

Department of Structural and Molecular Biology

UCL

A thesis submitted for the degree of Doctor of Philosophy

2015

DECLARATION

I, Laura Stoffels, confirm that the work presented in this thesis is my own. Where information has been derived from other sources, I confirm that this has been indicated in the thesis.

…….

Abstract

Widespread antibiotic resistance among pathogenic bacteria and the low specificity of these drugs cause a pressing need for the development of novel antibiotics. Endolysins are proteins that are produced by bacteriophage infected cells and digest the bacterial cell wall for phage progeny release. These efficient enzymes are highly specific for the target bacteria without affecting other species. Development of resistance against endolysins is rare, because they evolved to target molecules that are essential for bacterial viability. Taken together, this makes them promising novel antibiotics.

The development of recombinant endolysins as antibacterial agents requires an inexpensive and safe production platform. Microalgae emerged as an alternative expression platform in the last years. This study investigated therefore the production of endolysins in two distinct microalgal systems, the eukaryotic green microalga *Chlamydomonas reinhardtii* and the cyanobacterium *Synechocystis* sp. PCC 6803. *C. reinhardtii* is an attractive production platform for therapeutic proteins, due to the lack of endotoxins and infectious agents and its GRAS status (Generally Recognised as Safe). *Synechocystis* is a prokaryotic system and is natural transformable. Both offer established techniques for the expression of foreign genes and can be cultivated in full containment in simple photobioreactors.

Transgenic lines of *C. reinhardtii* and *Synechocystis* expressing endolysins specific to the human pathogens *Streptococcus pneumoniae* and *Staphylococcus aureus* were created. The *S. pneumoniae*-specific endolysin Pal has been purified in an active form and its specificity and efficiency in killing the target bacterium demonstrated *in vitro*. Another endolysin specific to *Propionibacterium acnes*, a bacterium involved in the skin condition acne vulgaris, was synthesised in *Synechocystis*. The synthesis of the endolysins in the microalgae was analysed under the influence of different expression elements and at different growth stages, and the yields of recombinant protein were quantified to evaluate microalgae as a production platform for antibacterial and other protein therapeutics.

Acknowledgement

First of all, I would to thank my supervisor **Dr Saul Purton** for the opportunity to do this PhD project in his lab, for all his advice, help and ideas in the last four years, and his support while writing the thesis.

Next, I would to thank my second supervisor **Dr Bambos Charalambous** for all his advice and for providing the clinical isolates of *Streptococcus pneumoniae, Streptococcus pyogenes, Staphylococcus aureus*.

I would like to express my gratitude to **Supreme Biotechnologies Ltd** and **UCL** for funding my PhD project. Furthermore, I would like to thank **Tony Dowd** for his trust, ideas and our interesting, helpful and instructive meetings in the last four years. I also would like to express my gratitude to **UCL Advances** for awarding me a PhD Enterprise Scholarship for the commercial evaluation of my PhD project.

I would like to thank all former and current members of the **Purton group** for the wonderful cooperative, supportive and friendly atmosphere in the group and wonderful four years. Firstly, I would like to thank here **Dr Henry Taunt** for establishing the endolysin project and several methods in our lab, for all his advice, all the very nice scientific and non-scientific discussions in the last years, for proof-reading and for teaching me useful microbiological applications for outside the lab. Secondly, I would like to thank **Dr Tommaso Barbi** for all his help, for all the nice discussions, for proof-reading and for all his advice regarding my project and regarding the world of scientists in general. Furthermore, I would like to express my gratitude to **Dr Janet Waterhouse** for continuous proof-reading throughout the last four years, her efforts teaching me British English and also her advice. I would also like to thank **Dr Sofie Vonlanthen** for proof-reading, wonderful discussions and times together in the last years, for all her advice and a great support and encouragement. Furthermore, I would like to thank very much **Dr Lamya Al´Haj** for advice and encouragement, very nice times in the lab, as well as for creating the *Synechocystis* transformation vectors. Thank you very much also to **Stephanie Braun Galleani** for proof-reading, very nice times in the lab and Marina Court, and her

continuous companionship for the conferences in the last years. Furthermore, I would like to thank **Noreen Hiegle** for very nice times together in the lab and Marina Court, all her advice and encouragement, as well as for creating the strains TN72*_pal-HA-His* and TN72*_φ11-HA-His*. I am also very grateful to **Dr Chloe Economou** for her help and encouragement, as well as to **Dr Amandine Maréchal** for all her advice regarding protein biochemistry. I am also very thankful to **Dr Rosie Young** for all her advice and help with molecular biology and for creating the transformation vector pSRSapI. I would like to thank **Dr Thanya Wannathong** for teaching me cloning in the beginning, for very nice times in London and Thailand and for creating the recipient strain TN72. Furthermore, I would like to thank **Dr Joanna Szaub** for her advice, encouragement and very nice times in London, Adelaide and Thailand. Thank you very much also to **Priscilla Rajakumar** for proof- reading, wonderful scientific discussions and her trust in the last two years. I want to thank **Max Blanchard** for proof-reading and for taking over the endolysin project. And I am grateful to **Marco Lizzul** for his advice and help regarding *Haematococcus pluvialis* and the UCL Advances PhD Enterprise Scholarship. Furthermore, I would like to thank **Dr Lucia Biffar** for wonderful times together and a great support throughout all the last years. Thank you very much also to **Umaima Al Hoqani, Alice Lui Yuen, Abbas Sayed, Dr Liam O´Hara, Ben Mackrow and Juliana Ramos** for a great time in the Purton lab. And, of course, thank you very much to **Thushi Sivagnanam** for her great effort in organising and running our lab.

I am very grateful to **Gary Sorhaindo** for all his amazing continuous support, encouragement and company in the last four years. And thank you very much for proof-reading and your assistance with printing last night.

I am endlessly grateful to my mum **Marlis Stoffels** for all her incredible support, encouragement and help throughout this PhD, my whole studies and my whole life. Furthermore, I am very grateful to my father **Volker Köditz** and for all his support, encouragement and help, as well as to **Jagoda Köditz** for all her encouragement and support in the last years.

Abbreviations

aadA	aminoglycoside-3''-adenyl-transferase gene
Amp	ampicillin
AMPS	ammonium persulphate
ATP	adenosine triphosphate
bp	base pairs
BSA	bovine serum albumin
BSAC	British Society for Antimicrobial Chemotherapy
CTB	cholera toxin subunit B
DNA	deoxyribonucleic acid
ECL	enhance chemiluminescence
e. g.	*exempli gratia* = for example
EDTA	ethylenediaminetetraacetic acid
ELISA	enzyme-linked immunosorbent assay
g	gram
GC	guanine and cytosine
GFP	green fluorescent protein
GOI	gene of interest
HA	hemagglutinin
His	histidine
HSM	high salt minimal medium
kb	kilo base pairs
kDa	kilo Dalton
Mb	mega base pairs
mg	milligram
min	minute
ml	mililitre
mM	millimolar
mRNA	messenger RNA
MWCO	molecular weight cut-off
OD	optical density

ORF	open reading frame
PCR	polymerase chain reaction
PSI	photosystem I
PSII	photosystem II
RNA	ribonucleic acid
SDS	sodium dodecyl sulphate
SDS-PAGE	sodium dodecyl sulphate polyacrylamide gel electrophoresis
sec	second
sup.	supernatant
TAP	tris-acetate-phosphate medium
TEMED	N, N, N', N'-tetramethylethylenediamine
TRA	turbidity reduction assay
tRNA	transfer RNA
TSP	total soluble protein
UTR	untranslated region
VFP	vivid green fluorescent protein
w/v	weight by volume
tRNA	transfer RNA
UTR	untranslated region
WHO	World Health Organization
WT	wild type

Table of contents

Table of figures

Table of tables

CHAPTER 1

Introduction

1 Introduction

1.1 The need for new antibiotics

After the discovery of penicillin in 1928 and the subsequent development of further antibiotics, these drugs became a potent and efficient weapon against infectious diseases. In 1967 the US Surgeon General William H. Stewart even declared that the war against infectious diseases was won, and this represented the general opinion of the medical community during this time (Spellberg et al. 2008; Fauci 2001). However, the increase of antibiotic resistance in the last decades has severely reduced the reliability of antibiotic treatments. In particular, the prevalence and range of multi-drug resistant strains has increased alarmingly (Levy & Marshall 2004).

The director of the Welcome Trust, Professor Jeremy Farrar, and the Chief Medical Officer for England, Professor Dame Sally Davies, warned in 2014 that antibiotic resistance has reached a tipping point at which it starts to become a threat also in Europe. The World Health Organization (WHO) had already made antimicrobial resistance the topic of World Health Day 2011, and released a global report on antimicrobial resistance in May 2014. The report stated that very high rates of antimicrobial resistance were observed in all WHO regions in bacterial pathogens such as *Escherichia coli*, *Klebsiella pneumoniae*, *Staphylococcus aureus* and *Streptococcus pneumoniae*. These bacteria cause common health-care associated and community-acquired infections such as urinary tract infections, wound infections, blood stream infections and pneumonia. The report warned that antimicrobial resistance is an "increasingly serious threat to global public health" and that there is a real risk of falling back into a pre-antibiotic era in the 21st century (WHO report 2014).

At the same time the development of new antibiotics has severely declined in the last few decades, mainly owing to the lower profitability of antibiotics compared to other drugs (Figure 1.1). Drug development generally requires very high costs, but antibiotics are short-course therapies, which make them less profitable than drugs for

chronic diseases (Spellberg et al. 2008). Furthermore, the risk of resistance development makes it important to limit the widespread use of newly-developed antibiotics to maintain their efficacy, which negatively affects the profits from that drug (Spellberg et al. 2008). The British Society for Antimicrobial Chemotherapy (BSAC) even established the global initiative Antibiotic Action, which seeks to inform and educate about the need for discovery, research and development of new antibiotics. The initiative is supported by several microbiological and medical societies, researchers, health professionals and politicians worldwide. In addition, the Infectious Disease Society of America (IDSA), which gives policy recommendations to the US government, has started the "10 x '20 initiative", which calls for the delivery of ten new antibiotics by the year 2020 to tackle the problem of antibiotic-resistant infections that costs the US health care system between $21 and $34 billion and over 8 million additional hospital days per year (Wright 2012; Infectious Diseases Society of America 2011).

Figure removed

Figure 1.1: Dates of the discovery of distinct classes of antibacterial drugs and the "discovery void" in the last few decades
The indicated dates represent the dates of the initial discovery or the patent. Reproduced from (WHO report 2014), originally from (Silver 2011).

Infectious diseases are the second-leading cause of death worldwide and also belong to the top causes of death in developed countries (WHO report 2004). Antibiotics are still the major weapons against severe infectious diseases and it is therefore very important to preserve the efficacy of the available antibiotics, but also to develop new antibiotics with different targets and new strategies to circumvent the resistance mechanisms of the microorganisms.

1.1.1 Antibiotics and the development of antimicrobial resistance

Antibiotics are substances that kill or prevent the growth of microorganisms. The term antibiotics can refer to substances that are produced by bacteria or fungi as a protection mechanism against other microorganisms, as well as to chemically modified semisynthetic antibiotics and synthetic antimicrobial drugs.

Arsphenamine is often described as the first antibacterial agent. It was discovered in the laboratory of Paul Ehrlich in 1909 and was sold under the trade name Salvarsan as a treatment against Syphilis. In 1928, the first natural substance with an antibacterial effect was discovered by Alexander Fleming. This antibiotic is produced by the fungus *Penicillium crysogenum* and was called penicillin (Madigan 2009). The large-scale production of penicillin G started in 1939, and the substance was first and very efficiently used for the treatment of staphylococcal and pneumococcal infections among soldiers before it became available for general use in 1945 (Madigan 2009). Alexander Fleming received the Nobel prize in 1945 for the discovery of penicillin, which revolutionised the treatment of infections (WHO report 2014). Shortly after 1945, pharmaceutical companies began to search for other antibiotics and discovered a variety of structurally different antibiotics with different mechanisms of actions. Furthermore, researchers developed semisynthetic antibiotics with different spectra and efficiencies by chemical modification of natural antibiotics in the following decades. However, the discovery and development of new antibiotics has declined severely in the last decades, and the last truly new class was discovered in the 1980s (Figure 1.1).

Over 2 billion years ago, antibiotics developed as a defence mechanism of microorganisms against competitors. At the same time mechanisms to resist the antimicrobial substances also evolved in microorganisms to keep up in the battle of competing microorganisms (Spellberg 2008).

Different mechanisms are known that cause resistance against antimicrobial agents. Some microorganisms, for example, are impermeable to certain antibiotics. Gram-negative bacteria have an outer membrane around their cell wall, which makes them impermeable to penicillin G, but not tetracycline or streptomycin (Figure 1.2) (Madigan 2009). The organism can also lack the target of the antibiotic. Bacteria of the genus *Mycoplama*, for example, lack a cell wall and are therefore resistant against β-lactam antibiotics that inhibit cell wall synthesis (Madigan 2009). Another resistance mechanism involves the rapid transport of the antibiotic out of the cell by antibiotic-efflux pumps (Figure 1.2). One type of efflux pump can often confer resistance against several antibiotics. For example, bacteria with RND-type pumps are resistant against tetracyclines, chloramphenicol and the fluoroquinolones (Levy & Marshall 2004; Nikaido 1996). Other organisms are able to modify or degrade the antimicrobial substance. The β-lactamase enzymes cleave the β-lactam ring and in doing so, destroy penicillins and cephalosporins (Figure 1.2). Hundreds of different β-lactamases have been discovered to-date (Levy & Marshall 2004). Other modifying enzymes can inactivate chloramphenicol and aminoglycosides by acetylation or phosphorylation of key chemical groups on the antibiotics. Furthermore, the modification of the target structure of the antibiotic or the affected metabolic pathway is also a common strategy to require resistance (Levy & Marshall 2004). The mechanism of action of penicillin and other β-lactam antibiotics is the inhibition of cell wall synthesis by binding to the enzyme that carries out the transpeptidation of two glycan linked peptide strands in the cell wall. This enzyme is therefore called penicillin-binding protein (PBP). Some bacteria exchanged the PBP for another, structurally different protein with greatly reduced affinity to β-lactam antibiotics (Antignac & Tomasz 2009). This exchange confers resistance against β-lactam antibiotics and combination drugs with β-lactamase inhibitors. Today, 15 classes of antibiotics are known that target different physiological and metabolic functions, but resistance mechanisms have developed against every class (Levy 2002).

Figure removed

Figure 1.2: Biological mechanisms of antibiotic resistance
The main mechanisms conferring antimicrobial resistance shown in the figure are antibiotic-efflux pumps, enzymatic deactivation of the antibiotic and impermeability for the antibiotic. Reproduced from Levy & Marshall (2004).

The genes for resistance are either encoded on the chromosome or on plasmids, and can spread by various mechanisms such as the exchange of plasmids, transfer via bacteriophages, the uptake of naked DNA and via transposons (Figure 1.3) (Levy & Marshall 2004). Microorganisms are able to duplicate the plasmids and to pass them to other closely or even distantly related organisms (a process termed conjugation). In this way resistance genes can be easily transferred and spread within the microbial population (Figure 1.3) (Madigan 2009). Chromosomal resistance genes can be released to the environment after cell lysis and some species can integrate these genes as free DNA in a process called transformation (Figure 1.3). Antimicrobial resistance genes are often located on transposons – mobile DNA elements that can change their position within the genome or from a plasmid to the genome (Levy & Marshall 2004).

Furthermore, integrons can be involved in the acquisition of resistance genes. Integrons are assembly platforms that integrate different genes by site-specific recombination under one promoter (Mazel 2006). A further propagation mechanism is the transfer of genes between different bacterial cells via virulent or temperate bacteriophage in a process called transduction. The continued exposure to antimicrobial drugs, kills the susceptible cells and selects for the resistant organisms, which then propagate in the population (Levy & Marshall 2004).

Figure removed

Figure 1.3: The genetics of antimicrobial resistance
The figure shows the location of antimicrobial resistance genes and mechanisms by which resistance genes can spread to other bacterial cells. The genes can be transferred via the exchange of plasmids, bacteriophages, the uptake of naked DNA and transposons. Reproduced from Levy & Marshall (2004).

1.1.2 Limitations of conventional antibiotics

Beside the increasing occurrence of resistance against conventional antibiotics, there are further limitations of these drugs. Most antibiotics have a broad-spectrum against a range of bacterial classes and therefore each treatment affects not only the pathogen, but also the beneficial and protective human bacterial flora. Not only does this increase the susceptibility to infections with pathogenic bacteria and fungi, but also can cause conditions such as obesity, type 1 diabetes, inflammatory bowel disease, allergies and asthma (Blaser 2011; Chen & Blaser 2007). Furthermore, reoccurring exposure to antibiotics results in the spread of antimicrobial resistance genes within the commensal bacterial flora, which functions as a reservoir for resistance genes and can pass the genes on to pathogenic bacteria (Schmelcher et al. 2012). It would be therefore highly desirable to develop narrow-spectrum antibiotics that specifically kill only the targeted pathogen, to reduce the collateral effects on the commensal bacterial flora and to decrease the spread of antimicrobial resistance genes (Blaser 2011).

However, to-date the available diagnostic methods are still limited and the usage of broad-spectrum antibiotics is a convenient way to handle daily practices in doctors' surgeries, since in most cases these drugs are effective even when the pathogen has not been identified. Nevertheless, the increasing occurrence of antibiotic-resistant bacteria makes it more and more important to accurately diagnose the pathogen and its susceptibility to different antibiotics. In the last few decades the number of available diagnostic methods has increased and the methods have greatly improved. However, further research needs to be done to develop accurate, but also rapid and practicable diagnostic methods. This is reflected by the choice of the Longitude Prize 2014, an inducement prize contest, in which the public voted for "antibiotics" as "the greatest challenge of recent times". The committee set the challenge as "the creation of a cost-effective, accurate, rapid and easy-to-use test for bacterial infections that will allow health professionals worldwide to administer the right antibiotic at the right time". With the development of better diagnostic methods and a growing awareness of the importance of the human microbiome, the demand for narrow-spectrum antibiotics will most likely greatly increase.

Furthermore, not many conventional antibiotics are available that can eliminate bacteria in biofilms. Biofilms on the mucosal membranes in the nasopharynx are seen as a major reservoir for pathogenic bacteria (e.g *S. pneumoniae and S. aureus*) in the population and are often the starting point of infections. The diminution of this reservoir would most likely have a great impact on the incidence of *S. pneumoniae* and *S. aureus* infections (Loeffler et al. 2003). The available antibiotics that can target bacteria on the mucosal membrane – namely, mupirocin and polysporin – have been used prophylactically in hospitals, which helped to prevent the spread of methicillin-resistant *S. aureus* (MRSA) strains in these facilities. However, strains with resistances to these antibiotics have appeared as well (Hudson 1994).

Moreover, many conventional antibiotics have side effects, and there are restrictions on the use, especially for the treatment of children (Payne et al. 2007). There is therefore a great need to develop novel and also improved classes of antibiotics, not only for the treatment of infections with multi-resistant pathogens but for all infections.

1.2 Bacteriophage endolysins as potential new generation antibiotics

1.2.1 Bacteriophages and phage therapy

Bacteriophages are viruses that infect bacteria and are the most abundant entities on the planet. It is estimated that the number of bacteriophage particles amounts to 10^{31}. The majority are tailed bacteriophages, which comprise of a tail and a head that encapsulates the DNA or RNA genome (Figure 1.4) (Elbreki et al. 2014). The nucleic acids can be single or double stranded, and some bacteriophages have a circular genome, while others carry a linear genome. The tail is involved in the attachment to the bacterial cell and the injection of the nucleic acids.

Figure removed

Figure 1.4: Electron micrograph of a *Acinetobacter baumannii* bacteriophage (A) and schematic representation of the structure of a tailed bacteriophage (B)
Modified from Elbreki et al. (2014), 3D model in (B) modified from www.wikipedia.com.

Felix d'Herelle characterised and named bacteriophages in 1917 and initiated experiments investigating the use of bacteriophages as treatments for bacterial infections (so-called 'phage therapy') in the early 1920s (Elbreki et al. 2014). Felix d'Herelle also participated in the establishment of the International Bacteriophage Institute in Tblisi, Georgia, which is also known as the Eliava Institute. This institute has performed extensive research into phage therapy since then and supplies countries

of the former Soviet Union with bacteriophage preparations for the treatment of bacterial infections. However, the production strongly declined after the break-up of the Soviet Union (O'Flaherty et al. 2009). In the 1930s, several companies in the US, France and Germany produced phage preparations as antimicrobials e.g. Eli Lilly (US). However, after the discovery and spread of antibiotics and only mixed success, phage therapy disappeared in Western countries in the 1940s (Elbreki et al. 2014).

The increase in antibiotic-resistant strains and the enormous expansion in our understanding of phage biology has now caused a rediscovery of phage therapy in western countries. Several companies and research groups have started to investigate the potential of bacteriophages for the treatment of infectious diseases and other applications, such as their use as food preservatives (O'Flaherty et al. 2009). With the rediscovery of phage therapy, attention was also drawn to bacteriophage-encoded endolysins. These enzymes are used by most bacteriophages to digest the peptidoglycan of the bacterial cell wall for phage progeny release at the end of the lytic cycle, and have the potential to be used on their own as antibacterial agents (Schmelcher et al. 2012; Loessner 2005; Fischetti 2008).

1.2.2 Endolysins play an important role in the lytic life cycle of bacteriophages

Endolysins are bacteriophage-encoded enzymes that are produced in bacterial cells after they have been infected by a bacteriophage. These proteins are also known as bacteriophage lysozymes, lysins or muralytic/mureolytic enzymes (Loessner 2005).

Bacteriophages have two types of life cycle. Virulent bacteriophages immediately enter the lytic life cycle (explained below), whereas the genome of temperate bacteriophages is first inserted into the host chromosome during the lysogenic cycle. The bacteriophage genome, often referred to as a prophage, is replicated together with the host chromosome during cell replication, and can remain silent for a long period of

time before environmental conditions prompt entry into the lytic cycle (O'Flaherty et al. 2009).

To infect a bacterial cell, bacteriophages attach to the cell surface, often to receptors, and insert their genetic material into the cell. In the case of virulent bacteriophages the infection results immediately in the hijacking of the cell metabolism. The bacterial DNA and protein synthesis machinery changes to produce bacteriophage particles and the host genome is degraded (Figure 1.5) (O'Flaherty et al. 2009). At the same time, endolysins and another type of proteins, called holins, are produced and accumulate in the cytoplasm of the infected bacterium (Loessner 2005). The holin proteins help to tightly control the moment of the endolysin-mediated cells lysis. At the end of the lytic cycle and once a critical holin concentration has been reached, the hydrophobic proteins assemble into oligomers and insert into the cell membrane (Schmelcher et al. 2012; Young et al. 2000). The insertion of the holin proteins results in the creation of pores, which allow the endolysin to pass across the cytoplasmic membrane and enter the peptidoglycan (Loessner 2005). Figure 1.6 shows the mechanism for the cell wall of Gram-negative bacteria (for the Gram-positive cell wall see figures 3.2 and 5.2). Subsequently, the endolysins cleave specific bonds of the peptidoglycan, which results in the disruption of the cell wall and the high internal pressure of 20 – 50 atmospheres causes the osmotic lysis and the death of the bacterial cell (Schmelcher et al. 2012). The cell lysis results in the release of the phage progenies, which can now infect new bacterial cells (Figure 1.5).

To-date, only a few exceptions have been described of endolysins that do not depend on a holin for release to the peptidoglycan. Two examples are an endolysin from a *Oenococcus oeni* bacteriophage and the *Lactobacillus plantarum*-specific bacteriophage Øg1e that are both attached to signal peptides and are exported by the host *sec* system (São-José et al. 2000; Kakikawa et al. 2002).

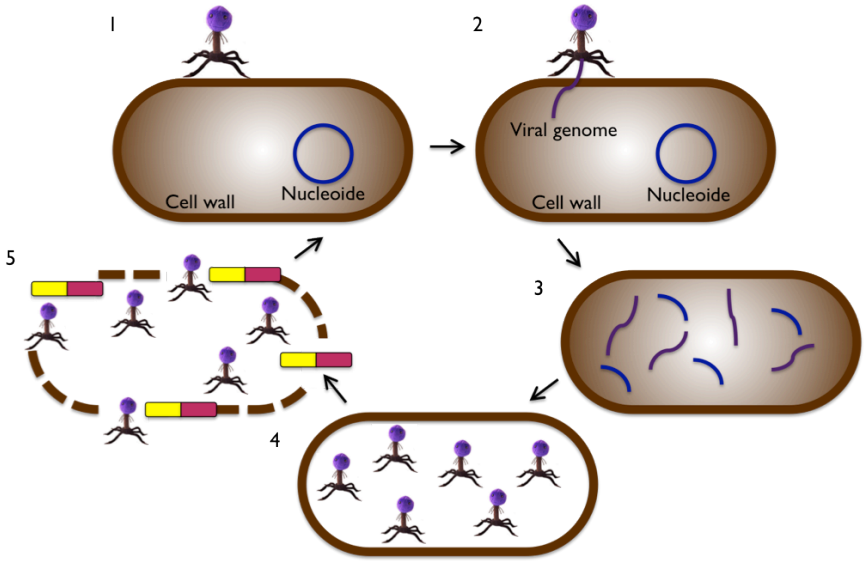

Figure 1.5: Bacteriophage lytic life cycle
The infection starts with the attachment of the bacteriophage to the target bacterium (1). Subsequently, the phage DNA or RNA is injected into the cell (2). The degradation of the host DNA is initiated and the bacterial DNA and protein synthesis machinery changes to produce bacteriophage particles (3) and (4). The release of endolysins via pores formed by holins causes the lysis of the bacterial cell wall and releases hundreds of new bacteriophages to the environment (5).

Figure removed

Figure 1.6: Schematic representation of the bacterial cell wall of (Gram-negative bacteria) and the peptidoglycan (type A1γ) showing the bonds that are targeted by different endolysins
The endolysins are produced in the cytoplasm of the bacterial cells that are infected by a bacteriophage. At the end of the lytic cycle, holin proteins are inserted into the cytoplasmic membrane, which results in pores (A). The endolysins can get through these pores to the cell wall, where the enzymes cleave specific bonds of the peptidoglycan (B). B shows the structure of type A1γ peptidoglycan, found for example in *E. coli* and *Listeria*. CCWP = carbohydrate cell wall polymer, LU = linkage unit, P = phosphate group, MurNAc = *N*-acetyl-muramic acid, GlcNAc = *N*-acetyl-glucosamine acid, Ala = alanine, Glu = glutamic acid, Lys = lysine, m-DAP = meso-diaminopimelic acid. Modified from Loessner (2005).

1.2.3 Endolysin structure & mode of action

Bacteriophages are highly specific to a target bacterium. In addition their endolysins are usually only effective against the species of bacteria in which they are naturally produced, or in some cases, against other species within the same genus (Borysowski et al. 2006).

Endolysins that are specific for Gram-positive bacteria usually have a modular organisation. Many of these endolysins have a two-domain structure with a N-terminal catalytic domain and a C-terminal cell binding domain connected by a linker (Figure 1.8, Figure 1.7) (Fischetti 2005). However, there are also endolysins with different domain architectures. Many staphylococcal endolysins, for example, have two catalytic domains followed by one cell binding domain (Navarre et al. 1999; O'Flaherty et al. 2005). Alternatively, the cell binding domain can be located in the middle of the enzyme and surrounded by two catalytic domains, which is the case for the endolysin λSA2 that is specific to *Streptococcus agalactiae* (Figure 1.8) (Pritchard et al. 2004). Despite their modular structure, nearly all known endolysins specific to Gram-positive bacteria are single polypeptides encoded by one gene. The only exception here is PlyC, an endolysin of the group A *Streptococcus* bacteriophage C1, which is encoded by two different genes (Nelson et al. 2006).

The cell binding domains of endolysins attach the enzyme tightly to its substrate after cell lysis. Endolysins are also able to enter and cleave the peptidoglycan of Gram-positive bacteria from outside of the cell (i.e. 'exolysins'). Therefore, the attachment prevents the endolysins from attacking surrounding cells of the target bacterium, which can still function as a host for the bacteriophage (Schmelcher et al. 2012). In contrast, the outer membrane of Gram-negative bacteria protects uninfected cells against lysis by endolysins from outside. Endolysins that are specific to Gram-negative bacteria are therefore usually smaller single-domain proteins without a cell binding domain (Cheng et al. 1994).

Figure removed

Figure 1.7: Crystal structures of the *S. pneumoniae*-specific endolysin Cpl-1 (A), the *Listeria* monocytogenes-specific endolysin PlyPSA (B) and a general schematic representation of two domain endolysins (C)
Reproduced from Hermoso et al. (2003) (A) and Korndörfer et al. (2006) (B).

Figure removed

Figure 1.8: Schematic representation showing the modular organisation of selected bacteriophage endolysins
CBD = Cell binding domain, ChBD = Choline binding domain, Cpl-7 = Cpl-7-like bindng domain, SH3b = Bacterial Src homology 3 domain (cell wall binding domain). Reference: (1) Zimmer et al. (2003), (2) Loessner et al. (1995), (3) García (1990), (4) García (1990), (5) O'Flaherty et al. (2005), (6) Pritchard et al. (2004), (7) Pritchard et al. (2007), (8) Briers et al. (2007). Reproduced from Schmelcher et al. (2012).

Furthermore, the cell wall binding domain is responsible to a large degree for the specificity of the endolysin for certain species or genera. The domain binds noncovalently to molecules in the cell envelope, which can be part of the peptidoglycan or other cell wall associated molecules. It has been shown that the LysM domain binds to the *N*-acetyl-glucosamine acid of the peptidoglycan (Visweswaran et al. 2011). The binding domains of several pneumococcal endolysins bind to the choline of the teichoic acids in the cell wall, whereas the Cpl-7 cell wall binding domain attaches to the Streptococcal cell wall in a mechanism independent of choline (Schmelcher et al. 2012). The SH3b binding domains can be found in a range of endolysins, including *Staphylococcus*-specific endolysins and lysostaphin, a bacteriocin that is produced by *Staphylococcus simulans* against *S. aureus* (Schindler

& Schuhardt 1964; Sass & Bierbaum 2006). It has been shown, for several endolysins, that the cell wall binding domain is required for full lytic activity (Sanz et al. 1992; Sass & Bierbaum 2006). The crystal structure of the *S. pneumoniae*-specific endolysin Cpl-1 suggests that the cell wall binding domain positions the catalytic domain in the right orientation towards the substrate, which might be the reason that the domain is required for full enzymatic activity in several endolysins (Hermoso et al. 2003; Schmelcher et al. 2012). In contrast, some endolysins remained fully active after the removal of the binding domain, or were even found to be more active (Cheng & Fischetti 2007; Low et al. 2005). These results and further studies encourage the engineering of tailor-made improved endolysins. Tailor-made endolysins have been created by removing the cell binding domains, combining domains from different endolysins or adding additional domains, as well as random and site-directed mutagenesis. Several studies found increased activities or extended lytic spectra for the new designed endolysins (Schmelcher et al. 2012).

The catalytic domain is responsible for the enzymatic cleavage of the peptidoglycan and can be an *N*-acetyl-β-D-glucosaminidase or *N*-acetyl-β-D-muramidase (lysozymes), which both cleave one of the two glycosidic bonds of the carbohydrate strand. Other catalytic domains have endopeptidase activity and cleave a specific bond of the peptide chains. Furthermore, these domains can be *N*-acetylmuramoyl-L-alanine amidases, which hydrolyse the amide bond between the sugar strand and the peptide chain (Figure 1.6 B) (Loessner 2005). Catalytic domains can also have an influence on the specificity of an endolysin. The peptidoglycan structures differ between both Gram-types, but also between different bacterial species. A pentaglycine bridge, for example, can be only found in *Staphylococcus* and very few other species. The absence or presence of the specific target bond contributes therefore to a limitation of the host range (Schmelcher et al. 2012). Furthermore, the catalytic domain contributes to the net charge of the endolysin, which can also have an influence on the host range (Low et al. 2011).

1.2.4 Bacteriophage endolysins as antimicrobial agents

Endolysins have been studied by different research groups and it has been shown for several endolysins, that when applied externally to Gram-positive bacteria, these enzymes are able to lyse and kill cells of the target bacterium (Fenton et al. 2010; Borysowski et al. 2006). This has been shown for endolysins purified from bacteriophage-infected bacteria and for recombinant endolysins that were mainly synthesized using the expression platform *Escherichia coli* (Garcia et al. 1983c; Sheehan et al. 1997; Loessner 2005). It was believed that endolysins could not be used as a treatment against Gram-negative bacteria, since the outer membrane represents a barrier for the enzymes. However, a few studies demonstrated recently the successful application *in vitro* of endolysins against Gram-negative bacteria (Lai et al. 2011; Lukacik et al. 2012).

Several promising pre-clinical trials have been performed with endolysins specific to different Gram-positive human pathogens. Table 1.1 gives an overview of the endolysins and the animal models of disease that have been used in *in vivo* studies. Overall, the studies found that the administration of the endolysin under study resulted also *in vivo,* in a significant decrease of the bacterial loads and therefore an increase of the survival rates of the infected animals. Moreover, numerous *in vivo* studies showed that endolysins can prevent the colonisation of the mucosal membrane by pathogens, which cannot be achieved by most conventional antibiotics (Loeffler et al. 2001; Loeffler et al. 2003; McCullers et al. 2007).

Most endolysins have a high specificity for the cell wall of bacterial species in which they are naturally produced. Some endolysins are even effective only against certain serotypes or strains, whereas others lyse bacteria within the same genus (López et al. 2004). In contrast to conventional antibiotics, which usually have a broad-spectrum, endolysins could be used to specifically eliminate the pathogen without harming the commensal bacterial flora. As already discussed in 1.1.2, the usage of narrow-spectrum antibiotics for the treatment is highly desirable, but requires accurate and practicable diagnostic methods. With the development of better diagnostic methods, the demand for narrow-spectrum antibiotics will most likely greatly increase.

Table 1.1: A selection of endolysins investigated in *in vivo* studies
Reproduced from www.phibiotics.org and Fenton et al. (2010)

Endolysin	Bacteriophage	Target bacterium	Catalytic activity	Model systems (Mode of administration)	Reference
Cpl-1	Cp-1	*Streptococcus pneumoniae*	1,4-N-acetylmuramidase	Murine model of pneumococcal bacteremia (intravenous) Murine model for acute otitis media (intranasal) Rat model of experimental endocarditis (intravenous) Infant-rat model of experimental pneumococcal meningitis (intracisternal, intraperitoneal)	Loeffler et al. (2003) McCullers et al. (2007) Entenza et al. (2005) Grandgirard et al. (2008)
Pal	Dp-1	*Streptococcus pneumoniae*	N-acetylmuramoyl-alanine amidase	Murine model of nasopharyngeal colonization (intranasal) Murine peritonitis-sepsis model (intraperitoneal)	Loeffler et al. (2001) Jado et al. (2003)
PlyGBS	NCTC11261	*Streptococcus agalactiae* *Streptococcus pyogenes*	1,4-N-acetylmuramidase	Murine model of vaginal and upper respiratory colonization (intranasal, intravaginal, oral)	Cheng et al. (2005)
PlyG	*Bacillus* phage γ	*Bacillus anthracis* *Bacillus cereus*	N-acetylmuramoyl-alanine amidase	Murine model of *Bacillus anthracis* infection (intraperitoneal)	Schuch et al. (2002)
PlyBH	Ames prophage	*Bacillus anthracis*	Amidase	Murine model of peritonitis (intraperitoneal)	Yoong et al. (2006)
PlyC	C1	*Streptococcus pyogenes*	Amidase	Murine model of oral colonization (oral)	Nelson et al. (2001)
MV-L	ϕMR11	*Staphylococcus aureus* *Staphylococcu simulans*	N-acetylmuramoyl-alanine amidase	Murine model of nasal colonization (intranasal) Murine model of MRSA bacteremia (intraperitoneal)	Rashel et al. (2007)

1.2.4.1 Resistance to endolysins

As discussed in 1.1.1, the number of multi-drug resistant bacteria has increased in recent decades and resistant strains have appeared against all classes of antibiotics that have been developed to-date. It is therefore desirable to develop novel classes of antibiotics, which are less susceptible to resistance development. As also mentioned in 1.1.2 the use of narrow-spectrum antibiotics could decrease the spread of antimicrobial resistance genes within the bacterial community by preventing selective pressure on the whole commensal flora of a patient with every treatment. The high specificity of endolysins is therefore advantageous to decelerate the development and spread of antibiotic resistance.

Since endolysins cleave the peptidoglycan from outside and do not need to get into the cell, several of the resistance mechanisms discussed in 1.1.1 cannot affect the activity of endolysins. Intracellular resistance mechanisms such as antibiotic-efflux pumps, cytoplasmic enzymes that degrade or modify antimicrobials, and the reduction of membrane permeability, can be therefore excluded (Schmelcher et al. 2012). However, resistance development due to target modification or the activity of extracellular enzymes is still conceivable.

Bacteriophages and their endolysins evolved over billions of years in parallel with the target bacterium. To ensure the survival of the bacteriophage, this co-evolution required that endolysins target components in the cell wall that are essential for the viability of the bacterium. It is therefore believed that endolysins target highly immutable structures within bacteria and that the development of resistance against endolysin is a rare event (Schmelcher et al. 2012).

A few studies have attempted to induce resistance against certain endolysins. Loeffler et al. (2001) showed that the repeated exposure of *Streptococcus pneumoniae* to low concentrations of the pneumococcal endolysin Pal (< 1 U) on agar plates (16 rounds) or increasing concentrations in liquid cultures did not cause the development of resistant strains (4.1.1). Another study exposed *Bacillus* cells to the mutagen methane-

sulphonic acid ethyl ester to accelerate resistance development against the endolysin PlyG. The treatment did not result in any PlyG-resistant strains, whereas the same treatment resulted in a 1,000 – 10,000-fold increase in resistance against the antibiotics streptomycin and novobiocin (Schuch et al. 2002; Schmelcher et al. 2012). However, antimicrobial resistance has been observed against other peptidoglycan hydrolases, for example human lysozyme and lysostapin, which has a similar modular organisation and a high sequence similarity to several *Staphylococcus* endolysins (Schmelcher et al. 2012). Therefore, the development of resistance against endolysins cannot be entirely excluded.

A strategy to decrease the risk of resistance development could be the administration of several endolysins in combination, or the combination of an endolysin with a conventional antibiotic. It has been shown that Cpl-1 has synergy with the antibiotics gentamicin and penicillin (Djurkovic et al. 2005). Furthermore, the endolysins Pal and Cpl-1 in combination were found to have a synergistic effect (4.1.1) (Jado et al. 2003). Synergy was also observed for the staphylococcal endolysin LysK in combination with lysostaphin (S. C. Becker et al. 2008). These results encourage the combinational use of endolysins and antibiotics to enhance on one hand the efficacy, and on the other hand to discourage the development of resistance.

1.2.4.2 Safety & immunogenicity

Despite the promise of endolysins, the application of whole enzymes as antibacterial agents to treat infections raises several concerns. The degradation of bacterial cells by endolysins releases cell debris such as peptidoglycan pieces, teichoic acids and liopteichoic acids, which can cause an inflammatory response, and even result in septic shock or organ failure. A study that investigated the inflammatory response after continuous intravenous application of Cpl-1 in rats observed indeed an increase of proinflammatory cytokines (Entenza et al. 2005). Vancomycin, which was used as a control in the study, also induced an inflammatory response, but levels were less pronounced. Furthermore, the study found that Cpl-1 eliminated *S. pneumoniae* cells

from the blood within 30 minutes, which was faster than vancomycin, and concluded that the findings support the use of Cpl-1 for intravenous treatment of infections, but that therapeutic concentrations and safety need to be further investigated. In contrast, a study by Witzenrath et al. treated mice intraperitoneally with Cpl-1 against a pneumococcal pneumonia infection and observed even lower levels of proinflammatory cytokines in Cpl-1-treated mice compared to untreated mice (Witzenrath et al. 2009).

Another concern that needs to be addressed when proteins are administered is a potential immune response and the generation of deactivating antibodies. Several studies showed that the intravenous and intraperitoneal treatment with endolysins, for example Pal and Cpl-1, results in the production of antibodies against the endolysins (Jado et al. 2003; Loeffler et al. 2003). The hyperimmune serum of rabbits after immunisation with Cpl-1 was shown to marginally decrease the *in vitro* activity of Cpl-1. However, the previous immunisation of mice with Cpl-1 or Pal, did not affect the eradication of *S. pneumoniae* from infected mice by a second treatment with the endolysins in comparison to unimmunised mice (Jado et al. 2003; Loeffler et al. 2003). The study by Jado et al. reported that no signs of anaphylaxis or adverse side effects were observed after treatment with Pal or Cpl-1. The first *in vivo* study that demonstrated the potential of an endolysin for the treatment of MRSA also found that the treatment with MV-L resulted in the production of antibodies. However, the antibodies did not decrease the bacteriolytic activity of MV-L and no harmful side effects were observed (Rashel et al. 2007).

Nevertheless, non-native proteins get degraded by the host immune system. It has been shown that the half-life of Cpl-1 after intravenous administration in rats was approximately 20 minutes, which is similar to the administration of other non-native proteins (Loeffler et al. 2003). Since several studies achieved promising results in *in vivo* studies, it has been suggested that the enzymatic activity of endolysins is fast enough to outcompete the degradation by the immune response (Schmelcher et al. 2012). An encouraging study by Resch et al. (2011) that created dimers of Cpl-1 via the introduction of cysteine residues for disulphide bridge formation demonstrated an enhanced enzymatic activity and a decelerated degradation in the plasma.

Nevertheless, endolysins could be good candidates for topical or mucosal membrane treatments, in which the enzymes are less affected by the clearance of the immune system and the risk of an inflammatory reaction is reduced.

1.2.5 Further applications of endolysins

Beside the use as novel antibiotics in human medicine, endolysins could be also used for different applications such as the control of bacterial contamination in food and feed, for the abolishment of bacterial pathogens on crop plants or the eradication of biofilms in food production (Schmelcher et al. 2012). Furthermore, applications in veterinary medicine, for example, the treatment of bovine mastitis have been suggested (Donovan et al. 2006).

Taken together, endolysins are promising candidates for use as a novel and improved class of antibacterial agent, both in human medicine and also for use in other fields.

1.3 The target bacteria *Streptococcus pneumoniae*, *Staphylococcus aureus* and *Propionibacterium acnes*

S. pneumoniae and *S. aureus* are major human pathogens that cause a range of serious infections and have a high proportion of antibiotic-resistant strains. Both species were listed in the WHO report about antibiotic resistance as "bacteria of international concern", and are the only two Gram-positive bacteria on this list (WHO report 2014). The potential of endolysins as a treatment against *S. pneumoniae* and *S. aureus* has been demonstrated *in vitro* and *in vivo* (Witzenrath et al. 2009; Rashel et al. 2007). Skin infections caused by *S. aureus* and infections starting in the nasopharynx caused by both bacteria could be treated by topical or mucosal membrane treatments, which would reduce the risk of a rapid degradation of the endolysins and potential inflammatory reactions. *S. pneumoniae* and *S. aureus* were therefore chosen as target bacteria for this study that investigates the production of endolyins in microalgae.

In addition, the production of an endolysin against *Propionibacterium acnes* in the cyanobacterium *Synechocystis* sp. PCC 6803 was investigated in this study. *P. acnes* has been associated with the skin condition acnes vulgaris and an endolysin effective against the bacterium could be therefore used in a topical treatment (Farrar & Ingham 2004).

1.3.1 *Streptococcus pneumoniae*

S. pneumoniae is a Gram-positive, aerotolerant bacterium and is a major cause of pneumonia, bacterial meningitis and sepsis and is responsible for a high percentage of otitis media infections in children (Bogaert et al. 2004). It is considered one of the major human pathogens due to the morbidity and mortality it causes in young children, elderly people and patients with immunodeficiencies (Loeffler et al. 2001). Nearly one million children under the age of five years die every year from pneumonia and invasive diseases caused by *S. pneumoniae,* which is equivalent to 11% of all deaths in this age group (O'Brien et al. 2009; WHO report 2014). *S.*

pneumoniae often colonizes asymptomatically the nasopharynx of healthy carriers, which is responsible for a majority of the transmission within the population (WHO report 2014).

The number of antibiotic-resistant *S. pneumoniae* strains has increased in the last decades and is now a worldwide major public health concern (Adam 2002). *S. pneumoniae* shows high rates of reduced susceptibility to penicillins and macrolides (Figure 1.9 shows the data for the EU/EEA countries in 2012), as well as lower rates of resistance to fluoroquinolones (5.2% in the 2012 ECDC report) (ECDC - Surveillance report 2012). Penicillin resistance is caused by the acquisition of altered PBPs with reduced affinities for the binding to penicillins. The successive addition of mutation in the PBPs has resulted in increasing degrees of resistance (ECDC - Surveillance report 2012). Different degrees of antimicrobial resistance are defined by the minimal inhibitory concentration (MIC) of the antibiotic that is needed to inhibit the visible growth of the bacterium. The classification ranges from susceptible over non-susceptible and intermediate resistance to full resistance, but the definition of each class and the terminologies vary between studies (WHO report 2014). Macrolide resistance is either caused by a macrolide efflux system or a target modification of the 23S subunit of the ribosome, which inhibits the binding of macrolides to the 23S subunit. Both mechanisms are caused by the acquisition of one gene, which results immediately in full resistance with high MIC values (ECDC - Surveillance report 2012). Fluoroquinolones resistance is mediated by a mutation in the *parC* gene encoding a subunit of the topoisomerase IV, the target of the fluoroquinolones, or an efflux pump.

Two vaccines against pneumococcal infections are available. The 23-valent vaccine consists of purified polysaccharides from 23 serotypes and covers theoretical 85 – 90% of known *S. pneumoniae* strains. However, the vaccine is not effective in children under two years, which represent a major risk group, due to a lower immune response of young children (Bogaert et al. 2004). The conjugated vaccine comprises of seven to 11 pneumococcal polysaccharides bound to a diphtheria toxin, which causes an effective immune response in children under the age of two. The

disadvantage of this vaccine is that it covers only a part of the circulating *S. pneumoniae* serotypes (Bogaert et al. 2004).

A

Figure removed

B

Figure removed

Figure 1.9: Antibiotic resistance of *Streptococcus pneumoniae* isolates in Europe
Percentage (%) of invasive isolates that are non-susceptible or resistant to macrolides (A) or both to penicillins and macrolides (B) in the EU/EEA countries in 2012. Reproduced from ECDC - Surveillance report (2012)

1.3.2 *Staphylococcus aureus*

Staphylococcus aureus is a Gram-positive, facultative anaerobic bacterium and member of the phylum Firmicutes. The bacterium colonises asymptomatically the skin and nasal cavity of approximately 30% of the population, but can also cause serious infections (ECDC - Surveillance report 2012). *S. aureus* is a common cause of a range of skin and soft-tissue infections and can also cause life-threatening diseases such as pneumonia, meningitis, endocarditis, toxic shock syndrome, food poisoning and sepsis. Furthermore, *S. aureus* is responsible for the majority of wound infections after surgeries (WHO report 2014).

It is a prominent example of an organism that developed multi-drug resistance. Resistance of *S. aureus* against penicillin mediated by β-lactamases was already observed in the 1940s. Subsequently, β-lactamase stable drugs (e.g. methicillin) and β-lactamase inhibitors (e.g. clavulanic acid) were developed, but by the 1960s *S. aureus* had developed resistance against these drugs as well by acquisition of a gene that encodes a variant of the PBP with a low affinity of β-lactams, called PBP2a. These strains were therefore termed methicillin-resistant *S. aureus* (MRSA). By 2003, over 50% of *S. aureus* strains isolated in the United States were MRSA strains (Arias & Murray 2009). Subsequently, MRSA developed resistance against the glycopeptide antibiotic vancomycin, followed by resistance to many other antibiotics, including aminoglycosides, macrolides, fluoroquinolones, rifampicin and even newer antibiotics such as daptomycin and linezolid (Levy 2005). Figure 1.10 shows the prevalence of MRSA strains and strains resistant against rifampicin in the EU/EEA countries in 2012 (ECDC - Surveillance report 2012). The resistance to rifampicin is mediated by a mutation in the *rpoB* gene, which results in a RNA polymerase with a decreased affinity for rifampicin (ECDC - Surveillance report 2012).

Despite extensive research and numerous clinical trials with promising vaccine candidates, the creation of an vaccine against *S. aureus* has not been successful to-date (Fowler & Proctor 2014).

A

Figure removed

B

Figure removed

Figure 1.10: Antibiotic resistance of *Staphylococcus aureus* isolates in Europe
Percentage (%) of invasive isolates that are resistant to methicillin and other β-lactam antibiotics (MRSA strains) (A) and to rifampicin (B) in the EU/EEA countries in 2012. Reproduced from ECDC - Surveillance report (2012).

1.3.3 *Propionibacterium acnes*

Propionibacterium acnes is a Gram-positive, anaerobic bacterium of the phylum Actinobacteria, and it is a prevalent human skin commensal that colonises mainly areas that are rich in fatty acids such as the face, scalp and upper back.
P. acnes is believed to play a role in the inflammatory stages of acne vulgaris. It has been shown that antibiotic treatments that reduced the number of *P. acnes* cells on the skin have a therapeutic effect on the severity of the acne condition (Farrar & Ingham 2004). Furthermore, patients with acne vulgaris who did not respond to an antibiotic treatment were more likely to carry *P. acnes* strains, which were resistant to this antibiotic (Eady et al. 1989). One study found that *P. acnes* stimulates the release of the proinflammatory cytokines TNF-α, IL-1β and IL-8, which could play a role in the association of the bacterium with inflammatory acne. However, the exact mechanisms of this association and acne vulgaris are still unclear (Farrar & Ingham 2004).

Acne vulgaris is a skin condition that affects about 80% of the population at some point in life, mainly in adolescence. It can be very painful, cause psychological problems and can result in lifelong scarring in severe cases (Farrar et al. 2007). Furthermore, *P. acnes* can cause eye lid infections and postoperative as well as device-related (e.g. joint prostheses) infections, especially in immunocompromised patients (Farrar et al. 2007). Acne vulgaris is treated with topical or oral antibiotics, but shows high levels of resistance against the prescribed antibiotics (Marinelli et al. 2012). Alternatively, chemical treatments with substances such as benzyl peroxide are used, which can have strong side effects.

Especially, for the treatment of skin infections in the face and upper body the use of a narrow-spectrum antibiotic would be desirable to reduce the risk of opportunistic infections by fungi or bacteria. An endolysin against acne could not only be used in a pharmaceutical treatment, but also in a cosmetic product against mild acne, which would open up a much larger market. Products for the treatment of acne vulgaris, have a market that generates a revenue of nearly $3 billion annually. Furthermore, the application of an endolysin in a cosmetic product would significantly reduce the regulatory requirements and clinical-trials to bring the product to the market.

1.4 Microalgae as a production platform for recombinant therapeutic proteins

The development of endolysins as antibacterial agents requires a suitable expression platform that can be used for efficient large-scale commercial production, but this platform also needs to fulfil all safety criteria for the production of therapeutic proteins.

Antibiotics are traditionally low-priced and the production of small molecule drugs does not involve high costs. In contrast, the production cost for recombinant proteins is generally considerably higher (Dove 2002). It would be therefore desirable to use a system with low costs for the production of recombinant endolysins in order to compete with small molecule drugs. However, the successful development of an endolysin treatment that offers clear advantages over small molecule antibiotics, for example efficacy against pathogens with multi-drug resistances, advantageous narrow-spectrum properties or effectiveness against bacteria in biofilms, would justify a higher retail price and therefore higher production costs. In addition, a production system that offers itself clear advantages, other than low-cost production, would justify higher costs as well.

In recent decades microalgae have started to get progressively more attention as production platforms for biological products. Primarily, the ability of photosynthetic organisms to utilise sunlight, inorganic nutrients and CO_2 for the production of biological products makes these organisms appealing as the world becomes more and more aware of the problems related to increasing CO_2 emission. Furthermore, the use of sustainable natural resources for production processes has become increasingly desirable.

One of the primary focuses was to use algae for the production of biodiesel, since the production of biodiesel in higher plants reduces the availability of fertile land, which could be used for the production of food. However, despite extensive research endeavours and the successful production of different kinds of biofuels, to-date biodiesel production in microalgae is still not commercially viable in comparison to

petroleum derived fuels (Chisti 2013). However, with inevitably increasing prices for petroleum derived fuels and a successful reduction of the costs for production of biofuels from algae, this is likely to change. Nonetheless, the usage of microalgae for the production of other biological products, mainly high-value products, is starting to get more and more attention.

Microalgae are believed to offer several advantages for the production of recombinant proteins. Some of these advantages are similar to the assets of transgenic plants as protein production platforms (Rasala et al. 2010). This includes simple and inexpensive nutrient requirements, which are believed to result in low costs for cultivation (Dove 2002; Specht et al. 2010; Rasala et al. 2010), and potentially in cost-efficient recombinant protein production (Gimpel et al. 2014). As mentioned above, the ability of photosynthetic organisms to grow using light, inorganic substances and CO_2, results not only in low nutrient requirements, but also has the potential to decrease the overall carbon footprint of recombinant protein production by consuming the CO_2 that is produced during other steps of the production process. Furthermore, both microalgae and plant production systems can be easily and rapidly scaled up (Rasala et al. 2010).

Several microalgae and plants are classified as GRAS organisms (**G**enerally **R**egarded **a**s **S**afe), which means these organisms are safe for human consumption. Furthermore, these microalgae and plants are free of endotoxins and viral or prion contaminants, which is important especially for the production of therapeutic proteins. Endotoxins are present in many bacteria, which makes it necessary to purify therapeutic proteins produced for example in the bacterium *Escherichia coli*. Viral and prion contaminations that can harm humans are often a concern when therapeutic proteins are produced in mammalian cell cultures (Specht et al. 2010). In addition, mammalian cell cultures are the most expensive production platform and are usually only used for complex mammalian proteins that cannot be produced in other systems. However, bacterial expression platforms with GRAS status do exist, such as lactic acid and coryneform bacteria, and the yields of recombinant proteins that can be achieved in these systems have increased in recent years (Ferrer-Miralles & Villaverde 2013;

Jørgensen et al. 2014). Nevertheless, bacterial systems can also have other drawbacks such as the aggregation of recombinant proteins and the formation of inclusion bodies.

In addition, microalgae are believed to offer advantages over transgenic plants. Firstly, microalgae can be easily grown in full containment under sterile conditions in simple photobioreactors (PBRs) (Figure 1.11) (Specht et al. 2010; Rasala et al. 2010), which prevents the release of transgenes to the environment. In contrast, a major concern regarding the open and semi-enclosed cultivation (in green houses) of transgenic plants is the potential flow of transgenes to surrounding plants including food crops (Dove 2002). Furthermore, growth in PBRs reduces the risk of environmental contamination of the production system and therefore the contamination of the therapeutic protein. In contrast, the open and semi-enclosed cultivation of transgenic plants carries a high risk of infections with parasites and pathogens, which can result in the loss of the production crop (Specht et al. 2010). However, it should be mentioned that transgenic plants can be grown in bioreactors in closed containment as well. One option is the cultivation as plant cell suspension cultures, which also greatly reduces the risk of transgene flow to the environment and the contamination of the production platform. However, the disadvantages of this method are slower growth of the cultures and often lower yields of recombinant protein compared to the production in whole plants (Michoux et al. 2011). Another method is the cultivation of leaf tissues in temporary immersion bioreactors, which results in yields of recombinant proteins that are comparable to the production in whole plants (Michoux et al. 2011). However, these systems have not reach the same scale as PBRs for the cultivation of microalgae, especially in comparison to outdoor microalgae PBRs. An advantage of outdoor PBRs is that wasteland (such as deserts or salt land) can be used that is not fertile enough for the cultivation of crop plants.

Moreover, the creation of transgenic plants requires in a lot of cases more time compared to transgenic microalgal strains. It takes between two and four weeks to create a transgenic microalgae, whereas the creation of a transgenic plant line can take months or even years (Specht et al. 2010).

A

B

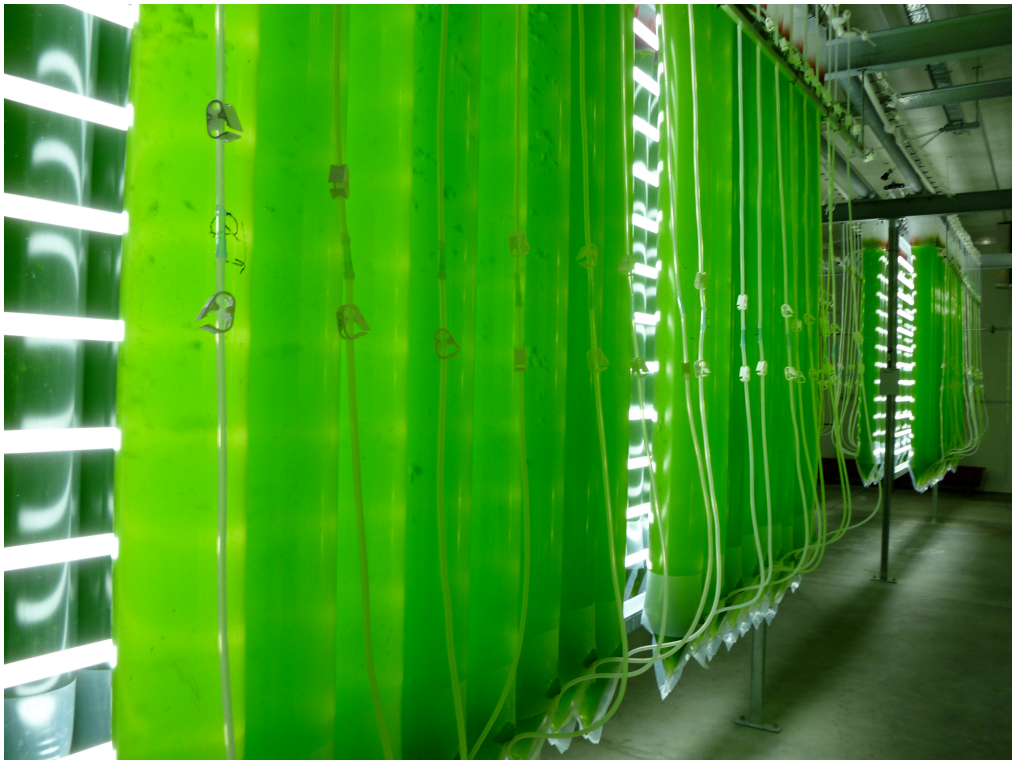

Figure 1.11: Photobioreactor systems that can be used for the contained cultivation of microalgae A shows an outdoor photobioreactor system located in the AlgaePARK in Wageningen, Netherlands. B shows an indoor photobioreactor system that comprises of 40 litre bags. This system is used by Supreme Biotechnologies Ltd, located in Nelson, New Zealand.

1.4.1 The definition of microalgae

Microalgae are a diverse and polyphyletic group of microorganisms that are capable of performing oxygenic photosynthesis. Some definitions of microalgae are restricted to eukaryotic, photosynthetic microorganisms such as green algae (chlorophyta), red algae (rhodophyta), dinoflagellates (dinoflagellata) and diatoms (bacillariophyceae). However, in this study the term "microalgae" refers to eukaryotic as well as prokaryotic, photosynthetic microorganisms and includes cyanobacteria (traditionally called blue-green algae). Microalgae can be found in nearly all habitats from marine and freshwater environments to terrestrial habitats and these organisms contribute considerably to the overall carbon fixation on earth.

In this study the chloroplast of the green microalga *Chlamydomonas reinhardtii*, an organism that has been used as a model organism for over 50 years, and the well-studied cyanobacterium *Synechocystis* sp. PCC 6803 were used to investigate the potential of microalgae as production platforms for therapeutic recombinant endolysins.

1.4.2 *Chlamydomonas reinhardtii* as a protein production platform

C. reinhardtii offers all of the advantages stated above for the production of therapeutic proteins. The microalga is classified as a GRAS organism and can be grown in close containment. Furthermore, it has been shown that its cultivation can be easily scaled up (Gimpel et al. 2014; Chen & Johns 1996). Moreover, *C. reinhardtii* offers already established genetic and genomic tools and has been successfully used for the expression of a variety of recombinant proteins, including many therapeutic proteins (Almaraz-Delgado et al. 2014).

1.4.2.1 The green microalga *Chlamydomonas reinhardtii*

C. reinhardtii is an unicellular, eukaryotic microalga that has a diameter of approximately 10 µm and can be found in freshwater and soil. The alga belongs to the chlorophyta or green algae, a group of micro- and macroalgae that all possess chlorophyll *a* and *b,* and produce starch as a storage compound. These are properties green algae share with higher plants. It is a member of the Chlamydomonadaceae*,* which is a family within the order Volvocales that comprises approximately 30 genera of microalgae with a cell wall and two to four flagella (Harris 2009).

Figure 1.12 shows the structure of the *C. reinhardtii* cell, which carries two anterior flagella and possesses a relatively thick cell wall with several layers made of glycoproteins. However, several viable mutants have been isolated or created that lack an intact cell wall structure. The flagella are responsible for the motility of *C. reinhardtii* and play a role in the mating process. The cell contains multiple mitochondria, but only one cup-shaped chloroplast. The chloroplast occupies approximately two thirds of the cell; estimates range from 40 – 80% of the cell volume. A pyrenoid is located within the chloroplast and is responsible for carbon fixation. Furthermore, the *C. reinhardtii* cell carries an orange eyespot, which is able to sense light and enables the cell to orientate itself in the right position towards a light source via phototaxis (Harris 2009).

C. reinhardtii has been used as a model organism to study a broad range of different fields including flagella function and assembly, photosynthesis, circadian rhythm, phototaxis and chloroplast biogenesis (Rochaix 1995). The nuclear genome of *C. reinhardtii* has a size of 120 Mb (mega base pairs) and was fully sequenced in 2007 (Merchant et al. 2007). The nuclear genome comprises of 17 chromosomes carrying 15,143 genes and has a relatively high guanine and cytosine (GC) content of approximately 64% (Merchant et al. 2007). The mitochondrial genome, which was sequenced already in 1993, has a size of 15.8 kb (Vahrenholz et al. 1993). The chloroplast carries between 80 and 100 copies of its genome, which is called the plastome. The plastome is circular and has a size of 203 kb and contains 99 genes. It was sequenced in 2002 by Maul et al. (2002) and has, in contrast to the nuclear

genome, a low GC content of 34%. The genes on the plastome encode ribosomal and transfer RNAs, an RNA polymerase, as well as ribosomal proteins. Furthermore, the plastome carries genes for core proteins of the photosynthetic apparatus (Maul et al. 2002). The availability of all three *C. reinhardtii* genome sequences has greatly contributed to the advancement of our understanding of the organism, but also to the development and improvement of genetic tools for the genetic manipulation of the microalga.

The replication of *C. reinhardtii* can happen either asexually or sexually. The vegetative cells are haploid, and divide usually by two (or three) rounds of binary fission before the lysis of the mother cell releases the daughter cells (Harris 2009). Vegetative cells are genetically fixed mating types, either mating type plus or mating type minus (mt^+ / mt^-) (Harris 2009). The entry into the sexual cycle is induced by nitrogen starvation or by other environmental stress conditions. The vegetative cells differentiate to gametes before two gametes with different mating types start pairing with their flagella before the cells fuse to a diploid cell, the zygote. The zygote develops into a dormant zygospore that is resistant to adverse environmental conditions. Under favorable conditions the zygote germinates and divides into four haploid daughter cells, which represent vegetative cells (Harris 2009). The daughter cells inherit the chloroplast genome from the mating type plus and the mitochondrial genome from the mating type minus gamete. The inheritance of the nuclear genome follows Mendel's law of inheritance.

A

B

Figure 1.12: Schematic representation of the *Chlamydomonas reinhardtii* cell
A shows the structure of the *C. reinhardtii* cell and was reproduced from Merchant et al. (2007). B shows an electron microscope image of *C. reinhardtii* cells and was reproduced from http://remf.dartmouth.edu/images/algaeSEM/source/1.html.

1.4.2.2 Genetic engineering of *Chlamydomonas reinhardtii*

C. reinhardtii has been used extensively for research into genetic engineering in recent decades, and has resulted in the establishment of robust methods for the transformation of all three genomes of *C. reinhardtii* (Specht et al. 2010). The nuclear genome can be transformed with several DNA delivery methods such as microparticle bombardment (biolistics), agitation in the presence of glass beads (mainly using a cell wall less mutant), electroporation, as well as *Agrobacterium* transfection (Debuchy et al. 1989; Kindle 1990; Brown et al. 1991; Kumar et al. 2004). The chloroplast and mitochondrial genomes have been transformed using biolistics (Boynton et al. 1988; Randolph-Anderson et al. 1993). Furthermore, the chloroplast genome can be transformed by agitating of a cell wall less mutant in the presence of glass beads (2.3.8.2).

The transformation of the nuclear genome has been successfully used for the expression of heterologous genes encoding, for example, the reporter protein GFP (Fuhrmann et al. 1999) and antibiotic resistance selectable markers such as the phleomycin resistance gene (*ble*) and the aminoglycoside 3''-adenyl-transferase gene (*aadA*) (Franklin & Mayfield 2004). The expression from the nuclear genome offers the advantage that proteins can be directed to different compartments of the cell or secreted out of the cell using signal peptides, unlike proteins produced in the chloroplast (Franklin & Mayfield 2004). However, in this study the chloroplast was used for the production of the therapeutic endolysins for reasons discussed in the next section.

The transformation of the chloroplast genome is performed with selectable markers that can be antibiotic resistance genes, such as *aadA* (spectinomycin/streptomycin resistance) or *aphA6* (kanamycin resistance). Furthermore, the restoration of phototrophic growth in a mutant lacking a particular photosynthesis gene or the restoration of an *arg9* mutant to arginine prototrophy can be used for selection (Purton et al. 2013). Chloroplast transformation vectors carry expression cassettes that are flanked by homologous sequences that target the insertion of the transgene to a

specific locus in the plastome (Purton et al. 2013). The transformation of *C. reinhardtii* and the system used in this study are further explained in 2.3.8.1.

Figure removed

Figure 1.13: Recombinant protein expression in different compartments of *C. reinhardtii*
Recombinant proteins (depicted in the figure as blue and red monoclonal antibodies) can be either expressed from the nuclear genome or the plastome. After expression from the nuclear genome the proteins accumulate in the cytoplasm or can be directed using specific signal peptides to the chloroplast, endoplasmic reticulum (ER) or secreted to the periplasm and transported out of the cell. The expression from the plastome results in the accumulation of the proteins in the chloroplast stroma. There are no known mechanisms that transport proteins from the chloroplast to the cytoplasm. The inserted figures show examples of proteins that have been expressed in the different compartments. (a) shows *gfp* expression from the nuclear genome and (b) shows LuxCT accumulation in the chloroplast. Blue areas (plus the neighbouring white areas) indicate the cytoplasm and the green lines indicate the two membranes of the chloroplast surrounding the chloroplast stroma. The mitochondria are indicated by brown ovals. Reproduced from Franklin & Mayfield (2004).

1.4.2.3 The *C. reinhardtii* chloroplast as a protein synthesis factory

There are several advantages of chloroplast expression over nuclear expression in *C. reinhardtii*. One major asset of chloroplast expression is that the levels of recombinant proteins that can be achieved in the organelle to-date are markedly higher compared to their expression from the nuclear genome (Potvin & Zhang 2010). This is most likely the result of silencing mechanisms in the nuclear genome (Specht et al. 2010). Another reason could be the polyploidy of the plastome, which provides a high copy number of the transgene and, therefore, most likely contributes to higher levels of gene expression.

The integration of transgenes into the plastome occurs exclusively via homologous recombination, which allows the insertion site to be easily defined. Furthermore, it ensures that only one copy of the transgene is inserted. In contrast, in the nuclear genome transgenes are inserted into random locations and multiple insertions can occur. A defined insertion site prevents complications related to random insertion such as variable levels of expression or gene silencing through position effects. Furthermore, the plastome does not have any other regulatory mechanisms such as RNA interference, which can affect transgene expression and therefore reduce the production of a recombinant protein (Potvin & Zhang 2010). Moreover, the plastome can be transformed with several genes at the same time by inserting the transgenes in different locations. Alternatively, the plastome has the ability to express multiple genes from polycistrons, in which several genes are expressed using one promoter (Specht et al. 2010). Finally, as mentioned above, in *C. reinhardtii* the chloroplast genome is inherited from the m^+ strain during the sexual cycle, which allows transgene containment by using mt^- type strains for the creation of transgenic lines.

1.4.2.3.1 The chloroplast offers advantages for the production of bacteriophage endolysins

The chloroplasts of green algae and higher plants originated from the endosymbiosis of a cyanobacterium by a heterotrophic, unicellular eukaryote at least 1.2 billion years ago, which is seen as the primary endosymbiotic event (Figure 1.14) (Parker et al. 2008). The chloroplast possesses, therefore, many properties that reflect its prokaryotic origin, such as a eubacterial-type transcription and translation machinery with, for example, 70S ribosomes (Purton et al. 2013). Furthermore, all chloroplast proteases that have been identified to-date are homologues of prokaryotic proteases (Adam et al. 2006). The presence of several genes of chlamydial origin in the genomes of photosynthetic eukaryotes indicates an ancient endosymbiosis of a *Chlamydiae* cell by the ancestor of primary photosynthetic eukaryotes that happened before the primary endosymbiotic event (Becker et al. 2008). This event might have helped to establish the formation of plastids by providing genes that facilitated the communication between the cyanobacterial endosymbiont and the eukaryotic host cell (Huang & Gogarten 2007).

These properties are most likely an advantage for the production of endolysins, which are naturally produced in bacteria and accumulate for a relatively long time inside the cell before their release to the peptidoglycan. It can therefore be assumed that these proteins are adapted to production by the prokaryotic transcription and translation machinery and that endolysins have a relatively high resistance against prokaryotic proteases. The chloroplast provides a prokaryotic environment, but at the same time lacks the target of the endolysins, the peptidoglycan. A study by Oey et al. (2009b) obtained results indicating that high levels of endolysin expression have a negative impact on bacterial expression systems (in this study *Escherichia coli*), which is potentially caused by interactions of the endolysins with the bacterial peptidoglycan, such as unspecific cleavage or binding. An expression system lacking peptidoglycan is therefore likely to present an advantage for the production of endolysins. It has been shown that the *S. pneumoniae*-specific endolysin PlyGBS can accumulate in the tobacco chloroplast to levels as high as 70% of total soluble protein, most likely as a result of low protein degradation (Oey et al. 2009a). Furthermore, the endolysins Pal

and Cpl-1 have been successfully produced in the tobacco chloroplast (Oey et al. 2009b), and Cpl-1 has also been shown to accumulate in the chloroplast of *C. reinhardtii* (Taunt 2013). Another advantage is that post-translational modifications, such as glycosylation, do not occur in the chloroplast, which is a further characteristic that the chloroplast shares with bacterial systems (Specht et al. 2010).

Figure removed

Figure 1.14: Endosymbiosis theory
The chloroplasts of green microalgae and higher plants originated from the endosymbiosis of a cyanobacterium by a heterotrophic, unicellular eukaryote, which is seen as the primary endosymbiotic event. Subsequently, further endosymbiotic events occurred, which resulted in plastids with multiple membranes as found in organisms such as dinoflagellates or apicomplexa. Reproduced from Parker et al. (2008).

1.4.2.3.2 The expression of therapeutic proteins in the *C. reinhardtii* chloroplast

Chloroplast expression in *C. reinhardtii* has been used for the production of a whole range of therapeutic proteins, including antibodies, immunotoxins and (oral) vaccines (Almaraz-Delgado et al. 2014). Table 1.2 shows a selection of therapeutic proteins that have been successfully produced in the *C. reinhardtii* chloroplast.

However, the recombinant protein yields that can be achieved in *C. reinhardtii* chloroplast are still lower compared to established production systems (TSP levels of more than 15% TSP are common in *E. coli*). Several studies have investigated factors that influence accumulation levels of recombinant proteins in the *C. reinhardtii* chloroplast. For example, it has been shown using the reporter protein GFP, that codon optimisation can result in an 80-fold increase in protein yields in the chloroplast (Franklin et al. 2002). Codon optimisation strategies are mainly based on the preferred (most common) codons for one amino acid in an organism, but can also take into account aspects such as preferred codon pairing. The codon usage table for the *C. reinhardtii* chloroplast by Nakamura et al. (2000) is shown and further discussed in chapter 6.

To-date, only endogenous promoter/5´UTR elements have been shown to be effective for transgene expression in the chloroplast. The promoter/5´UTR elements that result in the highest expression levels are from the genes *atpA*, *psaA* and *psbA* (Bateman & Purton 2000; Rasala et al. 2011). However, high expression levels under the *psbA* promoter/5´UTR were only observed in a *psbA* deficient mutant. Though, it was possible to reintroduce the *psbA* gene under the control of a different promoter to restore photosynthesis, which resulted only in a marginal decrease of the expression levels of the transgene (Manuell et al. 2007). It has been shown that an authentic 3'UTR is necessary for mRNA accumulation, since it stabilises the mRNA and plays a role in transcription termination and 3' formation, but all 3'UTRs of endogenous chloroplast genes analysed so far, resulted in similar mRNA and protein levels for transgenes (Barnes et al. 2005).

Table 1.2:Overview of selected therapeutic proteins produced in the *C. reinhardtii* chloroplast
Adapted from Specht et al. (2010) and Almaraz-Delgado et al. (2014), TSP = total soluble protein CTB = cholera toxin B subunit.

Recombinant Protein	Function	Application	Yield	Reference
HSV8-lsc	Human antibody against glycoprotein D from *Herpes simplex* virus	Therapeutic	Not reported	Mayfield et al. (2003)
CTB-VP1	Protein VP1 from foot and mouth disease virus fused to CTB	Vaccine	3 - 4 % TSP	Sun et al. (2003)
hTRAIL	Tumor necrosis factor-related apoptosis-inducing ligand	Therapeutic	0.43% - 0.67 % TSP	Yang et al. (2006)
M-SAA	Bovine mammary-associated serum amyloid	Therapeutic	3 - 5 % TSP	Manuell et al. (2007)
CSFV-E2	Swine fever virus structural protein E2	Vaccine	1.5 - 2 % TSP	He et al. (2007)
hGAD65	Human glutamic acid decarboxylase	Diagnostics and therapeutic	0.25 - 0.3 % TSP	Wang et al. (2008)
VP28	White spot syndrome virus protein 28	Vaccine	0.1 - 10.5 % TSP	Surzycki et al. (2009)
CTB-D2	D2 fibronectin-binding domain of *Staphylococcus aureus* fused to CTB	Oral vaccine	0.7 % TSP	Dreesen et al. (2010)
VEGF 14FN3	Human vascular endothelial growth factor Domian 14 of human fibronectin	Therapeutic	2 - 3 % TSP	Rasala et al. (2010)
Pfs25 and Pfs28	*Plasmodium falciparum* surface proteins	Oral vaccine	0.5%, 0.2% TSP	Gregory et al. (2012)
αCD22PE40	Antibody against DC22 surface protein from B-cells fused to two domains of an exotoxin from Pseudomonas aeruginosa	Immunotoxin	0.3 - 0.4 % TSP	Tran et al. (2013)
CtxB-Pfs25	*Plasmodium falciparum* surface protein 25 fused to CTB	Oral vaccine	0.09%	Gregory et al. (2013)

1.4.3 The potential of other eukaryotic microalgal species for the synthesis of recombinant proteins

The transformation of several other eukaryotic microalgae species has been established in recent years. For example, nuclear transformation was achieved for a range of other green algae such as *Dunaliella salina*, *Chlorella vulgaris, Chlorella sorokiniana, Haematoccus pluvialis* and for diatoms such as *Phaedactylum tricornutum* or *Cyclotella cryptica* (Geng et al. 2003; Chow & Tung 1999; Dawson et al. 1997). Furthermore, chloroplast transformation has been successfully performed for the red alga *Porphyridium sp.* and the euglenoid *Eugelena gracilis* (Lapidot et al. 2002; Doetsch et al. 2001). A comprehensive summary of algae species whose transformation was achieved until 2013, can be found in Vonlanthen (2013). The establishment of a robust transformation method is an important prerequisite for further investigations into the applicability of other microalgae as recombinant protein production platforms.

Different microalgae species to *C. reinhardtii* might offer advantages for the production of certain proteins. Higher growth rates and maximal cell densities, which can be reached for example by *Chlorella sorokiniana*, would result in faster production or in higher protein yields per litre of medium. Marine species offer the advantage that salt water instead of fresh water can be used. However, this is mainly of interest for large scale production of lower value proteins. Furthermore, certain microalgae species produce secondary metabolites providing health benefits such as astaxanthin or carotenoids, which might be of interest for combinations with certain recombinant proteins. The transformation of *H. pluvialis*, for example, was established with the aim of producing vaccines for the use in aquaculture in the microalgae. The aim is to deliver the vaccine together with astaxanthin, which is required in the diet of pink-fleshed fish, using dried *H. pluvialis* cells (Gutiérrez et al. 2012).

1.4.4 The cyanobacterium *Synechocystis* sp. PCC 6803 as a production platform for bacteriophage endolysins

The primary focus of the study was the investigation of the suitability of the *C. reinhardtii* chloroplast as a production platform for bacteriophage endolysins. However, for reasons that are discussed in 6.1 the investigation was expanded to the cyanobacterium *Synechocystis* sp. PCC 6803, which is introduced below and in 6.1.

1.4.4.1 An introduction to *Synechocystis* sp. PCC 6803

Synechocystis sp. PCC 6803 is a Gram-negative, fresh-water cyanobacterium that was originally isolated from a lake in California in 1968 by R. Kunisawa. It possesses coccoid, non-filamentous cells with a size of 1.5 to 2 µm (Ikeuchi & Tabata 2001). *Synechocystis* can grow photoautotrophically as well as mixotrophically or heterotrophically (with five minutes of light activation per day) using glucose or organic acids as additional carbon sources. The cyanobacterium is also able to grow under anaerobic conditions in the presence of carbon sources (Vermaas 1996). The organism is mesophilic and basophilic and achieves optimal growth at temperatures of 30°C to 34°C and at pH values between 8 and 10. The cell division of *Synechocystis* cells occurs by binary fission (Ikeuchi & Tabata 2001). Although cyanobacteria are classified as Gram-negative bacteria, they have a relatively thick peptidoglycan layer. *Synechocystis* cells are surrounded by a four layer cell envelope, which is composed of the cytoplasmic membrane, followed by the peptidoglycan cell wall and the outer membrane. The last layer is mostly formed by a S-layer or other carbohydrate structures (Liberton et al. 2006).

The cyanobacterium is naturally transformable, since it is able to take up exogenous DNA (Vermaas 1998). *Synechocystis* carries a genome that is comprised of one circular chromosome and seven additional plasmids. The main chromosome has a size of 3.5 Mb, whereas the sizes of the plasmids vary between 2.3 and 120 kb (Kaneko et

al. 1996). Multiple copies (approximately ten) of the genome are present in each *Synechocystis* cell (Vermaas 1998). The genome of *Synechocystis* has been fully sequenced and has a GC content of 47.7% (Kaneko et al. 1996). Furthermore, the genome is well annotated and gene functions have been extensively studied. The annotated genome and information about gene functions and mutants are available in the databases CyanoBase and CyanoMutants[1].

Many tools for the genetic manipulation of *Synechocystis* have been established in the last few decades, including several different promoter systems, selectable markers and transformation vectors. The majority of promoters and expression elements that are used in *Synechocystis* are derived from strongly expressed endogenous genes encoding for proteins involved in photosynthesis and carbon fixation such as *psbAII, psaA, psaD* and *rbcL* (Peca et al. 2008; Dexter & Fu 2009). Nevertheless, a few foreign promoters have been shown to result in efficient expression as well, such as the inducible *E. coli* promoters *trc10*, *trc20* and *A1lacO-1* (Huang et al. 2010). The expression elements used in this study are described in 6.2.1.

For the selection of *Synechocystis* transformants, antibiotic resistance genes are mainly used as selectable markers. Commonly used antibiotic resistance marker genes are *nptI and nptII* encoding for neomycin phosphotransferases conferring resistance against neomycin and kanamycin and the *aadA* gene, which confers resistances against streptomycin and spectinomycin (Koksharova & Wolk 2002; Vermaas 1998).

[1] CyanoBase: http://genome.microbedb.jp/cyanobase/
CyanoMutants: http://www.kazusa.or.jp/cyano/mutants/

1.5 Summary, aims and objectives

There is a pressing need for the development of new and improved classes of antibiotics to combat infections with multidrug resistant pathogens, and to minimise the spread of antibiotic resistance in the bacterial population. Furthermore, the development of narrow-spectrum antibiotics that do not harm the commensal microbial flora, and antibiotics that can target bacteria in biofilms is desirable. Bacteriophage endolysins are proposed as promising candidates for a novel class of antibiotics that potentially offer solutions for these problems. *S. pneumoniae*, *S. aureus* and *P. acnes* are examples of suitable target bacteria for a potential endolysin antibiotic treatment.
Microalgae have emerged as novel production platforms for therapeutic proteins in the last few years. These organisms offer several advantages such as simple nutrient and cultivation requirements and growth in closed containment. Furthermore, several species have GRAS status and are free of endotoxins and viral or prion contaminants, which is especially desired for the production of therapeutic proteins.

The aim of the research presented in this thesis was, therefore, to investigate the suitability of microalgae as production platforms for recombinant bacteriophage endolysins. With this aim, the following studies were performed:

- Production of endolyins targeting the human pathogens *S. pneumoniae* and *S. aureus* in the chloroplast of *Chlamydomonas reinhardtii,* followed by an analysis of the stability and production yields of the proteins in the chloroplast

- Demonstration of the antibacterial activity of the endolysins against the target bacteria and the development of purification strategies for the endolysins produced in *C. reinhardtii*

- Production of endolysins, whose production in the *C. reinhardtii* chloroplast has been proven to be difficult, in the cyanobacterium *Synechocystis* sp. PCC 6803, followed by a demonstration of the antibacterial activity

CHAPTER 2

Materials & methods

2 Materials and methods

2.1 Microalgal and bacterial strains

2.1.1 *Chlamydomonas reinhardtii* strains

Table 2.1: *Chlamydomonas reinhardtii* strains used or created in this study

Strain	Genotype/phenotype	Reference
TN72	mt^+, CW15.3A (cell-wall deficient), *psbH* partly deleted by *aadA* cassette, PSII-deficient mutant, spectinomycin resistant	Ninlayarn (2012)
TN72_control	TN72 transformed with the empty pASapI vector, carrying *atpA* promoter, *psbH* rescued	Ninlayarn (2012)
TN72_*pal-HA*	TN72 carrying *pal* with HA-tag sequence under *atpA* promoter, *psbH* rescued	This study
TN72_*ϕ11-HA*	TN72 carrying *ϕ11* with HA-tag sequence under *atpA* promoter, *psbH* rescued	This study
TN72_*pal-HA-His*	TN72 carrying *pal* with HA- and His-tag sequence under *atpA* promoter, *psbH* rescued	This study, by N. Hiegle
TN72_*ϕ11-HA-His*	TN72 carrying *ϕ11* with HA- and His-tag sequence under *atpA* promoter, *psbH* rescued	This study, by N. Hiegle
TN72_SR_control	TN72 transformed with the empty pSRSapI vector, carrying *psaA* exon 1 promoter, *psbH* rescued	R. Young, unpublished
TN72_SR_*pal-HA*	TN72 carrying *pal* with HA-tag sequence under *psaA* exon 1 promoter, *psbH* rescued	This study
TN72_SR_*pal-x*	TN72 carrying *pal* without a sequence for a tag under *psaA* exon 1 promoter, *psbH* rescued	This study
TN72_SR_*cpl-1-HA*	TN72 carrying *cpl-1* with HA-tag sequence under *psaA* exon 1 promoter, *psbH* rescued	Taunt (2013)

2.1.2 Bacterial strains

2.1.2.1 *Synechocystis* sp. PCC 6803 strains

Table 2.2: *Synechocystis* sp. PCC 6803 strains used or created in this study

Strain	Genotype/phenotype	Reference
Synechocystis sp. PCC 6803	Wild type, large, glucose-tolerant	Williams (1988)
Syn6803_*nrsB_pal-HA*	Carrying *pal* with HA-tag sequence under *nrsBRS* promoter system, kanamycin resistant	This study
Syn6803_*nrsB_ϕ11-HA*	Carrying *ϕ11* with HA-tag sequence under *psbAII* promoter, kanamycin resistant	This study
Syn6803_*AII_ϕ11-HA*	Carrying *ϕ11* with HA-tag sequence under *nrsBRS* promoter system, kanamycin resistant	This study
Syn6803_*nrsB_gp20*$_1$	Carrying *gp20*$_1$ with HA-tag sequence under *nrsBRS* promoter system, kanamycin resistant	This study
Syn6803_*AII_gp20*$_1$*-HA*	Carrying *gp20*$_1$ with HA-tag sequence under *psbAII* promoter, kanamycin resistant	This study
Syn6803_*nrsB_gp20*$_2$*-HA*	Carrying *gp20*$_2$ with HA-tag sequence under *nrsBRS* promoter system, kanamycin resistant	This study

2.1.3 *Escherichia coli* strains

Table 2.3: *E. coli* strains used for cloning or the expression of endolysin genes

Strain	Genotype/phenotype	Reference
DH5α	*fhu*A2 Δ(*argF-lacZ*)U169 *pho*A *gln*V44 Φ80 Δ(*lacZ*)M15 *gyr*A96 *recA*1 *relA*1 *endA*1 *thi*-1 *hsdR*17	Hanahan (1983)
DH5α_*pal-HA*	Carrying pASApI containing *pal* with HA-tag sequence under *atpA* promoter	This study
DH5α_*ϕ11-HA*	Carrying pASApI containing *pal* with HA-tag sequence under *atpA* promoter	This study
DH5α_control	Carrying pASApI without gene of interest under *atpA* promoter	This study

2.1.3.1 Target bacteria

Table 2.4: Target bacteria used for antibacterial activity studies

Species and strain	Genotype/phenotype	Reference
Streptococcus pneumoniae		
16 NP3	Serotype 19F, reference strain, penicillin resistant	Royal Free Hospital
H08212 0259	Serotype 6A, clinical isolate	Royal Free Hospital
H08052 0052	Serotype 6B, clinical isolate	Royal Free Hospital
H05252 0075	Serotype 6B, clinical isolate	Royal Free Hospital
H08432 0293	Serotype 27, clinical isolate	Royal Free Hospital
35 NP1	Serotype 6B, clinical isolate, intermediate resistance against penicillin (Minimal inhibitory concentration (MIC): 0.125 µg/ml) and co-trimoxazole (MIC: 6 µg/ml)	Royal Free Hospital
Streptococcus pyogenes		
ATCC 19615	*Streptococcus* group A	Royal Free Hospital
Staphylococcus aureus		
ATCC 28213	Reference strain	Royal Free Hospital
ATCC 43300	Clinical isolate, methicillin resistant strain (MRSA), resistant to methicillin, resistant to oxacillin	Royal Free Hospital
ATCC 25923	Clinical isolate, methicillin sensitive strain (MSSA)	Royal Free Hospital
Propionibacterium acnes		
ATCC 6919	DSM number: 1897, type strain, other collection numbers: NCTC 737	DSMZ - German Collection of Microorganisms and Cell Cultures
Agrobacterium tumefaciens		Obtained from T. Barbi

2.2 Plasmids

Table 2.5: Plasmids used in this study

Plasmid	Characterisation	Reference
pASapI	Carries an expression cassette with *atpA* promoter/5'UTR and *rbcL* 3'UTR, the *C. reinhardtii psbH* gene as selectable marker together with regions upstream and downstream of *psbH* for homologous recombination	Ninlayarn (2012)
pASapI_control	pASapI carrying an empty expression cassette	Ninlayarn (2012)
pASapI_*pal-HA*	pASapI carrying *pal* with HA-tag sequence	This study
pASapI_*ϕ11-HA*	pASapI carrying *ϕ11* with HA-tag sequence	This study
pASapI_*pal-HA-His*	pASapI carrying *pal* with HA- and His-tag sequence in expression cassette	This study, by N. Hiegle
pASapI_*ϕ11-HA-His*	pASapI carrying *ϕ11* with HA- and His-tag sequence in expression cassette	This study, by N. Hiegle
pSRSapI	Carries an expression cassette with *psaA exon1* promoter/5'UTR and *rbcL* 3'UTR, the *C. reinhardtii psbH* gene as selectable marker together with regions upstream and downstream of *psbH* for homologous recombination	Young & Purton (2014)
pSRSapI_control	pSRSapI carrying an empty expression cassette	Young & Purton (2014)
pSRSapI_*pal-HA*	pSRSapI carrying *pal* with HA-tag sequence under *psaA* exon 1 promoter, *psbH* rescued	This study
pSRSapI_ *pal-x*	pSRSapI carrying *pal* without a sequence for a tag under *psaA* exon 1 promoter, *psbH* rescued	This study
pSRSapI_*cpl-1-HA*	pSRSapI carrying *cpl-1* with HA-tag sequence under *psaA* exon 1 promoter, *psbH* rescued	Taunt (2013)
pLAH.*AII*	Carries an expression cassette with the *Synechocystis* sp. PCC 6803 *psbAII* promoter/5'UTR, upstream and downstream regions of *psbAII* for homologous recombination and Tn903 kanamycin resistance cassette for selection	Al'Haj (2014)
pLAH.nrsB	Carries an expression cassette with *Synechocystis* sp. PCC 6803 *nrsB* promoter/5'UTR and *nrsRS* regulatory elements, upstream and downstream regions of *psbAII* for homologous recombination and Tn903 kanamycin resistance cassette for selection	Al'Haj (2014)
pLAH.AII_*ϕ11-HA*	pLAH.AII carrying *ϕ11* with HA-tag sequence	This study

Plasmid	Characterisation	Reference
pLAH.AII_*gp20$_1$-HA*	pLAH.AII carrying *gp20$_1$* with HA-tag sequence	This study
pLAH.nrsB_*pal-HA*	pLAH.nrsB carrying *pal* with HA-tag sequence	This study
pLAH.nrsB_*ϕ11-HA*	pLAH.nrsB carrying *ϕ11* with HA-tag sequence	This study
pLAH.nrsB_*gp20$_1$-HA*	pLAH.nrsB carrying *gp20$_1$* with HA-tag sequence	This study
pLAH.nrsB_*gp20$_2$-HA*	pLAH.nrsB carrying *gp20$_2$* with HA-tag sequence	This study

2.3 Media and culture conditions

2.3.1 Media for the cultivation of *C. reinhardtii*

2.3.1.1 Gorman-Levine Tris-acetate phosphate (TAP) medium (Harris 1989, modified)

NH_4Cl	0.4	g/L
$MgSO_4 \bullet 7H_2O$	0.1	g/L
$CaCl_2 \bullet 2H_2O$	0.05	g/L
K_2HPO_4	0.108	g/L
KH_2PO_4	0.056	g/L
Tris	2.42	g/L
Glacial acetic acid	1	ml/L
Trace element stock solution	1	ml/L

The pH was adjusted to 7.0. Solid medium was prepared by the addition of 2% (w/v) Bacto agar.

2.3.1.2 Sueoka high-salt (HSM) medium (Harris 1989, modified)

NH_4Cl	0.4	g/L
$MgSO_4 \bullet 7H_2O$	0.1	g/L
$CaCl_2 \bullet 2H_2O$	0.05	g/L
K_2HPO_4	0.717	g/L
KH_2PO_4	0.363	g/L
Trace element stock solution	1	ml/L

The pH was adjusted to 6.9. Solid medium was prepared by the addition of 2% (w/v) Bacto agar.

2.3.2 Trace element stock solution

H_3BO_4	11.4	g/L
$ZnSO_4 \bullet 7H_2O$	22	g/L
$MnCl_2 \bullet 4H_2O$	5.06	g/L
$FeSO_4 \bullet 7H_2O$	4.99	g/L
$CoCl_2 \bullet 6H_2O$	1.61	g/L
$CuSO_4 \bullet 4H_2O$	1.57	g/L
$(NH_4)_6Mo_7O_{24} \bullet 4H_2O$	1.1	g/L

The trace elements were dissolved in 550ml ddH_2O in the order indicated above, then heated to 100°C. Subsequently, 50 g EDTA•Na_2 was dissolved in 250 ml H_2O by heating and added to the above solution. The mixture was reheated to 100°C, cooled to 80 - 90°C and adjusted to pH 6.5 - 6.8 with 20% KOH and adjusted to one litre. The stock was incubated at room temperature for two weeks and allowed to form a rust coloured precipitate and filtered through three layers Whatman No. 1 paper under suction until the solution was clear.

2.3.3 Media for the cultivation of *Synechocystis* sp. PCC 6803

2.3.3.1 BG11 (Blue Green Medium) (Castenholz 1988)

Ingredients for 1 L of 1x BG11

100x BG11	10	ml
Trace elements	1	ml
Iron stock	1	ml
Autoclave and allow to cool then add		
Phosphate stock	1	ml
Na_2CO_3 stock	1	ml
$NaHCO_3$ stock	10	ml
TES buffer (pH 8.2)	10	ml

Table 2.6: Stock solutions for BG11 medium

100x BG11	**g/L**
$NaNO_3$	149.6
$MgSO_4 \cdot 7H_2O$	7.49
$CaCl_2$	3.60
Citric acid	0.60
Na_2EDTA	1.12 ml 0.25M solution, pH 8.0
Trace elements	**g/100ml**
H_3BO_3	0.286
$MnCl_2 \cdot 4H_2O$	0.181
$ZnSO_4 \cdot 7H_2O$	0.022
$Na_2MoO_4 \cdot 2H_2O$	0.039
$CuSO_4 \cdot 5H_2O$	0.008
Iron stock	**g/100ml**
Ferric citrate	0.6
Or ferric ammonium citrate	1.11
Stock solutions	**g/100ml**
K_2HPO_4	3.05
Na_2CO_3	2.0
$NaHCO_3$	8.401
TES buffer (NaOH to pH 8.2)	22.9

Solid media BG11 medium was prepared by mixing 2x concentrated BG11 including 3 g of sodium thiosulphate with an equal volume of Difco Bacto-agar (3% w/v in distilled water) after both solutions had been autoclaved separately to reach a final concentration of 1x BG11 and 1.5% agar.

2.3.4 Medium for the cultivation of *Escherichia coli*

2.3.4.1 Lysogenic broth (LB) medium (Bertani 1951)

Bacto-tryptone	10.0	g/L
Yeast extract	5.0	g/L
Sodium chloride	10.0	g/L

Solid medium was prepared by the addition of 1.5% agar.

2.3.5 Media for the cultivation of the target bacteria

2.3.5.1 Trypticase soy yeast extract medium (DSMZ medium 92)

Trypticase soy broth	30.0	g/L
Yeast extract	3.0	g/L

The pH was adjusted to 7.0 – 7.2. Solid medium was prepared by the addition of 1.5% agar.

2.3.5.2 Skimmed milk tryptone glycerol glucose (STGG) medium (O'Brien et al. 2001)

Skimmed milk powder	20	g/L
Tryptone soy broth	30	g/L
Glucose	5	g/L
Glycerol	100	ml/L

2.3.5.3 Brain heart infusion medium

Brain heart infusion (SIGMA)	17.5	g/L
NaCl	5	g/L
Na_2HPO_4	2.5	g/L
Glucose	2	g/L
Peptone	10	g/L

Solid medium was prepared by the addition of 1.5% agar prior autoclaving.

2.3.6 Antibiotics

Antibiotic	**Stock solution**	**Final concentration**
Ampicillin	100 mg/ml in H_2O	100 µg/ml
Kanamycin	100 mg/ml in H_2O	50 µg/ml
Spectinomycin	100 mg/ml in H_2O	50 µg/ml
Chloramphenicol	100 mg/ml in EtOH	500 µg/ml

2.3.7 Culture conditions

2.3.7.1 *Chlamydomonas reinhardtii*

The *C. reinhardtii* strains used in this work are listed in Table 2.1. The strains were maintained on Gorman-Levine Tris-acetate phosphate (TAP) agar plates. For culture growth the plates were incubated at 20ºC and at a light intensity of 48 - 50 µmol/m^2/s using Gro-lux or Luxline plus fluorescent tubes (Osram Sylvania). Subsequently, the plates were stored under dim light (5 - 10 µmol/m^2/s) at 20ºC. The *C. reinhardtii* strains were transferred to fresh plates every six to eight weeks (Harris 1989).

Small liquid cultures (up to 50 ml) and pre-cultures were inoculated with a loop full of cells from plates, which had been freshly restreaked a few days before. The cultures

were grown in Erlenmeyer flasks (liquid medium to air ratio 1:5 or 1:4) in an illuminated incubator with a light intensity of 100 – 200 µmol/m^2/s, at 120 rpm shaking and at a temperature of 25ºC. Larger cultures (100 – 1,000 ml) were inoculated from liquid mid-log phase pre-cultures with a 1% inoculum and grown under the same conditions. In larger scale *C. reinhardtii* was grown in the photo bioreactor system of Supreme Biotech Ltd. in 30 - 40 litre bags under constant bubbling with air at 25ºC.

2.3.7.2 *Synechocystis* sp. PCC 6803

The *Synechocystis* sp. PCC 6803 strains are listed in Table 2.1. The strains were maintained on BG11 agar plates. Cultures on solid medium were grown in an illuminated incubator with a light intensity of 30 - 50 µmol/m^2/s at 30ºC and subsequently stored under dim light (5 - 10 µmol/m^2/s) at 20ºC. The *Synechocystis* strains were transferred to fresh plates every three to four weeks.
Liquid BG11 cultures were grown in Erlenmeyer flasks (liquid medium to air ratio 1:5 or 1:4) in an illuminated incubator with a light intensity of 100 – 200 µmol/m^2/s, at 120 rpm shaking and at a temperature of 25ºC. Small flasks and pre-cultures were inoculated with a loop full of cells from agar plates, whereas larger cultures of more than 50 ml were inoculated from a pre-culture with a 1% inoculum.

2.3.7.3 *Escherichia coli*

E. coli cultures were grown on LB agar plates or in LB liquid medium under constant shaking at 37ºC. If necessary the appropriate antibiotics were added in the concentrations stated in 2.3.6. For long-term storage, *E. coli* strains were stored as 25% (v/v) glycerol stocks. This was achieved by mixing equal volumes of grown bacterial cultures with 50% (v/v) sterile glycerol. The aliquots were snap frozen in liquid nitrogen and stored at -80°C.

2.3.7.4 *Streptococcus pneumoniae* and *Streptococcus pyogenes*

S. pneumoniae and *S. pyogenes* were grown on Columbia blood agar plates (SIGMA) overnight at 35 ºC under anaerobic or aerobic conditions, respectively. Alternatively, liquid cultures were grown in trypticase soy broth overnight at 35ºC without shaking. Anaerobic conditions were generated using Oxoid AGS CO_2Gen Compact gas packs and an anaerobic jar from Oxoid. For long-term storage of *S. pneumoniae,* cells were grown in STGG medium, snap frozen in liquid nitrogen and stored at -80°C (O'Brien et al. 2001). For long-term storage of *S. pyogenes,* glycerol stocks were prepared as described in 2.3.7.3.

2.3.7.5 *Staphylococcus aureus*

S. aureus was grown on Columbia blood agar plates overnight at 35 ºC. Liquid cultures were grown in ISO-Sensitest broth from Oxoid overnight at 35ºC with or without shaking. For long-term storage of *S. aureus,* glycerol stocks were prepared as described in 2.3.7.3.

2.3.7.6 *Propionibacterium acnes*

P. acnes was grown in liquid brain heart infusion medium at 30°C for five to seven days under anaerobic conditions. Alternatively, *P. acnes* was cultured on Columbia blood agar plates or brain heart infusion medium agar plates at 30 ºC under anaerobic conditions. For long-term storage of *P. acnes,* glycerol stocks were prepared as described in 2.3.7.3.

2.3.8 Growth measurements

2.3.8.1 *Chlamydomonas reinhardtii* and *Synechocystis* sp. PCC 6803

Growth of *C. reinhardtii* and *Synechocystis* was measured by recording the optical density at 750 nm with a Unicam UV/Vis Spectrometer (Thermo Electron Corporation, USA). Samples with an OD_{750nm} over 0.8 were diluted with the adequate medium. Alternatively, growth of *C. reinhardtii* was determined by counting cells with a haemocytometer. Therefore 10 µl of iodine tincture (19.7 mM iodine in 95 % (v/v) ethanol) was added to 1 ml of cell culture before the measurement to inhibit cell motility.

Furthermore the biomass of *C. reinhardtii* was analysed at several growth stages. Therefore 50 ml samples were taken and the cells were harvested by centrifugation at 5,000 x *g*. Subsequently, the cell pellet was washed one time with distilled H_2O. The cells were transferred to pre-weighed Eppendorf tubes and freeze-dried until the weight was constant. The dry weight in g/L of culture volume was calculated.

2.3.8.2 Heterotrophic bacteria

The growth of bacterial cultures was measured by recording the optical density at 600 nm with a Unicam UV/Vis Spectrometer (Thermo Electron Corporation, USA). Samples with an OD_{600nm} over 1.0 were diluted with the adequate medium.

2.4 Molecular genetic methods

2.4.1 Polymerase chain reaction (PCR)

In vitro gene amplification was carried out by the polymerase chain reaction (Mullis et al. 1992) using the Phusion polymerase (Fermentas or Thermo Scientific). The components and protocol of a 50 µl PCR reaction are listed in Table 2.7.

Table 2.7: Components and protocol used for PCR reactions

Components		**Concentration**		
HF buffer		1	x	
Template DNA		50 - 100	ng	
Primers		10	pmol each	
dNTPs		1	mM (250 µM each)	
Phusion polymerase		0.6	U	
ddH_2O		Add to a final volume of 50 µl		
Step		**Temperature**		**Time**
Initial denaturation		98ºC		2 min
	Denaturation	98ºC		10 sec
25 – 30 x	Annealing	T_m + 3ºC of the lower primer T_m		30 sec
	Elongation	72ºC		≈ 1 min/kb
Final elongation		72ºC		10 min

2.4.1.1 Oligonucleotide primers

The primers used for polymerase chain reactions in this study are shown in Table 2.8. All primers were synthesised by Eurofins MWG (Ebersberg, Germany).

Table 2.8: Oligonucleotide primers used in this study

Primer name	Sequence (5' to 3')	Function
FLANK1	GTCATTGCGAAAATACTG	PCR screening for successful transformation of *C. reinhardtii* with the vectors pASapI (A) or pSRSapI (B)
rbcL.Fn	CGGATGTAACTCAATCGGTAG	
rbcL.R	CAAACTTCACATGCAGCA	
atpA.R (A)	ACGTCCACAGGCGTCGT	
RYpsa.R (B)	GGATTTCTCCTTATAATAAC	
rbcL.R	CAAACTTCACATGCAGCA	Sequencing of pASapI (A) and pSRSapI (B) inserts
atpA.F (A)	CAAGTGATCTTACCACTCAC	
psa.F (B)	GTTCACGCGTAAGCTTTCTTAATTCAACATTT	
Pal.F	ATCTGCTCTTCTATGGGTGTTGATATTG	Attachment of a His-tag to *pal* and *ϕ11*
ϕ11.F	ACGTGCTCTTCTATGCAAGCTAAATTAAC	
Histag.R	TGTTGCATGCTTATTAATGATGATGATGATGAT GAGCGTAATCTGGAAC	
HAremoval.R	ATGCATGCTTAAACTTTAGATGTAATTAAACC ATCAGGTTC	Removal of the HA-tag together with Pal.Fw
psbAII.F (A)	CCCAGAACTATGGTAAAGGCG	PCR screening and sequencing for the insertion of the GOI into pLAH.AII (A) and pLAH.nrsB (B)
psbAII.R	GGTCTGCCTCGTGAAGAAGGTGTT	
nrsBseq.F (B)	CCGTCTCATCTTCCACCAGC	
Syn6803ϕ11.F	AGCGATTAATGCAAGCTAAATTAACAAAAAAC GAATTTATTG	Insertion of *ϕ11* into the vectors pLAH.AII and pLAH.nrsB
Syn6803ϕ11.R	TGATGGATCCTTATTAAGCGTAGTCTGGAACA TCG	
Syn6803pal.F	ATGCCATATGGGTGTTGATATTGAAAAAGGTG	Insertion of *pal* into the vectors pLAH.AII and pLAH.nrsB
Syn6803pal.R	TGATGGATCCTTATTAAGCGTAATCTGGAACA TCG	
Syn6803gp20.F	GCATATTAATGGTTCGTTATATTCCAGCTGC	Insertion of *gp20* into the vectors pLAH.AII and pLAH.nrsB
Syn6803gp20$_1$.R	GCATGGATCCTTATTAAGCATAGTCAGGTACA TCATA	
Syn6803gp20$_2$.R	GCATGGATCCTTATTAAGCGTAATCTGGAACA TCG	

2.4.2 Agarose gel electrophoresis

DNA fragments were separated on 1% (w/v) agarose gels made with 1x TAE buffer (40 mM Tris, 1 mM sodium EDTA, 17.5 mM glacial acetic) and 1 µg/ml ethidium bromide. The samples were mixed with 6x DNA Loading Dye (Fermentas) before loading onto the gel that had been submerged in 1x TAE buffer in an electrophoresis tank. The electrophoresis was performed at 85 V for 30 to 120 min. Subsequently, the DNA fragments were visualized using a UV transilluminator (UVP Gel Documentation System). The O'GeneRuler™ 1 kb Plus DNA Ladder (Fermentas) was used to estimate the size of the DNA fragments.

2.4.3 Plasmid isolation

Plasmid isolation was performed with the GENEJet Plasmid Miniprep Kit from Fermentas or the QIAprep Spin Midiprep Kit from Qiagen according to the manufacturer's instructions for lower quantities of a plasmid (up to 20 µg). For the isolation of larger quantities (up to 200 µg) of plasmids the commercial QIAfilter Plasmid Midi Kit (Qiagen) was used according to the manufacturer's instructions.

2.4.4 DNA purification and gel extraction

PCR products were purified using the QIAquick PCR purification Kit from Qiagen (Hilden, Germany) and Gel extraction of DNA bands was performed using the QIAquick Gel Extraction Kit from Qiagen.

2.4.5 Restriction enzyme digests, dephosphorylation and ligations

Restriction enzyme digests were performed using restriction endonuclease enzymes according to the manufacturer's instructions from New England Biolabs (NEB) and Fermentas (Thermo Scientific), respectively. Ligations were performed using T4 DNA ligase from NEB with 3 to 5 times more insert than vector according to the

manufacturer's instructions. To avoid relegation of digested vectors in some cases the 5' phosphate was removed after the digest using Antarctic phosphatase (NEB) according to the manufacturer's instructions.

2.4.6 DNA sequencing

DNA sequencing of plasmids and PCR products was performed using the Scientific Support Services of The Wolfson Institute for Biomedical Research, University College London. The sequencing results were aligned and analysed using MacVector 12.6.0.

2.4.7 Preparing competent *E. coli* cells

LB medium (10 ml) was inoculated with a single *E. coli* colony from an overnight culture on solid LB medium and grown under constant shaking at 37ºC overnight. Fresh LB medium (100 ml) was inoculated with 1% of the overnight culture and grown for 2.5 h under constant shaking at 37ºC to an OD_{600nm} of 0.3 to 0.6. The cells were pelleted in precooled tubes by centrifugation at 3,000 x *g* for 5 minutes. Subsequently, each cell pellet derived from 25 ml culture was resuspended in 10 ml of 50 mM $CaCl_2$ and incubated for 30 minutes on ice. Cell were pelleted by centrifugation as described above and resuspended in 1.5 ml of fresh 50 mM $CaCl_2$. Sterile glycerol was added to a final concentration of 15% before the competent cells were aliquoted and frozen at -80ºC.

2.4.8 Transformation of competent *E. coli* cells by heat-shock

An aliquot with 100 µl of competent *E. coli* cells were thawed and 1 µl of a plasmid preparation or 20 µl of a ligation product was added to the cells. The mixture was incubated for 30 minutes on ice before exposure to 42ºC for one minute. The transformed cells were added to 1 ml of LB medium and incubated at 37ºC for 1 h under continuous shaking. After incubation different volumes were platted on LB plates containing the appropriate antibiotic.

2.4.9 Transformation of the *C. reinhardtii* chloroplast

2.4.9.1 The transformation system

The vectors pASapI (Economou et al. 2014) and pSRSapI (Young & Purton 2014) carry the photosystem II gene *psbH*, whereas in the recipient strain TN72 of the chloroplast transformation *psbH* is partly replaced by an *aadA* cassette (Figure 2.1). Since *psbH* is essential for phototrophic growth, only cells of the recipient strain that restore *psbH* through homologous recombination with the DNA on the vector are able to grow phototrophically. Successful transformants can be therefore selected for restoration of phototrophic growth on minimal medium.

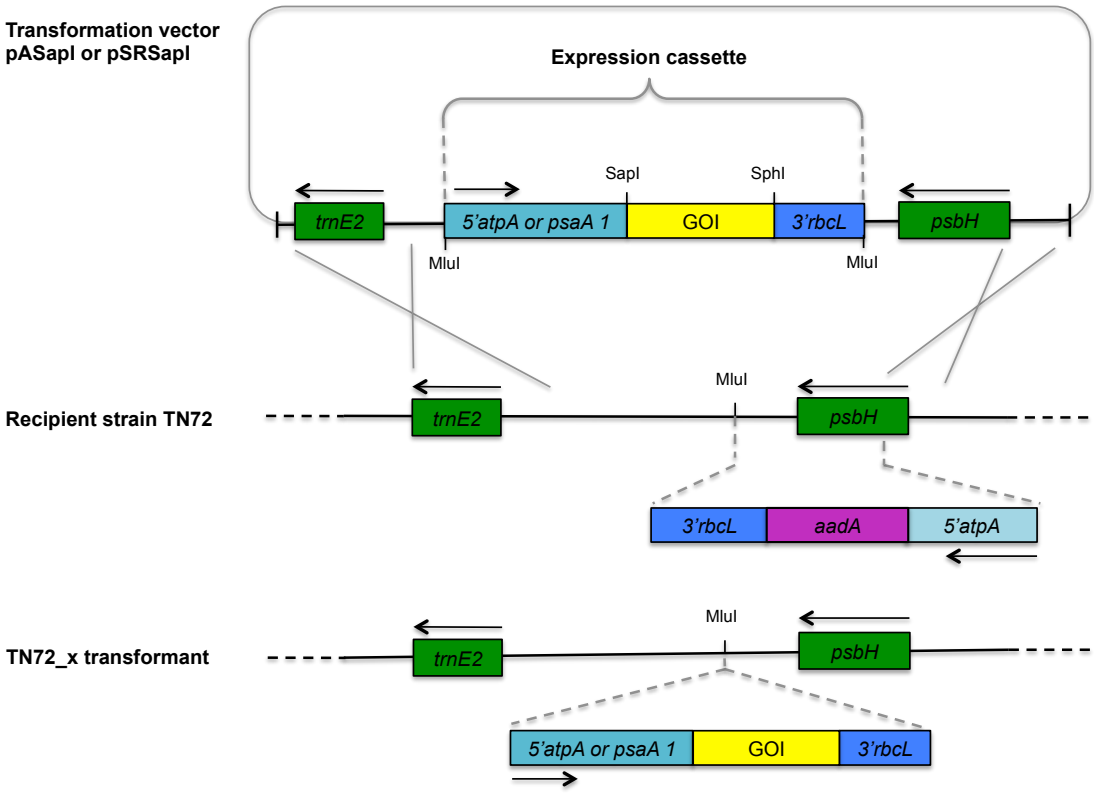

Figure 2.1: Chloroplast transformation system with the vectors pASapI and pSRSapI and the recipient strains TN72.
Homologous recombination (grey crosses) between chloroplast sequences (thick black lines) on the vectors and the plastome of the recipient strain (TN72) allows the restoration of *psbH*, which is necessary for phototrophic growth, combined with the introduction of the expression cassette including the gene of interest (GOI). Endogenous chloroplast genes are indicated in green, promoter/5'untranslated regions in blue and the GOI in yellow

The insertion site (SapI – SphI) for the gene of interest (GOI) on pASapI and pSRSapI is located directly downstream of *psbH* and therefore restoration of *psbH* by homologous recombination results also in the transfer of the GOI into a neutral region downstream of *psbH*. Furthermore, the insertion site is flanked by an expression cassette consisting of the promoter/5'untranslated region (UTR) of the endogenous chloroplast gene *atpA* in pASapI and *psaA* exon 1 in pSRSapI. Both vectors carry the 3'UTR of the chloroplast *rbcL* gene for the expression of the GOI (Figure 2.1).

2.4.9.2 Transformation of the *C. reinhardtii* chloroplast by agitation in the presence of glass beads

A liquid culture of the *C. reinhardtii* recipient strain TN72 was grown to mid-log phase (1 – 2 x 10^6 cells/ml) in TAP medium under continuous illumination. Cells were pelleted by centrifugation at 8,000 *x g* for eight minutes and the pellet was resuspended in fresh TAP medium to a concentration of 2 x 10^8 cells/ml. Sterile test tubes containing about 0.3 g of 0.4 mm diameter glass beads were filled with 300 µl of the previously prepared cell suspension and 2 – 20 µg of plasmid DNA. The test tubes were vortexed for 15 sec each using a Vortex genie-2 (Scientific industries). Top agar (TAP or HSM + 0.5% agar) was melted and cooled down to 42ºC before 3.5 ml of the agar were added to the test tubes. Cell suspension and top agar were mixed and instantly platted onto HSM plates. The plates were left for 1 h in the dark and 12 h in dim light before they were placed in bright light. Transformant colonies appeared 2 – 4 weeks later.

2.4.9.3 Isolation of DNA from *C. reinhardtii*

To confirm that the gene of interest had been correctly inserted into the *C. reinhardtii* plastome or to sequence the transgenic lines, DNA was extracted by resuspending a loop full of cells from an agar plate in 20 µl of sterile ddH_2O, followed by the addition of 20 µl ethanol (100%) and 200 µl of chelex (5%, w/v). The mixture was incubated at 98ºC for 10 minutes and centrifuged at 21,000 x *g* for 10 minutes at room temperature. Subsequently, 2 µl of the supernatants were used in 50 µl PCR reactions.

2.4.10 Transformation of *Synechocystis* sp. PCC 6803

The transformation method used was adapted from (Williams 1988) by (Al-Haj 2014). Liquid BG11 medium (50 ml) was inoculated with a loopful of *Synechocystis* cells from a freshly restreaked plate and allowed to grow in an illuminated shaking incubator at 25ºC and a light intensity of 50 - 100 µmol/m^2/s for four days. The cultures were grown to an OD_{750nm} of 0.4 – 0.8 and the concentration (cells/ml) was calculated by multiplying the OD_{750nm} value obtained by 1.15 x 10^8 (Bishop 2002). Subsequently, the culture was harvested by centrifugation at 3,000 x *g* for 10 minutes and washed in 2 ml of fresh BG11 medium and spun down a second time. The cell pellet was resuspended in BG11 medium to a final concentration of 4 x 10^8 cells/ml. In duplicates, 1-5 µg of the vector DNA was added to 200 µl of the cell suspension and incubated at 30ºC for 4-6 hours. The cells were spread onto BG11 plates, allowed to dry, and then incubated for 2-3 days to allow expression of the introduced resistance marker. Subsequently, the plates were overlaid with 3 ml of 0.6% (w/v) agar containing kanamycin to give a final concentration of 200 µg/ml in the plates. The plates were incubated for approximately two weeks in a light intensity of ~40 µmol/ m^2/s at 30ºC and were then examined for the presence of putative transformant colonies. The colonies were restreaked three times to reached homoplasmicity before the insertion of the GOI was analysed by PCR.

2.4.10.1 Isolation of DNA from *Synechocystis* sp. PCC 6803

To confirm that the gene of interest had been inserted into *Synechocystis* sp. PCC 6803 or to sequence the transgenic lines, DNA was extracted using the chelex-based method adapted from (Werner & Mergenhagen 1998). A loop full of cells from an agar plate was resuspended in 20 µl of sterile ddH_2O, followed by the addition of 20 µl ethanol (100%) and 200 µl of chelex (5%, w/v). The mixture was incubated at 98ºC for five minutes and centrifuged at 21,000 x *g* for two minutes at room temperature. Subsequently, 2 µl of the supernatants were used in 50 µl PCR reactions.

2.4.11 Bioinformatics

For the alignments of DNA and protein sequences, virtual restriction enzyme digests, reverse complementation of DNA sequences and translation of DNA sequences the software MacVector 12.6.0 was used. Furthermore, the following free online molecular analysis tools and databases were used in this study.

Table 2.9: Databases and websites used in this study

Protein and DNA sequence databases	
UniProtKB/Swiss-Prot	http://www.uniprot.org
NCBI	http://www.ncbi.nlm.nih.gov
C. reinhardtii chloroplast genome	http://www.chlamy.org/chloro/default.html
Bioinformatics tools	
Reverse complementation	http://www.bioinformatics.org/sms/rev_comp.html
Primer design	http://www.bioinformatics.org/sms2/
Restriction digest	http://tools.neb.com/NEBcutter2/
Conversion tool	http://www.attotron.com/cybertory/analysis/trans.htm
Sequence alignment	http://www.ebi.ac.uk/Tools/msa/clustalw2/
Protein and nucleotide BLAST	http://blast.ncbi.nlm.nih.gov/Blast.cgi
Endolysin database	
phiBIOTICS	http://www.phibiotics.org
Codon usage database	
Nakamura et al. 2000	http://www.kazusa.or.jp/codon/
Culture conditions of microorganisms	
DSMZ	http://www.dsmz.de

2.5 Protein analysis

2.5.1 Protein concentration assay

Protein concentrations were determined with the Bio-Rad protein assay, based on the method of Bradford, using the microassay procedure for 96-well microtitre plates. The standards (25, 50, 100, 200, 300, 400, 500 µg/ml) and samples were measured in triplicates. The assay was performed by mixing 160 µl of each standard or sample with 40 µl of Bio-Rad protein assay dye reagent concentrate, followed by incubation at room temperature for 10 minutes. Subsequently, the absorbance was measured at 595 nm.

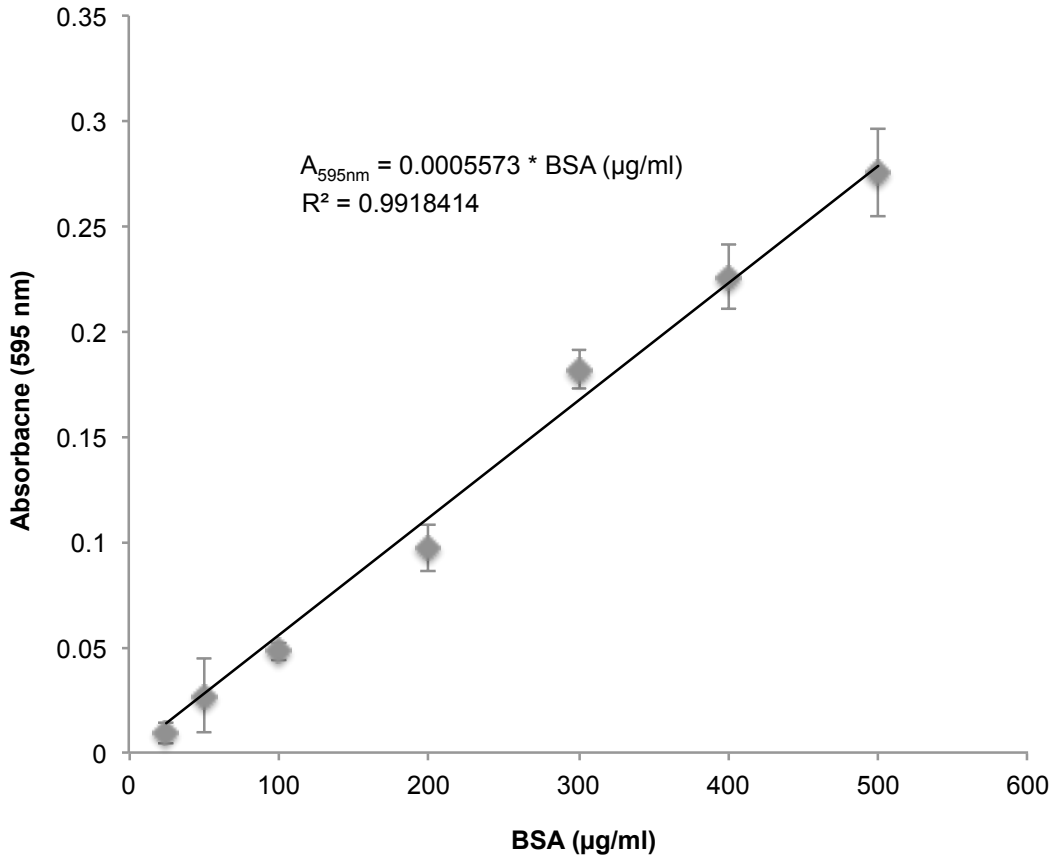

Figure 2.2: BSA standard curve for Bio-Rad protein assay
Calibration curve for the Bradford assay created using bovine serum albumin (BSA) at concentrations ranging from 25-500 µg/ml assayed at 595 nm. The error bars show ± one standard deviation (n = 3).

2.5.2 Sodium dodecyl sulphate polyacrylamide gels (SDS-PAGE)

SDS-PAGE was carried out using a Protein gel tank system from Biorad holding 80 x 83 x 1 mm gels with 10 wells. The gels were prepared based on the Laemmli gel recipe (Laemmli 1970) stated in table 2.10 with a lower 15% resolving gel and an upper 3.75% stacking gel. Samples were prepared in Solution A or by the addition of 4x protein gel sample loading buffer (Table 2.10), boiled at 99ºC for three minutes and centrifuged at 21,000 x *g* for 20 minutes before they were loaded onto the gel. The gels were run in reservoir buffer at 120V for 120 minutes. To visualize all proteins in the gel or to check if the western blotting was successful the gel was stained with Coomassie staining solution (Table 2.12) for one hour at room temperature and destained in destaining solution for at least two hours. Subsequently, the gel was scanned using the Odyssey® imaging system from LI-COR.

Table 2.10: Buffers and solutions used for SDS-PAGE performance

Protein gel sample loading buffer (4x)		
Tris-HCl pH 6.8	50	mM
SDS	2	%
Glycerol	10	%
β-Mercaptoethanol	1	%
EDTA (Ethylenediaminetetraacetic acid)	12.5	mM
Bromophenol blue	0.02	%
Solution A		
Tris-HCl pH 8.3	0.8	M
Sorbitol	0.2	M
β-Mercaptoethanol	1	%
SDS	1	%

Table 2.11: Laemmli gel recipe, buffers and solutions used during SDS-PAGE performance

15% Resolving gel (40 ml)	**Volume in 40 ml**	
Acrylamide/bisacrylamide (Sigma) 40% stock, acrylamide:bisacrylamide = 37:1	15	ml
Resolving buffer (8x stock) 0.25M Tris, 1.92M glycine, 1% SDS, pH8.3	5	ml
10% SDS	0.4	ml
Distilled H_2O	18	ml
10% ammonium persulphate (AMPS)	1.5	ml
Tetramethylethylenediamine (TEMED)	15	µl
3.75% Stacking gel (20 ml)	**Volume in 20 ml**	
Acrylamide/bisacrylamide (Sigma) 40% stock, acrylamide:bisacrylamide = 37:1	1.88	ml
Stacking buffer (4x stock) 0.5M Tris-HCl (pH 6.8)	5	ml
10% SDS	0.2	ml
Distilled H_2O	12	ml
10% ammonium persulphate (AMPS)	1.5	ml
Tetramethylethylenediamine (TEMED)	15	µl
Reservoir buffer (10 x)		
Tris	0.25	M
Glycine	1.92	M
SDS	1	%
The pH was adjusted to 8.3.		

Table 2.12: Coomassie staining and destaining solutions

Coomassie Blue R staining solution		
Coomassie Brilliant Blue R	3	mM
Methanol	50	% (v/v)
Acetic acid	10	% (v/v)
Destaining solution		
Methanol	40	% (v/v)
Acetic acid	10	% (v/v)

2.5.3 Western blot analysis (semi-dry)

After electrophoresis, the gel was soaked in Towbin buffer together with 8 pieces of 3MM Whatman paper and an Amersham™ Hybond™-ECL nitrocellulose membrane (GE Healthcare), all of the same size as the gel, for about 20 minutes. For the transfer a sandwich was assembled in the following order from the anode side: 4 pieces of 3MM Whatman paper, the nitrocellulose membrane, the gel, and another 4 pieces of Whatman paper on top. The transfer was performed at a voltage of 20 V for approximately one hour using a Trans-Blot SD semi-dry electrophoretic transfer cell from Biorad.

2.5.3.1 Immuno-detection

The membrane was subsequently blocked in blocking buffer under gently shaking at room temperature for one hour or at 4ºC overnight. After a quick rinse with TBS-T, the membrane was incubated with the primary antibody (all antibodies are stated in Table 2.15) in blocking buffer at room temperature for 1 – 3 hours under gently shaking. Afterwards the membrane was quickly rinsed and then washed for 5 – 10

minutes under vigorous shaking with TBS-T. The washes were repeated three times, before the secondary antibody in blocking buffer was applied for one hour, followed by three more washes. In experiments where horseradish peroxidase-linked secondary (ECL) antibodies were used, the membrane was first incubated with SuperSignal® West Pico Chemiluminescence Substrate (Thermo Scientific) for five minutes at room temperature. Subsequently, the membrane was exposed to a sheet of Hyperfilm ECL (GE Healthcare) in the dark room. The film was developed using a Xograph automatic film developer. The exposure time varied between 10 seconds and 20 minutes depending on the strength of the signal.

For quantitative western blot analysis IRDye® secondary antibodies (Dylight™ 800) were used and the infrared fluorescence signal (IR signal) was excited at 785 nm and detected using the Odyssey® Infrared Imaging system (Li-COR Biosciences).

Table 2.13: Buffers and solutions used in western blot analysis

Towbin buffer		
Tris	25	mM
Glycine	192	mM
Methanol	20	% (v/v)
TBS-T		
TBS buffer		
Tris base	20	mM
NaCl	137	mM
HCl pH 7.4	1	M
Tween-20	0.1	%
Blocking buffer		
TBS-T		
Skimmed milk	0.5 - 5	%

2.5.3.2 Quantification of western blot analysis

The infrared fluorescent signals of the bands in the western blot analysis measured using the Odyssey® Infrared Imaging system were analysed using the Image Studio Software 3.1.4 from LI-COR Biosciences for most analysis. For a few earlier analysis shown in this study the Odyssey® Infrared Imaging system application software 3.0 was used. Both programs express the signal in different value dimensions. The newer software expresses the signal in values of several millions, whereas the older software states values between 0.01 and 200.

To quantify the signal using the Image Studio Software, rectangles were drawn around each band to define the area for quantification. The program automatically subtracts a background value from the signal, which is determined as the median of the signal measured in an area of 2 pixels above and below the rectangle. LI-COR states that its system can be used to directly detect the amount of antigen in western blot analysis over a wide range of quantities (www.licor.com). The determination of the linear range for HA-tagged proteins in crude extracts is described in 3.2.4.

The Odyssey® Infrared Imaging system and the Image Studio Software can be therefore used to compare the amount of the protein of interest between samples of one performance. Quantifications were always performed with samples on the same gel and membrane, since gel to gel (and membrane to membrane) differences in the IR fluorescence signal can occur (Thomson et al. 2011). When more than nine samples were compared, which exceeded the capacity of one gel, the gels were run in parallel and were blotted at the same time onto nitrocellulose membranes. All further steps were performed under the same conditions and the membranes were scanned in the Odyssey® system at the same time, which greatly minimised variations between samples on different gels. In figures that show comparisons between samples from different gels and membranes, the borders of the membranes are indicated by black boxes.

2.5.4 Protein microarray

Western blot analysis of Pal with anti-HA antibodies resulted in clean blots with a single band at the size of Pal, which enabled immuno-detection using protein microarrays without separation on a SDS-PAGE. Chlorophyll causes a strong background when the Odyssey® Infrared Imaging system is used for detection. Protein microarrays were therefore only performed with samples that contained hardly any chlorophyll (after ultracentrifugation). The advantage is that a higher number of samples can be analysed in a single experiment compared to a western blot analysis.

For the performance of protein microarrays, 2 µl of the samples (ultracentrifugation supernatant, elutions and washes) were directly spotted onto a nitrocellulose membrane. The membrane was allowed to dry for 30 minutes before blocking at 4ºC overnight. Subsequently, the nitrocellulose membrane was treated as described in 2.5.3.1. The detection and quantification of the spots was in all cases performed using the Odyssey® Infrared Imaging system (Li-COR Biosciences). The IR signal was analysed using the Image Studio Software version 3.1.4 from LI-COR Biosciences as described in 2.5.3.2.

2.5.5 Enzyme-linked immunosorbent assay (ELISA)

For the performance of ELISA assays, a 96-well microtitre plate was coated with 50 µl of sample or serial dilutions of the sample and incubated at 37ºC for two hours or at 4ºC overnight. Afterwards the plate was washed three times with distilled H_2O containing 0.1 % (w/v) Tween 20. The wells were blocked with 350 µl of ELISA blocking buffer for 1.5 hours at 37ºC or at 4ºC overnight, followed by three washes with distilled H_2O. Subsequently, the wells were filled with 50 µl of the primary antibody (Table 2.15) in blocking buffer and incubated for two to three hours at 37ºC, followed by three washes with distilled H_2O containing 0.1 % Tween 20. The secondary antibody (ECL anti-rabbit) was applied in blocking buffer (50 µl in each well) for two hours at 37ºC. After the incubation the wells were washed with distilled H_2O containing 0.1 % Tween 20. To develop the reaction 100 µl of development

solution were filled in each well and the plate was incubated at room temperature until a stable blue colour appeared. The reaction was stopped by the addition of 50 µl 0.5 M H_2SO_4 in each well. Subsequently, the absorbance was measured at 450 nm.

Table 2.14: Buffers and solutions used in ELISA analyses

PBS-T		
PBS buffer		
KCl	2.7	mM
NaCl	137	mM
$Na_2HPO_4 \bullet 2H_2O$	10	mM
KH_2PO_4	2	mM
Tween-20	0.1	%
ELISA blocking buffer		
PBS		
BSA	2.5	%
Development solution (10 ml)		
H_2O	5	ml
0.2 M Na_2HPO_4	2.5	ml
0.1 M citric acid	2.5	ml
Tetramethylbenzidine	1	tablet
H_2O_2 (added just before loading)	10	µl
Stopping solution		
H_2SO_4	0.5	M

2.5.6 Antibodies

2.5.6.1 Custom made anti-Pal antibodies

To be able to detect untagged Pal, the company Eurogentec (Belgium) was commissioned to raise Pal-specific antibodies from synthetic peptides in rabbits. First, two peptide sequences of 17 amino acids with a predicted high immunogenicity were chosen within the Pal sequence (Figure 2.3). Subsequently, the peptides were synthesised and attached to keyhole limpet hemocyanin (KLH) carrier protein. Two rabbits were injected four times with the peptides in intervals of three to seven days. Preimmune bleeds, medium bleeds and final bleeds were taken. The final bleed was confirmed to contain antibodies against Pal and used for western blot analyses.

MGVDIEKGVAWMQARKGRVSY**SMDFRDGPDSYDCSSS**MYYALRSAGASSAG
WAVNTEYMHAWLIENGYELISENAPWDAKRGDIFIWGRKGASAGAGGHTGM
FIDSDNIIHCNYAYDGISVNDHDERWYYAGQPYYYVYRLTNANAQPAEKKL
GWQKDATGFWYARANGTYPKDEFEYIEENKSWFYFDDQGYMLAEKWLKHTD
GNWYWFDRDGYMATSWKRIGESWYYFNRDGSMVTGWIKYYDNWYYCDATNG
DMKSNAFIRYNDGWYLLLPDGR**LADKPQFTVEPDGLIT**AKV

Peptide 1: **C+ LADKPQFTVEPDGLIT**
Peptide 2: **SMDFRDGPDSYDCSSS**

Figure 2.3: Protein sequence of Pal with the peptide sequences used to raise custom made anti-Pal antibodies
The two peptide sequences highlighted in red and blue with a predicted high immunogenicity were chosen to raise custom made antibodies in rabbits by the company Eurogentec (Belgium). A cysteine was added to the N-terminus of peptide 2 to target the coupling site on the keyhole limpet hemocyanin (KLH) carrier protein.

2.5.6.2 Antibodies used in this study

Table 2.15: Antibodies used in this study

Antibodies	Source	Dilution
Primary antibodies		
Anti-HA (polyclonal, produced in rabbit)	Sigma-Aldrich	1:2,000 (Western blot) 1:750 (ELISA)
Anti-Pal (polyclonal, produced in rabbit)	Eurogentec	1:2,000 (Western blot) 1: 100 to 1:12,500 (ELISA)
Anti-D1 (polyclonal, produced in rabbit)	Gift from P. Nixon, Imperial College London, UK	1:2,000 (Western blot)
Anti-rbcL (polyclonal, produced in rabbit)	Gift from J. Gray, University of Cambridge, UK	1:20,000 (Western blot)
Secondary antibodies		
ECL anti-rabbit IgG, horseradish peroxidase-linked species-specific whole antibody (from donkey)	GE Healthcare	1:10,000 (Western) 1:1,000 (Anti-HA ELISA) 1:5,000 (Anti-Pal ELISA)
Anti-rabbit IgG (H&L), Dylight^{TM} 800 conjugated (from goat)	Thermo Scientific	1:20,000

2.6 Protein purification methods

2.6.1 Preparation of crude extract and soluble protein extract

C. reinhardtii cultures were grown to an OD_{750nm} of 2 to 3 and harvested by centrifugation at 8,000 x *g* for 10 minutes or using a cream separator (Motor Sich, Ukraine) (for 30 litre cultures). The cell pellet was resuspended in 20 mM NaPi-buffer (NaH_2PO_4, the pH was adjusted to 6.9 with NaOH) to a concentration of 100 times the culture volume. In some cases protease inhibitor (Roche cOmplete, EDTA-free) was added to the cell suspension. Subsequently, the cells were broken by three cycles of freezing in liquid nitrogen and thawing at 37ºC, followed by vortexing for 10 seconds. The broken cell suspension was centrifuged at 21,000 x *g* for five minutes (or 3,000 x *g* for 20 minutes for volumes above 2 ml) and the supernatant was recovered and is referred to as crude extract in this study. To remove further cell debris, membranes and non-soluble proteins and gain a soluble protein extract the crude extract was centrifuged at 100,000 x *g* for one hour in an ultracentrifuge.

2.6.2 Ammonium sulphate precipitation

The samples (soluble protein extract or combined DEAE cellulose elution fractions) were stirred on ice and grounded ammonium sulphate was slowly added to it until the desired percentage of ammonium sulphate saturation was reached. The stirring was continued for 30 minutes before the solution was centrifuged at 3,000 x *g* for 30 minutes. The pellet was resuspended in a smaller volume of 20 mM NaPi-buffer and used for further analyses. The supernatant was treated stepwise with higher concentrations of ammonium sulphate in the same way as described above.

2.6.3 Purification with anti-HA (influenza haemagglutinin peptide) resin

HA resin (100 – 200 µl) was incubated with 500 – 800 µl of the sample for 4 to 18 h at 4ºC on a rotating incubator. The tube was gently centrifuged 3 times to allow the

resin to settle down before the flow through of the sample was removed. Subsequently, the resin was washed five times with 1 ml NaPi-buffer. The HA tagged protein was eluted from the resin by incubation with 300 – 500 µl 0.1 M Glycine-HCl buffer (pH 2.5) for two minutes and immediately neutralized with 1 M Tris-HCl buffer (pH 8.0). Alternatively, the resin was eluted by incubation with 100 µg/ml HA peptide for 10 minutes.

2.6.4 Purification with diethylethanolamine (DEAE) cellulose

The purification of Pal with DEAE cellulose was for a first test performed in Eppendorf tubes with 100 to 300 µl of resin and subsequently in columns with 10 – 50 ml resin. In Eppendorf tubes the resin was incubated with the sample for one to two hours at room temperature on a rotating incubator and then washed with 1 ml each of wash buffer 1, 2 and 3. Pal was eluted with 100 – 300 µl of choline containing elution buffer.

When columns were used, the samples (soluble protein extracts of TN72_SR_*pal-HA* or TN72_SR_*cpl-1-HA*) were applied to the column using a peristaltic pump with a flow rate of 2 ml/min and the application of the sample was repeated two to three times. The resin was washed with six column volumes of wash buffer 1, eight volumes of wash buffer 2 and four volumes of wash buffer 3. Pal and Cpl-1 were eluted with two column volumes of elution buffer and 1 – 1.5 ml fractions of the elution were collected. The amount of Pal or Cpl-1 in the wash and elution fractions was analysed in a protein microarray as described in 2.5.4. Subsequently, the elution fractions with the highest amount of Pal or Cpl-1 were combined and dialysed using Slide-A-Lyzer G2 dialysis cassettes (Thermo Scientific) with a MWCO of 20,000. The combined and dialysed elution was concentrated using either Vivaspin 6 centrifugal concentrators (Sartorius Stedim Biotech) with a MWCO of 30,000 or by ammonium sulphate precipitation (2.6.2).

Table 2.16: Buffers and solutions used for the purification of Pal and Cpl-1 with DEAE cellulose

Wash buffer 1		
NaPi-buffer (pH 6.9)	20	mM
Wash buffer 2		
NaPi-buffer (pH 6.9)	20	mM
NaCl	1.5	M
Wash buffer 3		
NaPi-buffer (pH 6.9)	20	mM
NaCl	0.1	M
Elution buffer		
NaPi-buffer (pH 6.9)	20	mM
NaCl	0.1	M
Choline	6.5	% (w/v)

2.7 Antibacterial activity assays

2.7.1 Spot tests

A liquid culture of the target bacterium was grown overnight and 200 µl of the culture were spread onto Columbia blood agar plates or other appropriate nutrient agar plates. Subsequently, the plates were dried for five to ten minutes before 20 - 50 µl of each sample (*C. reinhardtii* crude extracts containing an endolysin and control extracts) were spotted onto the plates. The plates were incubated overnight regarding to the growth conditions of the target bacterium and inspected for inhibition zones on the next morning.

2.7.2 Counting colony forming units (cfu)

Cells from a liquid culture of the target bacterium were mixed with endolysin containing samples and control samples (crude extracts or purified endolysins) and incubated for 10 to 60 minutes. Subsequently, the mixture was diluted in serial 10 fold dilution steps before 20 µl of the dilutions were spotted on appropriate nutrient agar plates and incubated overnight regarding to the growth conditions of the target bacterium. On the next morning the colonies in each spot were counted and the colony forming units per ml of cell suspension were calculated. Furthermore, the differences in cfu between the endolysin treated and the control samples were calculated.

Alternatively, samples that had been first analysed in a TRA to follow the lysis of the target bacterium were used for the cfu assay. As soon as the decrease in OD_{750nm} in the presence of the endolysin had plateaued in the TRA, the mixtures of bacterial suspension and endolysin containing sample as well as the control assays were diluted and spotted on the agar plates as described above.

2.7.3 Turbidity reduction assays (TRAs)

A culture of the target bacterium of interest was grown according to the growth conditions described in 2.3. *S. pneumoniae* cultures were grown overnight, subcultured the next morning and grown for another six hours to ensure that the culture had not reached the stationary phase before the start of the assay. Subsequently, the cultures were harvested and the cells were resuspended in 20 mM NaPi-buffer. The TRAs were first performed in 1 ml cuvettes and the OD was measured at 600 nm manually over a times course. Subsequently, the TRAs were performed in 96-well microtitre plates with a final assay volume of 200 µl. An ELx 808 microplate reader (BIO-TEK INSTRUMENTS INC.) was used to measure the OD at 595 nm automatically every two minutes over times courses of 60 to 500 minutes at 37ºC. The start $OD_{595 \text{ or } 600 \text{ nm}}$ values of the bacterial suspensions were 0.1 to 1.0 depending on the assay. The assays were started by the addition of the endolysin containing samples and corresponding control samples. Most TRAs were performed by adding 20 µl of the endolysin or control preparation to 180 µl of suspension of the target bacterium.

2.7.3.1 Endolysin preparations used in the TRAs

C. reinhardtii samples containing endolysins used in the TRAs were prepared as described in 2.6.1 or 2.6.4. *Synechocystis*-produced endolysin samples were prepared by breaking *Synechocystis* cells by vortexing in the presence of glass beads (212 - 300 µm) for two minutes followed by two minutes on ice for five cycles. Subsequently, the supernatant was separated from the cell debris by centrifugation (21,000 x *g* for five minutes) and used in the TRAs.

E. coli-produced endolysin samples were prepared by breaking the cells with a French Pressure cell press at 10,000 psi for two cycles. The cell debris was pelleted by centrifugation at 5,000 x g for 20 minutes or 21,000 x *g* for five minutes. The supernatant was used in the TRAs.

CHAPTER 3 & 4

Synthesis of the *Streptococcus pneumoniae* specific endolysin Pal in the chloroplast of *Chlamydomonas reinhardtii*

3 Synthesis of the *Streptococcus pneumoniae* specific endolysin Pal in the chloroplast of *C. reinhardtii*

3.1 Introduction

3.1.1 The *S. pneumoniae* specific endolysin Pal

Pal is an endolysin encoded by the lytic bacteriophage Dp-1 of *S. pneumoniae*. Dp-1 is part of the *Siphoviridae*, a family of DNA viruses with a non-enveloped head and a flexible and non-contractile tail and has a genome that consists of a 57 kb double-stranded DNA (López et al. 1992). Dp-1 was the first described bacteriophage of *S. pneumoniae* (López et al. 1977) and Pal was the first pneumococcal phage-encoded endolysin to be purified and described (Garcia et al. 1983a). Pal was named in this study and stands for "phage-associated lytic activity" (Garcia et al. 1983a). Garcia et al. also biochemically characterized it as an amidase that requires choline for full biochemical activity (Garcia et al. 1983a; Garcia et al. 1983b). Sheehan et al. (1997) localized and characterized the gene coding for Pal and were the first to express it in *Escherichia coli*.

Pal has a two-domain structure with an N-terminal catalytic domain that exhibits *N*-acetyl-muramoyl-L-alanine amidase activity and has a high similarity (41.9% identity) to the N-terminal region of a protein (orf259) from the lactococcal bacteriophage BK5-T (Sheehan et al. 1997) (Figure 3.1). It cleaves the peptidoglycan of the *S. pneumoniae* cell wall between the L-alanine of the peptide chain and the *N*-acetyl-muramic acid of the sugar strand (Figure 3.2). The C-terminal binding domain binds specifically to choline in the teichoic acids of the cell wall and consists of six repeats of about 20 amino acids and a short C-terminal tail. This domain shows a high similarity to the choline-binding domains of several pneumococcal and clostridial proteins, and the highest similarity to the choline-binding domain of the major autolysin of *S. pneumoniae* LytA (64.6% identity, *S. pneumoniae* wild-type strain R6) (Figure 3.1). Sheehan et al. (1997) describe Pal therefore as the first example of a

natural chimeric enzyme of intergeneric origin and see it as a well-characterised support for the theory of the modular evolution of proteins.

Sheehan et al. presume that the open reading frame (ORF) just upstream of the *pal* gene on the Dp-1 genome, which shares a stop and start codon with *pal* (TAATG) encodes for the holin protein of the lytic system. This orf encodes a protein with two predicted membrane-spanning helical domains and a highly charged C-terminal tail, which resembles the protein structure of the Ejh holin of the pneumococcal phage EJ-1 (Díaz et al. 1996).

Pal requires choline-containing cell walls or *in vitro* incubation in the presence of free choline to become fully active and is for example unable to degrade cell walls, in which choline has been replaced by ethanolamine (Garcia et al. 1983a; Sheehan et al. 1997). Choline binding strongly stabilises the cell wall binding domain and causes a conformational change that transmits the stabilisation to the catalytic domain. This "conversion" is most likely responsible for the full activation of Pal by choline binding (Varea et al. 2004). The two domains of Pal interact as cooperative, interdependent units and their denaturation happens as a single process. Varea et al. predicts two to three choline binding sites per Pal monomer, which are located at the interface of two consecutive repeats of the cell wall binding domain. The activity of Pal is inhibited by higher concentrations of free choline and has an IC_{50} (50% inhibitory concentration) of 2 mM choline.

Furthermore, Varea et al. (2004) predicted the secondary structure of Pal using spectroscopic techniques and prediction methods. The catalytic domain is predicted to have a $\alpha\beta\alpha_2\beta_6$ structure, in which the single elements are connected by long loops. The six repeats of the cell wall binding domain are predicted to contain each one β–hairpin followed by a coiled region.

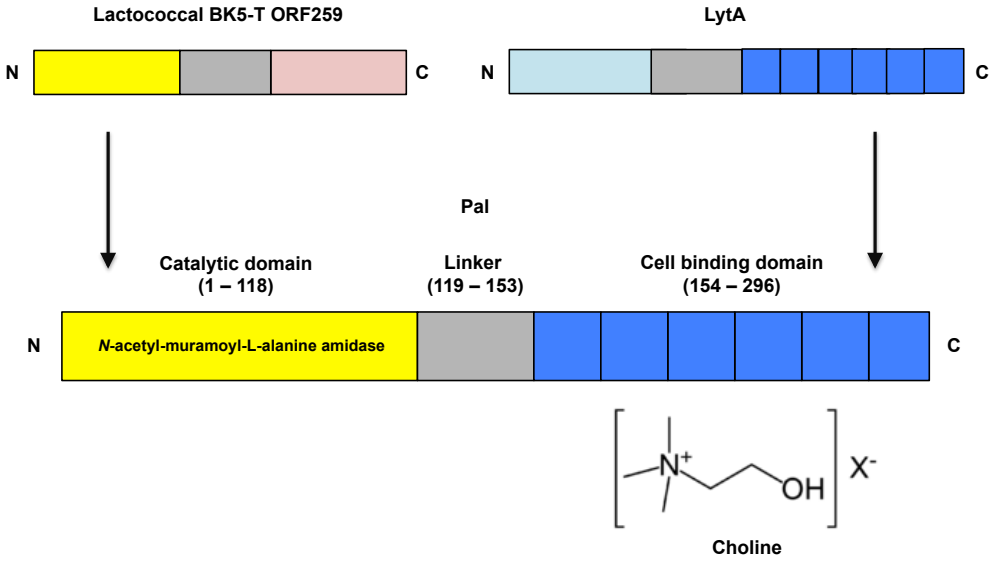

Figure 3.1: Modular organisation of the endolysin Pal
Pal consist of a N-terminal catalytic domain with *N*-acetyl-muramoyl-L-alanine amidase activity, which has a high sequence similarity to the lactococcal BK5-T open reading frame 259, and a C-terminal cell wall binding domain, which has a high similarity to the one of the major autolysin of *S. pneumoniae* LytA. The cell wall binding domain consists of six repeats and binds to choline of the teichoic acids of the pneumococcal cell wall.

Figure removed

Figure 3.2: Cleaving site of the *S. pneumoniae* specific endolysin Pal
The endolysin Pal is produced in the cytoplasm of *S. pneumoniae* cells infected with the bacteriophage Dp-1. At the end of the lytic cycle holin proteins are inserted into the cytoplasmic membrane, which results in pores (A). Pal can get through these pores to the cell wall, where it cleaves the peptidoglycan between the L-alanine of the peptide chain and the *N*-acetyl-muramic acid of the sugar strand (B). B shows streptococcal peptidoglycan (type A3α). CCWP = carbohydrate cell wall polymer, LU = linkage unit, P = phosphate group, MurNAc = *N*-acetyl-muramic acid, GlcNAc = *N*-acetyl-glucosamine acid, Ala = alanine, Glu = glutamic acid, Lys = lysine. Modified from Loessner (2005).

Besides expression in *E. coli*, Pal has been successfully expressed in active from in tobacco (*Nicotiana tabacum* cv. Petite Havana) chloroplasts, where it accumulated to up to 30% of the plants total soluble protein (Oey et al. 2009b). Oey et al. reported that cloning of Pal into their standard tobacco chloroplast expression vector in *Escherichia coli* was unsuccessful. They speculated that this was due to toxicity of Pal for *E. coli*. The same results were reported for the *S. pneumoniae* specific endolysin Cpl-1. Therefore a toxin shuttle vector was created in this study, which is based on premature transcription termination in *E. coli* using transcriptional terminator sequences that are specific for bacteria. This vector showed strongly decreased expression of the fluorescent protein GFP in *E. coli* and made it possible to clone *pal* and *cpl-1* into the expression system using *E. coli.* Whereas a ligation experiment with equal amounts of *pal* and *gfp* genes into the standard expression vector resulted in 100% *gfp* clones, the same ligation into the toxin shuttle vector resulted in similar amounts of *pal* and *gfp* clones (55% to 45%). Oey et al. (2009b) concluded therefore that their chloroplast vectors reached accumulation levels of Pal and Cpl-1, which became toxic to *E. coli.* At the same time, this study did not observe any effect of Pal or Cpl-1 against *E. coli* when the enzymes where applied from outside in turbidity reduction assays. Furthermore, this study describes a high stability of Pal and Cpl-1 in the tobacco chloroplast, since no decline of Pal and Cpl-1 accumulation was observed in older leaves despite that the protein biosynthesis decreases with leaf age (Oey et al. 2009b). Furthermore, Pal accumulated a high level of 30% of total soluble protein. Oey et al. (2009b) presumed that this was due to a high resistance of Pal and Cpl-1 (which are naturally produced and accumulate in bacteria) against prokaryotic-type proteases in the chloroplast. Oey et al. described also a very high stability of PlyGBS, a group B streptococcus specific endolysin, which accumulated to even 70% of total soluble protein in tobacco chloroplasts (Oey et al. 2009a).

Oey et al. (2009a,b) concluded therefore that chloroplasts are ideal expression platforms for endolysin-type antibiotics due to their prokaryotic origin and therefore prokaryotic-type proteases combined with the absence of the endolysin substrate peptidoglycan.

3.1.2 Aims and objectives

The aim of the experiments presented in this chapter was the expression of the endolysin Pal, a promising candidate as a novel protein antibiotic against *Streptococcus pneumoniae*, in the *C. reinhardtii* chloroplast, followed by an analysis of the accumulation and stability of the recombinant protein in the chloroplast. Subsequently, the maximal yields of Pal produced in *C. reinhardtii* were quantified to be able to examine the suitability of *C. reinhardtii* as a novel expression platform for Pal and other antimicrobial proteins in comparison to other protein production platforms such as bacteria or the tobacco chloroplast.

3.2 Results and Discussion

3.2.1 Creation of transgenic lines of *C. reinhardtii* carrying the *pal* gene in the plastome

Three different transgenic lines of *C. reinhardtii* carrying a synthetic *pal* gene in their plastome (together with corresponding control strains) were created to study the synthesis of the Pal protein in the algal chloroplast. The lines differ in regard to the promoters/5'untranslated regions (UTR's) used for the expression of *pal* and the presence of an epitope tag (Figure 3.1).

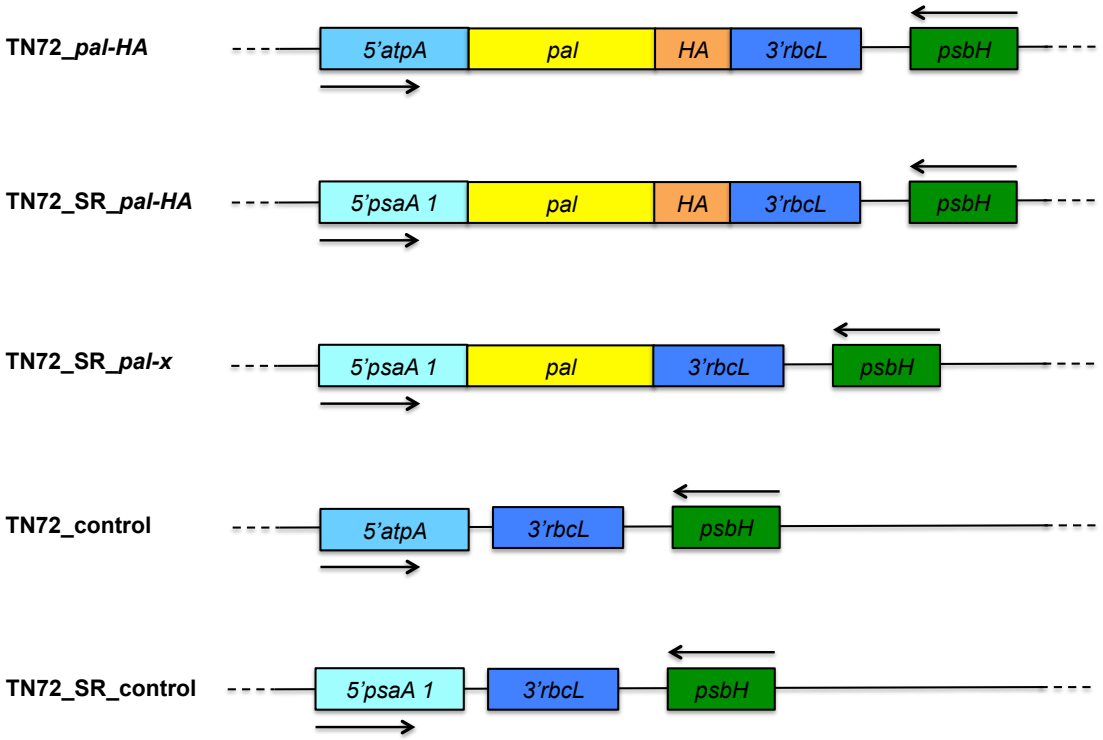

Figure 3.3: Pal expressing strains of *C. reinhardtii* TN72 created in this study and the corresponding control strains
The diagram shows the differences in the expression elements and tags of the three *C. reinhardtii* TN72 strains, which were created to study the expression of Pal in the *C. reinhardtii* chloroplast and the two corresponding control strains. Endogenous chloroplast genes are indicated in green, expression elements in blue, the gene of interests in yellow and the HA-tag in orange.

All lines were created using a *C. reinhardtii* chloroplast transformation system that consists of the cell wall-less recipient strain TN72 and the expression vectors pASapI or pSRSapI. This transformation system uses the photosystem II gene *psbH* as a selectable marker and inserts the gene of interest (GOI) in a neutral region downstream of *psbH*. Successful transformants are selected for restoration of phototrophic growth on minimal medium. For a detailed description of the transformation system see materials and methods 2.3.8.

3.2.1.1 Design and codon-optimisation of the synthetic *pal* gene

The sequence of the Pal protein was taken from the database UniProtKB/Swiss-Prot (Entry: O03979; Entry name: ALYS_BPDP1; Gene name: PAL; Protein name: Lysin, EC=3.5.1.28; Organism: Pneumococcus bacteriophage Dp-1 (Taxonomic identifier: 59241)). Pal is comprised of 296 amino acids and has a mass of 34,453 Da. The corresponding gene was codon-optimised for the *C. reinhardtii* chloroplast to a Codon Adaption Index (CAI) of 0.8 with respect to the codon usage table from Nakamura et al. (2000) (http://www.kazusa.or.jp/codon) and synthesised by GENEART (Regensburg, Germany) with the addition of a 5' SapI and a 3'SphI restriction sites for subsequent cloning and a C-terminal human influenza haemagglutinin (HA) epitope tag for detection. The codon-optimised DNA sequence of the *pal* gene is attached in the appendix. The created *pal* gene has a length of 888 bp and including the HA-tag coding sequence and two stop codons (TAA) a length of 921 bp. The HA-tagged Pal protein has a molecular mass of 35.6 kDa.

3.2.1.2 Promoters and 5'/3' untranslated regions used for the expression of *pal*

Previous studies had shown that the promoters/5'UTRs from the highly expressed endogenous chloroplast genes *atpA* and *psaA* exon 1 result in the highest levels for recombinant proteins in the *C. reinhardtii* chloroplast (Purton et al. 2013; Michelet et al. 2011). The expression of *pal* was therefore analysed under the control of these two

promoters/5'UTRs. The *atpA* gene encodes for the α subunit of the chloroplast ATP synthase complex CF_1/CF_0 in green algae, including *C. reinhardtii* and higher plants (Leu et al. 1992). The *psaA* gene encodes a subunit of photosystem I and is split into three exons that are located apart from each other on the *C. reinhardtii* plastome. It has been shown that an authentic 3'UTR is necessary for mRNA accumulation, since it stabilises the mRNA and plays a role in transcription termination and 3' formation, but all 3'UTRs of endogenous chloroplast genes analysed so far resulted in similar mRNA and protein levels for transgenes (Barnes et al. 2005). The 3'UTR of the *rbcL* gene has been successfully used in several previous studies and was therefore chosen for the expression of *pal* in this study (Barnes et al. 2005; Rasala et al. 2011). The *rbcL* gene encodes the large subunit of the very abundant enzyme Ribulose-1,5-bisphosphate carboxylase/oxygenase (Rubisco).

3.2.1.3 Creation of the transgenic lines

3.2.1.3.1 TN72_ *pal-HA*

In the transgenic line TN72_*pal-HA* the expression of *pal* is under the control of the *atpA* promoter and 5'UTR, and the *rbcL* terminator and 3'UTR. The *pal* gene contains the coding sequence for a C-terminal HA-tag (Figure 3.3). For the creation of TN72_*pal-HA* the expression vector pASapI was used (Table 2.5) (Economou et al. 2014). The *pal* gene was cloned from the GENEART vector pMK_*pal-HA* into pASapI using the SapI and SphI restriction sites. The successful cloning of *pal* into pASapI was confirmed by sequencing. The resulting plasmid pASapI_*pal-HA* was transformed into *C. reinhardtii* TN72 using the glass bead method. The obtained colonies were restreaked three times to achieve homoplasmicity. Insertion of *pal* into the correct location in the chloroplast genome and homoplasmicity were confirmed by PCR with the primers FLANK1, atpA.R and rbcL.Fn (Figure 3.4) and by sequencing between the primers atpA.F and rbcL.R. Of six transformants analysed by PCR, four contained the expression cassette with *pal* in the correct location. The analysed transformants reached homoplasmicity before the second round of restreaking (Figure 3.4).

3.2.1.3.2 TN72_SR_*pal-HA*

TN72_SR_*pal-HA* uses the *psaA* exon 1 promoter/5'UTR and the *rbcL* terminator and 3'UTR to drive the expression of *pal*. The *pal* gene contains the coding sequence for a C-terminal HA-tag (Figure 3.3). The vector pSRSapI was used for the creation of TN72_SR_pal-HA (Young & Purton 2014). The cloning was carried out as described for TN72_pal-HA. The correct insertion of pal into the chloroplast genome and homoplasmicity was confirmed by PCR with the primers FLANK1, RYpsa.R and rbcL.Fn (Figure 3.4, Figure 3.5) and sequencing. The PCR screening showed that all five analysed colonies had been successfully transformed and had reached homoplasmicity (Figure 3.5).

3.2.1.3.3 TN72_SR_*pal-x*

TN72_SR_*pal-x* uses the same expression cassette as TN72_SR_*pal-HA,* but it carries an untagged *pal* gene (Figure 3.3). The pal gene was amplified without the HA-tag sequence in a PCR with the primers Pal.Fw and HAremoval.Re. Afterwards, the PCR product was cloned into pJet, followed by digestion with SphI and SapI and cloning into pSRSapI. Subsequently, the construct was transformed into C. reinhardtii TN72 and the correct insertion was confirmed as describe for TN72_SR_pal-HA (Figure 3.4, Figure 3.5). The PCR screening showed that all eight analysed colonies had been successfully transformed and had reached homoplasmicity (Three out of eight are shown in Figure 3.5).

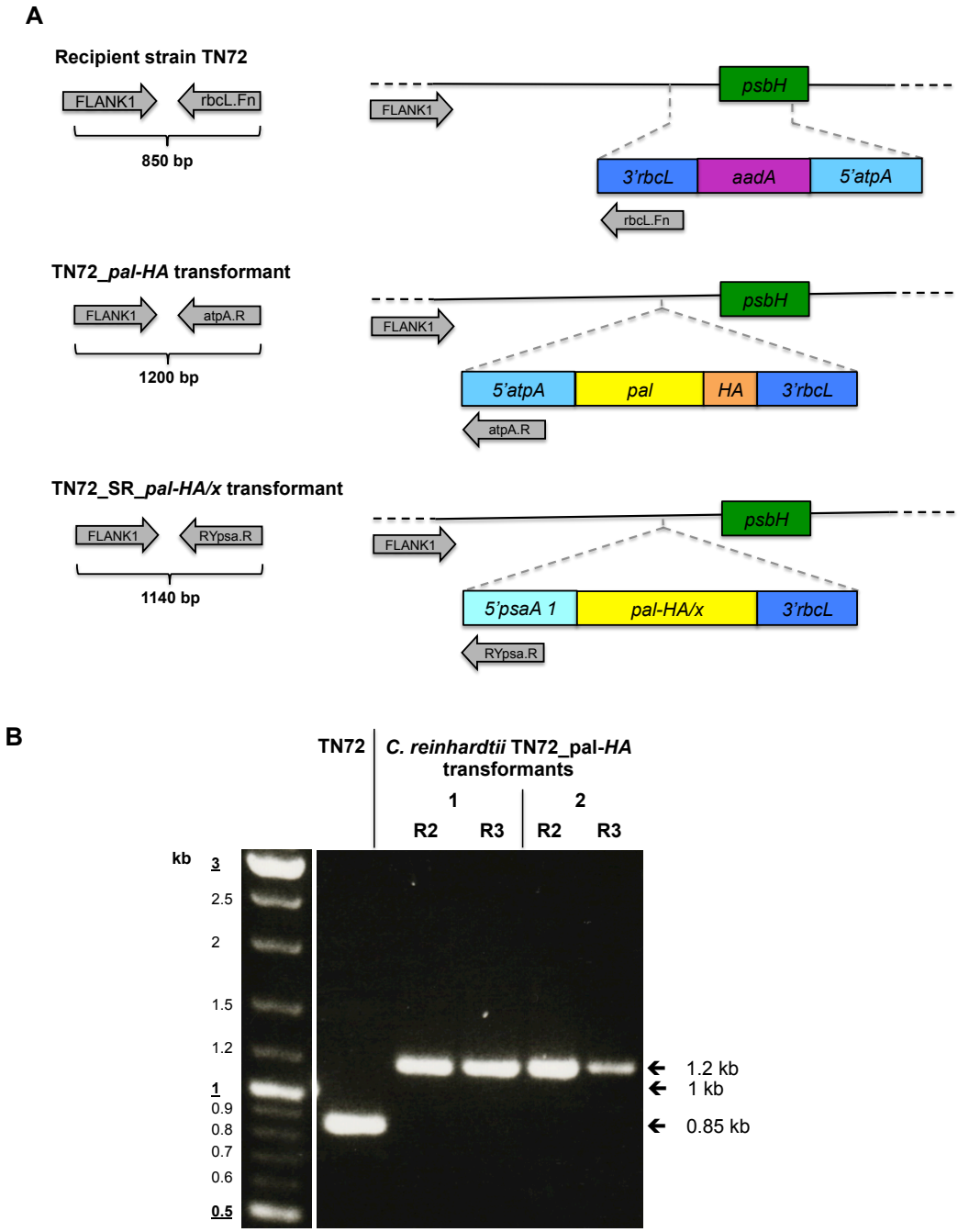

Figure 3.4: PCR screening for the successful transformation of the *C. reinhardtii* TN72 chloroplast

Schematic diagram showing the binding sites of the sets of primers and the expected fragment sizes for the recipient strain TN72 and successful TN72_*pal-HA* and TN72_SR_*pal-HA/x* transformants (A). PCR screening for putative transformants with TN72 as control (B). The primer FLANK1 binds to the plastome outside of the insertion area. RbcL.Fn binds within the *aadA* cassette of the untransformed recipient strain TN72 and results together with FLANK1 in a product of 0.85 kb. The third primers (atpA.R and RYpsa.R) bind to the promoters of the expression cassettes and result together with FLANK1 in a product of 1.2 kb for the *atpA* promoter and 1.14kb for the *psaA* exon 1 promotor. Homoplasmic transformants show only a band at 1.2 or 1.14 kb, respectively. Heteroplasmic transformants show additionally a 0.85kb band. (A) Grey arrows = primers, blue boxes = expression elements, green boxes = plastome genes. (B) 1, 2 = Transformant 1, 2; R2/3 = Second/third restreak.

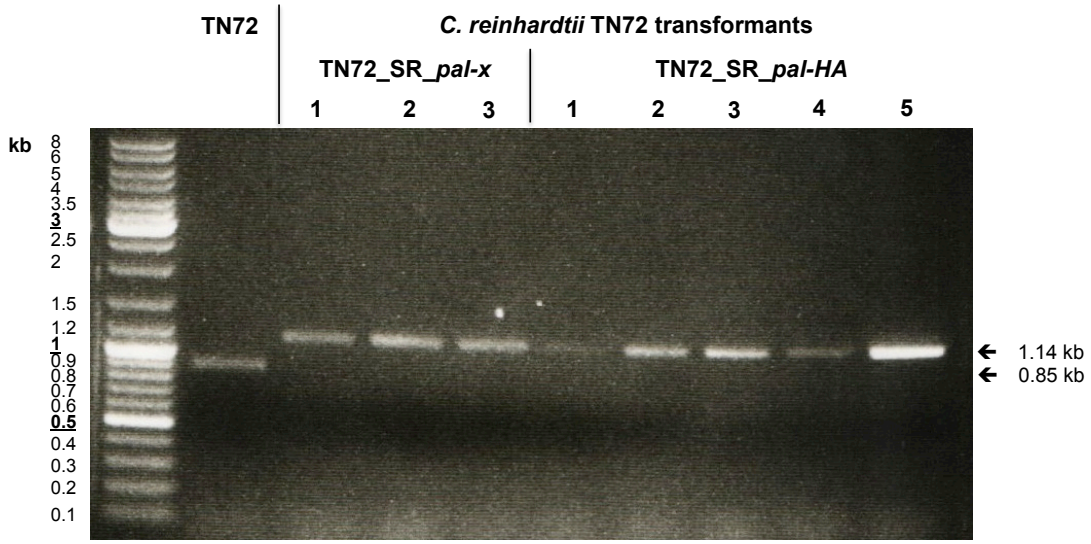

Figure 3.5: PCR screening for the successful transformation of the *C. reinhardtii* TN72 chloroplast with pASRSapI_*pal-HA* and pASRSapI_*pal-x*
In the PCR screening for putative TN72_SR_*pal-HA* and TN72_SR_*pal-x* transformants the primers FLANK1, rbcL.Fn and RYpsa.R were used. For binding regions of the primers see **Figure 3.4**. The primer FLANK1 binds to the plastome outside of the insertion area. RbcL.Fn binds within the *aadA* cassette of the untransformed recipient strain TN72 and results together with FLANK1 in a product of 0.85 kb. The third primer RYpsa.R binds to the promoter of the expression cassettes and result together with FLANK1 in a product of 1.14kb. Homoplasmic transformants show only a band at 1.2 or 1.14 kb, respectively. Heteroplasmic transformants show additionally a 0.85kb band. TN72 = Recipient strain; 1, 2, 3, 4, 5 = Transformant number 1, 2, 3, 4, 5; Expected band sizes are as follows: TN72 = 0.85 kb; Homoplasmic transformant = 1.14 kb; Heteroplasmic transformant: 0.85 kb and 1.14 kb.

3.2.1.3.4 Control strains

The corresponding control strains were created in previous studies by transformation of the recipient strain with the corresponding transformation vector carrying an empty expression cassette to ensure the same genetic background. TN72_control was transformed with pASapI and carries an empty expression cassette with the *atpA* promoter (Ninlayarn 2012). Similarly, TN72_SR_control was transformed with pSRSapI and carries the psaA exon 1 promoter, but no gene of interest (Young & Purton 2014) (Figure 3.3).

3.2.2 Expression of *pal* in the *C. reinhardtii* chloroplast

3.2.2.1 Confirmation of *pal* expression using anti-HA antibodies

Pal was synthesised with the addition of a C-terminal HA-tag to enable the detection of the Pal protein using commercially available anti-HA antibodies, since previous studies had shown that stable transformants of *C. reinhardtii* can occasionally fail to produce detectable levels of recombinant protein (Taunt 2013) (Rasala et al. 2010).
The transformant lines obtained were therefore analysed for the presence of the Pal protein by western blot analysis using antibodies against the HA-tag and in combination with IRDye® secondary antibodies and the Odyssey® Infrared (IR) Imaging System. Alternatively, horseradish peroxidase-linked secondary (ECL) antibodies were used and the resulting chemiluminescence was detected with photographic film.

Both detection systems confirmed the successful accumulation of Pal in the chloroplast of C. reinhardtii TN72_pal-HA and TN72_SR_pal-HA. Pal with the addition of the HA-tag (MW = 1.1 kDa) has a molecular weight of approximately 35.6 kDa and the observed band runs as expected slightly above the 35 kDa marker of the protein ladder (Figure 3.6, for TN72_pal-HA see Figure 3.10). The western blot analyses did not show any additional bands for TN72_pal-HA or TN72_SR_pal-HA that were not present in the control suggesting that no detectable levels of N-terminal degradation products are formed in the C. reinhardtii chloroplast (Figure 3.6). Transgenic lines that are created via the introduction of genes into the chloroplast genome by homologous recombination are genetically identical and are expected to show identical expression levels for recombinant proteins. This is further analysed in 5.2.2.1. For that reason one representative transformant of each strain was chosen for further experiments.

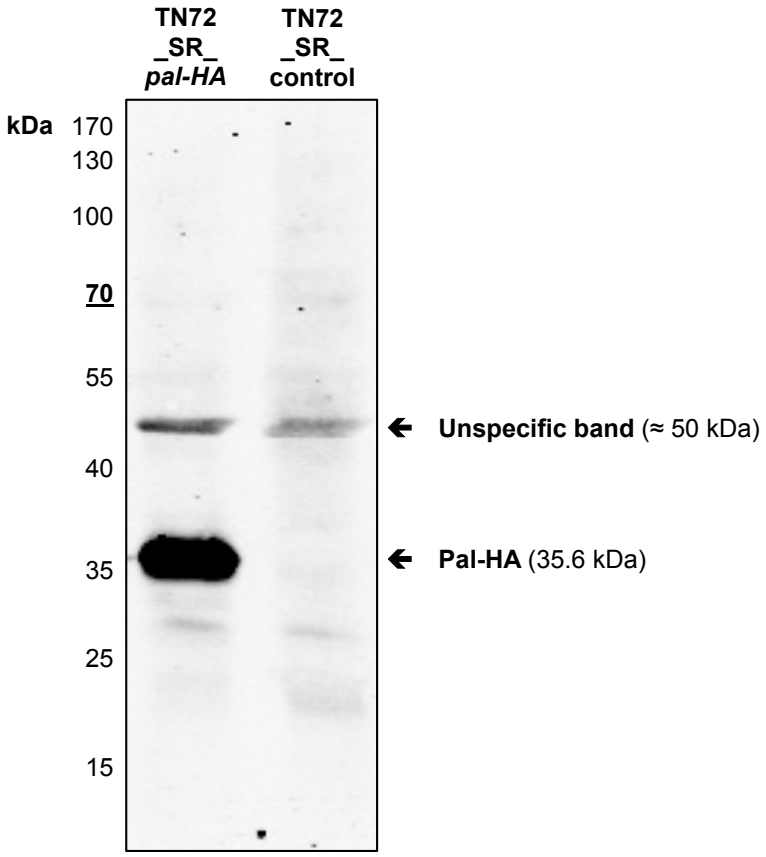

Figure 3.6: Western blot analysis of whole cell extracts of TN72_SR_*pal-HA* transformants showing the presence of HA-tagged Pal protein
The western blot was performed with whole cell extract (= suspension of whole cells that were broken by the addition of SDS (2% w/v) and boiling) and anti-HA antibodies, IRDye® secondary antibodies and the Odyssey® Infrared Imaging System for detection. TN72_SR_control was used as a negative control. The expected band size is 35.6 kDa. Protein sizes were determined using the PageRuler™ Prestained Protein ladder (Thermo Scientific).

3.2.2.2 Detection of Pal using custom made anti-Pal antibodies

Specific antibodies for the detection of Pal were not readily available. Since the success rate for the synthesis of recombinant proteins in the *C. reinhardtii* chloroplast to detectable levels is only around 50% to 70% (Rasala et al. 2010) (Rasala & Mayfield 2011), Pal was first attached with a HA-tag for an easy and inexpensive detection. Nevertheless, the addition of tags can affect the biological activity of proteins, and furthermore most tags are immunogenic, which is not desirable for human or veterinary therapeutics (Terpe 2003). Thus, it was of interest to remove the HA-tag and to analyse the activity of untagged Pal after the synthesis of HA-tagged

Pal had been confirmed with anti-HA antibodies. To be able to detect untagged Pal, the company Eurogentec (Belgium) was commissioned to raise Pal-specific antibodies from synthetic peptides in rabbits. Specific antibodies could be also used for sandwich ELISAs and highly specific purifications. Furthermore, they would enable the detection of N-terminal and mid-protein degradation products of Pal, which would not be detected with anti-HA antibodies owing to the lost of the HA-tag.

To check that antibodies had been successfully raised in the final bleed serum of the rabbits, an Enzyme-Linked Immunosorbent Assay (ELISA) with a series of concentrations of the peptide (15 ng, 7.5 ng, 3.75 ng) and a series of dilutions of the final bleed serum (1:100, 1:500, 1:2,500, 1:12,500, 1:62,500) from the rabbits was performed.

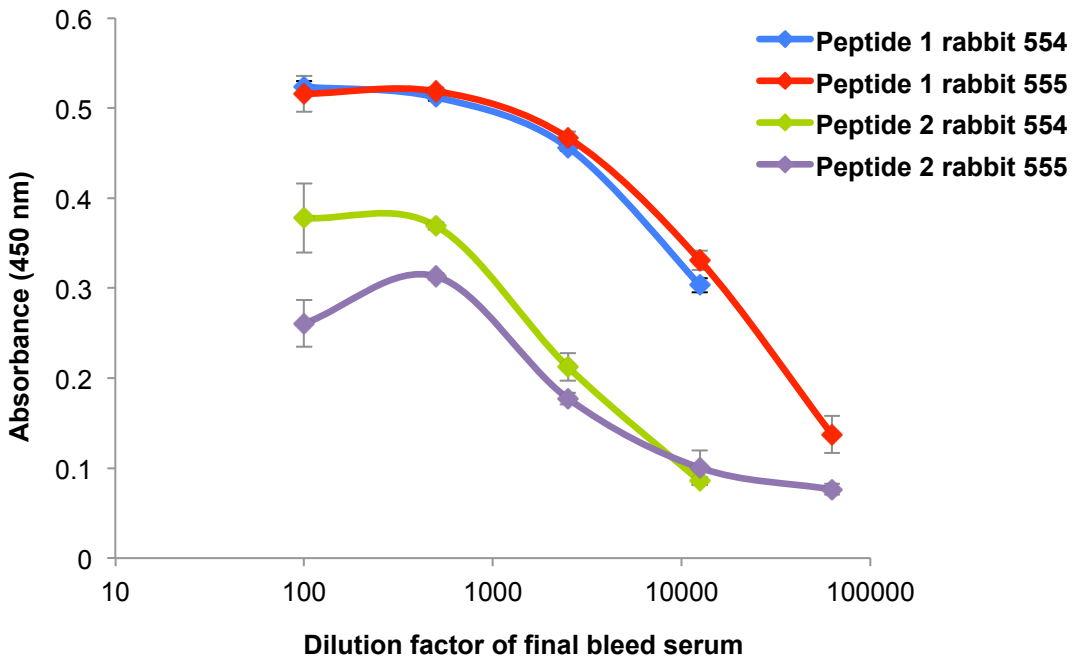

Figure 3.7: Enzyme-Linked Immunosorbent Assay (ELISA) to test the custom made anti-Pal antibodies against the peptides used to raise them
Eurogentec (Belgium) injected two rabbits (554 and 555) with two peptides from the sequence of Pal to raise custom made antibodies against Pal. An ELISA was performed with a series of dilutions of the final bleed from the two rabbits (1:100, 1:500, 1:2500, 1:12500, 1:62500) and the peptides in concentrations of 3.75, 7.5 and 15 ng. Horseradish peroxidase-linked secondary (ECL) antibodies were used for the assay and the ELISA signal was detected at 450 nm**.** The error bars show the standard error of triplicates.

The final bleed serum could be used to detect both peptides down to a dilution of 1:2,500 for all peptide concentrations tested proving that the antibodies had been successfully raised against both peptides. Peptide 1 could be detected down to a dilution of the serum of 1:12,500 and resulted in a stronger ELISA signal than peptide 2 at all dilutions. The sera from both rabbits showed similar results for peptide 1, but the serum of rabbit 555 showed a lower signal for peptide 2 than the serum of rabbit 554 at all dilutions (Figure 3.7). The serum of rabbit 554 was therefore chosen for further experiments.

Subsequently, a western blot analysis with the final bleed serum of rabbit 554 was performed to check whether the antibodies are able to detect full-length Pal in broken cell extract and to analyse the synthesis of untagged Pal in TN72_SR_*pal-x*. The final bleed serum was tested in three different dilutions (1:500, 1:1000, 1:2000) in western blots with horseradish peroxidase-linked secondary (ECL) antibodies for the detection of HA-tagged and untagged Pal in broken cell extract of TN72_SR_*pal-HA* and TN72_SR_*pal-x*, respectively. Incubation with all three dilutions of the final bleed serum resulted for both strains in bands around 35 kDa, which were not present in the negative control with TN72_SR_control proving that the custom made antibodies are able to detect full-length Pal. A dilution of 1:2000 resulted in the clearest western blot picture (Figure 3.8). Furthermore, the western blot analyses confirmed the production of untagged Pal in TN72_SR_*pal-x*. The bands for HA-tagged Pal and untagged Pal showed similar intensities at the same cell concentration in two performances of the western blot analyses indicating that both are expressed to similar levels and that the HA-tag does not interfere with the stability of Pal in the *C. reinhardtii* chloroplast.
The western blot analyses did not show any other bands in the lanes with samples of TN72_SR_*pal-HA* and TN72_SR_*pal-x*, which were not present in the lane of the negative control indicating that no degradation products of Pal are produced to detectable levels in the *C. reinhardtii* chloroplast (Figure 3.8).

However, the custom made anti-Pal antibodies showed a lower sensitivity than anti-HA antibodies in western blot analyses. The analyses of the yields of Pal synthesis in the *C. reinhardtii* chloroplast, which are discussed in the following sections, were therefore performed with TN72_(SR)_*pal-HA* and anti-HA antibodies.

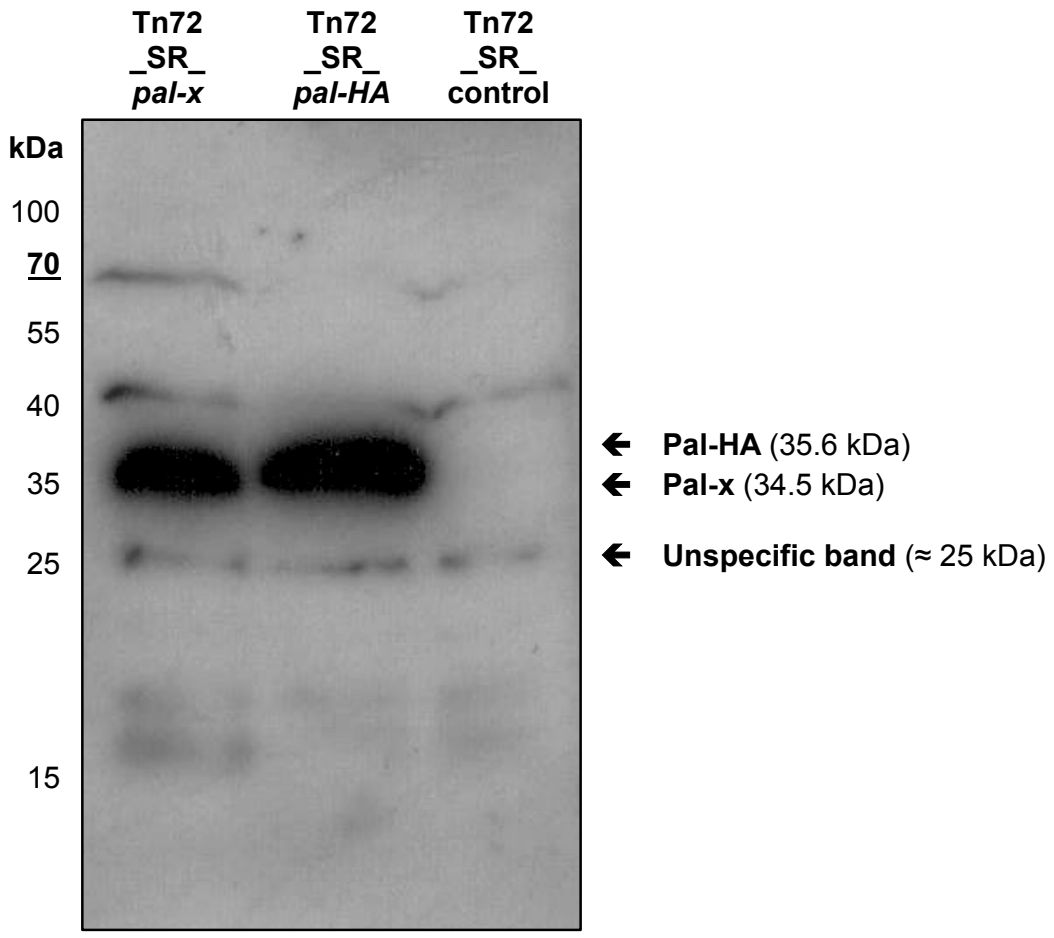

Figure 3.8: Western blot analysis with custom made anti-Pal antibodies showing the presence of untagged Pal and HA-tagged Pal in cell extracts
The western blot analysis was performed with whole cell extract of TN72_SR_*pal-x,* TN72_SR_*pal-HA* and TN72_SR_control, custom made anti-Pal antibodies raised by the company Eurogentec (Belgium) and horseradish peroxidase-linked secondary (ECL) antibodies. The resulting chemiluminescence was detected with photographic film. The expected band size for untagged Pal is 34.5 kDa and for HA-tagged Pal is 36.5 kDa. Protein size was determined using the PageRuler^{TM} Prestained Protein ladder (Thermo Scientific).

3.2.2.3 Expression of *pal* in *Escherichia coli* DH5α

Escherichia coli is widely used as an established expression system for the production of recombinant proteins. Therefore, it was of interest to compare the expression of *pal* in *E. coli* to the expression in the *C. reinhardtii* chloroplast. Previous studies had shown that the expression cassettes of pASapI and pSRSapI also allow the expression

of the gene of interest in *Escherichia coli* DH5α although the GOIs are codon-optimised for the *C. reinhardtii* chloroplast and the expression cassettes carry *C. reinhardtii* promoters and UTRs (Szaub 2012; Taunt 2013). This allows an easy, even though preliminary qualitative analysis of the expression of the GOIs in *E. coli* using the *C. reinhardtii* vectors. A quantitative comparison is not possible since neither the expression vectors nor the *E. coli* strain is optimised for recombinant protein expression. It can be assumed that the observed expression in this system is significantly lower than in an optimised *E. coli* expression system.

The construct pASapI_*pal-HA* was transformed into *E. coli* and a western blot analysis with anti-HA antibodies was performed on crude cell extracts. It was possible to detect a faint band close to 35 kDa that was not present in the negative control proving the successful synthesis of Pal in E. coli DH5α (Figure 3.9). Additionally, the blot showed multiple stronger bands of lower molecular weight in the sample of DH5α_pal-HA, which did not occur in the negative control with DH5α_control (Figure 3.9).

These bands could be N-terminal degradation products of Pal or the result of cryptic ribosome binding sites within the *pal* gene. A comparison of the estimated sizes of the smaller fragments with the Pal sequence showed that the majority of the five fragments do not end within the proximity of a methionine residue, which could have been coded by an additional AUG start codon. This indicates that the Pal fragments of lower molecular weight are most likely not the result of internal translation initiation regions, but rather degradation products generated by site-specific cleavage by *E. coli* proteases. An *E. coli* strain optimised for recombinant protein synthesis, for example a strain deficient for certain proteases, might therefore show a different pattern. On the other hand, it is conceivable that the accelerated degradation of Pal is due to toxicity of full-length Pal against *E. coli* as observed in Oey et al. (2009b). Nevertheless, this experiment indicates a faster degradation of Pal and suggests lower levels of full-length Pal protein compared to degradation products in *E. coli* DH5α. Overall, the results of the last sections suggest that Pal has a higher stability in the *C. reinhardtii* chloroplast compared to *E. coli* DH5α, which would exhibit an advantage of the *C. reinhardtii* chloroplast as an expression platform over *E. coli* DH5α.

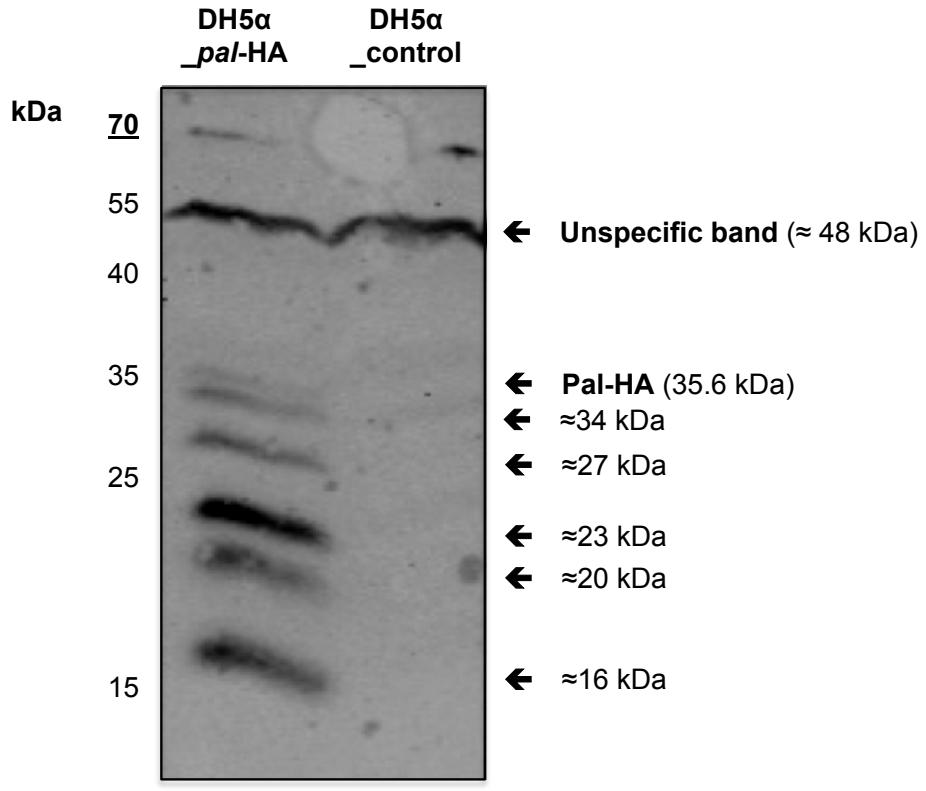

Figure 3.9: Western blot analysis with crude extracts of *Escherichia coli* DH5α *_pal-HA* transformants for the presence of HA-tagged Pal protein
The western blot was performed with anti-HA antibodies and IRDye® secondary antibodies and the Odyssey® Infrared Imaging System for detection. The expected band size is 35.6 kDa. Protein size was determined using the PageRuler™ Prestained Protein ladder (Thermo Scientific).

3.2.2.4 Comparison of *pal* expression when under the control of the promoter/5'UTR from either *atpA* or *psaA* exon 1

Two strains of *C. reinhardtii* TN72 expressing Pal, which use different promoters/5'UTRs elements were created in this study, to compare the expression levels of *pal* under the control of the two endogenous elements that had shown the highest recombinant protein yields in previous studies with the aim to maximise the production of Pal. In TN72*_pal-HA* the expression of *pal* is under the control of the *atpA* promoter/5'UTR, whereas TN72_SR*_pal-HA* uses the *psaA* exon 1 promoter/5'UTR (3.2.1.2).

Cultures of TN72_SR_*pal-HA* and TN72_*pal-HA* were grown in duplicate under the same conditions and samples were taken at multiple time points during growth to account for variations of protein levels at different growth stages. The samples were concentrated five times compared to the culture volume meaning they were normalised for the amount of Pal per culture volume. Subsequently, they were analysed in a western blot analysis with anti-HA antibodies and the Odyssey® Infrared Imaging System for the quantification of Pal. The western blot analysis for both strains is shown in figure 3.10 A. The graph in figure 3.10 and Table 3.1 show the average IR fluorescence of the duplicates measured by the Odyssey® Infrared Imaging System. The IR fluorescence values were divided by the OD_{750nm} of the cultures at the time of sampling to account for small variations in growth.

The amount of Pal in cells of TN72_*pal-HA* accounted at all growth stages for 8 - 31% of the amount measured in TN72_SR_*pal-HA*. This shows that the amount of Pal is between three to ten times higher (depending on the growth stage) when produced under the control of the *psaA* exon 1 promoter/5'UTR compared to the *atpA* promoter/5'UTR. The strain TN72_SR_*pal-HA* was therefore chosen for further investigations.

Table 3.1: Comparison of the amount of Pal produced under the control of the *atpA* and *psaA* exon 1 promoter/5'UTR
Cultures of TN72_SR_*pal-HA* and TN72_*pal-HA* were grown in duplicate under the same conditions and samples were taken at multiple time points during growth, harvested by centrifugation, concentrated five times in Na-Pi-buffer and 20 µl of the suspension were analysed in a western blot with anti-HA antibodies, IRDye® secondary antibodies and the Odyssey® Infrared Imaging System for detection and quantification. The IR fluorescence signals were divided by the optical density (750 nm) of the culture at the time of sampling and the percentage of Pal in TN72_*pal-HA* compared to TN72_SR_*pal-HA* was calculated for each growth stage. The standard deviation (±) is stated (n = 2).

Time (h)	**Signal (IR fluorescence) / OD_{750nm}**		**Amount of Pal produced using the *atpA* compared to the *psaA1* promoter/5'UTR (%)**
	TN72_SR_*pal-HA* *psaA1* promoter/5'UTR	**TN72_*pal-HA* *atpA* promoter/5'UTR**	
25	71 242 ± 30 188	16 190 ± 13 616	23
39.5	179 747 ± 83 567	22 145 ± 3 459	12
44	213 758 ± 22 302	23 135 ± 2 204	11
48	156 675 ± 60 774	26 160 ± 11 211	17
66	259 163 ± 160771	22 027 ± 1 026	8
72	81 344 ± 39 030	26 270 ± 12 321	32
89	110 020 ±33 747	22 455 ± 2 011	20
112	94 404 ± 15 524	29 654 ± 6 999	31
137	60 840	9 195	15

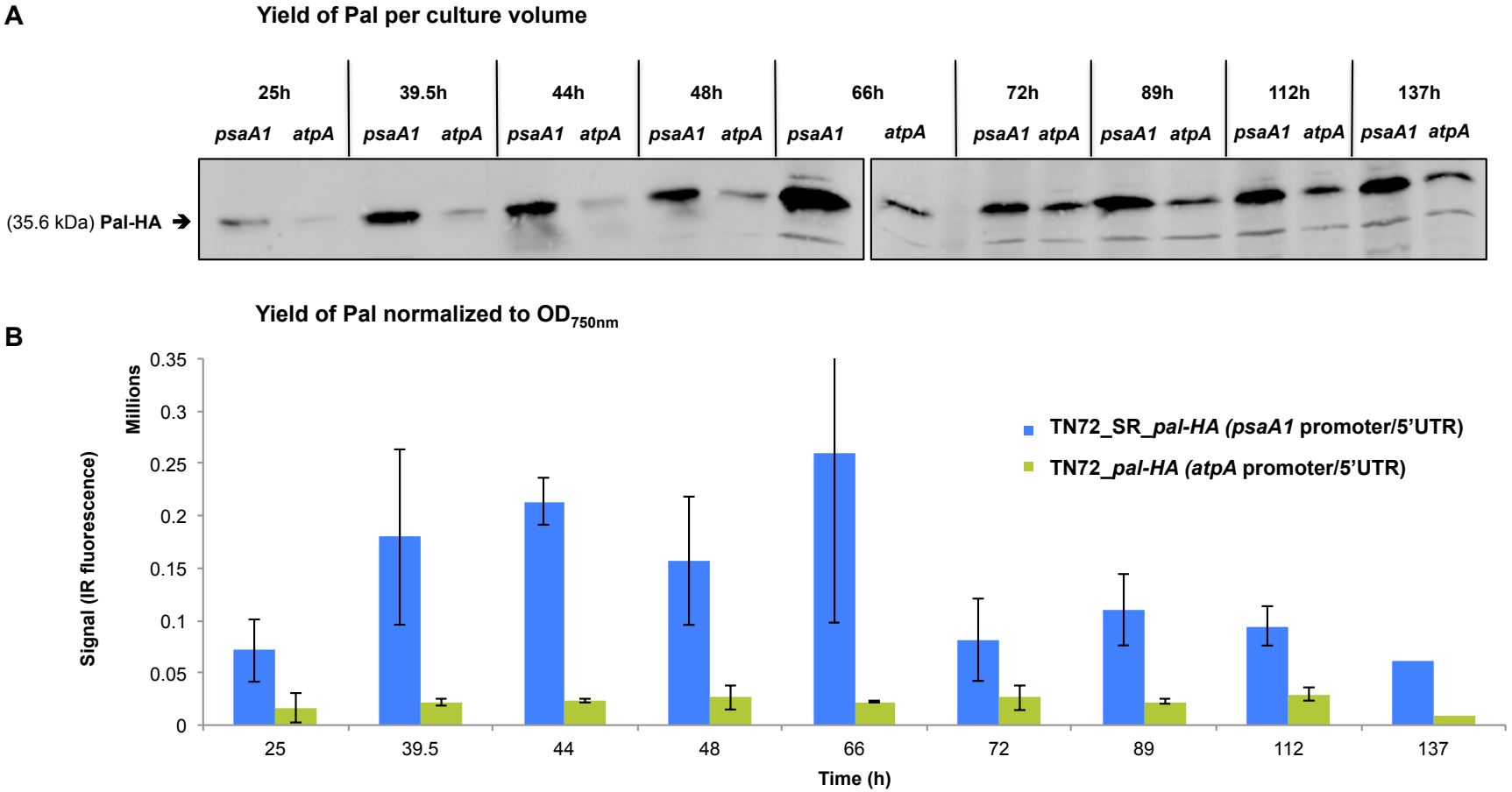

Figure 3.10: Comparison of the amount of Pal produced under the control of the *atpA* and *psaA* exon 1 promoter/5'UTR elements
Cultures of TN72_SR_*pal-HA* and TN72_*pal-HA* were grown in duplicate under standard conditions and samples were taken at multiple time points during growth, concentrated five times in Na-Pi-buffer and 20 µl were analysed in a western blot analysis with anti-HA antibodies, IRDye® secondary antibodies and the Odyssey® Infrared Imaging System for detection (A) and quantification. The IR fluorescence signals were divided by the optical density (750 nm) of the culture at the time of sampling and are shown in (B). The black frames indicate which samples were analysed on the same gel and membrane. The error bars show ± one standard deviation (n = 2).

3.2.3 Analysis of Pal accumulation and stability in the chloroplast

In section 3.2.2 the expression of *pal* was demonstrated using two different antibodies and it was shown that the expression of the gene is higher when driven by the *psaA* exon 1 promoter/5'UTR element than that from *atpA*. Subsequently it was of interest to analyse the accumulation and stability of Pal during the growth of *C. reinhardtii* with the aim to further maximise the yield of the endolysin.

C. reinhardtii is able to grow photoautotrophically, heterotrophically with acetate or mixotrophically. The highest growth rates and cell densities are reached during mixotrophic growth in liquid media with acetate, equal light exposure of all cells (200 - 400 µmol/m^2/s) and continuous shaking or bubbling for aeration of the culture and (Harris 2009). A recent study that analysed the steady-state level of the reporter protein VFP and the endolysin Cpl-1 in *C. reinhardtii* TN72 during growth under different conditions showed that growth in Tris-acetate phosphate (TAP) medium with continuous light of 200 µmol/m^2/s results in the highest yield of recombinant protein per culture volume (Braun Galleani 2014). The study revealed that the highest protein yield for VFP is achieved during growth at 30ºC, and for Cpl-1 at 25ºC. A second study confirmed higher yields of recombinant protein at 25ºC than at 30ºC for the endolysins Pal and Cpl-1 (Young, unpublished). These conditions (TAP medium, 25ºC, 200 µmol/m^2/s, continuous shaking) were therefore chosen to analyse the amount of Pal in *C. reinhardtii* and defined as standard conditions.

3.2.3.1 The production of Pal in the chloroplast does not interfere with the growth of *C. reinhardtii*

The synthesis of a recombinant protein is a metabolic burden for a cell, since it uses amino acids and metabolic energy for the production of a protein that is not of any use to the organism. The antimicrobial effect of the endolysin Pal relies upon the cleavage of the peptidoglycan in the streptococcal cell wall, and despite *C. reinhardtii*

not containing any peptidoglycan, it was nevertheless important to ensure that Pal does not have any toxic effect on the alga. It was therefore analysed if the production of Pal has a negative impact on the growth of *C. reinhardtii.*

TN72_SR_*pal-HA* and TN72_SR_control were grown under standard conditions in the Algem photobioreactor (Algenuity, Stewartby (UK)). The OD_{750nm} was automatically recorded every 0.5 h and the biomass (cell dry weight) was determined at four time points during growth. In the shown experiments TN72_SR_*pal-HA* was, in fact, found to grow slightly faster than TN72_SR_control and reached a slightly higher biomass (TN72_SR_*pal-HA*: 0.79 ± 0.00 g dry weight / litre culture volume, TN72_SR_control: 0.72 ± 0.01 g dry weight / litre culture volume) showing that Pal does not appear to have a negative effect on the growth of *C. reinhardtii.* No negative impact on the growth rate or the final OD_{750nm} was observed at any other time when both strains were cultured in parallel.

Table 3.2: Final biomass of *C. reinhardtii* TN72_SR_*pal-HA* and TN72_SR_control
TN72_SR_*pal-HA* and TN72_SR_control were grown under continuous shaking at 120 rpm, 25ºC and with a light intensity of 200 µmol/m^2/s in Gorman-Levine Tris-acetate phosphate (TAP) medium in the Algem photobioreactor (Algenuity, Stewartby (UK)) and the biomass (cell dry weight) was determined at four time points during growth. The standard deviation (±) is stated.

	TN72_SR_*pal-HA*	**TN72_SR_control**
Maximal biomass (g dry weight/L)	0.79 ± 0.00 (n = 2)	0.72 ± 0.01 (n = 2)

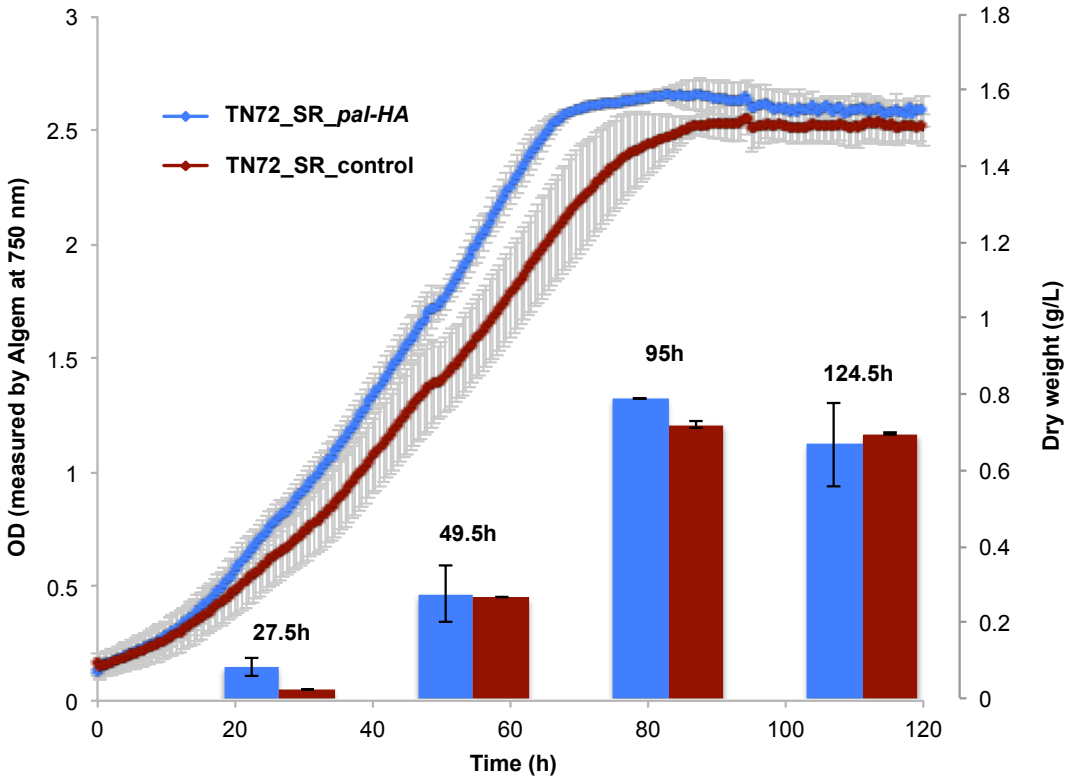

Figure 3.11: Growth of *C. reinhardtii* TN72_SR_*pal-HA* compared to TN72_SR_control
TN72_SR_*pal-HA* and TN72_SR_control were grown under continuous shaking at 120 rpm, 25ºC and with a light intensity of 200 µmol/m^2/s in Gorman-Levine Tris-acetate phosphate (TAP) medium in the Algem photobioreactor (Algenuity, Stewartby (UK)). The OD_{750nm} was automatically recorded every 0.5 h and the biomass (cell dry weight) was determined at four time points during growth. The error bars show ± one standard deviation for the optical density measurements (n = 4) and the dry weight measurements (n = 2).

3.2.3.2 Yield of Pal at different growth stages

The yield of recombinant Pal protein in cells of TN72_SR_*pal-HA* was determined at different growth stages to analyse its expression and stability in the chloroplast. Furthermore, it was highly desirable to determine the growth stage that yields the highest amount of Pal for the quantification of the maximal yield and for further experiments with Pal.

In these analyses TN72_SR_*pal-HA* was grown under standard conditions, the culture growth was recorded by measuring the OD_{750nm} and samples were taken at

multiple time points during growth. Subsequently, the samples were analysed and quantified in a western blot analysis with anti-HA antibodies and the Odyssey® Infrared Imaging System. To understand the synthesis and stability of Pal in the chloroplast it was of interest to analyse the yield of Pal per batch of cells.

To obtain the same cell density in every sample, the cells were harvested and pelleted and then resuspended in a volume depending upon the OD750nm of the culture at the time of sampling (Figure 3.10). These experiments showed an initial increase in the amount of Pal per cell from the lag phase to the logarithmic phase. During the logarithmic phase the amount of Pal per cell stayed approximately the same and decreased from the logarithmic to the stationary phase by about 60% (Figure 3.10, Figure 3.12 (light blue bars)). This shows that the amount of Pal per cell is highest during the logarithmic phase of growth and indicates that Pal synthesis, degradation and the dilution of the Pal concentration during cell division is at an approximate equilibrium in the logarithmic phase. Furthermore the results indicate that the synthesis decreases and the degradation of Pal increases under these conditions towards the end of the logarithmic phase and the beginning of the stationary phase, respectively.

In order to determine the growth stage that provides the highest yield of Pal per culture volume, all samples were resuspended in the same volume after harvesting (Figure 3.13). The previously described results already suggest that the highest level of Pal protein per culture volume could be obtained at the end of the logarithmic phase before the amount of Pal per cell drops and when the culture has reached a high cell density. The second experiment confirmed this suggestion since it showed the lowest levels of Pal during the beginning of the logarithmic phase, the highest signal at the end of the logarithmic phase and a decrease by about 40% from the logarithmic to the stationary phase (Figure 3.13 (light blue bars in B)).

Both experiments indicate that the highest level of Pal per culture volume is obtained after about 60 h (2.5 days) of growth, an OD_{750nm} of 2.8 to 3.8. The maximal OD_{750nm} is influenced by the quality of the light penetration. *C. reinhardtii* stops logarithmic

growth under the investigated conditions (in 25 ml to 500 ml flasks) at an OD_{750nm} of 3 to 4, but can continues growing at a slower rate to an OD_{750nm} of up to 5. The *C. reinhardtii* chloroplast contains several energy-dependent proteases and it has been shown that decreased stromal ATP levels induced by uncouplers (e.g. CCCP) or incubation in the dark slow down the degradation of the chloroplast protein D1 (Preiss et al. 2001). Furthermore, UV light can have a negative impact on proteins (Teresa et al. 2012). The yield of Pal was therefore additionally investigated in cultures that were transferred to the dark, at the beginning of the stationary phase. These cultures maintained similar levels of Pal per cell in the stationary phase as seen in the logarithmic phase, unlike the culture maintained in the light. This observation indicates that the degradation of Pal is slowed down in the dark (Figure 3.12 (dark blue bars in B)).

Growing *C. reinhardtii* completely heterotrophically in the dark would make it possible to use already established fermenter-based culture systems for its cultivation, as used for heterotrophic growth of industrially important bacteria and yeast. Therefore it was of interest to compare the production of Pal under heterotrophic and mixotrophic conditions. The maximal OD_{750nm} of *C. reinhardtii* cultures grown entirely heterotrophically in the dark (with 17.4 mM acetate) was found to be approximately three times lower than of mixotrophically grown cultures (Heterotrophic: $OD_{750nm} \approx 1.7$, Mixotrophic: $OD_{750nm} \approx 5$), which results in about 40 – 70% (depending on the growth stage) lower yields of Pal per culture volume in heterotrophic compared to mixotrophic cultures, despite the reduced degradation in the dark (Figure 3.13).

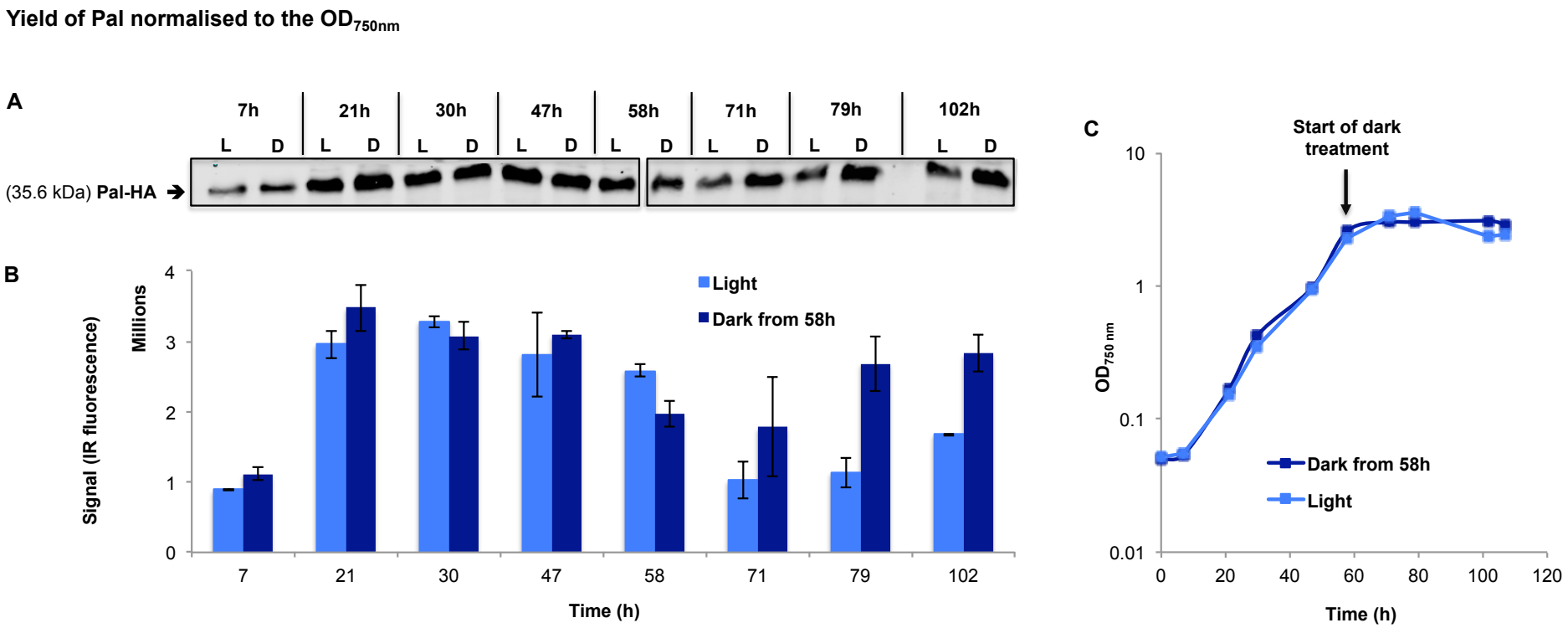

Figure 3.12: Yield of Pal synthesis at different growth stages and the influence of darkness on the protein stability during stationary phase
Cultures of TN72_SR_*pal-HA* were grown under standard conditions and samples were taken at multiple time points during growth. After harvesting the samples were normalised to the OD_{750nm} at the time of sampling. The samples were analysed in western blot analyses with anti-HA antibodies, IRDye® secondary antibodies and the Odyssey® Infrared Imaging System for detection and quantification. All cultures were grown in the light (200 µmol/m^2/s) at the beginning of the experiment. Then one half was moved to the dark after 58 h (dark blue) and the other half remained in the light (light blue). A shows one of the western blot pictures, B the averages of the Odyssey IR fluorescence signals and C the growth of the cultures. The black frames in A indicate separate gels and membranes in the western blot. The error bars in B show ± one standard deviation (n = 2).

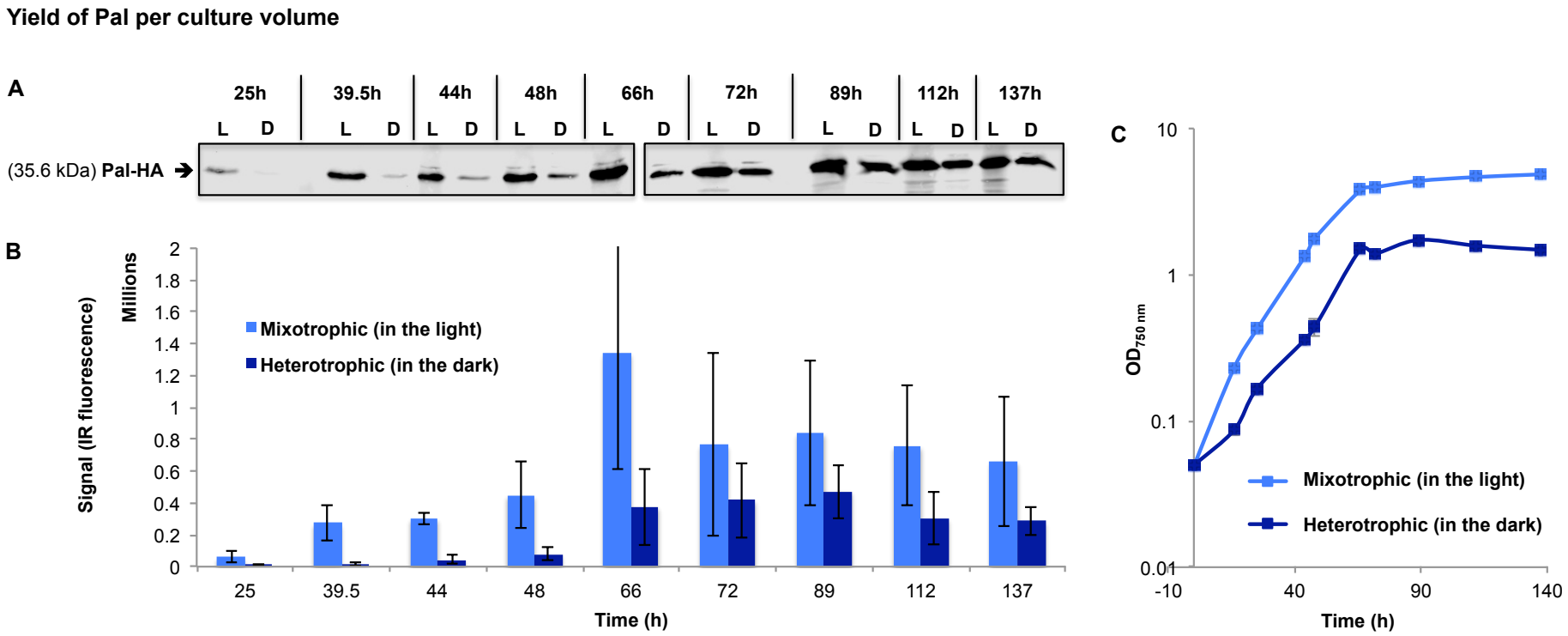

Figure 3.13: Yield of Pal synthesis per culture volume at different growth stages during mixotrophic and heterotrophic growth
Cultures of TN72_SR_*pal-HA* were grown with acetate under mixotrophic conditions in the light (light blue) and heterotrophic conditions in the dark (dark blue). Samples were taken at multiple time points during growth, after harvest all samples were resuspended in an equal volume (a five times concentration of the culture volume). The samples were analysed in western blot analyses with anti-HA antibodies, IRDye® secondary antibodies and the Odyssey® Infrared Imaging System. A shows one of the western blot pictures, B shows the average of the Odyssey IR fluorescence signals and C the growth curves of the cultures The black frames in A indicate separate gels and membranes in the western blot. The error bars in B show ± one standard deviation (n = 4, two cultures, each analysed in duplicates), the error bars in C show the standard deviation between the two cultures (n = 2). L = Culture grown mixotrophic in the light, D = Culture grown heterotrophically in the dark.

Several previous studies have investigated whether higher acetate concentrations increase the cell density in the dark, but found that higher concentrations (above 15 or 20 mM, respectively) inhibit the growth of *C. reinhardtii* (Sager & Granick 1953; Chen & Johns 1994). Sager & Granick showed that by adding more acetate once growth has ceased, another doubling of the cell density is possible. This study also investigated whether other carbon sources can be used for heterotrophic cultivation of *C. reinhardtii.* They tested 32 different carbon sources (including glucose, galactose, sucrose, lactose, maltose, mannose, ribose, starch, glycerol, citrate, fumarate and succinate), but found that none of them supports the growth of *C. reinhardtii* in the dark (Sager & Granick 1953). It is therefore difficult to increase the maximal cell densities of *C. reinhardtii* grown in batch cultures in the dark.

3.2.3.3 Stability of Pal in the light and the dark following inhibition of the protein synthesis in the chloroplast using chloramphenicol

The experiment described in 3.2.3.2 indicates that the synthesis and degradation of Pal is at an approximate steady state during the logarithmic phase and that the yield of Pal decreases towards the stationary phase in the light. Furthermore the results suggest that incubation in the dark slows protein degradation in the stationary phase. Nevertheless, the findings allow only limited conclusions to be drawn concerning the stability of Pal in the chloroplast. To analyse the stability and the degradation of Pal in the chloroplast more closely, protein synthesis in the organelle was specifically blocked by the 70S ribosome inhibitor, chloramphenicol (Hoobert & Blobel 1969). The yield of Pal was then determined over a time course after inhibition in both the light and in the dark.

Cultures of TN72_SR_*pal-HA* were grown until an OD_{750nm} of 1.0 and split equally into eight flasks. Four flasks were treated with 500 µg/ml of chloramphenicol (dissolved in ethanol) while the other four were supplemented with the same volume of the solvent ethanol, as a control. A concentration of 500 µg/ml chloramphenicol was chosen, because it showed an impact on culture growth and the greenness of the

culture in the first performance of the experiment (unlike 200 µg/ml) indicating that the concentration is sufficient to inhibit protein synthesis in the chloroplast. After addition of chloramphenicol, samples were taken at different time points over a period of 122 h. The samples were then normalised to the same cell density and analysed in a western blot analysis with anti-HA antibodies. The Odyssey® Infrared Imaging System was used for the quantification of Pal.

As shown in figure 3.14, the amount of Pal per cell in the light-grown cultures decreased stepwise during the time course in the chloramphenicol-treated and the control cultures, but was at most time points lower in the chloramphenicol-treated cultures compared to the controls. Nevertheless, Pal was still detectable 122 h after the inhibition of the protein synthesis by chloramphenicol. In the dark the amount of Pal per cell did not decrease stepwise during the first 71 h (the data indicated a decrease at 25 h, but this was followed by a subsequent increase) and only decreased in the death phase of the culture (after 122 h). The amount of Pal was also in the dark in the chloramphenicol-treated cultures at most time points lower than in the control cultures, which were still able to synthesise proteins in the chlroroplast. Nevertheless, Pal was still detectable 122 h after the chloramphenicol inhibition of protein synthesis, and the amount was similar in both the treated and non-treated cultures.

The samples of the experiment performed in the light were additionally analysed with an anti-D1 antibody as a control. The D1 protein is encoded in the chloroplast and is part of photosystem II. Only 3 h after the addition of chloramphenicol, the amount of D1 protein was lower in the treated cultures compared to the control cultures and had decreased to non-detectable levels after 6.5 h. Furthermore the chloramphenicol treatment had a strong impact on the growth of the cultures in the light, but not in the dark. The proteins in the chloroplast are mainly involved in photosynthesis and therefore do not play a major role during growth in the dark. Taken together, these data, indicate that the concentration of chloramphenicol (500 µg/ml) was sufficient to inhibit the protein synthesis in the chloroplast and shows that the degradation of the endogenous chloroplast protein D1 is a lot faster than the degradation of Pal in the *C. reinhardtii* chloroplast. A recent study that investigated the stability of recombinant human growth hormone produced in the *C. reinhardtii* chloroplast showed that only 6

h after the start of the experiment the levels of recombinant human growth hormone were lower in the chloramphenicol treated samples compared to the control samples and that the levels were strongly reduced 24 h after inhibition by chloramphenicol (Waterhouse, unpublished).

Overall the experiments indicate that Pal exists as a stable protein in the *C. reinhardtii* chloroplast and that it is able to withstand the degradation processes in the chloroplast of *C. reinhardtii* for at least 122 h, unlike D1 or the human growth hormone. Additionally, it supports the theory of Oey et al. (2009a,b) that endolysins show a very high stability in chloroplasts due to eubacterial-type proteases and the resistance of endolysins against the proteases of their host bacteria. Furthermore the experiment confirms the results of section 3.2.3.2, which suggested that the degradation of Pal is slowed down during incubation in the dark.

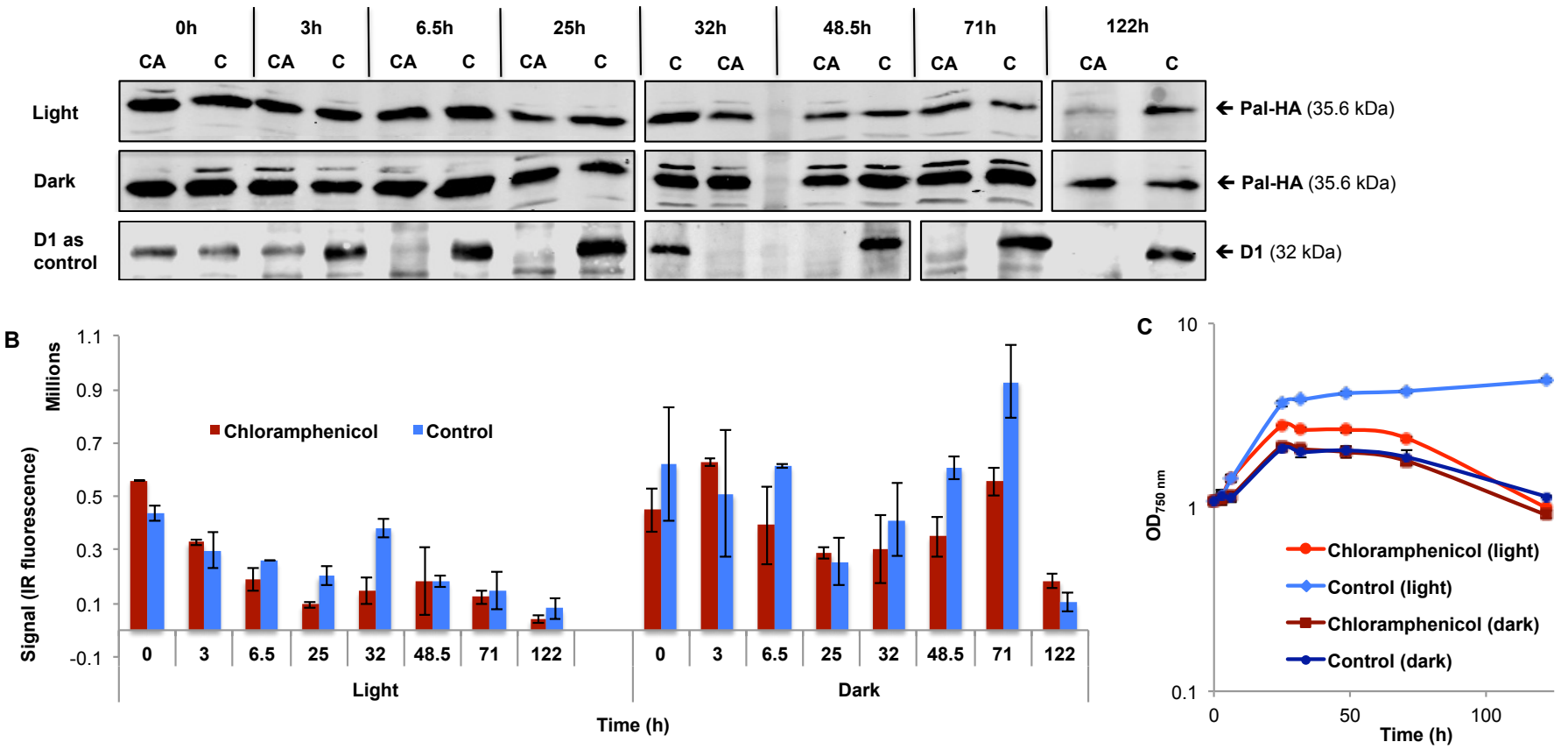

Figure 3.14: Stability of Pal after inhibition of the protein synthesis in the chloroplast by chloramphenicol in the light and the dark
Cultures of TN72_SR_*pal-HA* were grown under standard conditions to an OD_{750nm} of 1 and then split between eight flasks. One half was treated with 500 µg/ml of chloramphenicol and the other half was supplemented with an equal volume of the solvent ethanol as a control, one half was placed in the dark and one half in the light, samples were taken over a time course of 122h, normalised to the same cell density and analysed in a western blot analysis with anti-HA or anti-D1 antibodies, IRDye® secondary antibodies and the Odyssey® Infrared Imaging System. The black frames in A indicate separate gels and membranes in the western blot. A shows one set of the western blot pictures, B the average of the Odyssey IR fluorescence signals, C the growth of the cultures The error bars in B and C show ± one standard deviation (n = 2). The expected band size for Pal is 35.6 kDa and for D1 32kDa. CA = chloramphenicol treated cultures, C = control cultures.

3.2.4 Quantification of Pal produced in the *C. reinhardtii* chloroplast

In order to evaluate the potential of the *C. reinhardtii* chloroplast as an alternative expression platform to other established platforms, it was important to determine the yields of recombinant Pal protein.

Western blot analyses with infrared fluorescence secondary antibodies, the Odyssey® Infrared Imaging System and HA-tagged standard proteins were used for the quantification. The Odyssey® system measures the infrared (IR) fluorescence signal of a fluorophore bound to the IRDye® secondary antibody. A laser excites the fluorophore during measurement and the fluorescence is measured over a time course. The corresponding software quantifies the total fluorescence signal and subtracts the background in an area of 2 pixels above and under (or alternatively right and left of) the band from the signal value. LI-COR states that its system can be used to directly detect the amount of antigen in western blot analysis over a wide range of quantities (www.licor.com). Several studies have used infrared fluorescence antibodies and the Odyssey® system for protein quantification in cell extracts (Wang et al. 2007; Thomson et al. 2011).

3.2.4.1 Evaluation of purified CARHSP1 as a standard for the quantification of Pal in whole cell extracts

In order to quantify the HA-tagged Pal, it was first necessary to obtain a purified HA-tagged protein of known quantity. A tagged recombinant human CARHSP1 (calcium-regulated heat stable) protein with a known concentration was therefore purchased from Abcam.

The quantifications were performed with suspensions of whole cells that had been broken by the addition of 2% SDS and boiling (= whole cell extracts) to ensure that the total cellular amount of Pal protein was released for measurement. Firstly, it was

important to determine a linear range for Pal in whole cell extracts and to establish whether the purified standard protein could be used to quantify the concentration of another protein in whole cell extracts. For this purpose cultures of *C. reinhardtii* TN72_SR_*pal-HA* were grown under standard conditions to an OD_{750nm} of 2, harvested and diluted/concentrated to 0.25x, 0.5x, 1x, 2.5x, 5x, 10x, 20x and 50x of the culture volume. Subsequently, the cells were broken and analysed in western blot analyses with anti-HA antibodies. These western blot analyses revealed that the IR fluorescence signal of HA-tagged Pal shows a linear correlation for whole cell extracts with concentrations ranging from 0.25x to 5x of the culture volume (Figure 3.15).

Following this step, the samples were analysed together with different quantities of the HA-tagged standard protein CARHSP1 on the same gel and membrane in western blot analyses with anti-HA antibodies. Observations during this study and that by Thomson et al. (2011) suggest that quantitative comparison of samples should ideally be done between samples on the same gel and membrane, since gel-to-gel (and membrane-to-membrane) differences in the IR fluorescence signal can occur. The CARHSP1 quantities were plotted against the corresponding IR fluorescence signals and the resulting equations were used to calculate the quantities of Pal (Figure 3.15). The three to four dilutions of the whole cell extracts that revealed the best standard curve were chosen on each membrane for the calculations. The lower molecular weight of Pal compared to CARHSP1 was taken into account for the quantification.

Furthermore, it was considered whether the IR fluorescence signal of a purified protein (here CARHSP1) could be directly compared to the signal of a protein in cell extract, since the extract contains a lot of other proteins and cell debris that can bind to the nitrocellulose membrane and might reduce the binding capacity of the membrane for the protein of interest. Therefore, the quantification was performed with both pure CARSHP1 and with CARSHP1 that was added to the extract from TN72_SR_control with a concentration of 5x the culture volume to mimic the conditions in the most concentrated extract used in this experiment.

The results obtained for the quantification of Pal with pure CARSHP1 and CARSHP1 mixed with the cell extract were within the same range and with overlapping standard deviations (Pure CARSHP1: 5.0 ± 0.9 mg / L culture volume, CARSHP1 plus cell extract: 6.1 ± 1.8 mg / L culture volume) (Table 3.3, Table 3.4). These results indicate therefore that other proteins and cell debris in the extract do not saturate the binding capacity of the nitrocellulose membrane and that the IR fluorescence signal of a purified protein can be compared to the signal of a protein in a whole cell extract.

Table 3.3: Comparison of the quantification of Pal in whole cell extract with pure CARHSP1 and CARHSP1 plus TN72_SR_control extract as standards
Cultures of TN72_SR_*pal-HA* were grown under standard conditions to an OD_{750nm} of 2 and the cells were broken by the addition of SDS and boiling. Dilution series of TN72_SR_*pal-HA* whole cell extract and of pure CARHSP1 or CARHSP1 mixed with TN72_SR_control whole cell extract were analysed on the same gel and membrane in western blot analyses with anti-HA antibodies and IRDye® secondary antibodies. Standard curves of CARHSP1 quantities against the IR fluorescence signal of the Odyssey® Infrared Imaging System were used for the quantification of Pal, taking the lower molecular weight of Pal into account (see figure 3.15). The dilutions of the whole cell extracts with Pal on each membrane that revealed the best standard curve were chosen for the calculations. The standard deviations (±) are stated (n = x).

	Membrane	Pal (mg) / L culture volume	Average
Pure CARSHP1 standard	1	5.8 ± 0.5 (n = 3)	5.0 ± 0.9 (n = 3)
	2	4.0 ± 0.8 (n = 4)	
	3	5.1 (n = 1)	
CARSHP1 standard added to TN72_control whole cell extract (5x culture volume)	1	7.3 ± 2.4 (n = 3)	6.1 ± 1.8 (n = 2)
	2	4.8 ± 1.0 (n = 4)	

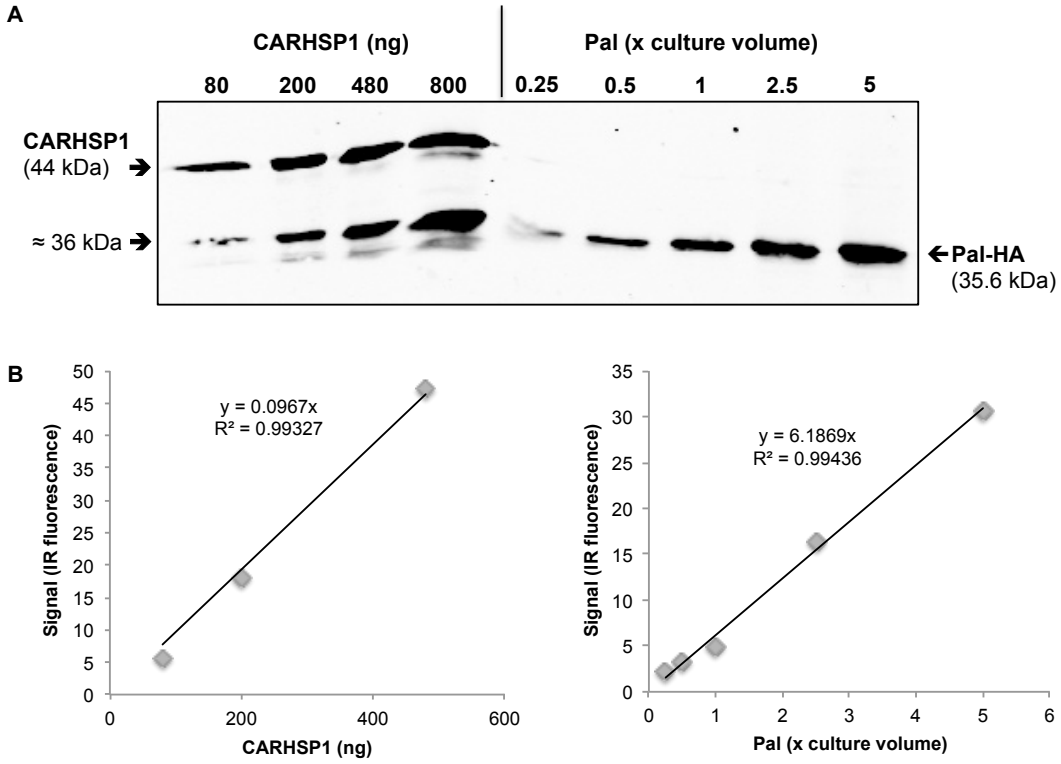

Figure 3.15: Western blot analysis with whole cell extracts of TN72_SR_*pal-HA* and the pure HA-tagged standard protein CARHSP1 for the quantification Pal
Different quantities of CARHSP1 and different dilutions of whole cell extracts of *C. reinhardtii* TN72_SR_*pal-HA* were analysed on the same gel and membrane in western blot analyses with anti-HA antibodies and IRDye® secondary antibodies (A). Standard curves of the CARHSP1 quantities against the IR fluorescence signal of the Odyssey® Infrared Imaging System were used for the quantification of Pal, taking the lower molecular weight of Pal into account (B).

3.2.4.2 Quantification of Pal using CARHSP1 and a multiple tag fusion protein as standards

In section 3.2.4.1 it was established that the IR fluorescence signal of a purified protein could be used to quantify a protein in a whole cell extract. However, a complication of the commercial standard, CARHSP1 was that it contained two degradation products of ~36 kDa in addition to the full-length protein of 44 kDa. Furthermore, the intensity of the degradation products increased over time, even when stored at -80ºC. The sum of the IR fluorescence signals of all three bands was used for the quantification of Pal, since it was assumed that they all originated from full-length CARHSP1. Nevertheless, the appearance of degradation products

decreased the reliability of this protein as a standard. Therefore, a second standard, a commercial available multiple tag fusion protein (antibodies-online.com GmbH, Germany), was used to confirm the results obtained with CARHSP1. This was also done, because it is conceivable that two different proteins show a variable behaviour during western blot analyses (e.g. differences in the transfer properties to the nitrocellulose membrane, access and binding of antibodies to the protein) and that it might therefore be difficult to compare the IR fluorescence signals of two different proteins directly.

Quantification was performed using two cultures: a culture in the mid-logarithmic phase with an OD_{750nm} of 2, to ensure that the Pal yields per cell (per cell dry weight) are at the highest level, and with a culture at the end of the logarithmic phase at an OD_{750nm} of 3.8. At this stage the highest yields per culture volume can be gained. Samples of the cultures were analysed in two different concentrations together with a dilution series of CARHSP1 or the multiple tag fusion protein. The yields were quantified as described in 3.2.4.1 (Figure 3.16). The quantification with the two different standard proteins gave results for both cultures with no significant difference (OD750nm of 2: $p = 0.22443$, OD750nm of 3.8: $p = 0.7273$) and overlapping standard deviations (Table 3.4). This suggests that any protein specific behaviour in western blot analyses plays a minor role. Furthermore, the results using the multiple tag fusion protein confirmed the results of the quantification with CARHSP1 (Table 3.3, Table 3.4).

Besides quantifying the maximal amount of Pal per culture volume, it was also of interest to determine the yield of Pal per gram of cell dry weight. For that reason, the cultures used for the quantifications were freeze-dried and then used to determine the amount of Pal per cell dry weight. Overall the performed quantifications suggested that the maximal yield of recombinant Pal produced in the chloroplast of *C. reinhardtii* during mixotrophic growth and the conditions used in this study is about 10 mg per litre of culture volume. Furthermore, the quantification indicated that Pal accounts for about 13 mg per g of cell dry weight in the logarithmic phase (Table 3.4).

A yield of 13 mg recombinant Pal per g of cell dry weight is comparable to a recent study that produced bovine Milk Amyloid A (MAA) in the *C. reinhardtii* chloroplast at pilot greenhouse scale and achieved recombinant protein yields of 12 mg per g of cell dry weight (Gimpel et al. 2014). Furthermore, the results of these quantifications suggest that the yield of Pal is higher than yields that were achieved for the *S. aureus* vaccine candidate CTB-D2 (Table 1.2, 1.4.2.3.2), which accumulated to 1.6 mg per g of cell dry weight in the *C. reinhardtii* chloroplast (Dreesen et al. 2010).

Most studies quantify the recombinant proteins produced in the *C. reinhardtii* chloroplast as percentage of total soluble protein (TSP) (Table 1.2, 1.4.2.3.2). Dreesen et al. (2010) state that TSP accounts for 23% of the total dry weight of lyophylized algae. Using this numbers, Pal would account for approximately 5% of TSP, a yield that has otherwise only been reached by a very few recombinant proteins. An example of such a protein is M-SAA (bovine mammary-associated serum amyloid), produced *C. reinhardtii* strain that was created by replacement of the endogenous *psbA* gene with a *psbA-m-saa* gene (Manuell et al. 2007).

However, a protein that accumulates to 5% TSP should be clearly visible and stand out when cell extract of the strain is analysed on a Coomassie stained SDS-PAGE gel. Manuell et al. (2007) show a Coomassie stained SDS-PAGE with *C. reinhardtii* cell extract, in which M-SAA is clearly visible despite all other protein bands. However, Pal is hardly visible when cell extract of *C. reinhardtii* TN72_SR_*pal-HA* is analysed on a SDS-PAGE gel as shown in figure 4.16 and figure 4.21. One explanation for this could be that Pal does not retain the Coomassie stain as well as other proteins e.g. M-SAA. However, another explanation could be that the quantification with CARSPH1 and the multiple tag protein overestimate the amount of Pal. This could be caused by differences in the transfer behaviour of Pal to the nitrocellulose membrane or differences in the accessibility of Pal for the anti-HA antibodies in comparison to the two standard proteins. Nevertheless, the quantification should therefore be repeated with purified Pal as a standard to assure the result of the described quantification.

Table 3.4: Quantification of Pal at two different growth stages using CARHSP1 and a multiple tag fusion protein as standards
Cultures of TN72_SR_*pal-HA* were grown under standard conditions to an OD_{750nm} of 2 and 3.8; the cells were broken by the addition of SDS (2% w/v) and boiling. Dilution series of CARHSP1 or the multiple tag fusion protein were analysed together with two dilutions of TN72_SR_*pal-HA* whole cell extract on the same gel and membrane in western blot analyses with anti-HA antibodies and IRDye® secondary antibodies. Standard curves of quantities of the standard protein against the IR fluorescence signal of the Odyssey® Infrared Imaging System were used for the quantification of Pal, taking the lower molecular weight of Pal into account (see figure 3.15). The percentage of total soluble protein was determined with *C. reinhardtii* soluble protein extract gained after centrifugation at 13,000 *x g* for 15 min. The standard deviations (±) are stated (n = x).

Standard protein	OD_{750nm} of culture	Pal (mg) / L culture volume	Pal (mg) / g of cell dry weight
CARSHP1 as standard	**2**	6.5 ± 0.8 (n = 4)	12.6 ± 0.7
	3.8	9.6 ± 1.6 (n = 4)	NA
Multiple tag fusion protein as standard	**2**	7.2 ± 0.8 (n = 4)	14.0 ± 0.7
	3.8	10.6 ± 5.0 (n = 4)	NA

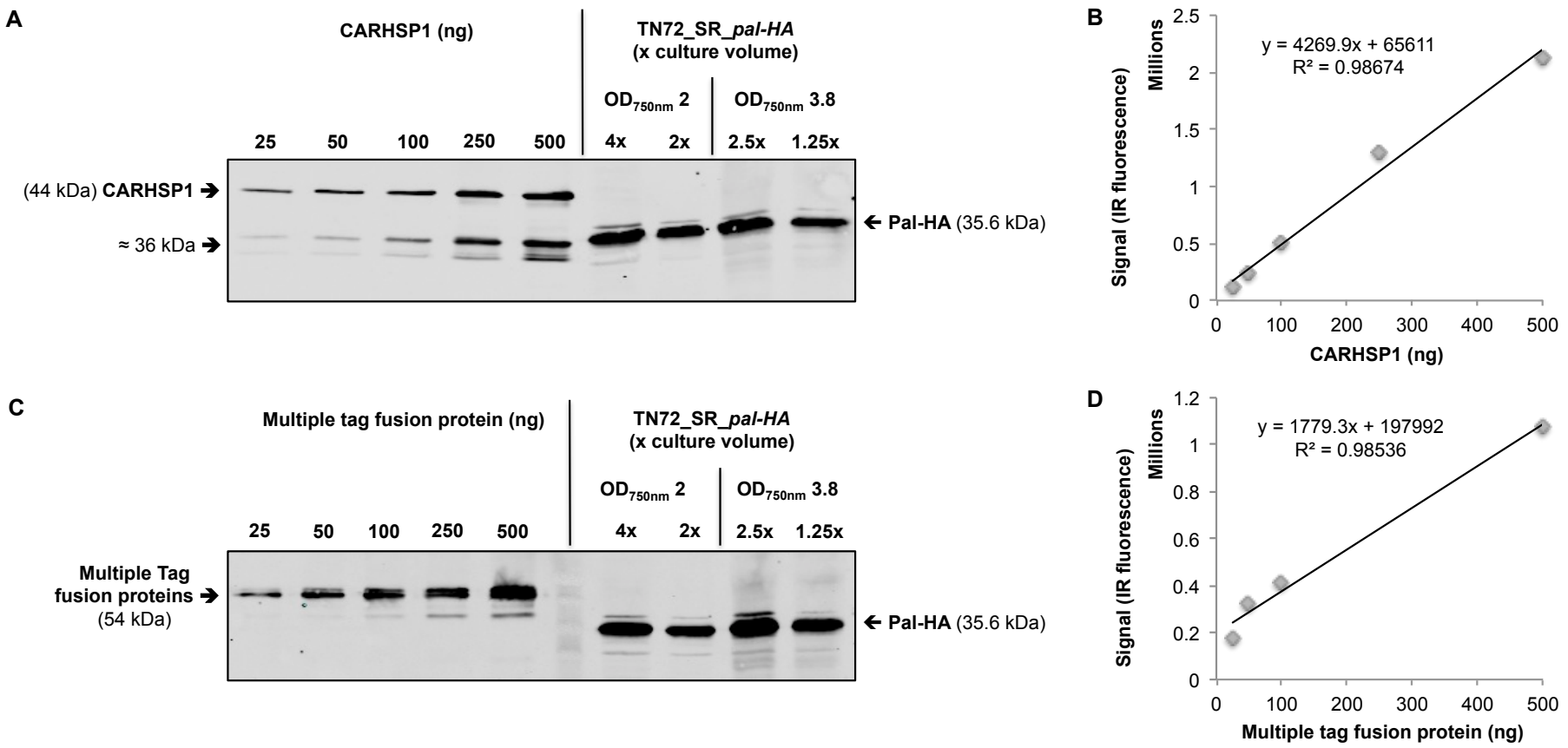

Figure 3.16: Quantification of Pal in whole cell extracts of TN72_SR_*pal-HA* using purified CARHSP1 (A, B) and multiple tag fusion protein (C, D) and the Odyssey® Infrared Imaging system

Cultures of TN72_SR_*pal-HA* were grown under standard conditions to an OD_{750nm} of 2 and 3.8; the cells were broken by the addition of SDS (2% w/v) and boiling. Dilution series of CARHSP1 or the multiple tag fusion protein were analysed together with two dilutions of TN72_SR_*pal-HA* whole cell extract on the same gel and membrane in western blot analyses with anti-HA antibodies and IRDye® secondary antibodies (A, C). Standard curves of quantities of the standard protein against the IR fluorescence signal of the Odyssey® Infrared Imaging System were used for the quantification of Pal, taking the lower molecular weight of Pal into account (B, C).

3.3 Conclusion and future work

The study described in this chapter investigated the synthesis of the endolysin Pal, a potential candidate for use as a novel antibiotic against *S. pneumoniae*, in the *C. reinhardtti* chloroplast to evaluate its suitability as a novel expression platform.

Transgenic lines with a transgene encoding Pal inserted in the plastome were created, both with and without a HA-tag and under the control of two different promoters/5'UTRs. Subsequently the expression of *pal* was confirmed with anti-HA antibodies and specific anti-Pal antibodies. Furthermore these western blot analyses showed that no degradation products accumulate to detectable levels in the *C. reinhardtii* chloroplast, whereas an analysis of *E. coli* DH5α expressing *pal* showed that degradation products accumulate to even higher levels than full-length Pal protein in the bacterium. The choice of promoter/5'UTR element was found to have a marked effect on *pal* expression and a comparison of two elements (those from *atpA* and *psaA* exon 1) that had shown high levels of recombinant protein in previous studies (Purton et al. 2013; Michelet et al. 2011) revealed that the expression of *pal* is three to ten times higher under the influence of the *psaA* exon 1 compared to the *atpA* promoter/5'UTR.

Growth studies showed that the accumulation of Pal in the chloroplast does not have a negative impact on the growth of *C. reinhardtii* proving that the endolysin does not have a toxic effect on *C. reinhardtii.* In contrast, a toxic effect of Pal for *E. coli* was reported by Oey et al. (2009b) and is further discussed in chapter 6.

The synthesis of Pal was subsequently investigated during mixotrophic growth in acetate containing medium, since the highest growth rates and cell densities can be reached under these conditions in batch cultivation (Harris 2009) and these conditions consequently also result in the highest yields of recombinant protein per culture volume (Braun Galleani 2014). The study showed that the yield of Pal protein per cell is highest in the logarithmic phase under these conditions and that production, dilution and degradation of Pal are at equilibrium in this phase. Upon entry into the stationary

phase, the amount of Pal per cell decreases by about 60%. Transferring the culture into the dark can limit this decrease, indicating that the protein degradation in the stationary phase is partially light depended. Nevertheless, cultures that were grown in the dark from the start only reached approximately one third of the final OD_{750nm} that mixotrophic cultures achieved, and had therefore 40 – 70% (depending on the growth stage) lower yields of Pal per culture volume, despite of the reduced protein degradation.

These findings indicate that the best strategy for obtaining maximal yields of Pal protein per culture volume in batch cultivation is mixotrophic cultivation and harvesting of the cells at the end of the logarithmic phase. The start of the stationary phase and the final cell density of *C. reinhardtii* cultures is influenced by the quality of light penetration and can therefore vary with the culture volume, the speed of mixing and the light intensity, and therefore needs to be determined individually for every cultivation set up. An alternative for large-scale production is the cultivation of *C. reinhardtii* in continuous cultures, in which fresh media continuously replaces used media and cells. The previous results suggest a flow rate that keeps the culture in the late-logarithmic phase would result in the highest yields during continuous cultivation. Nevertheless, the optimal conditions for continuous cultivation and other specific set ups need to be individually determined.

The cultivation of *C. reinhardtii* in the dark for the production of Pal is nevertheless an interesting option for large scale cultivation (Chen & Johns 1996a), since it makes it possible to use established fermentation vessels that are used for the growth of bacteria or yeast. Furthermore it makes the installation of growth lights dispensable and it is not necessary to use transparent materials and vessels with a small diameter to ensure sufficient light penetration of the culture. This might decrease the costs for the set up of the culture facilities and the costs of cultivation enough to compensate for the lower Pal yields gained during heterotrophic batch cultivation. Furthermore, continuous heterotrophic cultivation can increase the yield of biomass to up to 1.5 g per litre of culture volume (Chen & Johns 1996a). Alternatively, the biomass yields of heterotrophic cultures can be increased in fed-batch cultures or to a even higher

degree (up to 9 g per litre) in hollow-fibre cell-recycle systems (HFCRS), in which the media is replaced without cell removal (Chen & Johns 1996b).

In this chapter, the stability and degradation of Pal in the chloroplast was investigated by inhibiting the protein synthesis by chloramphenicol. This experiment showed that Pal is able to withstand degradation processes for up to 122 h in both the light and the dark unlike the endogenous protein D1 or the human growth hormone proving that Pal exists as a remarkable stable protein in the *C. reinhardtii* chloroplast and indicates that Pal has a high degree of resistance to the proteolytic processes in the plastid.

Furthermore it illustrated once more that the amount of Pal per cell stays at a higher level in cultures that are transferred to the dark. This observation indicates that the degradation of Pal is slowed down in the dark, this could be caused by a drop of stromal ATP levels, which decreases the activity of energy-dependent proteases (Preiss et al. 2001; Harris 2009). These results might help to narrow down which proteases in the *C. reinhardtii* chloroplast are involved in the degradation of Pal and other recombinant proteins. This knowledge could be useful for the identification of possible candidates for specific knockouts or knockdowns of nuclear genes encoding energy-dependent proteases with the aim of increasing the yields of recombinant protein. However, it is also conceivable that UV light has a negative impact on the stability of Pal (Teresa et al. 2012).

To be able to compare quantitatively the levels of different recombinant proteins produced in the *C. reinhardtii* chloroplast, and to compare the production of Pal to that in conventional expression systems, a quantification was performed using two different HA-tagged standard proteins. This quantification revealed a maximal yield of recombinant Pal protein of about 10 mg per litre of culture volume, and that Pal accounts for about 13 mg per g of cell dry weight in the logarithmic phase, which is comparable to a recent study that produced bovine Milk Amyloid A (MAA) in the *C. reinhardtii* chloroplast at pilot greenhouse scale. The quantification in this study was performed with two different standard proteins to ensure no protein specific differences occurred in western blot analyses. However, the quantification should be further improved by using purified Pal as a standard, thus ensuring that the Pal protein

does not behave differently in western blot quantifications in comparison to the two standard proteins.

Taken together, the results of this study suggest that the *C. reinhardtii* chloroplast can be used as a suitable production platform for the endolysin Pal, since reliable expression of predominantly full-length Pal, with a high stability was achieved. In contrast, expression in *E. coli* DH5α resulted in an accumulation of mainly degradation products compared to full-length protein. Nevertheless, it is of great importance that the recombinant Pal protein is fully active against the target bacterium *Streptococcus pneumoniae.* This is investigated, together with strategies for the purification of Pal, in chapter 4.

4 Purification of *Chlamydomonas reinhardtii*-produced Pal and analysis of its antimicrobial activity against *Streptococcus pneumoniae*

4.1 Introduction

4.1.1 Previous studies investigating the antimicrobial activity of the endolysin Pal

Different research groups have studied the antimicrobial activity of *E. coli*-produced Pal. Loeffler et al. (2001) showed that Pal is effective in killing 15 different clinical isolates of *S. pneumoniae* including three penicillin resistant strains, while the endolysin does not affect the commensal *Streptococcus* strains *S. gordonii, S. mutans, S. salvarius, S. intermedius, S. crista* and *S. parasanguis,* even when they were challenged with 100 times higher dosages. Pal had also an effect on exponentially growing *S. oralis and S. mitis* strains, but at a significantly lower rate compared to *S. pneumoniae*. The study also showed that a capsule-deficient strain (R36A) and a mutant lacking a capsule and the major pneumococcal autolysin LytA (Lyt 4-4) have identical susceptibilities to Pal as the clinical isolates. Loeffler et al. concluded that the capsule of *S. pneumoniae* does not hinder Pal from accessing the cell wall and that LytA does not play a significant role in the lysis caused by Pal. Furthermore, Loeffler et al. (2001) performed electron microscopy with *S. pneumoniae* cells exposed to Pal. After one minute of exposure to Pal, protrusions of the cytoplasmic membrane and the cytoplasm were clearly visible and five minutes later only empty cell walls remained.

Loeffler & Fischetti (2003), Jado et al. (2003) and Rodríguez-Cerrato et al. (2007) have described a synergistic effect of Pal in combination with another *S. pneumoniae* specific endolysin Cpl-1. In the latter study, the chequerboard technique (Lorian 2005) - a method in which combinations of substances are tested at different concentrations in microtiter plates - was used to analyse synergistic effects between Pal, Cpl-1, LytA

and the antibiotics cefotaxime and moxifloxacin. The study determined minimal inhibitory concentration (MIC) values for Pal of 32, 32, 128 and 256 mg/L for four different clinical isolates of *S. pneumoniae*. The chequerboard technique revealed synergy for Pal and Cpl-1 for three out of four strains and values very close to synergy for Pal and LytA for all strains, but no synergistic effect was observed for Pal and the two antibiotics and no antagonism for any of the substances. In time-kill assays, which analysed a decrease in colony forming units (cfu) over a time course *in vitro*, Pal and the combination of Pal with LytA decreased the cfu titres by more than two or 3 three log units, respectively.

Another study indicated that Pal can kill bacteria within biofilms without affecting the structure of the biofilm (Domenech et al. 2011). Domenech et al. reported as well that the pH optimum of Pal is between 6.0 and 9.0. The optimum temperature for the enzyme activity of Pal is 37°C and the specific enzyme activity of Pal determined by Domenech et al. using an assay with radioactively labelled purified cell walls was 3.4 x 10^4 units/mg[1].

The first study describing Pal isolated from *S. pneumoniae* cells infected by the bacteriophage Dp-1 showed that the activity of Pal is inhibited by temperatures of 50°C and above, the pneumococcal Forssman antigen (1 µg/ml), cardiolipin (IC_{50} > 50 µg/ml), 0.1% (w/v) deoxycholate, 0.1% (w/v) SDS, proteases such as trypsin, pronase E and proteinase K (50 µg/ml), as well as 10 mM $CaCl_2$, $FeSO_4$, $CuSO_4$, $ZnCl_2$, $HgCl_2$, while 10 mM of LiCl, NaCl and KCl or 1% (w/v), whereas Triton X-100 did not affect the activity (Garcia et al. 1983a). This study observed also a strong stimulating effect of DTT (10 mM) on the activity of Pal. Nevertheless, this effect was only observed with Pal isolated from Dp-1 infected pneumococci, but not recombinant Pal produced in *E. coli* (Sheehan et al. 1997).

Two animal studies have been conducted so far with *E. coli*-produced Pal. In the study by Loeffler et al. (2001), Pal was tested in a mouse model of nasopharyngeal

[1] Domenech et al. (2011) One unit of enzymatic activity is defined as the amount of enyzyme that catalyses the hydrolysis of 1 µg of pneumococcal cell walls in 10 min using cell walls that are radioactively labeled with [*methyl*-^{3}H]choline.

colonization. Intranasally infected mice were treated by one nasal and pharyngeal wash 42 h after infection with 1400 units[2] of Pal. The treatment with Pal decreased *S. pneumoniae* cfu to undetectable levels within 5 h, whereas high levels of cfu were found in the untreated controls. The same treatment with 700 units eliminated *S. pneumoniae* from five of eight mice and strongly decreased titers in the other three.

Furthermore, pneumococci were exposed to low concentrations of Pal (<1 U) on agar plates for 16 rounds or to increasing concentrations in liquid cultures for three rounds in this study. The exposed cells did not shown any difference in the susceptibility to Pal in an *in vitro* assay compared to unexposed cells indicating that the occurrence of resistance against Pal is a rare event. Loeffler et al. (2001) explained these findings by the fact that Pal evolved to bind to choline in the pneumococcal cell wall and the presence of this molecule is critical for *S. pneumoniae.* The replacement of choline in the pneumococcal cell wall by ethanolamine results in marked changes of the cell physiology (López et al. 1997). Loeffler et al. concluded that *S. pneumoniae* cells on mucosal membranes are highly susceptible to the action of the lytic enzyme Pal. The mucosal membranes in the nasopharynx are seen as a major reservoir for *S. pneumoniae* in the population and the diminution of this reservoir would have a great impact on the incidence of *S. pneumoniae* infections. So far there are no treatments available to eliminate *S. pneumoniae* colonization on mucous membranes in humans without harming the beneficial bacterial flora. Loeffler et al. anticipate that Pal and similar endolysins are promising candidates to control nasopharyngeal carriage and thereby reduce the prevalence of *S. pneumoniae* infections.

Jado et al. (2003) used a murine sepsis model, in which mice were injected intraperitoneally with a serotype 6B clinical isolate of *S. pneumoniae* with resistances to β-lactam, tetracycline, chloramphenicol and erythromycin antibiotics. Single doses of 40 µg of Pal 10 minutes after the bacterial challenge (5×10^7 cfu, a dose with a 100% mortality rate) or 200 µg one hour after the bacterial challenge, resulted in the full recovery of all mice. The bacterial titres in the blood of the mice dropped by ≈4

[2] Loeffler et al. (2001) One unit of Pal is defined as the reciprocal of the highest dilution, which caused 50% decrease in absorbance after 15 minutes incubation at 37°C, as compared with the absorbance of the control, in a turbidity reduction assay (OD_{600nm} 1.3) with equal volumes of *S. pneumoniae* suspension and Pal solution.

log units two hours after injection and were completely cleared after four to five days. No toxic effects were observed upon intraperitoneally administration of 200 µg of Pal. Heat-inactivated Pal did not rescue the mice challenged with *S. pneumoniae* proving that the observed effect is enzyme-specific. A dose of 10 µg was found to be the minimal effective dose, which rescued two to three out of four mice. The synergy of Pal and Cpl-1 was confirmed *in vivo* in this study, since 2.5 µg of Pal together with 2.5 µg of Cpl-1 rescued 100% of the infected mice, whereas 5 µg of Pal or Cpl-1 alone did not protect the mice (Jado et al. 2003).

Furthermore, the immune response 10 days after the injection of Pal was analysed, and it was found that the titres of specific IgG antibodies to the *S. pneumoniae* serotype 6B polysaccharide were eight times higher in hyperimmune compared to preimmune serum. Additionally, the immune serum from the mice was shown to be active against Pal in western blot analyses. However, mice that got a second bacterial challenge and Pal treatment ten days after the first all recovered indicating that the immune response does not decrease the activity of Pal *in vivo*. Furthermore, no signs of anaphylaxis or adverse side effects were observed. Taken together, this makes the endolysin Pal a promising candidate for use as a novel, highly specific antibacterial agent against *Streptococcus pneumoniae.*

4.1.2 Aims and Objectives

The aim of the experiments presented in this chapter was to analyse the endolysin Pal produced in the *C. reinhardtii* chloroplast to see if it shows a specific lytic and bactericidal activity against *S. pneumoniae*, including clinical isolates. This was followed by a quantification and characterisation of the antimicrobial activity. Furthermore, different strategies for the purification of Pal were investigated to be able to analyse the antibacterial activity of *C. reinhardtii*-produced Pal without the interference of other cell components. During the performance of these experiments a strong antibacterial activity of *C. reinhardtii* extracts against *S. pneumoniae* was observed and partly characterised.

4.2 Results and discussion

4.2.1 Production of Pal protein preparations for the performance of activity assays

4.2.1.1 The cell wall less *C. reinhardtii* strain TN72 can be broken by simple mechanical methods

For initial western blot analysis confirming and analysing the synthesis of Pal in the *C. reinhardtii* chloroplast, cells were broken by the addition of 2% SDS (w/v) and boiling. For the performance of activity assays, it was necessary to break the cells and recover Pal without denaturing the enzyme. The *C. reinhardtii* strain TN72 lacks an intact cell wall and is therefore more sensitive to mechanical and osmotic damage than walled strains. A cell wall-less background was specifically chosen for the recipient strain TN72 to enable transformation using the simple and quick glass bead method, which is very inefficient for the transformation of cell-wall containing strains. Accordingly, the lack of a cell wall should also be an advantage for cell breakage and the extraction of Pal using simple mechanical methods. For initial antimicrobial activity assays, algal extracts were applied onto nutrient agar plates followed by overnight incubation. Therefore it was desired to keep the extracts sterile during preparation. A few simple mechanical methods that do not risk the contamination of the extracts were therefore tested to determine whether they can lyse the cells and whether Pal can be recovered and separated from the cell debris afterwards.

TN72*_pal-HA* cells were broken by freezing in liquid nitrogen, thawing at 30ºC and vortexing (ten seconds) for three or six cycles (F+T), in one case followed by grinding with a pestle. Alternatively, the cells were incubated in a sonication bath for 15 minutes. Both methods (except for the pestle treatment) can be done in enclosed tubes preventing contamination, which can easily occur using cell breakage equipment such as a cell disrupter or French pressure cell press.

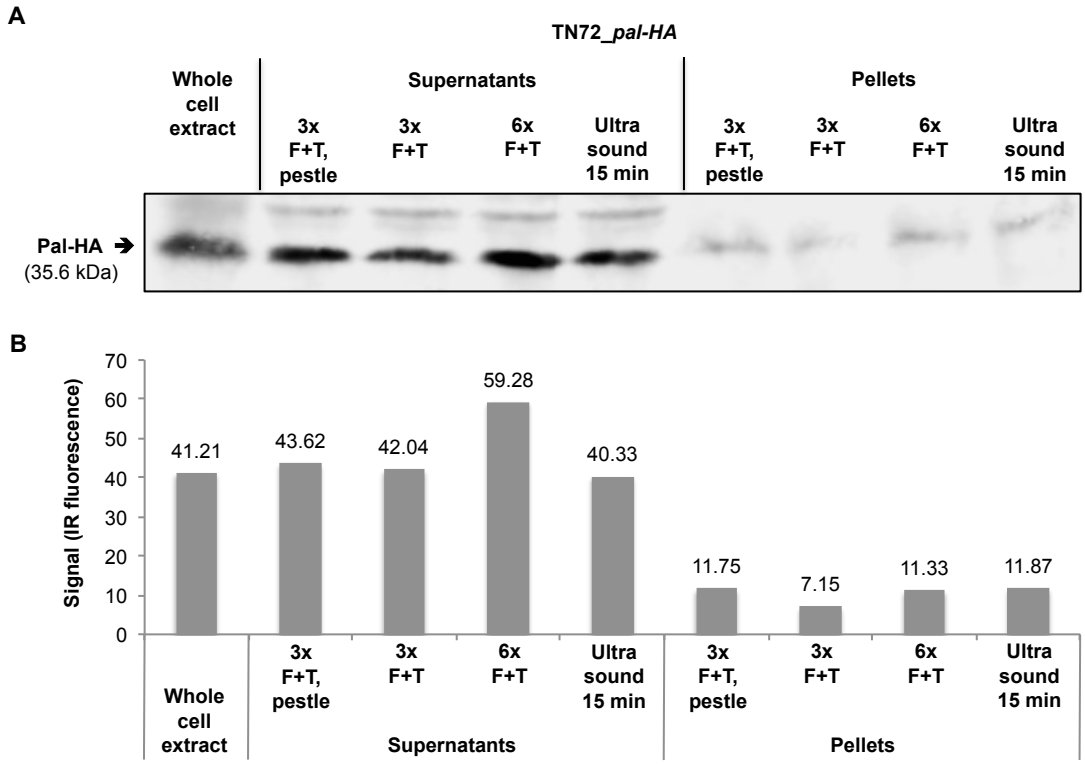

Figure 4.1: Western blot analysis showing the recovery of Pal in the supernatant after different methods of cell breakage and centrifugation
Tn72*_pal-HA* cells were broken by freezing in liquid nitrogen, thawing at 30ºC and vortexing for 10 sec (F+T) for three or six cycles, in one case followed by grinding with a pestle. Alternatively, the cells were put into a sonication bath for 15 min. Subsequently cells were centrifuged at 21,000 x *g* for 2 min. The presence of Pal in the supernatants and the pellets were determined by western blot analysis with anti-HA antibodies, IRDye® secondary antibodies and the Odyssey® Infrared Imaging system. A shows the western blot picture and B shows the corresponding Odyssey IR fluorescence signals.

After breakage, the cells were centrifuged (21,000 *x g*, 2 min) to pellet cell debris. The presence of Pal in the supernatants and the pellets was determined by western blot analysis. Prior to that, the pellets were resuspended in the previous volume of fresh buffer and these samples were additionally treated with SDS and boiling to break leftover unbroken cells. All four methods (three cycles of F+T, three cycles of F+T plus pestle treatment, six cycles of F+T, sonication bath) were sufficient to recover the majority of Pal in the supernatant (70 to 83% (comparison between the amount of Pal in the supernatants and in the pellets regarding to the signal values of the Odyssey system)) showing that the cell-wall less strain TN72 can be easily broken by simple mechanical methods (Figure 4.1, Figure 4.16). The presence of Pal in the cell pellets is presumably caused by a portion of unbroken cells or an insoluble fraction of Pal.

The cells that had been broken by three cycles of freezing and thawing were additionally examined with a light microscope before and after breakage. Before breakage the vast majority of cells were clearly visible as round and intact cells, whereas the vast majority of cells were broken into pieces or showed an irregular shape after freezing and thawing indicating that the treatment was sufficient to break the cells (Figure 4.2).

Three cycles of freezing and thawing was used routinely in the following assays in this chapter, since the western blot analysis indicated a recovery of approximately 80% of Pal into the supernatant. Furthermore, it is a quick and easy method that prevents contamination of the protein preparations. The whole extracts were routinely frozen additionally in aliquots at -20ºC for storage and as a first step of breakage. The supernatant obtained after breakage and centrifugation is referred to as "crude extract" in the following sections.

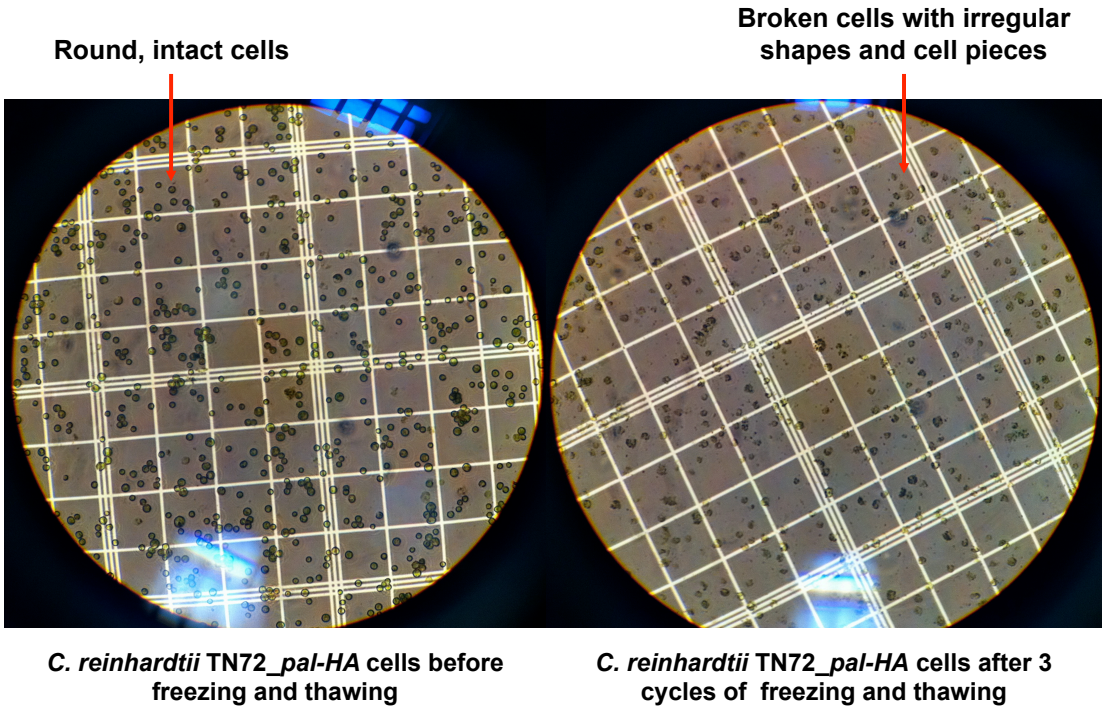

Figure 4.2: Microscopy of *C. reinhardtii* TN72_*pal-HA* cells before and after breakage by freezing and thawing
Cells were frozen in liquid nitrogen, thawed in a 30ºC water bath and vortexed for 10 seconds for three cycles. The cells were analysed before and after treatment with an Olympus microscope at 400x magnification.

4.2.1.2 Production of protein preparations can be done at high cell densities

For the performance of assays analysing the antimicrobial activity of Pal, it was of interest to produce protein preparations with a high concentration of Pal. However, a previous study had shown that the endolysin Cpl-1 precipitates and cannot be recovered in the supernatant when suspensions of TN72_(SR)_*cpl-1-HA* with high cell densities were used for cell breakage (Taunt 2013). Suspensions of whole cells that were concentrated more than 5x the culture volume resulted in lower amounts of Cpl-1 in the supernatant compared to less concentrated suspensions and concentrations of 100x the culture volume caused complete precipitation of Cpl-1 to the pellet after breakage (Taunt 2013). The recovery of Pal into the supernatant after the breakage of TN72_SR_*pal-HA* by freezing and thawing was therefore analysed at different cell densities.

TN72_SR_*pal-HA* cultures were grown to an OD_{750nm} of 2.0, harvested and concentrated to different cell densities (100x, 50x, 10x and 5x the culture volume). Subsequently the cells were broken by freezing and thawing (three cycles), followed by centrifugation at 21,000 x *g* for 5 min. The amount of Pal in the whole cell extracts before centrifugation and in the supernatants (= crude extracts) after breakage and centrifugation was determined by western blot analysis with anti-HA antibodies. The samples were additionally treated with SDS and boiling to ensure that all cells in the whole cell extract are broken. Just before the samples were loaded onto the western blot, all samples were diluted to the same cell density (to 5x the culture volume) to ensure that the samples are analysed within the linear range of the detection method and to make it easier to compare them afterwards. The western blot analyses showed similar amounts of Pal in the supernatants at all densities, indicating that the cell density within the analysed range does not have any influence on the solubility and therefore the recovery of Pal into the supernatant after cell breakage and centrifugation (Figure 4.3).

Furthermore, the amount of Pal in the whole cell extracts before centrifugation (which were additionally broken by SDS and boiling) and in the supernatant fractions after centrifugation were found to be similar. These results confirm that freezing and

thawing for three cycles is a suitable method for the cell breakage of *C. reinhardtii* TN72 and the recovery of Pal. These western blot analyses also indicated that the treatment with SDS and boiling does not improve the cell breakage and recovery of Pal. Only the supernatant of the 50x culture volume sample contained about 30% less Pal than the corresponding whole cell extract.

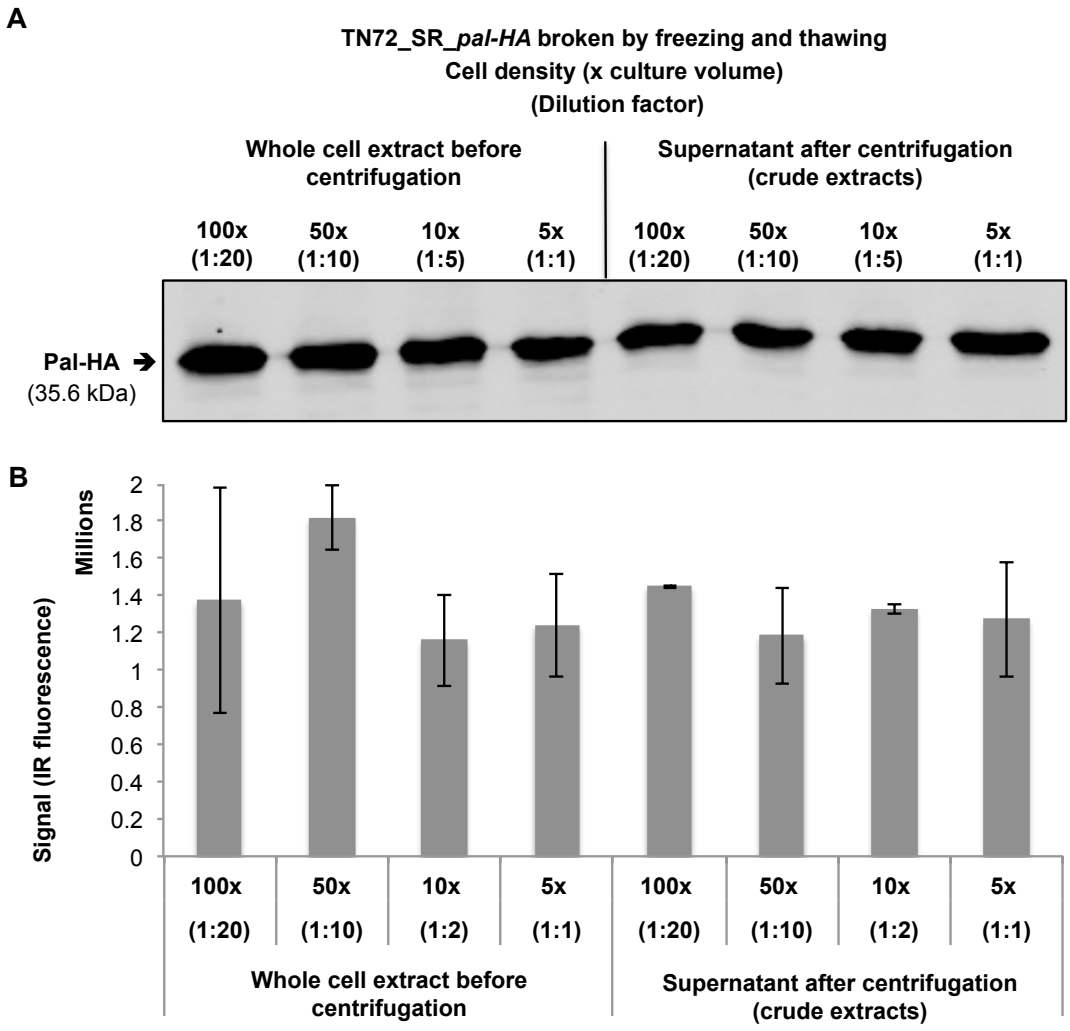

Figure 4.3: Western blot analysis showing the recovery of Pal in the supernatant after cell breakage by freezing and thawing at different cell densities
TN72_SR_*pal-HA* cultures were concentrated to different cell densities and broken by freezing in liquid nitrogen, thawing at 30ºC and vortexing for 10 sec for three cycles, followed by centrifugation at 21,000 x *g* for 5 min. The presence of Pal in the whole cell extracts before centrifugation and in the supernatants after breakage and centrifugation was determined by western blot analysis with anti-HA antibodies, IRDye® secondary antibodies and the Odyssey® Infrared Imaging system was used for detection (A) and for quantification (B). The expected band size for Pal-HA is 35.6 kDa. The error bars show ± one standard deviation (n = 2).

4.2.2 Antimicrobial activity of Pal against *S. pneumoniae*

Expression of a recombinant protein in a different expression system can result in changes or even abolishment of the activity, since for example reductant levels, availability of cofactors and the protein folding as well as the proteolytic machinery vary in different organisms. It was therefore of great importance to show that the Pal protein produced in the *C. reinhardtii* chloroplast exhibits full antimicrobial activity against the target bacterium *Streptococcus pneumoniae*. Therefore the bacteriolytic and bactericidal activity of Pal was analysed and quantified, and the findings are discussed in the following sections.

4.2.2.1 Bacteriolytic activity of Pal-HA in crude extracts of *C. reinhardtii*

Pal cleaves the peptidoglycan of the *S. pneumoniae* cell wall between the L-alanine of the peptide chain and the *N*-acetyl-muramic acid of the sugar strand, which results in a rapid cell lysis and subsequent death of the cell (Loeffler et al. 2001). As lysed cells make a significantly lower contribution to the light scattering (measured as 'optical density' = OD) of a suspension than do intact cells, the activity of a lytic enzyme can be measured as a decrease in OD. This type of assay is often referred to as turbidity reduction assay (TRA) and has been used in several studies to measure the lytic activity of endolysins (Schmelcher et al. 2012). The antimicrobial activity of Pal produced in the *C. reinhardtii* chloroplast was therefore analysed by measuring its lytic activity using TRAs.

Cells of a *S. pneumoniae* culture were harvested and resuspended in NaPi-buffer, before the addition of crude algal extracts from either TN72_SR_*pal-HA* or TN72_SR_control. Subsequently, the OD was measured at 600 nm in 1 ml cuvettes or 595 nm in 96-well plates using a plate reader over a time course. During the first performances of the TRAs, it was observed that the OD decreased over time without the addition of crude extracts or in the presence of the control extracts. *S. pneumoniae* produces autolysins, which lyse the cells in the stationary phase and play a role in the

virulence of *S. pneumoniae* (Berry et al. 1989; Mellroth et al. 2012). The observed decrease of the OD was therefore most likely caused by the autolysis of the cells. It was found that cells from overnight cultures, where a high proportion of cells had already reached the stationary phase, lysed much faster than cells in the logarithmic phase (data not shown). *S. pneumoniae* cells were therefore grown in overnight cultures, sub-cultured the following morning and grown for six hours before the performance of the TRAs, to ensure that the cells are in the logarithmic phase. The TRAs performed with the TN72_SR_*pal-HA* crude extracts showed a more rapid decrease of the OD compared to the negative controls, confirming the lytic activity of *C. reinhardtii*-produced Pal in crude extracts against *S. pneumoniae* (Figure 4.4).

The decrease in OD plateaued in all TRAs after a certain amount of time and never decreased to an OD value close to zero (Figure 4.6 A). Looking at figure 2 in Loeffler et al. (2001), it is not surprising that the OD did not decrease completely to zero, since empty cell walls remain after the lysis of *S. pneumoniae* by Pal, which still contribute to the optical density of the solution. To be able to determine if the residual OD is caused by empty cell walls or by residual intact cells, the bile salt detergent deoxycholate (0.05% w/v) was used as a positive control and to determine the maximal possible decrease in OD of a *S. pneumoniae* suspension. Deoxycholate induces the rapid autolysis of *S. pneumoniae* cultures already in the stationary phase (Mellroth et al. 2012). The activation of the autolysis by deoxycholate is specific to *S. pneumoniae* and is used in the diagnostic to distinguish it from other alpha-hemolytic *Streptococcus* strains (Neufeld 1900; Avery & Cullen 1920). A concentration of 0.05% (w/v) deoxycholate was chosen, because it was effectively used in other studies for the lysis of *S. pneumoniae* (Park et al. 2007). However, an analysis of *S. pneumoniae* lysis by deoxycholate at three different concentrations (0.0125%, 0.025% and 0.05% w/v) during this study did not show a difference in the speed or efficiency of the lysis (data not shown).

The described assays were performed with crude extracts that had been prepared from cell suspensions concentrated to 100x of the culture volume. The assay shown in Figure 4.4 was performed with 20 µl of crude extract, which contained approximately

5 µg of Pal protein, in a 200 µl reaction. This amount of Pal was sufficient to decrease the OD to nearly the same extent as the addition of deoxycholate (0.05% w/v).

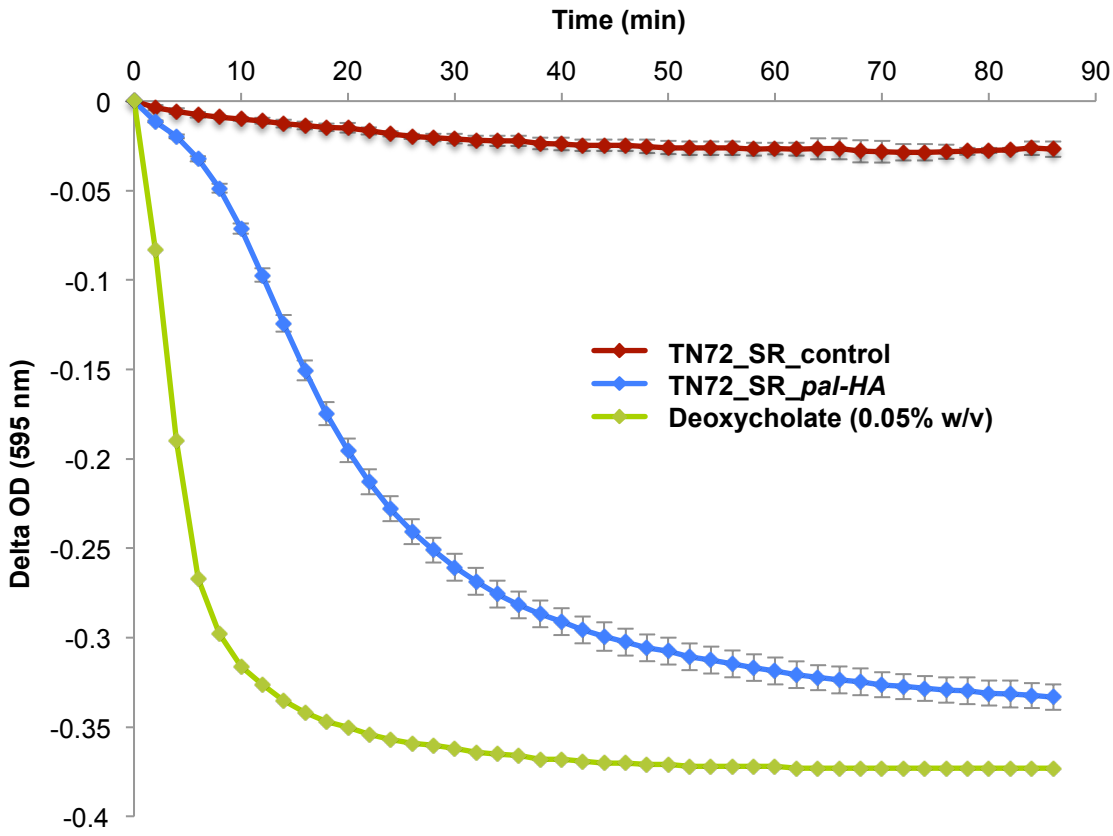

Figure 4.4: Turbidity reduction assay showing the lytic activity of Pal-HA in crude extract of *C. reinhardtii* against *Streptococcus pneumoniae*
S. pneumoniae cells were resuspended in NaPi-buffer to an optical density (OD_{595nm}) of 0.45 in a 96-well plate. *C. reinhardtii* TN72_SR_*pal-HA* or TN72_SR_control crude extract (= supernatant after cell breakage and centrifugation at 21,000 x *g* for 5 min) was added (20 µl with approximately 5 µg Pal protein) to the cell suspension in a 200 µl reaction and the OD_{595nm} was measured over a time course of 90 min. Deoxycholate (0.05% w/v) was used as a positive control. The assays were performed at 37ºC. The error bars show ± one standard deviation (n = 3).

4.2.2.2 Bacteriolytic activity of untagged Pal against *S. pneumoniae*

The addition of N- or C-terminal tags can reduce or eliminate the activity of enzymes in some cases *e.g.* by hampering the correct folding (Economou, unpublished; Rehm 2006). It was therefore important to analyse the activity of untagged Pal compared to HA-tagged Pal. For this purpose the strain TN72_SR_*pal-x* was created, which

synthesizes Pal without the addition of a tag. Western blot analysis with anti-Pal antibodies confirmed similar expression levels of Pal in TN72_SR_*pal-x* and TN72_SR_*pal-HA* (Figure 3.8). Subsequently TRAs were performed with *C. reinhardtii* crude extracts of TN72_SR_*pal-HA,* TN72_SR_*pal-x* and as a negative control Tn72_SR_control. In the assays with TN72_SR_*pal-HA* and the ones with TN72_SR_*pal-x* crude extract the OD_{595nm} decreased at the same rates and to a similar extent during the time course (Figure 4.5). The assay was repeated five times with different preparations of crude extracts and different cultures of *S. pneumoniae*, but no difference between TN72_SR_*pal-HA* and TN72_SR_*pal-x* was observed indicating that the HA-tag does not interfere with the lytic activity of Pal.

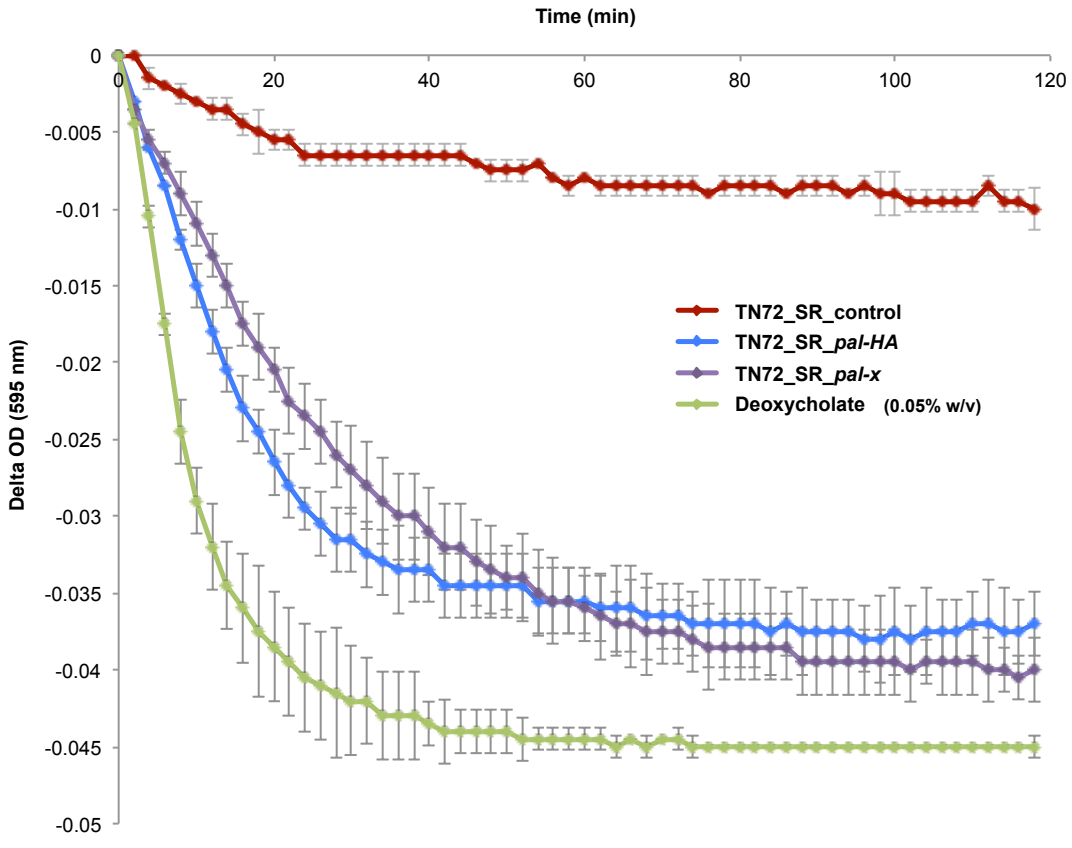

Figure 4.5: Turbidity reduction assay showing the lytic activity of *C. reinhardtii*-produced HA-tagged Pal and untagged Pal
S. pneumoniae cells were resuspended in NaPi-buffer to an optical density (OD_{595nm}) of 0.1. *C. reinhardtii* TN72_SR_*pal-HA,* TN72_SR_*pal-x* or as a control Tn72_SR_control crude extract was added to the cell suspension (20 µl crude extract (prepared from whole cell extract that had been concentrated to 100x the culture volume) in a 200 µl reaction) and the OD_{595nm} was measured. The error bars show ± one standard deviation (n = 2).

4.2.2.3 Specificity of *C. reinhardtii*-produced Pal

As discussed in the introduction, endolysins are generally very specific for the host species of the corresponding bacteriophage. In particular, endolysins targeting Gram-positive bacteria are often only effective against one or a few species of bacteria or even specific only against certain sub-species (Fischetti 2005). Pal produced in *E. coli* has been shown to lyse 15 strains of *S. pneumoniae,* while it showed no activity against commensal *Streptococcus* strains including *S. gordonii, S. mutans, S. salvarius, S. intermedius, S. crista and S. parasanguis*. The study showed that it is able to lyse *S. oralis* and *S. mitis,* which contain choline in their cell walls, but at a lot lower rate than *S. pneumoniae* (Loeffler et al. 2001). Oey et al. showed that *E. coli*–produced Pal does not have any effect on *E. coli* when it is applied from outside to the cells, even when it seemed to have a toxic effect on *E. coli* when expressed in high concentrations inside the cell (Oey et al. 2009b).

To test the specificity of Pal produced in *C. reinhardtii*, TRAs were performed with *Escherichia coli, Streptococcus pyogenes* and *Staphylococcus aureus*. *C. reinhardtii* crude extract containing Pal, which caused a strong decrease in the OD_{600nm} of a *S. pneumoniae* suspension, did not have any spectrophotometrically measurable effect on live *E. coli* and *S. pyogenes* cells nor on a heat-inactivated suspension of *S. aureus* (Figure 4.6). These results indicate that *C. reinhardtii*-produced Pal shows also a high specificity for *S. pneumoniae* when it is applied from outside to the cells.

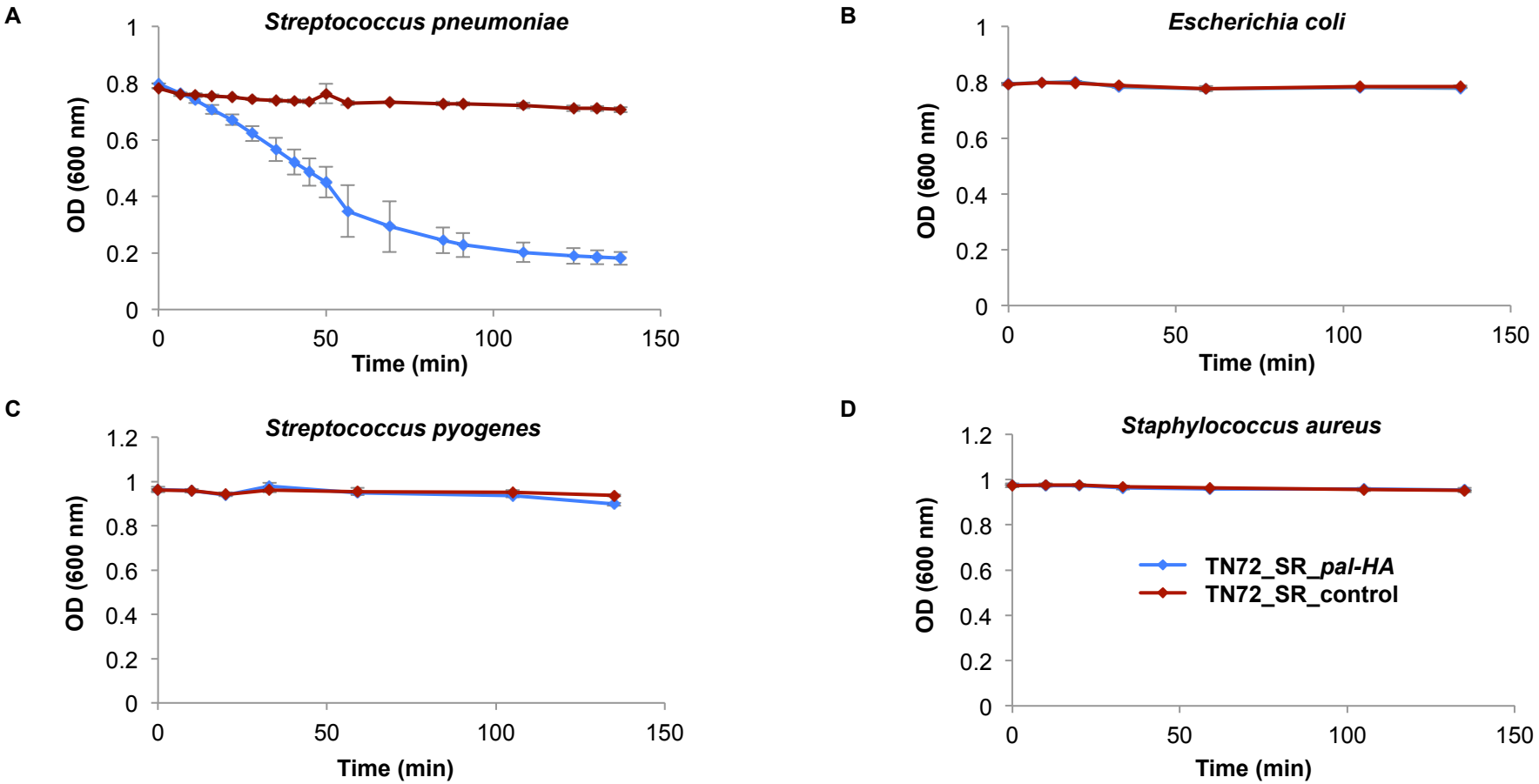

Figure 4.6: Turbidity reduction assays showing the specific lytic activity of Pal-HA produced in *C. reinhardtii* against *Streptococcus pneumoniae* (A) compared to *Escherichia coli* (B), *Streptococcus pyogenes* (C) and *Staphylococcus aureus* (D)

All strains were resuspended in NaPi-buffer to an optical density (OD_{600nm}) of 0.8. to 1.0. *C. reinhardtii* TN72_SR_*pal-HA* or TN72_SR_control crude extract (50 µl) (prepared from whole cell extract that had been concentrated to 100x the culture volume) was added to the cell suspension in a 1 ml reaction and the OD_{600nm} was measured over a time course of 150 min at room temperature. *S. aureus* cells had been heat inactivated at 80ºC for 10 min before the assay, the other species were used alive just after harvest. The error bars show ± one standard deviation (n = 2).

4.2.2.4 Quantification of the bacteriolytic activity of *C. reinhardtii*-produced Pal

After it had been demonstrated that Pal produced in the *C. reinhardtii* chloroplast shows lytic activity against *S. pneumoniae,* it was of interest to quantify the activity and to determine specific enzyme activities. It was important to compare the enzymatic activity of *C. reinhardtii*-produced Pal to *E. coli*- or tobacco-produced Pal to show that the algal-produced endolysin is fully active. Furthermore, quantification and standardisation facilitates the comparison of different conditions, different preparations of Pal and the comparison to other enzymes.

4.2.2.4.1 Determination of specific enzyme activities

Some of the previous studies that produced Pal in *E. coli* determined enzyme activities for the endolysin. However, most of these studies used different methods to analyse the antimicrobial activity of Pal and defined all their own units to quantify the activity (4.1.1), which makes it difficult to compare the enzyme activities in these studies with each other. In a review by Schmelcher et al. (2012) about bacteriophage endolysins, the authors raise the criticism that different labs use different assays and unit definitions, and emphasize the need for a standardization of assays and units. Schmelcher et al. cite Briers et al. (2007) as a good approach to standardize the quantification of murein hydrolase activity. The method of Briers et al. was therefore used in this study to quantify the activity of *C. reinhardtii*-produced Pal.

This method involves spectrophotometric turbidity reduction assays (TRA) with isolated peptidoglycan, whole cells or outer membrane-permeabilized Gram-negative cells as substrate. After the addition of the enzyme, in TRAs with an excess of substrate, an initial linear decrease of optical density occurs that gradually decelerates when the enzyme and/or the substrate becomes limited. The slope of the linear part of the decrease in turbidity is usually used as direct measure for the activity of an enzyme. Briers et al. criticize that there are often no specifications in the literature

how to define the linear region. Therefore they define the linear region in their method as the region with the data points that result in the highest determination coefficient (R^2) of a linear regression. The value of R^2 increases the more data points are included and decreases outside the linear region. Maximizing R^2 ensures therefore that the most reliable data set is used for the determination of the enzyme activity. The activity is then calculated using the corresponding slope of the linear regression and is expressed as a decrease in optical density per minute (ΔOD_{600nm}/min). The method takes into account the reaction volume and expresses the activity in units/mg enzyme. The formula is shown in Figure 4.7 A. The calculation of activity should be performed with different quantities of the enzyme, since in the presence of high amounts of enzyme a gradual saturation occurs and eventually the maximal activity of an enzyme is reached.

In this study, TRAs using *S. pneumoniae* cells from logarithmic phase cultures as described in 4.2.2.1 were performed to determine specific enzyme activities for Pal. The amount of enzyme used in the assays was determined in western blot analyses with the HA-tagged standard protein CARHSP1 as described in 3.2.4 and two dilutions of the analysed crude extract (Figure 4.7 C). Subsequently, the enzyme activities were calculated using the formula shown in Figure 4.7 A.

When the assays were performed with three different concentrations of TN72_SR*_pal-HA* crude extract (undiluted, 1:2, 1:10 corresponding to 5.2, 2.6 and 0.52 µg Pal in the reaction), a dosage dependency of the lysis reaction was observed (Figure 4.8). Furthermore, the different concentrations of crude extract containing Pal analysed in the same TRA resulted in comparable enzymatic activities with overlapping standard errors indicating that the amounts of enzyme used in the assay are within the dosage dependent and therefore linear range of the method (Table 4.2).

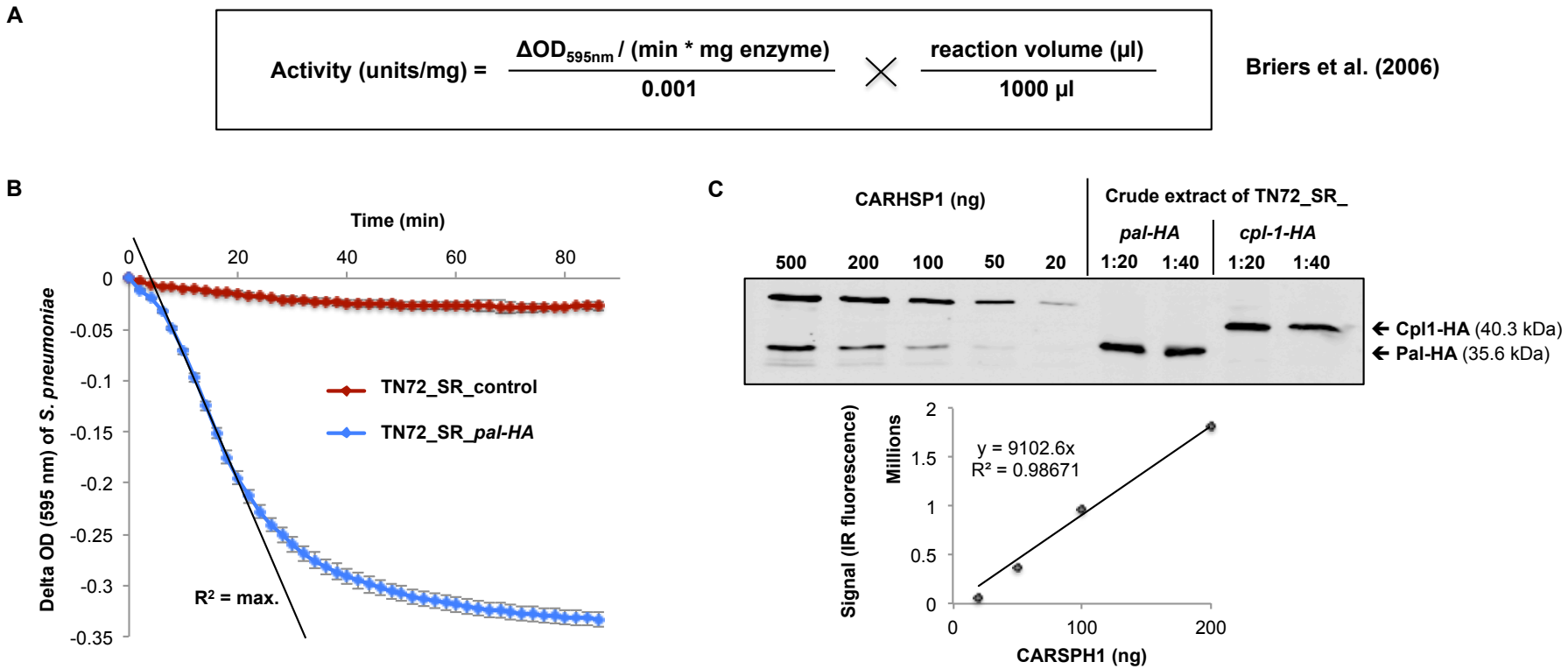

Figure 4.7: Determination of specific enzyme activities of Pal

The method described by Briers et al. (2006) was used to determine specific enzyme activities for Pal produced in *C. reinhardtii*. Briers at al. describe a standardized approach for accurate quantification of murein hydrolase activity (A). The method is based on turbidity reduction assays, in which the slope of the linear region of the drop in turbidity after the addition of the enzyme is used to determine the enzyme activity. The linear region is defined as the data set that results in the maximal determination coefficient (R^2 = max.) of a linear regression (B). The activity is then calculated using the corresponding slope of the linear regression and is expressed as a decrease in optical density per minute (ΔOD_{600nm}/min) and takes into account the reaction volume (µl) and the amount of enzyme in mg. (A). The amount of Pal (or Cpl-1) used in the assays was determined in western blot analyses with the HA-tagged standard protein CARHSP1 (C).

Table 4.1: Specific enzyme activities of *C. reinhardtii*-produced Pal determined with different amounts of crude extract containing Pal
The specific enzyme activities were determined using turbidity reduction assays with suspension of *S. pneumoniae* logarithmic phase cells at an OD_{595nm} of 0.15 and the method by Briers et al. (2006). The amount of Pal was determined by western blot analyses with HA-tagged CARHSP1 protein as a standard. 100x CE = crude extract prepared by freezing and thawing from whole cell extract that had been concentrated to 100x the culture volume. The standard deviations (±) are stated (n = 4).

Start OD_{595nm} of the *S. pneumoniae* suspension	**Concentration of Pal** (100x CE with ≈ 5 µg Pal)	**Specific enzyme activities of Pal** (Units/mg protein)
OD_{595nm} 0.15	**Undiluted (≈ 5 µg Pal)**	37.4 ± 3.7
	1:2 (≈ 2.5 µg Pal)	41.5 ± 6.9
	1:10 (≈ 0.5 µg Pal)	38.9 ± 5.1

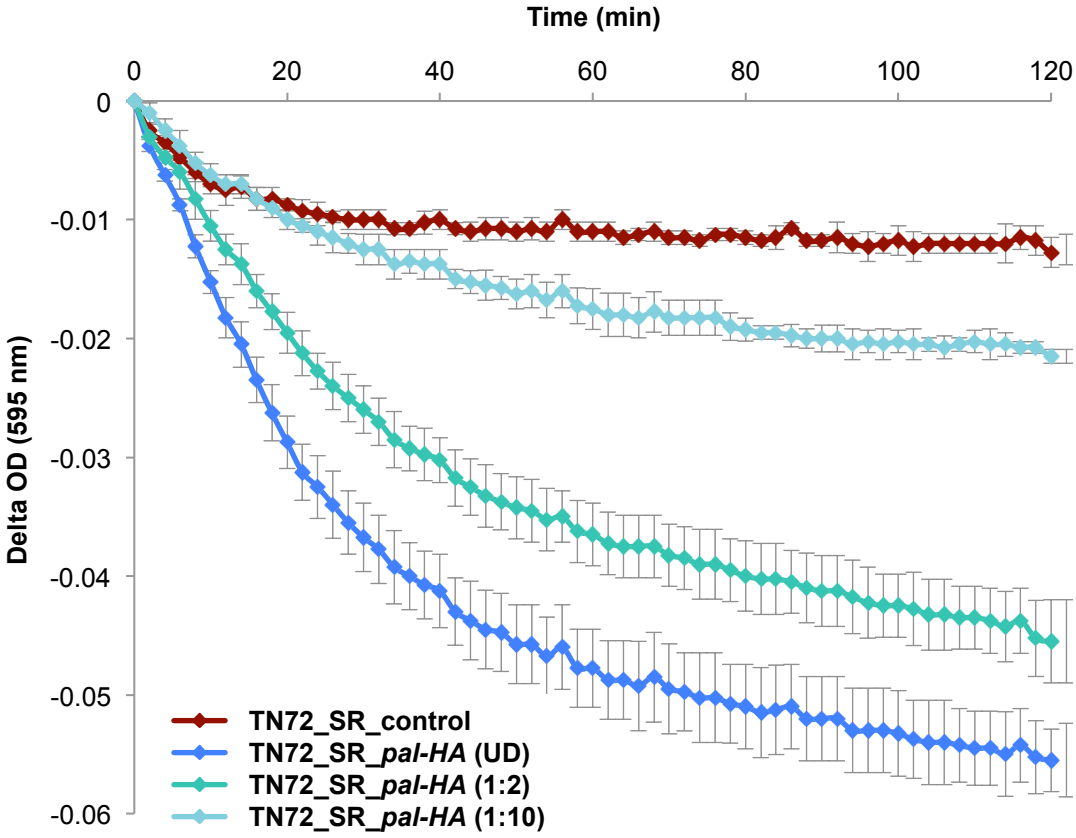

Figure 4.8: Turbidity reduction assay showing the lytic activity of Pal against *Streptococcus pneumoniae* using different amounts of Pal containing crude extract of *C. reinhardtii*
S. pneumoniae cells were resuspended in NaPi-buffer to an optical density (OD_{595nm}) of 0.15 in a 96-well plate. *C. reinhardtii* TN72_SR_*pal-HA* or TN72_SR_control crude extract (= supernatant after cell breakage and centrifugation at 21,000 x *g* for 5 min) was added (UD = 20 µl containing ≈ 5 µg Pal) to the cell suspension in a 200 µl reaction and the OD_{595nm} was measured over a time course. The assays were performed at 37ºC; UD = undiluted. The error bars show ± one standard deviation (n = 4).

However, during several performances of the experiment it was observed that the OD_{595nm} of the *S. pneumoniae* suspension used in the assay has a strong effect on the calculated enzyme activities of Pal (Table 4.2). The performance of the TRA with cells from the same *S. pneumoniae* culture at an OD_{595nm} of 0.1 compared to 0.5 resulted in ten times higher activity values. Interestingly, the increase in activity plotted against the start OD_{595nm} of the *S. pneumoniae* suspension showed a clear linear correlation (Figure 4.9).

It is conceivable that this was because the substrate (here the *S. pneumoniae* cells) was not in excess and represented the limiting factor. However, experiments with smaller concentrations of Pal resulted in comparable activity values and resulted in an earlier plateauing of the final OD_{750nm} (Table 4.1, Figure 4.8, Figure 4.23), which both indicates that the substrate was not the limiting factor in the reactions. Furthermore, it was demonstrated in a dilution series with *S. pneumoniae* cells that OD_{595nm} 0.1 to 0.5 is within the linear range of the spectrophotometer.

The same assays performed with *C. reinhardtii* crude extract containing the endolysin Cpl-1 (TN72_SR_*cpl-1-HA*), showed also a slight increase in the enzyme activities of Cpl-1 in correlation to an increase of the start OD_{595nm} of the *S. pneumoniae* suspension, but the increase was much less pronounced (Table 4.2, an increase of the OD_{595nm} from 0.1 to 0.5 resulted in doubling of the activities). Rodríguez-Cerrato et al. (2007) analysed the interactions of Pal and Cpl-1 with the major autolysin of *S. pneumoniae* LytA in a chequerboard technique assay. The analyses resulted in values very close to synergy for Pal and LytA and showed a clear additive effect of the two enzymes for all four *S. pneumoniae* strains tested. The same analyses showed for Cpl-1 and LytA only an additive effect for two out of four strains and the values were not close to synergy. When Garcia et al. (1983a,b) described the endolysin Pal isolated from Dp-1-infected *S. pneumoniae* cells for the first time, they observed an apparent involvement of the host autolysis activity in the release of Dp-1 phage particles. Autolysis-defective pneumococcal mutants for example showed an increased resistance to Dp-1 infection, which could be reversed by coating the cells with LytA or Pal (Garcia et al. 1983a; Garcia et al. 1983b). It is therefore conceivable that a release of LytA or other autolysins combined with an additive interaction of these

enzymes with Pal causes the observed increase in the speed of the cell lysis by Pal when the cell density of *S. pneumoniae* in the assay is increased.

On the other hand, Loeffler et al. (2001) showed that the antimicrobial activity of a LytA deficient strain is comparable to wild-type strains and concluded that LytA does not contribute to the lysis by Pal. However, this study analysed only a LytA deficient strain and not if there is an involvement of any other *S. pneumoniae* autolysins. Furthermore, a decrease in cfu was used to analyse the enzyme activities in this study, which does not monitor the speed of the reaction as closely as TRAs.

Additionally, the speed of lysis of *S. pneumoniae* by deoxycholate, increased when the cell densities in the TRAs were increased. The drop in ΔOD_{595nm}/min induced by deoxycholate increased by 18 fold when the start OD_{595nm} was changed from 0.1 to 0.5 (OD_{595nm} 0.1: -0.0048 ΔOD_{595nm}/min; OD_{595nm} 0.1: -0.0860 ΔOD_{595nm}/min) and the increase in activity showed a linear correlation to the start OD_{595nm} as well. Furthermore, it took 18 minutes to reach 90% of the maximal drop in OD_{595nm} in the assay with a start OD_{595nm} of 0.1 and only eight minutes in the one with a start OD_{595nm} of 0.5 (not shown). The lysis of *S. pneumoniae* by deoxycholate is a result of the induction of autolysins and is LytA-dependent (Δ*lytA* mutants are not susceptible to lysis by deoxycholate) (Mellroth et al. 2012). This study showed as well that deoxycholate causes a strong release of intracellular LytA to the surroundings. Therefore it seems to be logical that a higher cell density causes a faster lysis of even more cells when lysis is triggered by deoxycholate. Since the lysis caused by Pal also showed a response to increasing cell densities, it is conceivable that this could be due to a release of autolysins after the *S. pneumoniae* cells have been lysed by Pal. Nevertheless, to confirm this hypothesis more experiments need to be performed.

Furthermore, the calculated activities varied between assays performed with different cultures of *S. pneumoniae,* even when Pal preparations from the same *C. reinhardtii* culture were used (Table 4.2, Table 4.3). This might have been also due to slightly different growth stages of the *S. pneumoniae* cultures and therefore different amounts of accumulated autolysins.

Table 4.2: Specific enzyme activities of Pal and Cpl-1 determined at different *S. pneumoniae* cell densities
The specific enzyme activities were determined using turbidity reduction assays with suspensions of *S. pneumoniae* logarithmic phase cells at different OD_{595nm} in 96 well plates and the method by Briers et al. (2006). The amounts of Pal and Cpl-1 used in the assays were determined by western blot analyses with HA-tagged CARHSP1 protein as a standard. The standard deviations (±) are stated (n = 3).

Start OD_{595nm} of the *S. pneumoniae* suspension	**Specific enzyme activities** (Units/mg protein)	
	Pal	**Cpl-1**
OD_{595nm} 0.5	146.1 ± 8.7	22.4 ± 1.6
OD_{595nm} 0.3	73.0 ± 2.9	16.6 ± 2.2
OD_{595nm} 0.2	44.6 ± 2.9	16.9 ± 0.4
OD_{595nm} 0.1	14.7 ± 0.8	9.8 ± 0.6

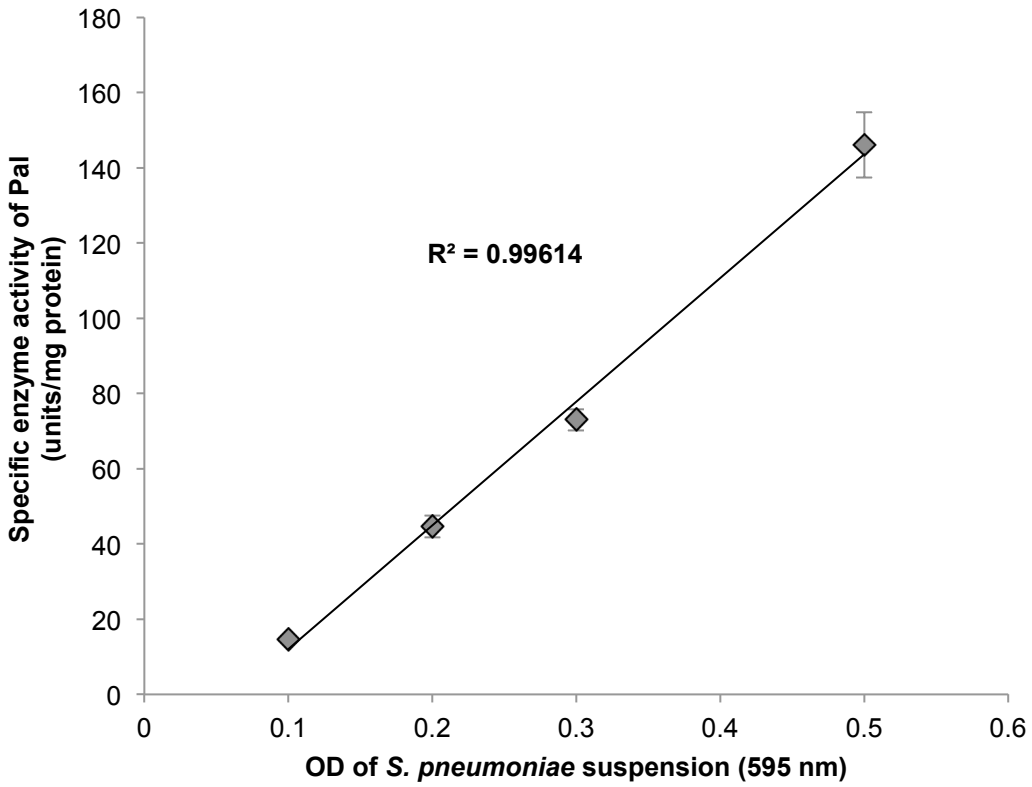

Figure 4.9: Correlation between the start OD_{595nm} of the *S. pneumoniae* suspension used in TRAs and the calculated specific enzyme activity of Pal
The specific enzyme activities were determined using turbidity reduction assays with suspension of *S. pneumoniae* logarithmic phase cells and different start OD_{595nm} in 96 well plates and the method by Briers et al. (2006). The amounts of Pal used in the assays were determined by western blot analyses with HA-tagged CARHSP1 protein as a standard. The error bars show ± one standard deviation (n =

3).

The Cpl-1 protein preparations were prepared in the same way as described for Pal in 4.2.1.2 and the specific enzyme activities were calculated as described above. The activities (per mg of protein) measured for Cpl-1 using crude extracts were in all performed assays lower compared to those of Pal. This was surprising, since purified Cpl-1 showed an even higher antibacterial activity than purified Pal (4.2.4.5) and previous studies described higher enzyme activities for Cpl-1 compared to Pal when both enzymes were produced in *E. coli* (Rodríguez-Cerrato et al. 2007; Domenech et al. 2011). The experiments analysing the activity of Cpl-1 using crude extracts shown in this study were all performed with TN72_SR_*cpl-1* cells prepared from one culture. To accurately determine the specific enzyme activities of Cpl-1 and to conclude if Cpl-1 in crude extracts has a decreased activity, the experiments need to be repeated with cells from different cultures.

4.2.2.4.2 Evaluation of the determined enzyme activities and the bacteriolytic activity of *C. reinhardtii*-produced Pal

The specific enzyme activities determined in the previous section showed strong variations depending on the cell densities and growth stages of the *S. pneumoniae* cells. It is therefore difficult to use these activities for comparisons to Pal produced in other expression systems or between assays performed with different *S. pneumoniae* cultures. However, the assay described here allows the comparison of different preparations of Pal, and of Pal to other enzymes, in TRAs with *S. pneumoniae* cells from the same culture diluted to the same OD_{595nm}.

To decrease fluctuations of the specific enzyme activities an alternative would be to use isolated cell walls radioactively labelled with [*methyl*-^{3}H]choline as used in a few studies for the analysis of *E. coli*-produced Pal (Sheehan et al. 1997; Domenech et al. 2011; Jado et al. 2003). To avoid the use of assays involving radioactivity, it might be possible to just use isolated *S. pneumoniae* cell walls and measure their degradation spectrophotometrically as described for other bacterial species, for example

Staphylococcus aureus (Navarre et al. 1999). Alternatively, a mutant deficient for LytA and other autolysins could be used for TRAs. Additionally, experiments with autolysin deficient mutants would help to further understand the possible involvement of autolysis in the lysis of *S. pneumoniae* by Pal.

Nevertheless, some of the previously described studies used TRAs with live *S. pneumonia*e cells (Oey et al. 2009b; Loeffler et al. 2001). Oey et al. state that 100 µg of total soluble protein from tobacco leaves expressing Pal in a one millilitre reaction was sufficient to decrease the OD_{600nm} in a TRA until only residual optical density of the bacterial lysate was left. In the assay shown in the publication, the OD_{600nm} dropped from around 0.6 to 0.25 within one hour (Oey et al. 2009b). They state that Pal accounts for 30% of the total soluble protein in the tobacco leaves, which means the assays were performed with approximately 30 µg of Pal protein per millilitre. In the assay shown in Figure 4.4 the OD_{595nm} decreased also by 0.35 from 0.5 to 0.15 in a 200 µl reaction within one hour and was performed with approximately 25 µg/ml Pal protein. This indicates that the bacteriolytic activity of Pal produced in *C. reinhardtii* is comparable to the activity of tobacco-produced Pal.

Loeffler et al. (2001) used TRAs only to define units for the performance of *in vivo* studies and assays analysing the bactericidal effect of *E. coli*-produced Pal. Most other studies analysed either the degradation of radioactively labelled cell walls or the bactericidal effect of Pal. To be able to compare the *C. reinhardtii*-produced Pal to *E. coli*-produced Pal while avoiding experiments involving radioactivity, assays analysing the bactericidal activity, for example by measuring a decrease in colony forming units after a treatment with Pal, need to be performed.

4.2.2.5 Antibacterial activity against clinical isolates of *S. pneumoniae*

It was of particular interest to test whether Pal produced in *C. reinhardtii* shows activity against clinical isolates, including antibiotic-resistant strains, since effective killing of these strains would highlight the potential of Pal as a treatment when traditional antibiotics fail. TRAs were therefore performed with five clinical isolates of *S. pneumoniae*: Serotype 6A strain H08212 0259, serotype 6B strain H08052 0052, serotype 6C strain H05252 0075, serotype 27 strain H08432 0293, serotype 6B strain 35 NP1. The strain 35 NP1 shows intermediate resistant against penicillin (Minimal inhibitory concentration (MIC): 0.125 µg/ml) and co-trimoxazole (MIC: 6 µg/ml).

The OD_{595nm} of all five strains decreased significantly during the time course of the assays in the presence of Pal when compared to the controls, which indicates that *C. reinhardti*-produced Pal has antibacterial activity against all five clinical isolates and shows that Pal is effective against a range of *S. pneumoniae* serotypes (Table 4.3, Figure 4.10, Figure 4.11). To determine specific enzyme activities of Pal against the clinical isolates, TRAs with four of the five strains and the reference strain were performed. The starting ODs were kept at 0.5 for all strains (except 35 NP1) to make the assays more comparable. As shown in Figure 4.10, the specific enzyme activities and also the speed of the reaction in comparison to the lysis caused by deoxycholate varied between the different strains. Rodríguez-Cerrato et al. also observed varying minimal inhibitory concentrations (MIC) when they analysed the effect of *E. coli*-produced Pal against four different *S. pneumoniae* clinical isolates. Their study determined MIC values ranging from 32 to 256 µg/ml (Rodríguez-Cerrato et al. 2007). Pal produced in *C. reinhardtii* showed (in all repetitions of the experiment) higher activities against the two serotype 6B strains and the reference strain with the serotype 19F, compared to the serotypes 6A and 6C. The OD_{595nm} of suspensions of serotype 6A and 6C also decreased in the presence of Pal eventually until only residual optical density of the bacterial lysate was left when the TRAs were performed for a longer period of 600 min. In contrast, the enzyme activities of Cpl-1 showed smaller differences between different strains, but need to be confirmed in more repetitions of the experiment as already mentioned in 4.2.2.4.1.

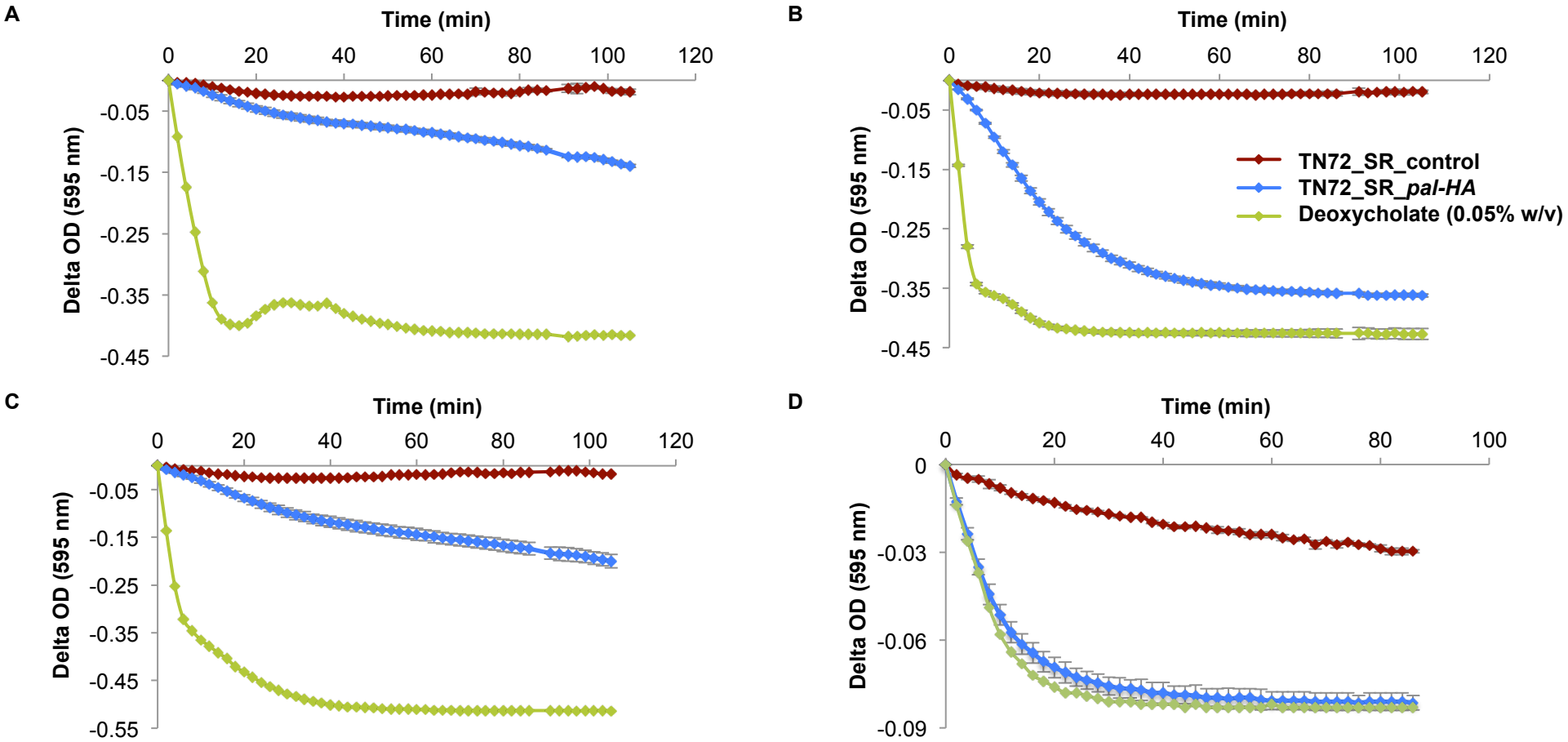

Figure 4.10: Turbidity reduction assays showing the lytic activity of *C. reinhardtii*-produced Pal against four clinical isolates of *S. pneumoniae*
The *S. pneumoniae* clinical isolates were resuspended in NaPi-buffer to an optical density (OD_{595nm}) of around 0.5, with the exception of NP1 with an OD_{595nm} of around 0.15. *C. reinhardtii* TN72_SR_*pal-HA* or TN72_SR_control crude extract (20 µl containing around 5 µg Pal protein) was added to the cell suspension in a 200 µl reaction and the OD_{595nm} was measured over a time course of 100 min at 37ºC. Clinical isolates of *S. pneumoniae* : A = Serotype 6A H08212 0259; B = Serotype 6B H08052 0052; C= Serotype 6C H05252 0075; D = 35 NP1 serotype 6B. The error bars show ± one standard deviation (n = 3).

Table 4.3: Specific enzyme activities of Pal and Cpl-1 against different clinical isolates of *S. pneumoniae*
The specific enzyme activities were determined using turbidity reduction assays with suspensions of *S. pneumoniae* at a start optical density (OD_{595nm}) of 0.5, for NP1 of 0.15, and the method by Briers et al. (2006). The amounts of Pal and Cpl-1 used in the assays were determined by western blot analyses with HA-tagged CARHSP1 protein as a standard. The standard deviations (±) are stated (n = 3).

***S. pneumoniae* strain**	**Serotype**	**Strain number**	**Specific enzyme activities** (Units/mg protein)	
			Pal	**Cpl-1**
Reference strain	**19F**	**16 NP3**	462.8 ± 20.4	53.6 ± 1.5
Clinical isolates	**6A**	**H08212 0259**	53.8 ± 8.2	30.4 ± 2.1
	6B	**H08052 0052**	400.6 ± 14.0	34.5 ± 2.8
	6C	**H05252 0075**	99.0 ± 11.9	62.0 ± 0.7
	6B	**35 NP1**	190.2 ± 18.5	85.8 ± 2.9

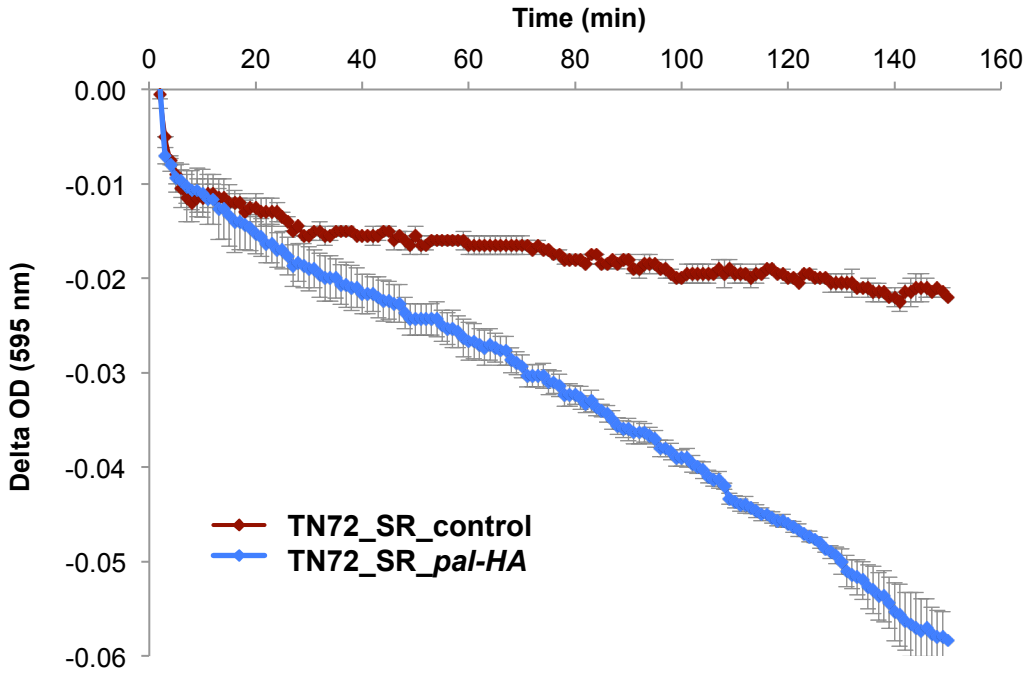

Figure 4.11: Turbidity reduction assay showing the lytic activity of *C. reinhardtii*-produced Pal against a clinical isolates of *S. pneumoniae* serotype 27 strain H08432 0293
The *S. pneumoniae* strain was resuspended in NaPi-buffer to an optical density (OD_{595nm}) of around 0.35. *C. reinhardtii* TN72_SR_*pal-HA* or TN72_SR_control crude was added to the cell suspension and the OD_{595nm} was measured over a time course. The error bars show ± one standard deviation (n = 3 for TN72_SR_*pal-HA* and n = 2 for TN72_SR_control).

4.2.2.6 Activity assays analysing the bactericidal activity of Pal

The TRAs described in the previous sections proved that the recombinant Pal protein produced in the *C. reinhardtii* chloroplast is able to lyse *S. pneumoniae* cells, including clinical isolates and different serotypes. Subsequently, it was desired to have a direct demonstration that the endolysin efficiently kills the target bacterium and to compare the activity of Pal produced in this study to studies that only assayed the bactericidal activity of *E. coli*-produced Pal. Therefore, the following experiments analysing the bactericidal activity of Pal in crude extracts against *S. pneumoniae* were performed. In spot tests, crude extracts of TN72_*pal-HA* and TN72_control were spotted onto a lawn of *S. pneumoniae* cells, which had been plated onto Columbia blood agar plates. After incubation overnight, the plates were analysed for inhibition zones in the area of the spots. Alternatively, the crude extracts were mixed with a suspension of *S. pneumoniae* cells, and spotted in different dilutions onto agar plates. On the next day, the numbers of colony forming units (cfu) were determined and the cfu/ml calculated. However, it was found that both assays were hampered by an endogenous activity in the *C. reinhardtii* crude extracts, including the control extracts, that had a growth-inhibiting or bactericidal effect against *S. pneumoniae*. This is despite the observations above that the control extract does not induce lysis of the bacterial cells.

Ghasemi et al. (2007) already described antimicrobial activity of *C. reinhardtii* culture supernatant and methanolic extracts against different bacterial species including *Staphylococcus aureus* and *Staphylococcus epidermis*. Furthermore, earlier studies had shown that *C. reinhardtii* solvent extracts had antibacterial activity against *B. subtilis* (Cannell et al. 1988; Jørgensen 1962). The next section (4.2.3) discusses the antimicrobial activity of *C. reinhardtii* in more detail. However, in order to analyse the bactericidal activity of Pal produced in *C. reinhardtii,* different strategies for the purification of Pal were examined to separate the recombinant endolysin from the endogenous antimicrobial substance in the algal crude extracts and are described in 4.2.4.

4.2.3 Endogenous antimicrobial activity of *C. reinhardtii* crude extracts

As mentioned in 4.2.2.6, an inhibitory effect against *S. pneumoniae* growth was observed for *C. reinhardtii* crude extracts, both with and without Pal. Crude extract (prepared from whole cell extract concentrated to 100x the culture volume) caused clear inhibition zones in lawns of *S. pneumoniae* platted on blood agar plates (Figure 4.12 A). In further experiments, the crude extract was mixed in a ratio of 1:1 with *S. pneumoniae* suspensions from an overnight culture. The mixture was spotted in different dilutions onto blood agar plates and on the next day the colony forming units (cfu) were counted. In the spots treated with crude extract, no *S. pneumoniae* colonies grew at all, whereas the control with buffer contained 695,833 ± 153,922 cfu/ml (Figure 4.12 B). The same experiment performed with *Streptococcus pyogenes*, which is the causative agent of group A streptococcal infections like skin infections or pharyngitis, showed a growth inhibiting effect of the algal extracts against this species as well. The control contained 330 million cfu/ml, whereas the samples treated with *C. reinhardtii* crude extract contained between 0.9 and 6.6 million cfu/ml (Figure 4.12 C).

To analyse whether the crude extract just inhibits the growth of *S. pneumoniae* or actually kills the cells, the following experiment was performed. Crude extract was mixed with *S. pneumoniae* suspensions or NaPi-buffer as described above and incubated for one hour. Subsequently, one part of cells that had been incubated with crude extract and the cells incubated with NaPi-buffer were washed three times with buffer and spotted in different dilutions on blood agar plates. After overnight incubation the plates were inspected for colony forming units. The controls that were incubated with buffer showed strong, uncountable growth at all dilutions, whereas the spots with *S. pneumoniae* cells that had been incubated with *C. reinhardtii* crude extract did not contain any cfu, independent of whether the cells had been washed after the treatment or not (Figure 4.12 D). These results suggest that the crude extract not just inhibits the growth, but rather that it contains a substance that kills *S. pneumoniae* cells, albeit without lysis as demonstrated by the TRAs.

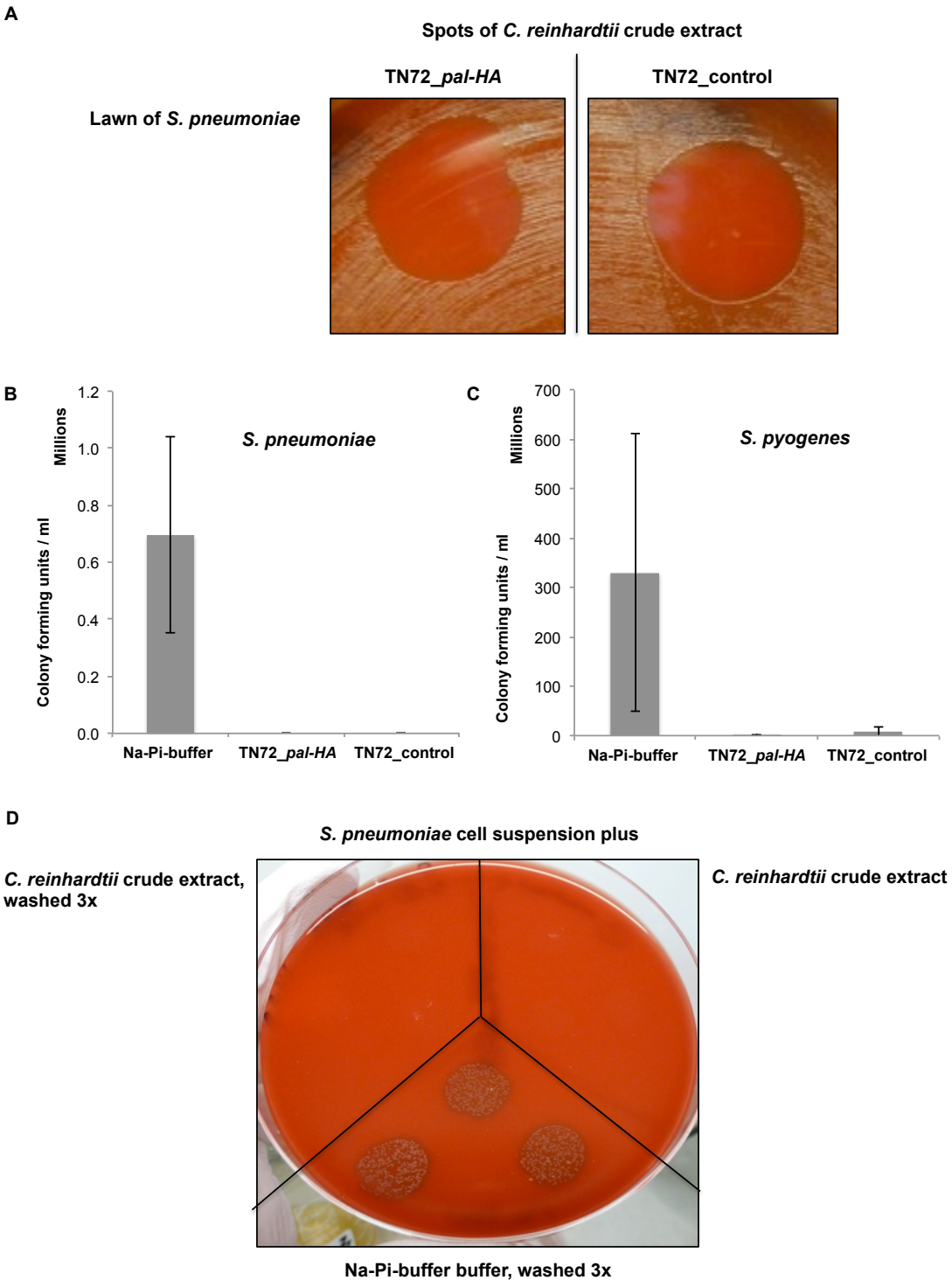

Figure 4.12: Antimicrobial activity of *C. reinhardtii* TN72_x crude extract against *Streptococcus pneumoniae* (A, B, D) and *Streptococcus pyogenes* (C)
S. pneumoniae cells were spread onto Colombia blood agar plates, subsequently crude extract of TN72_*pal-HA* and TN72_control were spotted onto the lawn before the plates were incubated overnight at 35ºC (A). *S. pneumoniae* or *S. pyogenes* cells were mixed with crude extract or NaPi-buffer, incubated and spotted at different dilutions onto blood agar plates. After overnight incubation the colony forming units (cfu) were counted and the cfu per ml calculated (B, C). After incubation with crude extract or buffer, cells were washed three times with NaPi-buffer before spotting; the figure shows the 1:100 dilution (D). The error bars in B and C show ± one standard deviation (n = 4).

The antimicrobial effect of *C. reinhardtii* crude extract was also tested against *Propionibacterium acnes*, *Agrobacterium tumefaciens* and *Escherichia coli* by either mixing suspensions of the bacteria with crude extract and spotting the mixture on appropriate growth medium or spotting crude extract on a lawn of the bacterium. In none of the experiments was an antimicrobial effect against any of the three species observed (Figure 4.13).

Subsequently, experiments to further characterize the unknown antimicrobial substance were performed. Preliminary experiments indicated that the substance is or binds to something that is larger in size than 30 kDa, because when crude extract was separated with centrifugal concentrators with a MWCO of 30,000, the antimicrobial substance did not pass the selective membrane (not shown). The antibacterial activity precipitated during ultracentrifugation at 100,000 x *g* for one hour, which suggests that the substance is not soluble in aqueous solution, since soluble molecules are expected to stay in the supernatant during ultracentrifugation (Figure 4.14 B). Another preliminary experiment did not show an effect of proteinase K or pronase E (0.2 mg/ml) on the unknown antimicrobial activity against *S. pneumoniae* suggesting that the substance is not a protein (not shown). To investigate the thermostability of the substance, crude extracts of TN72*_pal-HA* and TN72_control were heated to different temperatures for three minutes. Subsequently, the extracts were spotted on lawns of *S. pneumoniae* incubated overnight and inspected for inhibition zones. Above temperatures of 50ºC TN72_control did not cause inhibition zones anymore, whereas TN72*_pal-HA* still caused an inhibition of *S. pneumoniae*, although the effect was reduced, after incubation at 65ºC (Figure 4.14 A). The results were confirmed in two repetitions of the experiment. Endolysins are described as remarkably heat stable in the literature (up to 60°C) (Fischetti 2005) and Schmelcher et al. observed residual activity after incubating a *Listeria* bacteriophage endolysin at 90°C (Schmelcher et al. 2011). It is therefore conceivable that Pal survived the heat treatments at 55ºC and 65ºC, whereas the unknown endogenous substance lost its activity above 50ºC. On the other hand, Garcia et al. state that temperatures above 50ºC destroy the activity of Pal purified from Dp-1-infected *S. pneumoniae* cells (Garcia et al. 1983a), but they heated the samples for five minutes and Pal in crude extract might exhibit a higher stability than in purified form. Taken together, the results suggest that the endogenous

substance losses its antibacterial effect above temperatures of 50ºC and that Pal has bactericidal activity against *S. pneumoniae*. Nevertheless, the bactericidal activity of Pal needs to be confirmed with purified Pal to avoid any interference of the unknown antibacterial substance in the *C. reinhardtii* crude extract.

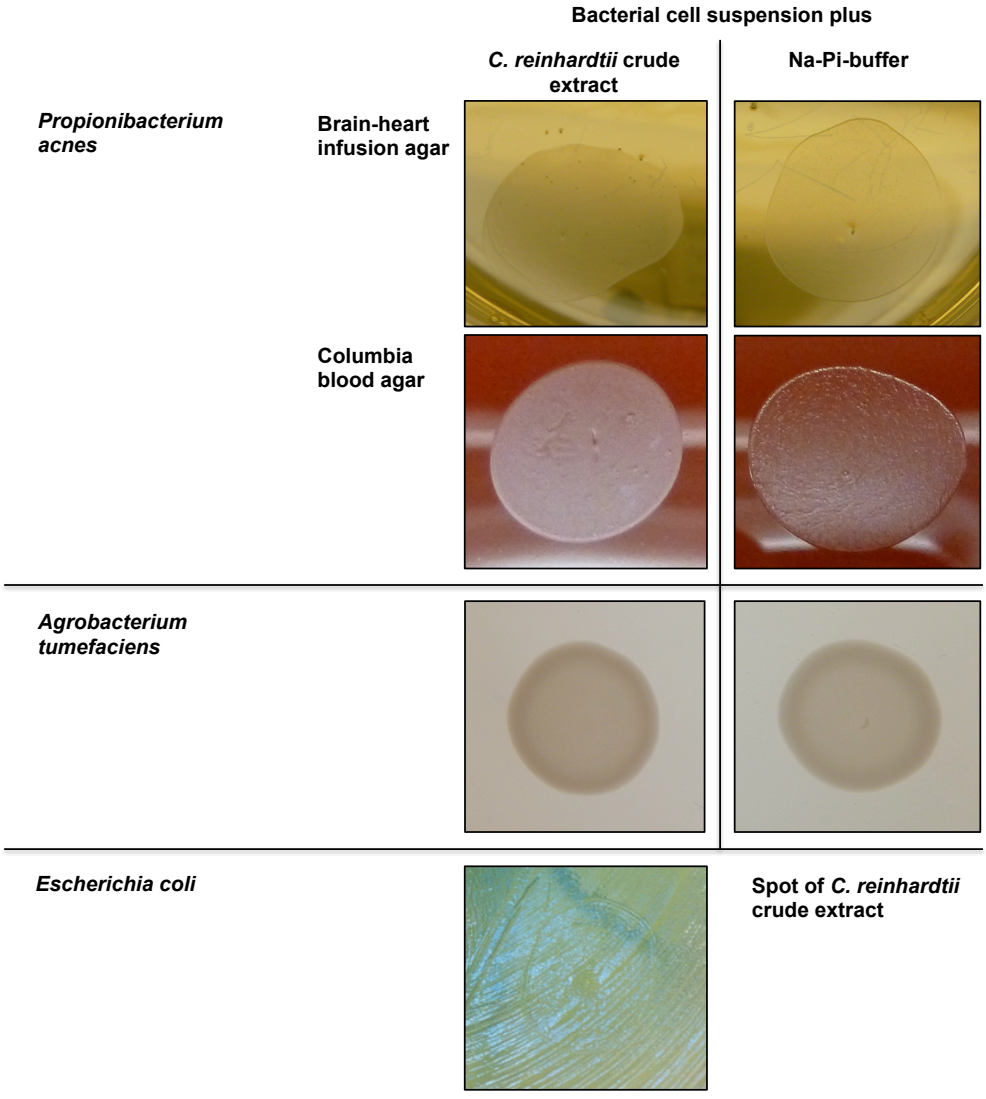

Figure 4.13: Effect of *C. reinhardtii* TN72_x crude extract against *Propionibacterium acnes*, *Agrobacterium tumefaciens* and *Escherichia coli*
P. acnes and *A. tumefaciens* cell suspensions were mixed with *C. reinhardtii* crude extract TN72_x in a ratio of 1:1 and incubated for 1.5 h (*P.acnes*) or 0.5 h (*A. tumefaciens*) at room temperature. Subsequently the mixture was spotted onto agar plates and incubated for 5 days (*P.acnes*) or overnight (*A. tumefaciens*). The mixture with *A. tumefaciens* was spotted in different dilutions onto the agar plates (undiluted, 1:10, 1:100, 1:1000), the undiluted spot is shown. *E. coli* was spread onto an agar plate and *C. reinhardtii* crude extract TN72_x (100x culture volume) was spotted onto the lawn before incubation overnight. *C. reinhardtii* crude extract did not show antibacterial activity against the three tested species under the used experimental conditions.

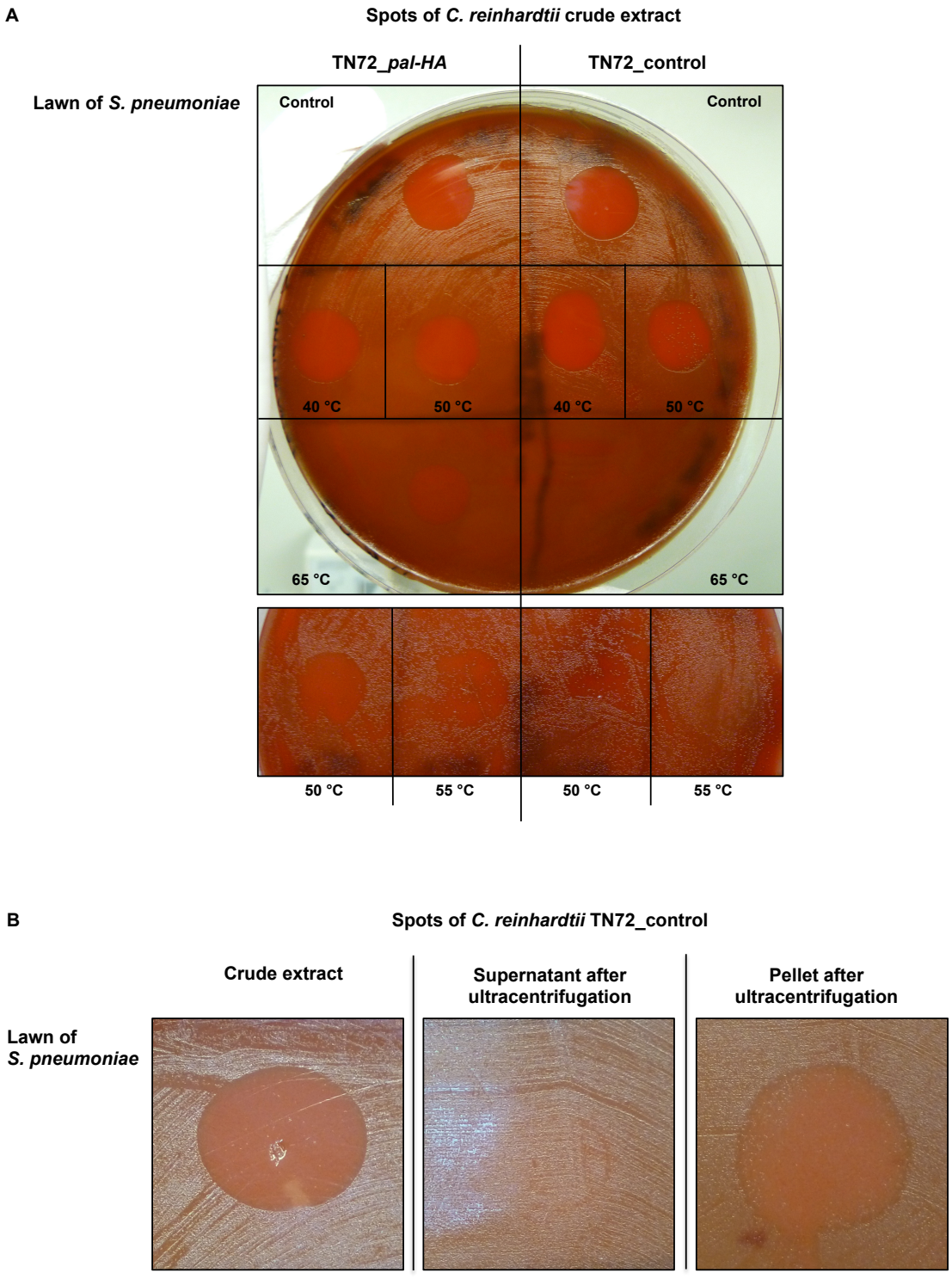

Figure 4.14: Effect of different temperature (A) and ultracentrifugation (B) on the antibacterial activity of *C. reinhardtii* crude extract against *Streptococcus pneumoniae*
Crude extracts of *C. reinhardtii* TN72_*pal-HA* and TN72_control were heated to different temperatures for 3 minutes (A). Crude extract of TN72_control was separated by ultracentrifugation at 100,000 x *g* for 1 h and the pellet was resuspended in the previous volume (B). Subsequently, the samples were spotted on *S. pneumoniae* cells plated on Colombia blood agar plates. After incubation overnight the plates were inspected for inhibition zones. Control in A = unheated extract.

A few studies have already described antimicrobial activities of *Chlamydomonas* species. Ghasemi et al. described an antimicrobial activity found in the culture supernatant of *C. reinhardtii* and in methanolic extracts that was effective against *Bacillus subtilis*, *Escherichia coli, Salmonella typhi, Pseudomonas aeruginosa*, *Staphylococcus aureus* and *Staphylococcus epidermis* (Ghasemi et al. 2007). In the here described study, no antibacterial effect against *E. coli* was observed with the used experimental procedure and algal extracts prepared as described in 4.2.1.1. The crude extracts of TN72_x showed in a few assays an effect against *Staphylococcus aureus*, but the results were not consistent and therefore not seen as conclusive.

Furthermore, Ghasemi et al. (2007) found an antifungal activity in *C. reinhardtii* culture supernatants against *Candida kefyr, Aspergillus niger* and *Aspergillus fumigatus*. The study analysed 60 strains of microalgae and found that 21 showed antibacterial and 17 antifungal activity. Most of them were *Chlorella, Chroococcus, Nostoc* or *Anacystis* species. Kellam & Walker (1989) had previously shown that a hexane extract of *Chlamydomonas vectensis* has antibacterial activity against *S. aureus* and *B. subtilis,* whereas the extract did not have any effect against *Escherichia coli* and *P. aeruginosa.* Cannell et al. (1988) observed antibacterial activity of *C. reinhardtii* methanolic extracts against *B. subtilis*, but stated that the extracts did not show activity against *E. coli* or *S. aureus*. In this study, 300 eukaryotic microalgae were analysed and 36 showed antimicrobial activity. Furthermore, the study showed that the growth medium has an influence on the production of the antimicrobial compounds (Cannell et al. 1988). Jørgensen (1962) first described the antibacterial activity of *C. reinhardtii* ether and ethanol extracts as well as culture supernatant against *B. subtilis* and is the only study that further characterized the antimicrobial substances. This study used paper chromatography and analyses of absorption spectra to show that chlorophyllides and other derivatives of chlorophyll cause the observed antimicrobial activity. The activity described in this study was dependent on illumination during the experiment and Jørgensen concluded that a substance formed by chlorophyllides during illumination probably by photo-oxidation is responsible for the antibacterial activity against *B. subtilis.*

The ability of chlorophylls to strongly absorb visible and near-infrared light and to store the energy in long-lived excited states, which is beneficial for photosynthesis, also render them highly phototoxic. Whenever the energy in the chlorophylls excited states cannot be used productively, triplet states can be formed, which can react with oxygen to form reactive oxygen species, which belong to the most aggressive agents found in nature (Scheer 2012). Several previous studies have shown that chlorophyll derivatives have antimicrobial activity and these substances were even used as antimicrobial treatments for wound healing and against infected ulcerative lesions in the 1940s and 1950s (Smith 1955). One conspicuous observation from the experiments described in this chapter is that the endogenous antimicrobial substance in the crude extracts was always found in the 'green fraction' after purification steps such as ultracentrifugation, ammonium sulphate precipitation, and separation with centrifugal concentrators (MWCO 30,000). The 'green fraction' contains presumably chlorophyll derivatives in addition to the bulk chlorophyll. This suggests that the antimicrobial activity that was observed in *C. reinhardtii* TN72_x extracts during this study could have also been caused by chlorophyll derivatives.

Several examples of eukaryotic microalgae that use free fatty acids as defense mechanism against other microorganisms have been described. The free fatty acids are mainly part of the cell membranes and storage structures and are released after cell breakage and the action of lipolytic enzymes (Desbois & Smith 2010; Smith et al. 2010). Ohta et al. showed that linolenic acid (18:3) from the green algae *Chlorococcum* HS-101 shows antibacterial activity against *S. aureus*, including MRSA strains (Ohta et al. 1994). The diatom *Phaeodactylum tricornutum* releases eicosapentaenoic acid (EPA, 20:5 (5, 8, 11, 14, 17)) after cell breakage through lipase activity, and EPA has antibacterial activity against a wide range of Gram-positive and Gram-negative bacteria (Desbois et al. 2009). Furthermore, it has been shown that butanoic acid (4:0) from the green alga *Haematococcus pluvialis* has an effect against *E. coli* and *S. aureus* (Amaro et al. 2011; Santoyo et al. 2009). Moreover, it has been shown that numerous other free fatty acids have antibacterial, antifungal and antiviral activity (Smith et al. 2010; Desbois & Smith 2010).

Table 4.4 shows a comparison between the fatty acids found in *C. reinhardtii* according to Giroud et al. (1988) and fatty acids that have been shown to exhibit antibacterial activity. The table shows that several fatty acids that are found in *C. reinhardtii* have antibacterial properties. Some of these fatty acids (16:0, 16:1 (Δ 7), 18:2 (Δ 9,12), 18:3 (Δ 9, 12, 15)) have even been shown to be effective against *S. pneumoniae* and other *Streptococcus* species (Kabara et al. 1972). Palmitic acid (16:0) represents about 22% of the total lipids, and the fatty acids stated in the table that have been shown to have antibacterial activity represent together about 80% of the total lipids in *C. reinhardtii*.

It is therefore conceivable that the observed antibacterial activity against *S. pneumoniae* and *S. pyogenes* of *C. reinhardtii* TN72_x is at least partly caused by antibacterial fatty acids. The previously mentioned observation that the antibacterial activity was found in the 'green fraction' (the chlorophyll containing fraction) after purification steps such as ultracentrifugation, ammonium sulphate precipitation and separation using centrifugal concentrators (MWCO 30,000) does not contradict this. The chlorophyll is connected to membrane proteins and to the cell membranes. Furthermore, membrane lipids and chlorophyll have similar polarities. It would be therefore not surprising that membrane lipids and chlorophyll react in similar ways in these purification steps. Membrane lipids are, for example, known to precipitate during ultracentrifugation. On the other hand, the observed temperature sensitivity of the substance is contradictory, since free fatty should be able to withstand temperatures of 55 to 60ºC. In contrast, it is conceivable that chlorophyll is sensitive to temperature within this range.

It is conceivable that a combination of different substances including chlorophyll derivatives and certain fatty acids are responsible for the antibacterial activity of *C. reinhardtii* TN72_x against *Streptococcus* species observed in this study. Nevertheless, more experiments need to be performed to identify and characterize the substances that cause this activity.

Table 4.4: Comparison between fatty acid composition of *Chlamydomonas reinhardtii* and fatty acids that have been show to have antibacterial properties
Column one shows the fatty acid composition of total lipids from *C. reinhardtii* 137c regarding to Giroud et al. (1988), in bold are fatty acids that represent more than 10% of the total lipids, the other columns show antibacterial fatty acids, the organisms they were effectively tested on and the reference. The fatty acids are named with their lipid numbers (C:D) and the Δ^x nomenclature, which counts the double bonds starting from the carboxyl acid end, the fatty acids are *cis* unless stated, t = *trans*.

Fatty-acids in *C. reinhardtii* (Giroud et al. 1988)	**Antibacterial fatty acids**	**Susceptible test organisms**	**Reference**
16:0	16:0 Palmitic acid	Several Gram- marine pathogens	Benkendorff et al. (2005)
		Several Gram+	Galbraith et al. (1971)
		Several Gram+, incl. *S. pneumoniae*	Kabara et al. (1972)
16:1 (7)	16:1 (7) 16:1 (9) Palmitoleic acid 16:1 (9t) Palmitelaidic acid	*Neisseria gonorrhoeae*	Bergsson et al. (1999)
16:1 (9)		*Bacillus larvae*	Feldlaufer et al. (1993)
		Several Gram+, incl. *S. pneumoniae*	Kabara et al. (1972)
16:1 (3t)	-	-	-
16:2 (7, 10)	-	-	-
16:3 (4, 7, 10)	-	-	-
16:3 (7, 10, 13)	-	-	-
16:4 (4, 7, 10, 13)	-	-	-
18:0	18:0 Stearic acid	Several Gram- marine pathogens	Benkendorff et al. (2005)
		Several Gram+	Galbraith et al. (1971)
18:1 (9)	18:1 18:1 (9) 18:1 (11) 18:1 (*cis)* 18:1 (*trans*)	Several Gram- marine pathogens	Benkendorff et al. (2005)
18:1 (11)		Several Gram+	Galbraith et al. (1971)
		Streptococcus group A	Kabara et al. (1972)
		Bacillus larvae	Feldlaufer et al. (1993)
18:2 (9,12)	18:2 (9, 12) 18:2 Linoleic acid	Several Gram+	Galbraith et al. (1971)
		Several Gram+, incl. *S. pneumoniae*	Kabara et al. (1972)
		Bacillus larvae	Feldlaufer et al. (1993)
18:3 (5, 9, 12)	18:3 18:3 (9, 12, 15) 18:3 (6, 9, 12) Linolenic acid	Several Gram+	Galbraith et al. (1971)
18:3 (9, 12, 15)		Several Gram+, incl. *S. pneumoniae*	Kabara et al. (1972)
		Bacillus larvae	Feldlaufer et al. (1993)
18:4 (5, 9, 12, 15)	18:4	Several Gram- marine pathogens	Benkendorff et al. (2005)

4.2.4 Purification of Pal

The purification of Pal is essential in order to study the activity of *C. reinhardtii*-produced Pal without the interference of other cell components, especially the endogenous antibacterial substance present in the alga. Furthermore, for the performance of *in vivo* studies, Pal needs to be purified to remove transgenic DNA and immunogenic compounds. The long-term goal is to use *C. reinhardtii*-produced Pal as a therapeutic agent. Therefore an efficient and economical method for the purification of Pal needs to be developed. Different purification and enrichment steps/methods were performed during this study and are discussed in this chapter.

4.2.4.1 Ultracentrifugation as a first step for the purification of *C. reinhardtii*-produced Pal

Previous studies described ultracentrifugation as a first step for the purification of *Escherichia coli*-produced Pal (Jado et al. 2003) (Loeffler et al. 2001). Ultracentrifugation can be used to remove cell debris, membrane pieces and non-soluble proteins, whereas most soluble proteins stay in solution.

Cells were broken by freezing and thawing and major cell debris was removed by centrifugation at 5,000 x *g* for 15 min (= low speed centrifugation), before ultracentrifugation at 100,000 x *g* for one hour. The majority of Pal (about 80% regarding to the IRF[3] signals) remained in the supernatant during low speed centrifugation. The amount of Pal that was detected in the pellet is presumably caused by a portion of unbroken cells or Pal that got trapped in or bound to major cell debris (Figure 4.15). As shown in Figure 4.15, the vast majority of Pal also remained in the supernatant during ultracentrifugation (98% (comparison between UC↵ supernatant and pellet), 82% (comparison between 5K↵ and UC↵ supernatant)) suggesting that the majority of Pal exists as a soluble protein in the chloroplast of *C. reinhardtii*.

[3] IRF = The Infrared fluorescence signals measured by the Odyssey® Infrared Imaging system were used to estimate the amount of Pal present in samples that were analysed in western blots.

An analysis of the protein extracts before (5K↵ supernatant) and after ultracentrifugation (UC↵ supernatant) on a Coomassie stained SDS-PAGE showed that ultracentrifugation can be used as an effective first step to remove a high proportion of cell debris and non-soluble proteins. It also removes the membrane-associated chlorophyll, which interferes with western blot detection systems by increasing the background of blots detected by the Odyssey infrared (IR) fluorescence system. Furthermore, chlorophyll increases the background in SDS-PAGE analyses (Figure 4.15 C) and photometric turbidity reduction assays.

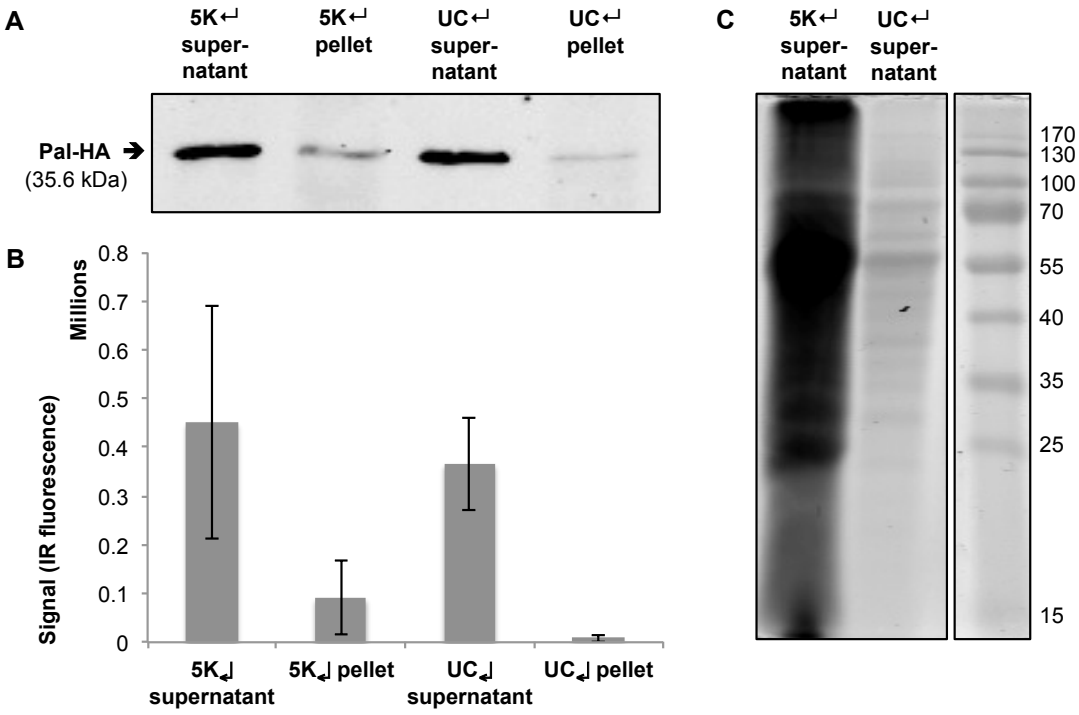

Figure 4.15: Western blot analysis (A, B) and SDS-PAGE (C) showing ultracentrifugation as a first step for the purification of *C. reinhardtii* TN72_SR_*pal-HA*

C. reinhardtii cells (whole cell extract that had been concentrated to 100x the culture volume, grown to an OD_{750nm} of 2) were broken by freezing and thawing and major cell debris was removed by low speed centrifugation (5,000 x *g* for 15 min). Ultracentrifugation was performed at 100,000 x *g* for 1 h. Samples were collected after each centrifugation step and analysed by western blot analysis with anti-HA antibodies and IRDye® secondary antibodies. The Odyssey® Infrared Imaging system was used for detection (A) and for quantification (B). Samples were also analysed on a Coomassie stained SDS-PAGE (C). The error bars in B show ± one standard deviation (n = 2).

4.2.4.2 Enrichment of Pal using ammonium sulphate precipitation

Ammonium sulphate precipitation is an inexpensive purification method, which can be used in large-scale protein purifications (Burgess & Jendrisak 1975; Lohman et al. 1986). Proteins differ markedly in their solubility at different concentrations of ammonium sulphate and therefore can be easily separated by this method.

The ammonium sulphate concentration of UC↵ supernatant was increased stepwise and the extract was centrifuged (3,000 x *g* for 15 - 30 minutes) at the end of each step. The pellet of precipitated proteins was resuspended in fresh buffer (with 10% of the previous volume), whereas the supernatant was treated with a higher concentration of ammonium sulphate (Deutscher, 1990). The majority of Pal (approximately 85% suggested by the IRF signals) precipitated between 25% and 30% saturation (= 30% AS). Smaller amounts of Pal precipitated at an ammonium sulphate concentration of 20%, 25% and 35% saturation (Figure 4.16 A, B). The findings were confirmed in two repetitions of the experiment.

An analysis of the UC↵ supernatant and the 30% AS fraction on a Coomassie stained SDS-PAGE showed that ammonium sulphate precipitation is a further useful step for the enrichment of Pal, since it separates Pal from a high number of other proteins (Figure 4.16 D). Furthermore, it easily allows the concentration of the protein extract. In the experiments shown the protein extract was concentrated by a factor of 10 (Figure 4.16 A, B; Figure 4.17 A, B), but the concentration factor could be further increased.

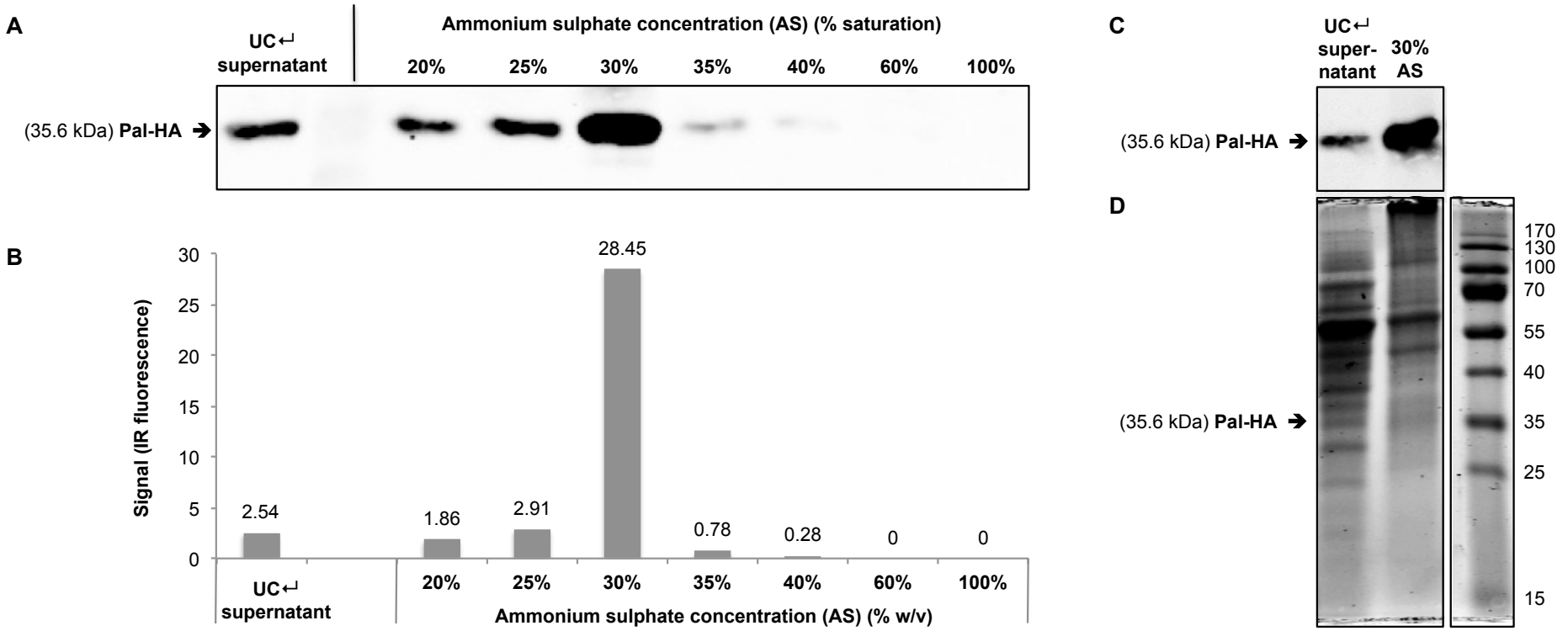

Figure 4.16: Western blot analysis (A, B, C) and Coomassie stained SDS-PAGE (D) showing the enrichment of Pal using ammonium sulphate precipitation
The ammonium sulphate concentration of ultracentrifugation supernatant (gained at 100,000 x *g* for 1h (= UC↵ supernatant)) of *C. reinhardtii* TN72_SR_*pal-HA* was increased stepwise, stirred on ice for 15 min and centrifuged (3,000 *x g*, 15 min) at the end of each step. The pellet was resuspended in fresh buffer with 10% of the previous volume. Samples from resuspended pellets (20%, 25% etc. ammonium sulphate concentration (% saturation)) were analysed by western blot with anti-HA antibodies, IRDye® secondary antibodies and the Odyssey® Infrared Imaging system. A shows the western blot picture, B the corresponding Odyssey IR fluorescence signals. C and D show the UC supernatant before the ammonium sulphate precipitation and the precipitated fraction (30% AS) with the highest amount of Pal. D shows the total protein content on a Coomassie stained SDS-PAGE and C the corresponding anti-HA western blot. The expected band size for Pal is 35.6 kDa.

4.2.4.3 Immunoprecipitation with monoclonal anti-HA agarose conjugate resin for the purification of Pal

Anti-HA antibody conjugated agarose resin (Sigma-Aldrich) can be used for the purification of HA-tagged proteins. The antibodies bind with high specificity to HA-tagged proteins, and the proteins can be eluted by a pH shift to 2.5 or by using high concentrations of HA peptide.

The fraction of proteins that precipitated between 25% and 30% ammonium sulphate concentration (30% AS) was incubated with anti-HA agarose (volume ratio of sample to resin: 3-5:1) for 4 – 16 h at 4ºC. After five washes with NaPi-buffer, Pal was eluted by Glycine-HCl buffer (pH 2.5) with a volume equal to the volume of the loaded sample, followed by neutralisation (pH 7). Alternatively, Pal was eluted with 100 µg/ml of HA peptide to exclude inactivation of the protein by the low pH. In both cases a second elution at pH 2.5 was performed to ensure complete elution of Pal from the resin.

As shown in Figure 4.17 (A, B) the resin was able to bind Pal and it was possible to elute the majority of bound Pal in one step when using Glycine-HCl (pH 2.5) as eluent. However, the flow through still contained a high amount of Pal (approximately 35% of the applied sample in the shown experiment). Extension of the incubation time to 16 h did not improve the binding capacity (not shown). A decrease of the sample to resin ratio from 5:1 to 3:1 decreased the loss of Pal into the flow only to about 20% (not shown). Nevertheless, it was possible to detect a faint band in the lane of the first elution on the Coomassie stained gel at the size of Pal (36.5 kDa) and to remove the majority of other proteins (Figure 4.17 C), which were still present in the 30% AS fraction (Figure 4.16 D). HA peptide could also be used to elute Pal (Figure 4.17 D, E), however, this procedure was not as effective, since the following elution at pH 2.5 still contained about 70% of the amount of Pal eluted with the HA peptide (Figure 4.18 D, E).

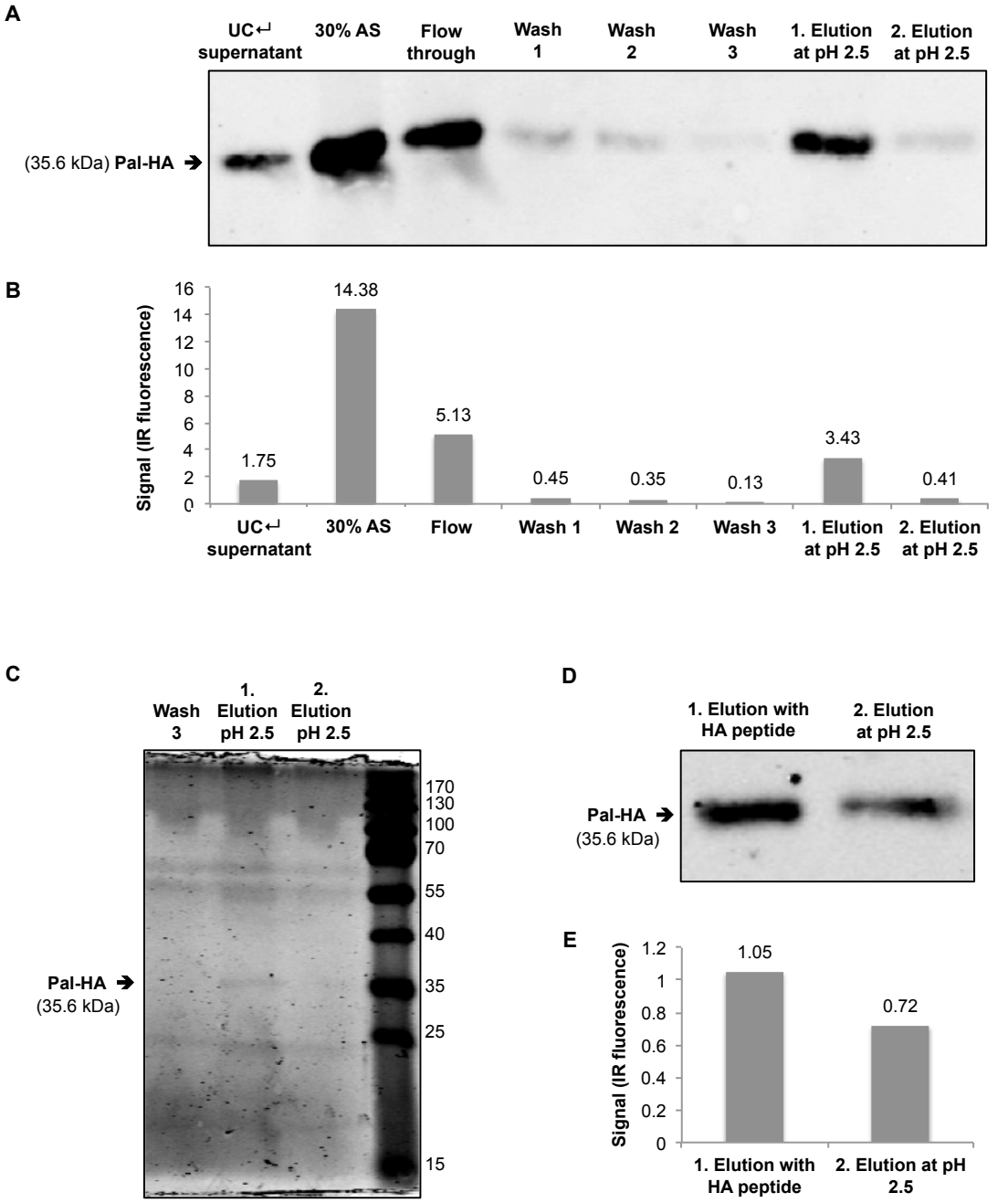

Figure 4.17: Purification of *C. reinhardtii*-produced Pal protein with monoclonal anti-HA agarose conjugate resin

Ultracentrifugation supernatant of TN72_SR_*pal-HA* was precipitated with ammonium sulphate. Anti-HA agarose was incubated with the suspension of proteins that precipitated between 25% and 30% ammonium sulphate concentration (= 30% AS) for 5 h at 4ºC. After 5 washes with NaPi-buffer, Pal was eluted in the same volume of Glycine-HCl buffer (pH 2.5) as the loaded sample, followed by pH neutralisation. Samples taken before and after this purification step were analysed by western blot with anti-HA antibodies and IRDye® secondary antibodies. The Odyssey® Infrared Imaging system was used for detection (A, D) and quantification of the bands (B, E). The elution samples were additionally analysed on a Coomassie stained SDS-PAGE protein gel (C). In a second experiment Pal was first eluted with HA peptide (100 µg/ml), followed by a second elution at pH 2.5 (D, E). UC↵ supernatant = supernatant after ultracentrifugation at 100,000 x *g* for 1h.

In a combination of ultracentrifugation, ammonium sulphate precipitation and immunoprecipitation with monoclonal anti-HA agarose conjugate resin, Pal could be sufficiently purified and enriched that it could be visualized as a faint band on a Coomassie stained SDS-PAGE. However, the binding capacity of the resin for Pal was exceeded in all repetitions of the experiment. Anti-HA agarose is relatively expensive (£160-300/ml with a binding capacity of 30-50 nmol/mL (SIGMA July 2014)) and therefore not feasible for large-scale purifications. Furthermore, in spite of the high specificity of the antibody-conjugated resin, there were still other proteins present in the elution from the anti-HA resin (Figure 4.17 C).

4.2.4.4 Purification with diethylaminoethanol (DEAE) cellulose and choline as specific eluent

Diethylaminoethanol (DEAE) cellulose was used in previous studies for the purification of *Escherichia coli*-produced Pal with choline as the specific eluent (Loeffler et al. 2001; Jado et al. 2003). The method used in these study is based on the methods reported by Sanchez-Puelles et al. (1992) and Sanz et al. (1988). Pal and other *S. pneumoniae* cell wall hydrolases (e.g Cpl-1, LytA) bind specifically to choline residues of the teichoic acids in the pneumococcal cell wall. The binding is required for the hydrolytic activity of these enzymes. DEAE is a choline analogue (Figure 4.18) and can bind these hydrolases as well (Sanchez-Puelles et al. 1992). The binding is strong enough to withstand a high salt wash at 1.0 or 1.5 M NaCl, which removes a high number of contaminant proteins, while choline-binding hydrolases can be specifically eluted with a buffer containing choline (2 to 6.5%). Henry Taunt (Taunt 2013) established the method for the purification of the *S. pneumoniae* endolysin Cpl-1 produced in *C. reinhardtii*. The purification with DEAE cellulose and choline described in this section is based on his findings and the previously mentioned studies.

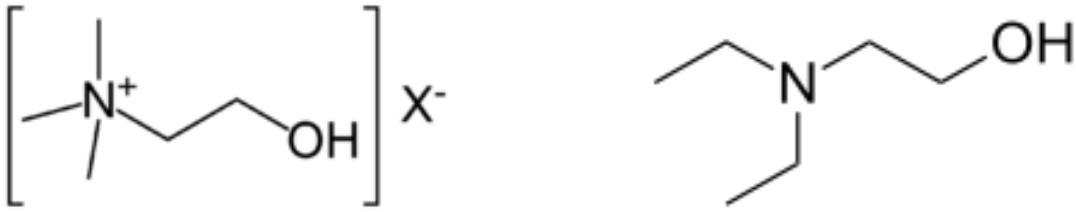

Choline **Diethylaminoethanol (DEAE)**

Figure 4.18: Comparison of the structural formulae of choline and the choline analogue diethylaminoethanol (DEAE). (Source: www.wikipedia.com)

Cells of TN72_SR_*pal-HA* and TN72_SR_control were concentrated to 100x the culture volume, broken by freezing and thawing followed by low speed centrifugation and ultracentrifugation. The UC↵ supernatants were loaded onto a column with DEAE cellulose with a sample to column volume ratio of 1:1 or 1.5:1. The loading was repeated three to four times. Subsequently, the column was washed with six column volumes of NaPi-buffer (pH 6.9), followed by washes with eight column volumes of NaPi-buffer containing 1.5 M NaCl and four column volumes of NaPi-buffer plus 0.1 M NaCl. The elution was performed with NaPi-buffer containing 0.1 M NaCl and 6.5% (w/v) choline and collected in 1 or 1.5 ml samples.

The elution samples were analysed together with samples from previous steps in protein microarrays on nitrocellulose membrane with anti-HA antibodies and the Odyssey® Infrared Imaging system. Protein microarrays allow the simultaneous analysis of high numbers of samples. However, since chlorophyll fluorescence causes a strong background signal, this type of protein microarray is only suitable for samples containing hardly any chlorophyll (e.g. after ultracentrifugation). Cells of the corresponding negative control strain were processed in the same way and samples were analysed in the same protein microarray. The IR fluorescence signals that were detected in the protein microarray of the negative control, were subtracted from the corresponding samples with Pal before the analyses to account for background fluorescence.

The DEAE cellulose columns were able to bind the vast majority of the *C. reinhardtii*-produced Pal using the described experimental procedure, since the signals of the

protein microarrays detected in the flow through were only around 5% [4] of the signals detected in the UC↵ supernatants that were applied to the columns (Figure 4.19 A, B). Furthermore, a western blot analysis with anti-HA antibodies of the flow through did not show any band at the size of Pal-HA, whereas the applied UC↵ supernatant showed a strong band (Figure 4.21 B).

In all purification attempts, it was possible to elute the majority of Pal in three to five elution fractions (Figure 4.19 A, B). During the first attempt with one litre cultures and a sample column ratio of 1:1, the concentration of Pal could be doubled in the elution fractions with the highest amount of Pal (E7 and E8) compared to the UC↵ supernatant that was applied to the column (5.62 (UC↵) : 11.06 (E8), Figure 4.19 A) as indicted by the IR fluorescence signal values of the protein microarray. An analyses of the IR fluorescence signal values of the protein microarray suggested that approximately 72% [5] of the amount of Pal applied to the column could be recovered into the elution fractions in the experiment shown in Figure 4.19.

[4] Percentage of Pal in flow through compared to amount applied to the DEAE column: Performance 1: 100% / (IR fluorescence signal (IRF) of the UC↵ supernatant minus the IRF of the corresponding control sample (6.92 – 1.3)) = 5.62 x IRF of flow through (0.33 – 0.07) = 4.6%; Performance 2: (100% / 818653) * 40149 = 4.9%.

[5] Percentage of Pal recovered in the elution fractions: IRF of the applied UC↵ supernatant (6.92 – 1.3) = 5.62 x 9 ml (volume applied to the column) = 50.58; IRF's of 1 ml elution fractions with Pal: 10.24 + 11.05 + 7.95 + 3.99 + 1.75 + 1.04 + 0.52 = 36.54; percentage recovered: 100% / 50.58 x 36.54 = 72%.

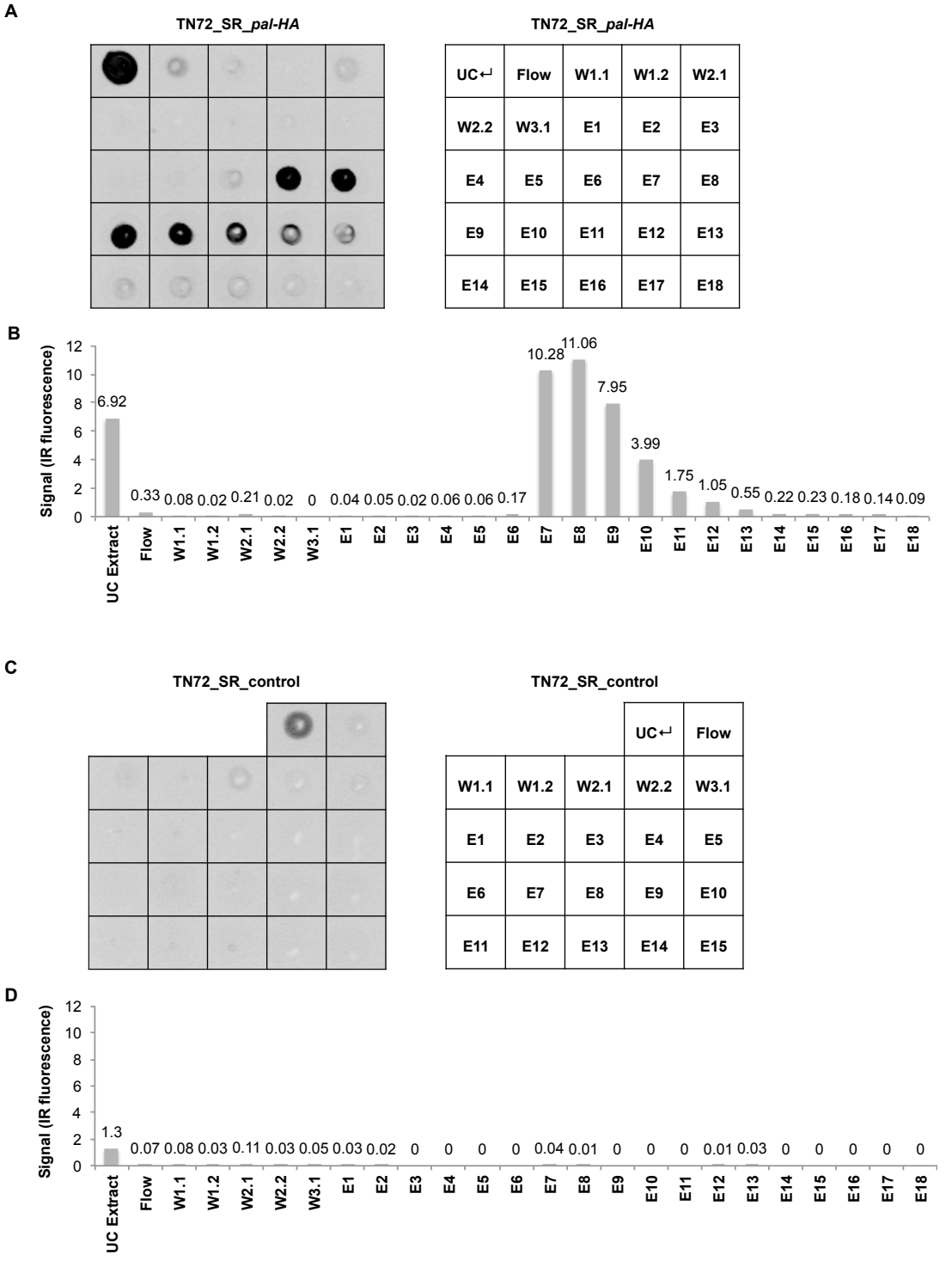

Figure 4.19: Protein microarray showing the enrichment of *C. reinhardtii*-produced Pal protein with diethylaminoethanol (DEAE) cellulose and choline as specific eluent
Ultracentrifugation supernatant (= UC extract) of *C. reinhardtii* TN72_SR_*pal-HA* (A, B) and of TN72_SR_control (C, D) were applied to DEAE cellulose columns (total volume 9 ml). After high salt washes, Pal was specifically eluted with choline (1 ml elution fractions). Samples of the different steps of the purification were spotted onto a nitrocellulose membrane, which was incubated with anti-HA antibodies and IRDye® secondary antibodies. The Odyssey® Infrared Imaging system was used for detection (A, C) and quantification (B, C). Flow = flow through; W1.1, 1.2 = Wash with NaPi-buffer (pH 6.9); W2.x = wash with NaPi-buffer + 1.5 M NaCl; W3.x = wash with NaPi-buffer + 0.1M NaCl.

The binding to choline in the cell wall is essential for the function of Pal and therefore free choline bound to the binding sites of Pal inhibits its activity (Domenech et al. 2011). For this reason, the eluted fractions with the highest amounts of Pal were combined and dialysed against NaPi-buffer to remove the choline. The dialysis caused no marked loss of Pal, since western blot analysis and Coomassie stained SDS-PAGE gels showed similar signals for the samples before and after dialysis (Figure 4.20 A, B; Figure 4.21 C).

Centrifugal concentrators (MWCO 30,000) were used as a next step to concentrate the amount of Pal in the combined and dialysed elution fractions. In the experiment here reported the previous volume was reduced to a quarter. However, the amount of Pal measured by western blot analysis suggested only an increase by a factor of two (76.61 / 37.43 = 2.05) (Figure 4.21 A, B). The use of centrifugal concentrators resulted in losses of a similar extent in repetitions of this experiment and in other experiments. Additionally, the concentrated elution fractions and the UC↵ supernatant (that was applied to the column) were analysed on a Coomassie stained SDS-PAGE for their total protein content. A faint band was visible for the concentrated elution fraction and it was possible to remove most other proteins beside traces of a 55 kDa protein, presumably the large subunit of the abundant Rubisco protein (Figure 4.20 C).

To decrease losses during the last concentration step and to remove the traces of the 55 kDa protein, further concentration/purification steps were considered. It has been shown in section 4.2.4.2 that ammonium sulphate precipitation is an efficient method for the concentration of Pal. Furthermore, it separates proteins depending on their solubility in the presence of different concentrations of ammonium sulphate. Therefore, Pal in the combined and dialysed elution fractions was precipitated in one step with an ammonium sulphate concentration of 35% saturation. A one step precipitation with a concentration of 35% saturation was chosen to minimize losses of Pal, since although the majority of Pal precipitates at 30%, smaller fractions of Pal precipitate in a range of 20% up to 35% saturation (4.2.4.2) and at 20% saturation and below hardly any proteins precipitated overall (not shown).

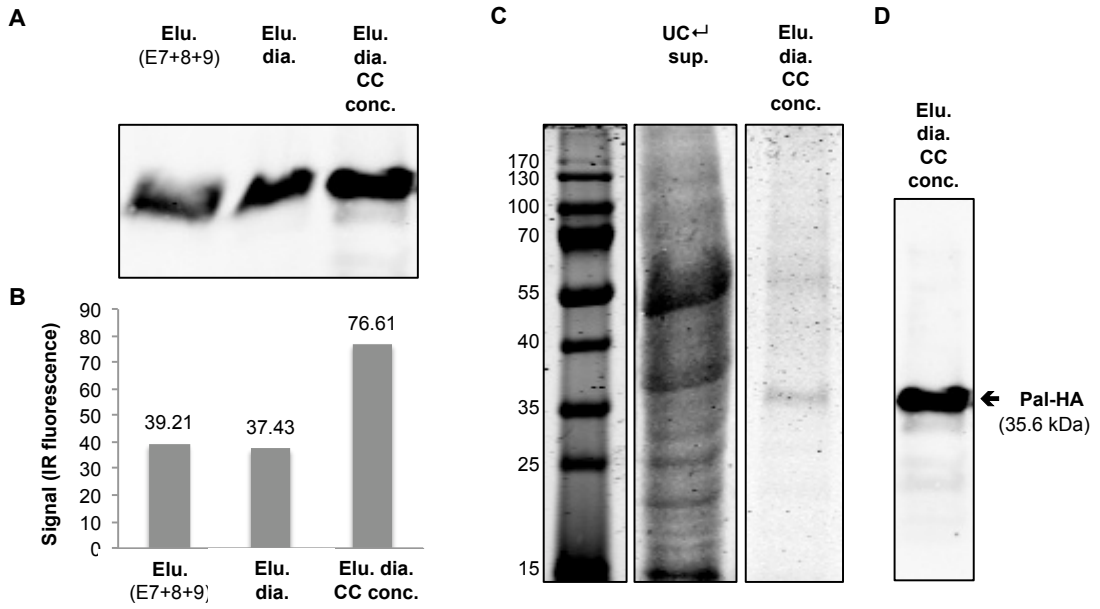

Figure 4.20: Western blot analysis showing the dialysis and concentration of Pal (A, B, D) and SDS-PAGE showing the purification of Pal with diethylaminoethanol (DEAE) cellulose and choline as specific eluent (C)
Ultracentrifugation supernatant of *C. reinhardtii* TN72_SR_*pal-HA* was purified using DEAE cellulose and choline as specific eluent. The elution fractions containing Pal were combined and dialysed against NaPi-buffer to remove the bound choline and concentrated to a quarter of the previous volume using a centrifugal concentrator (MWCO 30,000) (A, B). The combined, dialysed and concentrated elution fractions as well as the UC supernatant before purification were compared on a Coomassie stained SDS-PAGE (C), the corresponding western blot analysis of the elution is shown in D. UC supernatant = ultracentrifugation supernatant before application to the column; E, Elu. = elution; dia. = dialysed; CC conc. = concentrated with centrifugal concentrator (MWCO 30,000).

Figure 4.21 B, D shows a Coomassie stained SDS-PAGE and the corresponding western blot analysis of all previous purification steps and of the elution concentrated by ammonium sulphate (AS) precipitation. The AS precipitated elution revealed a strong band at the size of Pal-HA on the SDS-PAGE and at the same time there were no other bands visible in the same lane. The corresponding western blot analysis with anti-HA antibodies confirmed a strong band at the same size.

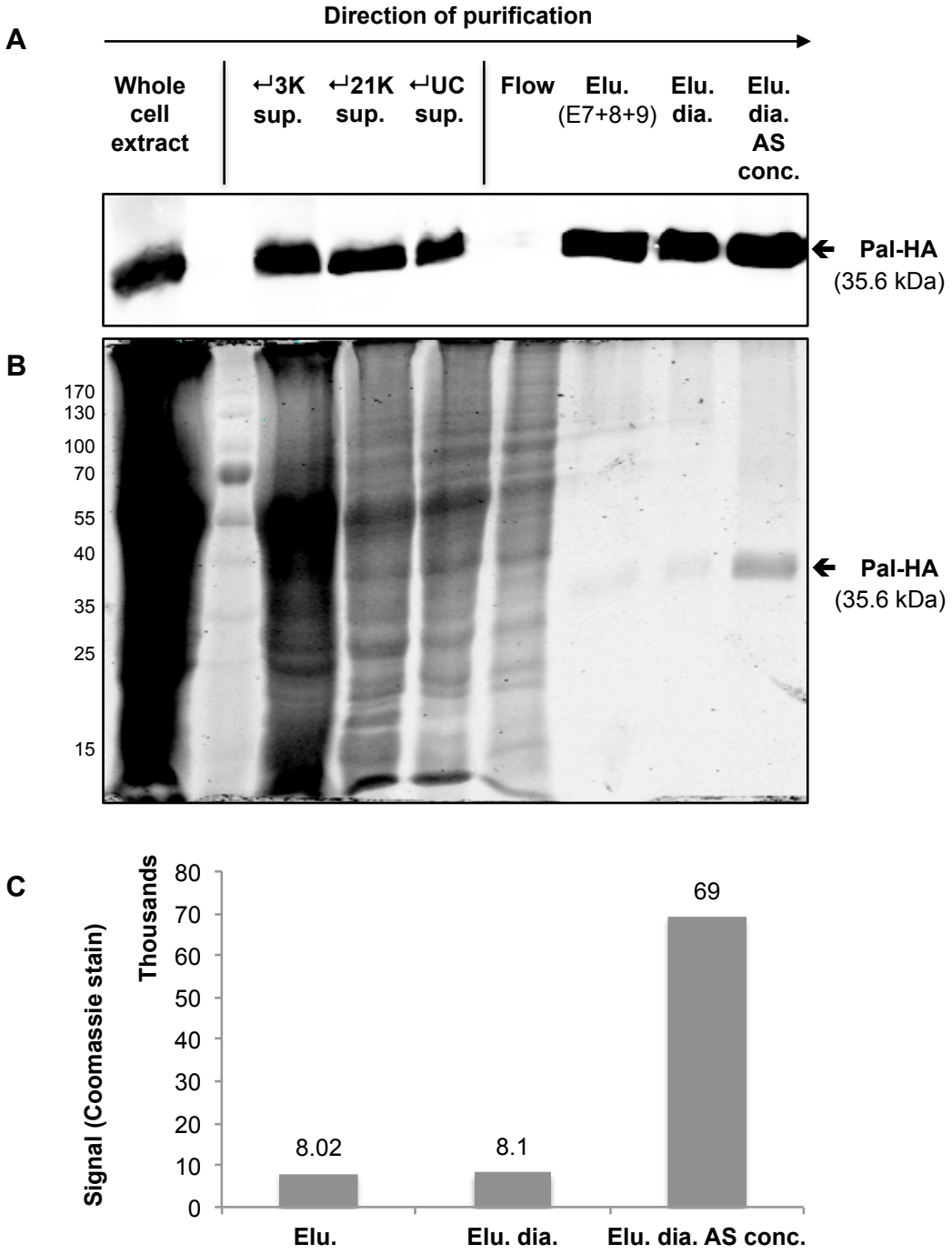

Figure 4.21: Western blot analysis (A) and Coomassie stained SDS-PAGE (B, C) showing the purification of Pal using ultracentrifugation, diethylaminoethanol (DEAE) cellulose with choline as specific eluent and ammonium sulphate precipitation
Ultracentrifugation supernatant (= UC sup.) of *C. reinhardtii* TN72_SR_*pal-HA* was purified using DEAE cellulose and choline as specific eluent. Subsequently the elution fractions with the highest amount of Pal were combined, dialysed and precipitated with 35% ammonium sulphate (% w/v) (= AS conc.). Samples of the UC sup, flow through and elution fractions were analysed in a western blot with anti-HA antibodies and IRDye® secondary antibodies and the Odyssey® Infrared Imaging system (A) and on a Coomassie stained SDS-PAGE (B). The bands of Pal in the combined, the dialysed and the AS precipitated elution were quantified using the Odyssey® Infrared Imaging system (C), CE = crude extract, sup. = supernatant, elu. = elution, dia. = dialysed, flow = flow through.

In the experiment shown in Figure 4.22, the pellet of precipitated proteins obtained after AS precipitation and centrifugation was resuspended in NaPi-buffer with 10% of the previous volume. A quantitative analysis of the SDS-PAGE using the Odyssey® Infrared Imaging system showed an increase in the strength of the Pal band by 8.5 times when the bands of the samples before and after AS precipitation were compared (Figure 4.21 C). The corresponding western blot analysis could not be used for quantification in this experiment, since the intensity of the bands exceeded the linear range of the Odyssey® Infrared Imaging system. In another performance of the purification the AS precipitated elution was resuspended in 20% of the previous volume and the signal of the western blot analysis increased by 3.6 times (not shown). This suggests that the losses during concentration of the elution samples using AS precipitation are less compared to losses of approximately 50% when centrifugal concentrators were used. The use of AS precipitation as a last step also allows the recovery of all the Pal protein from those fractions with lower concentrations of the enzyme (E11 - E13 in Figure 4.19 B). This can be done by pooling the fractions and concentrating the combined pool using AS precipitation. Furthermore, no bands of other proteins were detectable on the SDS-PAGE when AS precipitation was used as a last step.

Overall, using a combination of ultracentrifugation, DEAE cellulose with choline as eluent and ammonium sulphate precipitation, it was possible to visualize Pal as a strong single band on a Coomassie stained SDS-PAGE in the absence of any with this method detectable contaminant proteins.

4.2.4.5 Antimicrobial activity of Pal purified with ultracentrifugation diethylaminoethanol (DEAE) cellulose and ammonium sulphate precipitation

C. reinhardtii-produced Pal purified using ultracentrifugation, DEAE cellulose and choline, as well as ammonium sulphate precipitation was subsequently used to analyse the antibacterial activity of *C. reinhardtii*-produced Pal without the interference of other cell components. This was of particular interest, since it was now possible to analyse the bactericidal activity of Pal without the inference of the endogenous antimicrobial substance in *C. reinhardtii*.

4.2.4.5.1 Bacteriolytic activity of purified Pal

The first aim was to show that the purification procedure does not destroy the activity. The activity of Pal is reduced by 50% in the presence of 2 mM choline (IC_{50}) (Domenech et al. 2011) and here Pal was eluted from the DEAE cellulose column with 625 mM choline. Therefore the presence of residual choline could inhibit the activity of Pal after purification. Additionally, proteases, oxidation processes or other conditions that Pal was exposed to during the purification process, could have destroyed its antimicrobial activity.

For that reason, TRAs as described in 4.2.2.1 were performed with purified Pal and the control strain processed in the same way, as well as crude extracts of TN72_SR_*pal-HA* and TN72_SR_control. Figure 4.21 shows a western blot analysis and a Coomassie stained SDS-PAGE of the purified Pal (Elu. Dia. AS conc.) and the crude extract containing Pal (21K Sup., CE) used in this TRA in Figure 4.22. In the presence of purified Pal and TN72_SR_*pal-HA* extract, the OD of the *S. pneumoniae* suspension decreased significantly compared to the corresponding controls. The decrease in the presence of purified Pal was five times faster compared to the decrease in the presence of TN72_SR_*pal-HA* crude extract (ΔOD_{595nm}/min: -0.0065 (purified

Pal), -0.0013 (CE)) in the shown experiment (Figure 4.22). This shows that purified Pal retained its bacteriolytic activity during the purification and that the concentration of Pal protein during the purification resulted in a five fold concentration of the antibacterial activity of Pal.

However, analyses of the bacteriolytic activity of samples from different steps of the purification showed opposite trends during different purifications and TRAs, and the results were therefore not seen as conclusive (not shown). For that reason, it was not possible to determine quantitatively whether stages of the purification cause losses of the enzymatic activity of Pal. Nevertheless, an analysis of the bacteriolytic activities of samples from every purification step combined with an analysis of the amount of Pal in the samples, would be very useful to determine whether certain purification steps result in a reduction of the enzymatic activity of Pal and would be of great help to improve the purification of Pal. Furthermore, it would make it possible to investigate whether the endogenous activity in crude extracts of *C. reinhardtii* has an additive effect on the lysis of *S. pneumoniae* by Pal.

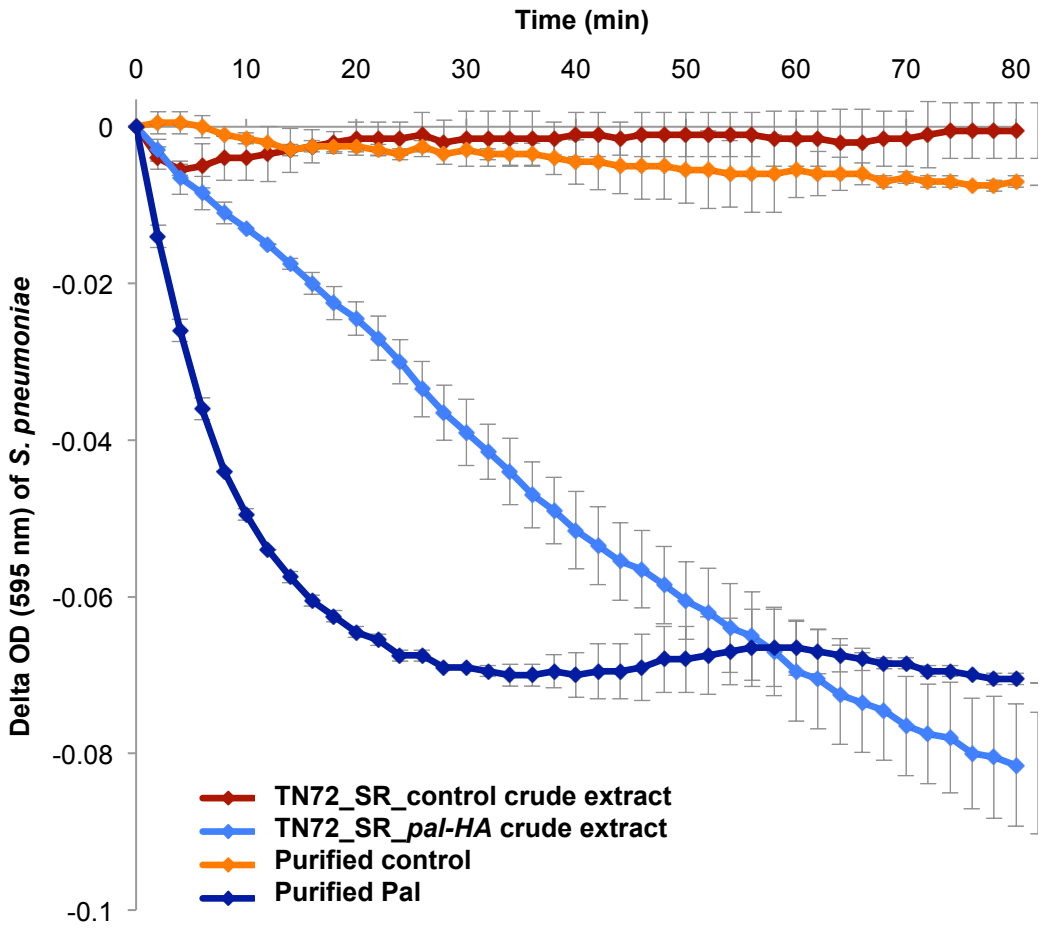

Figure 4.22: Turbidity reduction assay showing the bacteriolytic activity of purified Pal and Pal in *C. reinhardtii* crude extract against *S. pneumoniae*
Cultures of TN72_SR_*pal-HA* and TN72_SR_control were grown to an OD_{750nm} of ≈2, harvested and concentrated to 100x the culture volume. Pal was purified with ultracentrifugation, diethylaminoethanol (DEAE) cellulose and choline as specific eluent, as well as ammonium sulphate precipitation. *S. pneumoniae* cells were resuspended in NaPi-buffer to an optical density (OD_{595nm}) of 0.23. Crude extract of TN72_SR_control, TN72_SR_*pal-HA*, purified Pal or control extract treated in the same way were added to the cell suspension and the OD_{595nm} was measured. The error bars show ± one standard deviation (n = 2).

TRAs performed with purified Pal showed also a clear dosage dependent response (Figure 4.23). Furthermore, these TRAs showed (even clearer than in Figure 4.8) that lower amounts of Pal enzyme in the assay not only result in a lower speed of the lysis reaction, but also in a plateauing of the lysis before reaching the maximal decrease, which was defined by deoxycholate (Figure 4.23). Moreover, a second addition of Pal enzyme after the reaction had plateaued resulted in a further decrease of the OD_{595nm} until the level of the deoxycholate lysis was reached. These results reflect the nature of Pal and other endolysins with cell binding domains. The cell binding domains bind

tightly to specific molecules within the cell envelope. The recognition and binding of specific molecules is on one hand responsible for the high specificity of these endolysins. On the other hand, it binds the endolysins to cell debris after cell lysis, which prevents that the enzymes lyse surrounding uninfected cells of the target bacterium. (Schmelcher et al. 2012). This mechanism means that single Pal molecules most likely are only able to cleave the peptidoglycan once unlike typical enzyme molecules that can carry out the same reaction multiple times.

The occurrence of the plateauing of the lysis depending on the amount of Pal as shown in the TRAs in Figure 4.8 and Figure 4.23 supports the theory that once bound to the cell wall Pal cannot move on to cleave other *S. pneumoniae* cells. This mechanism decreases the efficiency of Pal. However, both domains are most likely required for the activity as the choline binding causes a conformational change that is transmitted to the catalytic domain (Varea et al. 2004). Furthermore, it has been shown for several endolysins that both domains are needed for full antimicrobial activity (Schmelcher et al. 2011; Sass & Bierbaum 2006). A truncation of the cell wall binding domain of Pal would therefore likely result in a loss or reduction of the enzymatic activity. However, it might be possible to modify the choline binding sites by site-directed mutagenesis in a way that weakens the binding without destroying it. This might result in a scenario, in which Pal can still bind to choline to induce the interaction between his two domains, but is released after the reaction and is able to cleave more *S. pneumoniae* cells. Overall, the changes would hopefully result in a higher efficiency and an extended lytic activity of a designer Pal.

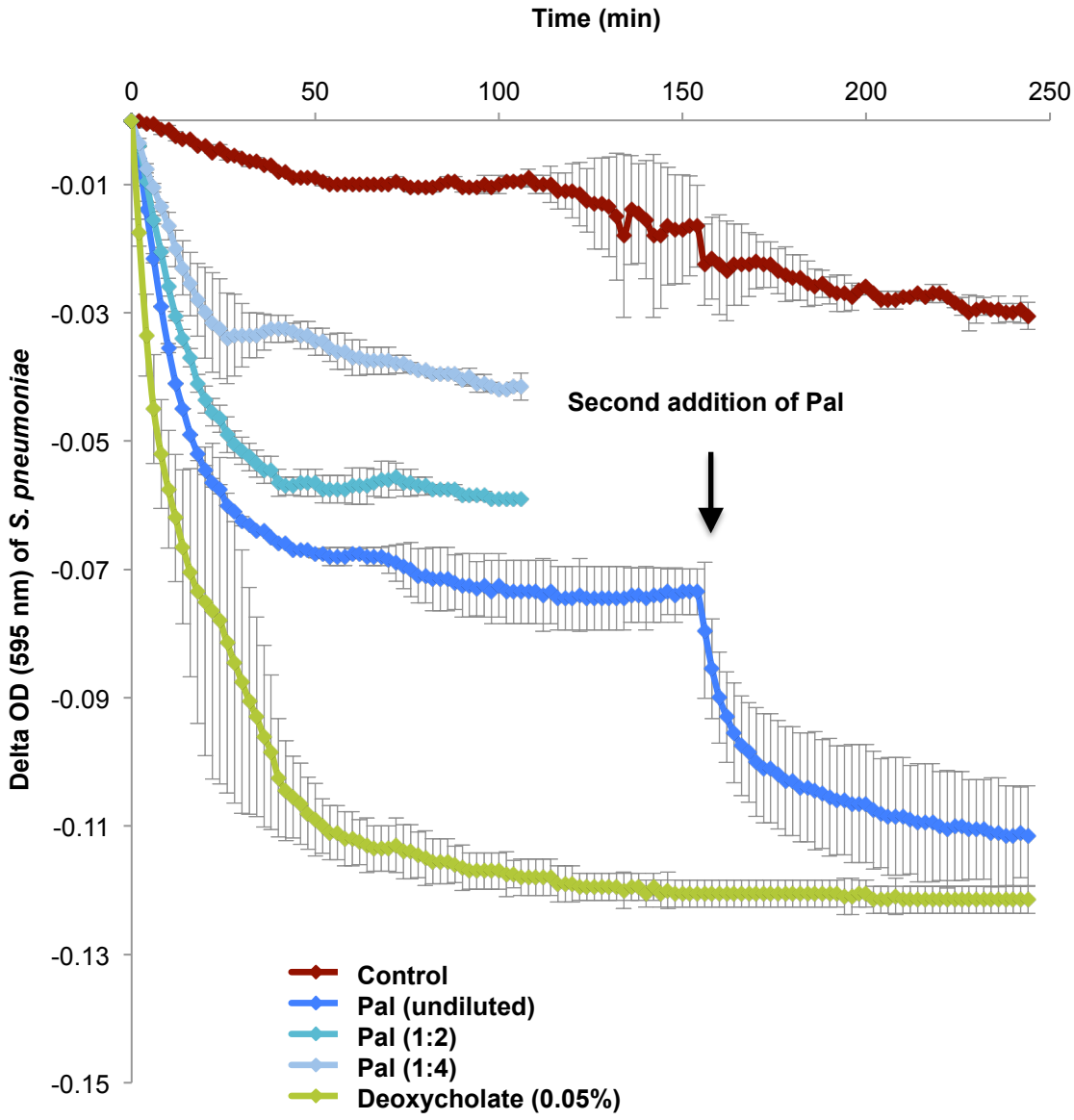

Figure 4.23: Turbidity reduction assay showing the dosage dependent bacteriolytic activity of purified Pal against *S. pneumoniae*
Pal was purified with ultracentrifugation, diethylaminoethanol (DEAE) cellulose and choline as specific eluent, as well as ammonium sulphate precipitation. *S. pneumoniae* cells were resuspended in NaPi-buffer to an optical density (OD_{595nm}) of 0.19. Purified Pal or control extract treated in the same way was added in different dilutions to the cell suspension and the OD_{595nm} was measured. After 150 minutes, the Pal and control suspensions were added a second time. The assay was performed at 37°C. The error bars show ± one standard deviation (n = 2).

4.2.4.5.2 Effect of choline on the bacteriolytic activity of purified Pal

It was of interest to examine whether free choline also inhibits *C. reinhardtii*-produced Pal, as described for *E. coli*-produced Pal (Domenech et al. 2011, Sheehan et al. 1997). This was on the one hand of interest to further characterise the endolysin produced in this study and on the other hand to evaluate whether the dialysis is a necessary step during purification, since it is a step that takes 16 hours and adds a further day to the purification procedure.

Therefore, TRAs were performed with preparations of Pal before and after dialysis. During the dialysis step, the Pal protein preparation was not concentrated and western blot analysis as well as Coomassie stained SDS-PAGEs did not show a marked loss of Pal protein during dialysis (Figure 4.20 A, B, Figure 4.21 C). However, the TRAs showed a strong decrease in the bacteriolytic activity of Pal in the presence of choline (6.5% v/w, 625 mM) before dialysis compared to the activity of Pal after dialysis (Figure 4.24) showing that the bacteriolytic activity of *C. reinhardtii*-produced Pal is also inhibited by free choline and that the dialysis is a necessary step during the purification of Pal. The concentration of choline used for the elution was performed with 625 mM, which is a lot higher concentration than the IC_{50} of 2 mM described by Domenech et al. (2011). To determine the IC_{50} for choline of *C. reinhardtii*-produced Pal, assays with a range of lower choline concentrations need to be performed.

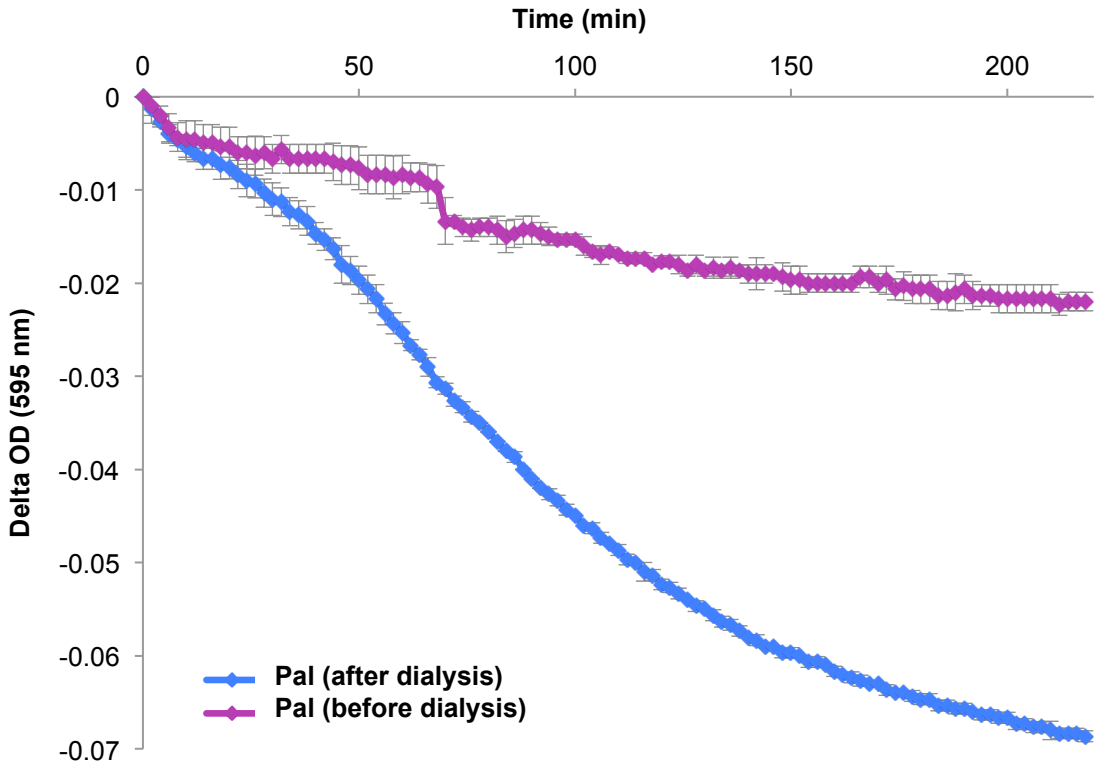

Figure 4.24: Turbidity reduction assay showing the inhibition of Pal by choline before dialysis
Pal was purified with ultracentrifugation, diethylaminoethanol (DEAE) cellulose and choline as specific eluent. *S. pneumoniae* cells were resuspended in NaPi-buffer to an optical density (OD_{595nm}) of 0.13. Samples of Pal preparations before and after dialysis were added to the suspension and the OD_{595nm} was measured. The assay was performed at 37°C. The error bars show ± one standard deviation (n = 3).

4.2.4.5.3 Bactericidal activity of purified Pal and Cpl-1

The purification of Pal allowed now to analyse the bactericidal activity of Pal without the inference of the endogenous antimicrobial substance in *C. reinhardtii* (4.2.3). The bacteriolytic activity of the endolysin Cpl-1 had been shown previously for purified enzyme and crude extracts, however the bactericidal effect had not yet been analysed (Taunt 2013). Cpl-1 was purified in the same way as Pal using ultracentrifugation, a DEAE cellulose column with choline as eluent and ammonium sulphate precipitation. The only difference to the purification of Pal was that Cpl-1 was precipitated with 50% ammonium sulphate instead of 35%.

Subsequently TRAs were performed with purified Pal, purified Cpl-1, deoxycholate and NaPi-buffer to follow the lysis of the *S. pneumoniae* cells (Figure 4.25 A). After the addition of further endolysins did not result in a further decrease of the OD_{595nm}, samples of the TRAs were spotted in different dilutions onto blood agar plates to analyse the number of colony forming units that had survived. After incubation overnight the plates showed only a few colonies in the spots of the undiluted samples that had been treated by Pal, Cpl-1 or deoxycholate, whereas the buffer control needed to be diluted 1:10,000 to reach a countable level (Figure 4.25 C).

Calculations of the cfu/ml showed that the samples treated with Pal contained 0.00047 ± 0.0005 million cfu/ml, the sample treated with Cpl-1 0.0003 ± 0.0001 million cfu/ml, whereas the control contained 2.5 ± 1 million cfu/ml. The sample treated with deoxycholate contained with 0.00122 ± 0.00025 million cfu/ml, more cfu than the samples treated with Pal or Cpl-1, despite that the OD_{595nm} measured in the TRA decreased more in presence of deoxycholate (Figure 4.25 A). This indicates that the decrease in OD_{595nm} is not directly related to the number of killed cells. Pal and Cpl-1 cleave only one specific bond of the peptidoglycan, whereas deoxycholate might trigger several autolysins that cleave different bonds. The lysis by Pal and Cpl-1 might result in larger cell pieces compared to the lysis by deoxcholate. Loeffler et al. showed that empty cell envelopes remain after the lysis by Pal, which still contribute to an OD_{595nm} measurement (Loeffler et al. 2001).

Overall, the number of cfu/ml decreased in the presence of Pal and Cpl-1 compared to the control by close to 4 log units (Pal: 3.54 log units, Cpl-1: 3.83 log units), which shows that both endolysins have bactericidal activity against *S. pneumoniae.*

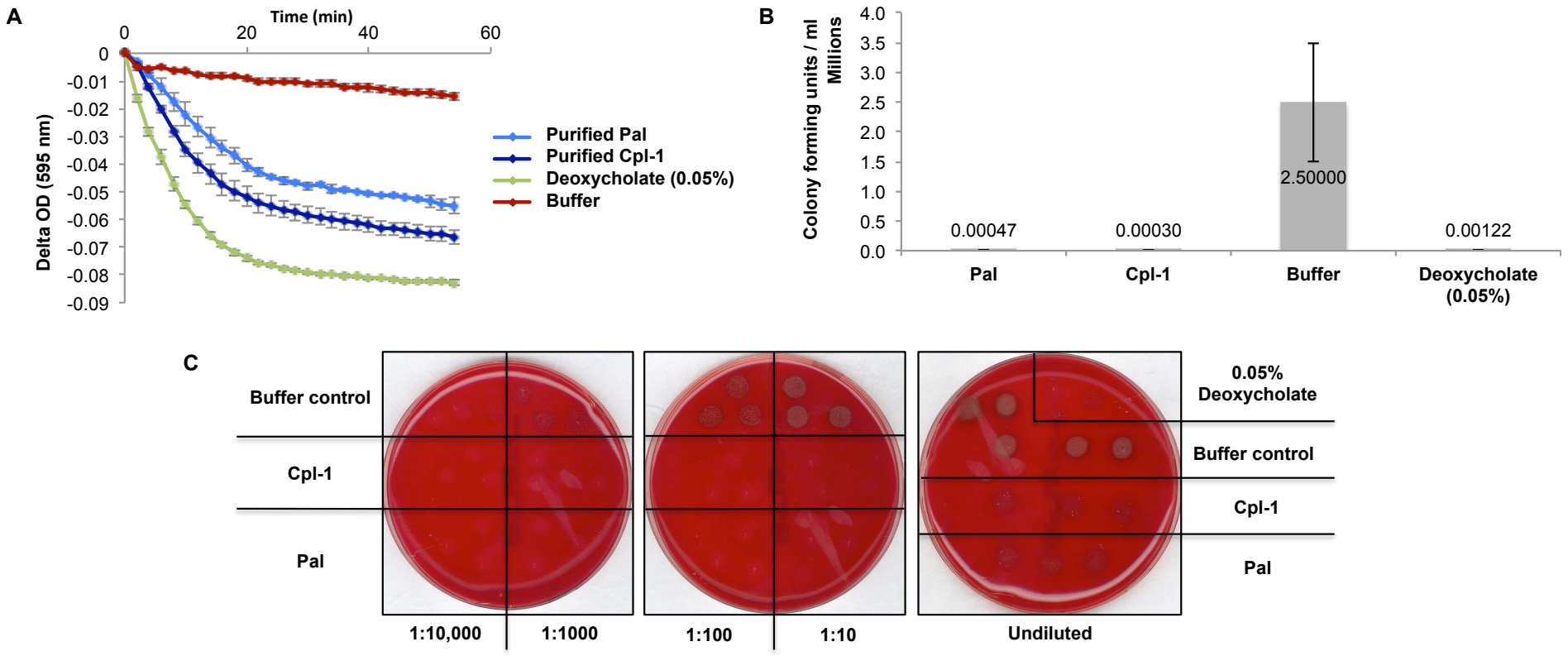

Figure 4.25: Bacteriolytic (A) and bactericidal (B, C) activity of purified Pal and Cpl-1
A turbidity reduction assay with *S. pneumoniae* cells (start OD_{595nm} 0.13) (A) was performed with purified Pal and Cpl-1, as well as deoxycholate (0.05% w/v) and buffer as positive and negative control, respectively. After the TRA, the samples were spotted onto blood agar plates in different dilutions to analyse the number of colony forming units (cfu) that had survived the treatments (C), subsequently the cfu/ml were calculated (B). The error bars in A and B show ± one standard deviation (n = 3).

4.2.4.5.4 Evaluation of the bactericidal activity of Pal and Cpl-1

Having analysed the bactericidal activity of Pal and Cpl-1, it was now possible to evaluate the antimicrobial activity of the endolyins produced in *C. reinhardtii* in comparison to these endolysins produced in *E. coli.*

Loeffler & Fischetti (2003) state that a freshly produced and purified batch of both endolysins is approximately 1 U/µg and found minimal inhibitory concentration (MIC) values of 50 to 200 U/ml for Pal and 25 to 50 U/ml for Cpl-1. A study by Rodríguez-Cerrato et al. (2007) states MIC values measured with four different strains of *S. pneumoniae* of 32, 32, 128 and 256 µg/ml for Pal and 8, 16, 16, 32 µg/ml for Cpl-1. The protein concentrations used in the experiment described in 4.2.4.5.3, were determined using a Bradford protein assay. The experiment was performed with 25 µg/ml of Pal and 15 µg/ml of Cpl-1. The concentrations used were therefore within the same range as the MIC values determined by Rodríguez-Cerrato et al. and even lower than the MIC values determined by Loeffler & Fischetti (2003).

Furthermore, Rodríguez-Cerrato et al. performed experiments similar to the one described in the last section with concentrations of 0.25x the MIC (in the case of Pal between 8 and 64 µg/ml, for Cpl-1 between 2 and 8 µg/ml). These experiments showed in average (of the four strains) a decrease in cfu of 2.71 log units after 5 h of incubation with Pal, and a decrease of 2.66 log units for Cpl-1, which is around one log (ten times) unit less compared to the results described in the last section of this chapter with only maximal three times (Pal) or 7.5 times (Cpl-1) less enzyme. In Loeffler & Fischetti, concentrations of 0.25x MIC (6.25 – 12.5 U/ml) decreased the cfu by 3 to 4 log units for Pal and 1 to 2 log units for Cpl-1. Loeffler et al. (2001) showed for 15 clinical isolates that the treatment with Pal (100 U/ml) (about 100 µg/ml) results in a decrease of cfu by around 4 log units, a result that was nearly reached in this study as well with around 25 µg/ml.

Taken together, these results suggest that Pal and Cpl-1 produced in the *C. reinhardtii* chloroplast have bactericidal activities, which are comparable to the activities of these endolysins produced in *E. coli.*

Oey et al. (2009b) determined also the amount of cfu after the treatment with Pal produced in tobacco (*Nicotiana tabacum*). This study states that after incubation for one hour with 300 µg of protein extract (equal to about 90 µg of Pal) the number of cfu of a *S. pneumoniae* suspension decreased to 7%, which is only just over one log unit. The experiment is not described for Cpl-1 in this article. But the article describes TRAs with Cpl-1 and states that 20 µg of Cpl-1 was sufficient to decrease the OD_{595nm} to a residual low OD_{600nm}, which meant from about OD_{600nm} 0.6 to 0.2, which was reached in TRAs performed during this study as well (not shown). This indicates that the *C. reinhardtii*-produced endolysins have antibacterial activities that are comparable to Pal and Cpl-1 produced in tobacco.

Overall, these results indicate that Pal and Cpl-1 are produced and accumulate in the *C. reinhardtii* chloroplast as proteins that are as active as the *E. coli* or tobacco produced enzymes. Furthermore, the data suggest that the purification of Pal and Cpl-1 did not cause major harm to the antibacterial activity of the endolysins.

4.2.4.6 Comparison of different purification/enrichment steps

Ultracentrifugation, ammonium sulphate precipitation, immunoprecipitation with anti-HA agarose and ion exchange chromatography with choline as specific eluent were all investigated for the purification of Pal. Ultracentrifugation removed the majority of cell debris, non-soluble proteins and the chlorophyll as well as most other pigments without a considerable loss of Pal, and proved to be a very effective first step for the purification of Pal. Ammonium sulphate precipitation can be used to separate Pal from numerous proteins, but still leaves a considerable number of contaminants when it is performed with ultracentrifugation supernatant. It is a very useful tool for the concentration of a protein suspension. Furthermore, ammonium sulphate precipitation is a purification method, which is used in large-scale protein purifications (Burgess & Jendrisak 1975, Lohman et al. 1986).

In a combination of ultracentrifugation, ammonium sulphate precipitation and immunoprecipitation with anti-HA agarose, Pal could be purified and enriched to such a degree that it could be visualized as a faint band on a Coomassie stained SDS-PAGE. However, the binding capacity of the resin for Pal under the assay conditions was exceeded in all repetitions of the experiment. Anti-HA agarose is expensive and therefore makes large-scale purifications uneconomical. Furthermore, in spite of the high specificity of antibody-conjugated resin, there were still contaminations with other proteins in the elution from the anti-HA resin. In another attempt, Pal was purified using ultracentrifugation and DEAE cellulose with choline as specific eluent. It was possible with this method to visualise a band for Pal on a Coomassie stained SDS-PAGE and to remove nearly all other proteins beside traces of a protein around 55kDa. Furthermore, it could be shown that Pal had been purified in an active form. DEAE cellulose can be easily used for scaling up and is used in industrial scale purifications (Burnouf et al. 2011) (Zhang et al. 2000). The addition of ammonium sulphate precipitation as a last step allowed the concentration of Pal without major losses and resulted in the removal of the 55 kDa protein. These results show that Pal can be purified using a combination of ultracentrifugation, DEAE cellulose with choline as eluent and ammonium sulphate precipitation and indicate that this purification method does not decrease the antibacterial activity of the endolysin.

4.3 Conclusion and future work

The experiments presented in this chapter analysed the antibacterial activity of the endolysin Pal synthesized in the *C. reinhardtti* chloroplast using crude extracts and purified enzyme. Furthermore, different purification methods for Pal were investigated and an antibacterial activity of *C. reinhardtii* extracts against two *Streptococcus* species was observed and further analysed.

As a first step, it was established that the cell wall less strain of *C. reinhardtii* TN72_x can be easily disrupted under sterile conditions by freezing and thawing or alternatively in a sonication bath. After cell breakage by these methods, Pal could be separated from the cell debris by centrifugation even at high cell densities. The breakage of cell-wall containing algae or bacteria species can be difficult and requires specialised equipment such as a French pressure cell press or other cell disrupter at lab-scale. These methods often result in marked losses of the extract and it is difficult to perform the breakage under sterile conditions. For large-scale cell disruption high-speed agitator bead mills or high-pressure homogenization methods are used. These methods can generate small pieces of cell fragments that are often difficult to remove. In contrast, breakage by freezing and thawing resulted in larger pieces, often just burst whole cells (Figure 4.2) that could be more easily separated by centrifugation than cell debris from cells broken by a cell disrupter. The acquisition of specialised equipment causes major costs and the operation is energy- and time-consuming. A cell wall less strain that can be easily disrupted by simple methods and simplifies the extraction of the desired protein is therefore a major advantage for a recombinant protein production platform.

As a next step, the bacteriolytic activity of *C. reinhardtii*-produced Pal against *S. pneumoniae* was demonstrated in turbidity reduction assays (TRAs). Moreover, the results suggest that the HA-tag does not hamper the antibacterial activity of the produced Pal. *C. reinhardtii*-produced Pal had no photometrically measurable effect on *Escherichia coli, Streptococcus pyogenes* or *Staphylococcus aureus,* which indicates that it has a high specificity for *S. pneumoniae*. On the other hand, it was

shown that Pal has bacteriolytic activity against not only the reference strain, but also five clinical isolates and five different serotypes of *S. pneumoniae*, including a strain with penicillin and co-trimoxazole resistance.

Moreover, an attempt was made to determine specific enzyme activities for *C. reinhardtii*-produced Pal using TRAs with live *S. pneumoniae* cells in this study. This determination was complicated by an autolytic activity of the *S. pneumoniae* cells. Cells from overnight cultures showed lysis in the control assays and even before the start of the TRAs. However, the performance of the TRAs with mid-logarithmic phase cells allowed the investigation of the lysis by Pal without major lysis in the control assays. Nevertheless, a strong dependency of the calculated enzyme activities on the start OD_{595nm} was observed. The more *S. pneumoniae* cells were added at the beginning to the TRA the quicker was the change in ΔOD_{595nm}. The same phenomenon was observed to a more extreme extent for the lysis by deoxycholate and to a lesser extent for the lysis by Cpl-1. On the other hand, TRAs performed at the same OD_{595nm} with different concentrations of Pal showed a clear dosage dependent response and identical specific enzyme activities per mg of Pal. It was considered whether the effect could be caused by an involvement of autolysins that might be released after lysis by Pal and have an additive bacteriolytic effect together with Pal. Nevertheless, more experiments, for example with mutants deficient for specific autolysins or autolysis inhibitors, need to performed before it can be concluded whether autolysins play a role in the cell lysis of *S. pneumoniae* by Pal. The results suggest that the determination of specific enzyme activities using such a complex substrate as live *S. pneumoniae* cells causes major variations in the resulting activities. To avoid major fluctuations of the activity values between different performances, an alternative would be to use isolated cell walls radioactively labelled with [*methyl*-^{3}H]choline as described in a few studies for the analysis of *E. coli*-produced Pal (Sheehan et al. 1997; Domenech et al. 2011; Jado et al. 2003) or non radioactive, purified and isolated *S. pneumoniae* cell walls for TRAs. Alternatively, it might be a solution to perform TRAs with mutants deficient for certain autolysins or heat-inactivated *S. pneumoniae* cells. Nevertheless, the method described in this study can be still used to compare different preparations of Pal, samples from different

purification steps or for the comparison to other enzymes, when cells from the same *S. pneumoniae* culture and the same start OD_{595nm} are used.
During this study it was possible to purify Pal in active form using a combination of ultracentrifugation, DEAE cellulose with choline as specific eluent and ammonium sulphate precipitation. A subsequent analyses of the antibacterial activity indicated that the purification procedure did not cause major harm to the antibacterial activity of the endolysin. The different steps performed for the purification of Pal are discussed in 4.2.4.6. Subsequently, purified Pal and additionally purified Cpl-1 were used to demonstrate the bactericidal activity of these endolysins against *S. pneumoniae*.

As a next step, TRAs with crude extracts and assays analysing the bactericidal activity with purified endolysins were used to demonstrate that the antibacterial activity of Pal and Cpl-1 produced in *C. reinhardtii* is at least as high as the bacteriolytic and bactericidal activities of the same endolysins produced in *E. coli* and tobacco. This was shown with two independent methods that used two different ways for the quantification of the amount of enzyme used in the assays. The amount of enzyme in the crude extracts was determined using western blots analysis with the HA-tagged standard protein CARHSP1 and the amounts of purified endolysins was analysed using Bradford protein assays and both resulted in values within the same range. This study did not determine minimal inhibitory concentrations (MIC) for Pal and Cpl-1. A careful determination of MIC values for Pal and Cpl-1 would enable a better comparison of the enzymatic activities of the two endolysins produced in *C. reinhardtii* to the enzymes from other production platforms and might even reveal higher activities for the algal produced ones. It is conceivable that Pal produced in *C. reinhardtii* has a higher enzymatic activity than the *E. coli*-produced one, since experiments described in 3.2.2.3 indicated that Pal is quickly degraded in *E. coli* and that more degradation products accumulate in the bacterium, which presumably have less or no activity, than full-length Pal.

An important further step would be now to perform *in vivo* studies with *C. reinhardtii*-produced Pal and Cpl-1 to investigate how the endolysins perform in mouse models in comparison to the *E. coli*-produced ones. The results of the quantification discussed in section 3.2.4 suggest that 10 mg of Pal are produced per litre of *C. reinhardtii* culture

volume (Cpl-1 accumulates to a similar level in the chloroplast (Taunt 2013)) and single doses of 40 – 200 µg Pal per mouse as used in Jado et al. (2003), with the created *C. reinhardtii* strains it is possible to produce 50 – 250 single doses for mice per litre of culture volume. Taken a loss of 50% during purification into account, this would be still 25 – 125 single dose per litre of *C. reinhardtii* culture. The facilities in the Purton lab allow the growth of 90 litres of culture at the same time. It seems therefore feasible to produce enough Pal and Cpl-1 with the created *C. reinhardtii* strains to conduct animal studies.

During this study a strong bactericidal activity of *C. reinhardtii* crude extracts against *S. pneumoniae* and also *S. pyogenes* was observed. On one hand, this was masking the measurements of the bactericidal activity of Pal and made it necessary to purify Pal. On the other hand, it adds an interesting feature to *C. reinhardtii* as a production platform for an antibacterial protein against *S. pneumoniae*. It was not directly demonstrated in this study that the unknown antimicrobial substance and Pal have an additive effect in killing *S. pneumoniae* cells, but it is conceivable. It would be very interesting to investigate whether this is the case, for example by quantitatively comparing the bactericidal activities of crude extract of *C. reinhardtii* containing Pal and *E coli* or tobacco extract with the same concentration of Pal. Additionally, the activity of Pal in crude algal extract could be analysed quantitatively in comparison to purified Pal.

The demonstration of an additive antibacterial effect would make the use of crude *C. reinhardtii* extracts containing Pal not only interesting from a commercial point of view (because it saves the costs for purification), but also because it would increase the therapeutic potency. *C. reinhardtii* is classified as GRAS (Generally recognised as safe) organism, which means that the alga is even safe for consumption. The use of crude extracts for topical and veterinary applications would therefore be conceivable. Another possibility would be to use *C. reinhardtii* crude extract containing Pal as a nasal wash for the elimination of *S. pneumoniae* in the nasopharynx. The nasopharynx is seen as the major reservoir for *S. pneumoniae* in the population and Loeffler et al (2001) propose that the diminution of this reservoir would have a great impact on the incidence of *S. pneumoniae* infections.

A literature research revealed two possible explanations about the nature of the endogenous antibacterial substance in *C. reinhardtii*. Jørgensen (1962) showed that chlorophyll derivatives from *C. reinhardtii* extracts have antibacterial activity against the Gram-positive bacterium *Bacillus subtilis* and this explanation agrees with the observation that the antibacterial activity was found in the 'green fraction' after all performed purification steps. A second explanation would be that certain fatty acids are responsible for the effect. It has been demonstrated that several microalgae contain fatty acids with antibacterial properties (Desbois & Smith 2010; Smith et al. 2010; Ohta et al. 1994). A comparison of the fatty acids found in *C. reinhardtii* and fatty acids that have been shown to possess antibacterial properties showed that a majority of fatty acids in the green microalgae do have antibacterial activity. Some studies demonstrated even an antimicrobial activity of some of the fatty acids against *S. pneumoniae*. It is therefore likely that fatty acids are at least partly responsible for the observed activity. A simple experiment to analyse whether chlorophyll derivatives or fatty acids are more likely to cause the antibacterial activity would be to nitrogen starve *C. reinhardtii*, which increases the amount of lipids and decreases the amount of pigments including chlorophylls. Followed by an analysis of the antibacterial activity of extracts from the starved and non-starved cells.

The occurrence of fatty acids with antimicrobial properties in *C. reinhardtii* and other microalgae makes microalgae in general more interesting as production platforms specifically for antibacterial proteins and makes the use of crude algal extract for the administration more attractive. This can be especially interesting for the use of endolysins against Gram-negative bacteria. The outer membrane represents a barrier that most endolysins against Gram-negative bacteria cannot cross. The mechanism of the antibacterial action of fatty acids is not fully understood yet, but the cell membranes are most likely the main target (Desbois & Smith 2010). Free fatty acids have an amphipathic structure and therefore detergent properties. This enables them to interact or even insert into cell membranes, which can result in pores, a higher fluidity of the membranes or at higher concentration solubilisation of the membranes (Desbois & Smith 2010). An antibacterial activity against Gram-negative bacteria has been shown for several fatty acids and also for some extracts of *C. reinhardtii* (Ghasemi et al 2007; Benkendorff et al. 2005). In a combination of Gram-negative specific

endolysins and algae extract, the ability of certain fatty acids to disintegrate membranes could be of great help to open the way for the Gram-negative specific endolysins to cross the outer membrane to get to the peptidoglycan. Ghasemi et al. (2007) demonstrated an antibacterial effect of extracts of *C. reinhardtii* against three Gram-negative bacterial species after extraction with methanol. Using a different extraction method (e.g. with methanol or chloroform) might allow the extraction of the fatty acids against Gram-negative bacteria together with synthesised endolysins. Furthermore, a proceeding approach could be to increase the percentage of fatty acids with the desired properties or introduce new ones in *C. reinhardtii* by metabolic engineering. For example, capric acid (10:0) and lauric acid (12:0), which are not present in *C. reinhardtii*, have been shown to have considerable antibacterial activities against *Chlamydia trachomatis* and *Neisseria gonorrhoeae* (Bergsson et al. 1999).

Overall, the results of this study strongly support the feasibility of the *C. reinhardtii* chloroplast as a platform for the synthesis of antimicrobial proteins, since reliable accumulation of predominantly full length Pal with a remarkable high stability was achieved. Moreover, it was possible to demonstrate a bacteriolytic and bactericidal activity against *S. pneumoniae* for *C. reinhardtii*-produced Pal and a second endolysin Cpl-1 and the results suggest that the enzymatic activities of both endolysins are comparable to the one of endolysins produced in *E. coli* or tobacco. Furthermore, the cell wall less *C. reinhardtii* strain TN72_x enables breakage by simple methods and easy extraction of the synthesised enzymes. The observation of an endogenous antibacterial activity of *C. reinhardtii* and the occurrence of several fatty acids with antibacterial properties in *C. reinhardtii* and other microalgae adds a very interesting argument for the use of microalgae as production platform for antimicrobial proteins and the use of crude algal extract for administration.

CHAPTER 5

Synthesis of the *Staphylococcus aureus* specific endolysin ϕ11 in the chloroplast of *Chlamydomonas reinhardtii*

5 Synthesis of the *Staphylococcus* specific endolysin ϕ11 in the chloroplast of *Chlamydomonas reinhardtii*

5.1 Introduction

5.1.1 The *Staphylococcus* specific endolysin ϕ11

The endolysin ϕ11 is encoded by the temperate bacteriophage ϕ11 of *Staphylococcus aureus*. The bacteriophage ϕ11 belongs, like Dp-1, to the family *Siphoviridae*, which is a member of the tailed bacteriophages of the order Caudovirales (Navarre et al. 1999). The genome of ϕ11 consists of a 44 kb double-stranded DNA molecule and the bacteriophage infects phage lytic group III strains of *S. aureus* including many strains that are human and animal pathogens (Iandolo et al. 2002).

The endolysin ϕ11 has a size of 54 kDa and two catalytic domains, an N-terminal D-alanyl-glycyl endopeptidase and a central *N*-acetylmuramoyl-*L*-alanine amidase, which have high sequence similarity to the catalytic domains of endolysins from other *S. aureus* specific bacteriophages such as Twort, ϕPVL, ϕ187 and α80 (Figure 5.1) (Sass & Bierbaum 2006; Navarre et al. 1999). The N-terminal catalytic domain belongs to the group of CHAP (cysteine, histidine-dependent amidohydrolase/peptidase) domains and cleaves the peptidoglycan between the D-alanine of the peptide chain and the first glycine of the glycine bridge and seems to be the more effective activity, whereas the second catalytic domain cleaves between the L-alanine of the peptide chain and the *N*-acetyl-muramic acid of the sugar strand (Figure 5.2) (Navarre et al. 1999). The C-terminal cell wall binding domain is homologous to the cell wall binding domain of the staphylolytic bacteriocin lysostaphin, which is produced by *Staphylococcus simulans* biovar *staphylolyticus,* and the protein ImlB, which occurs on the surface of *Listeria monocytogenes* (Figure 5.1) (Navarre et al. 1999). The domain belongs to the SH3b_5 cell wall binding domains, which are found in a large subset of staphylococcal peptidoglycan hydrolases (Becker et al. 2009).

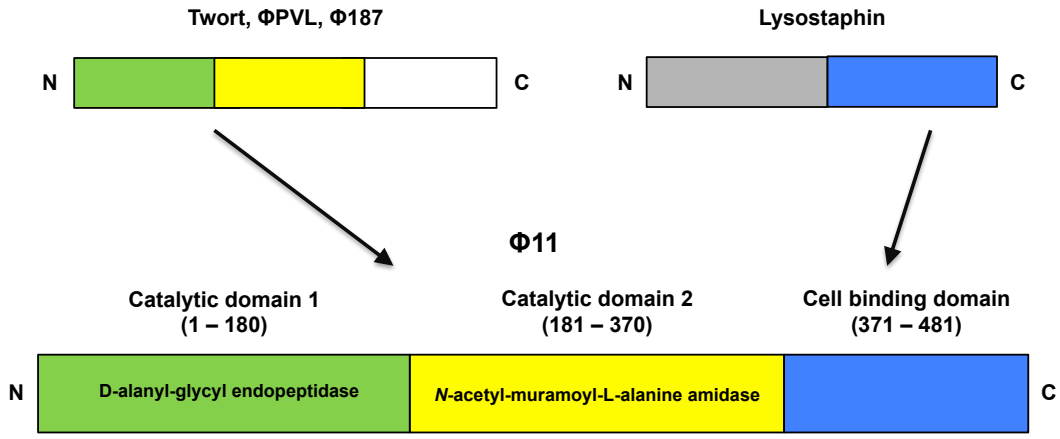

Figure 5.1: Modular organisation of the endolysin ϕ11
The endolysin ϕ11 has a *N*-terminal catalytic domain with D-alanyl-glycyl endopeptidase activity and a second central catalytic domain with *N*-acetyl-muramoyl-L-alanine amidase activity, which both have a sequence similarity to the catalytic domains of other *S. aureus* specific bacteriophages like Twort, ϕPVL and ϕ187. The C-terminal cell wall binding domain is homologous to the staphylolytic bacteriocin lysostaphin. (Figure based on Navarre et al. 1999 and Sass & Bierbaum 2006).

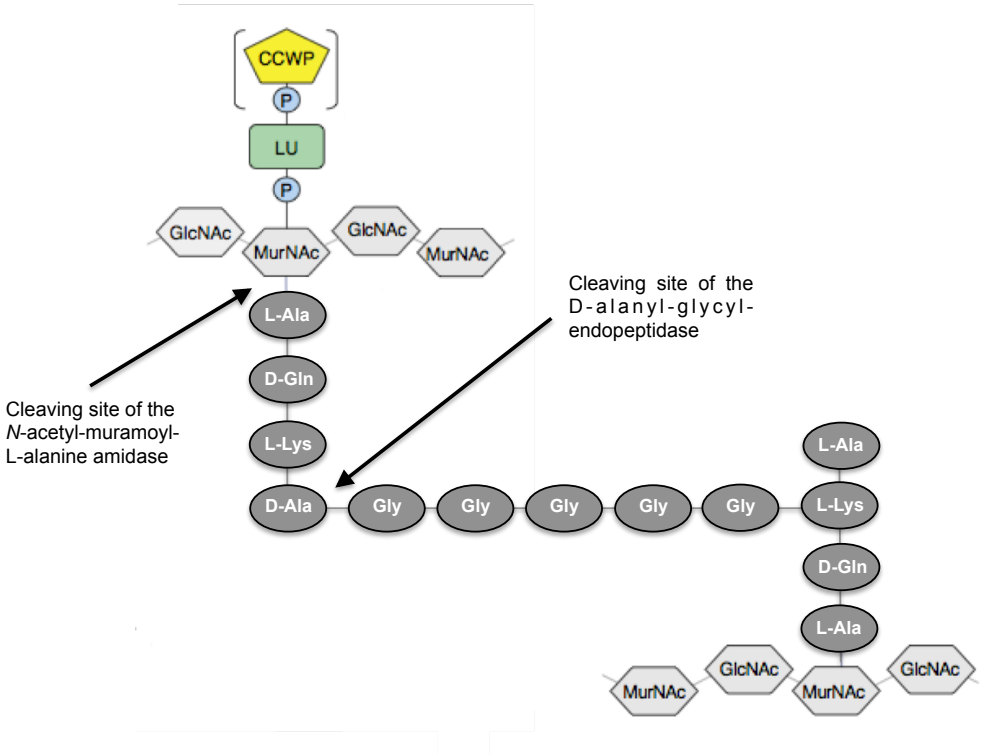

Figure 5.2: Cleaving sites of the *S. aureus* specific endolysin ϕ11
The first catalytic domain has D-alanyl-glycyl endopeptidase activity and cleaves the peptidoglycan between the D-alanine of the peptide chain and the first glycine of glycine bridge, whereas the second catalytic domain with *N*-acetyl-muramoyl-L-alanine amidase activity cleaves between the L-alanine of the peptide chain and the *N*-acetyl-muramic acid of the sugar strand. The structure of *S. aureus* peptidoglycan shown. CCWP = carbohydrate cell wall polymer, LU = linkage unit, P = phosphate group, MurNAc = *N*-acetyl-muramic acid, GlcNAc = *N*-acetyl-glucosamine, Ala = alanine, Gln = glutamine, Lys = lysine, Gly = glycine. Reproduced from (Navarre et al. 1999).

It has been shown for some hydrolases, amongst others lysostaphin, that the SH3b domain is essential for correct species-specific targeting to the *S. aureus* cell wall (Becker et al. 2009; Baba & Schneewind 1996). Furthermore, it has been shown that this domain is necessary for full staphylolytic activity (Becker et al. 2009).

Navarre et al. (1999) were the first to characterise the two different catalytic activities of ϕ11 and expressed a deletion mutant that lacks the amidase domain (Δ181 – 381) in *Escherichia coli*. The amidase deletion mutant still exhibited lytic activity against crude staphylococcal cell walls. The study found that the activity of the amidase deletion mutant is inhibited by *p*-hydroxymercuribenzoic acid, which is an organic mercurial that forms stable complexes with cysteine thiol residues. Furthermore, the enzyme was partly inhibited by EDTA (5 mM). Sequence alignments of the N-terminal endopeptidase domain of ϕ11 with the catalytic domains of the *S. aureus* specific endolysins Twort, ϕPVL, ϕ187 and α80 revealed the presence of one conserved cysteine. Navarre et al. concluded that this conserved cysteine residue is essential for the alanyl-glycyl endopeptidase activity of ϕ11 (Navarre et al. 1999).

Two further studies created a variety of deletion mutants to analyse the involvement of the three domains in the lytic activity of ϕ11. Sass & Bierbaum (2006) found that all three domains were essential for full lytic activity of ϕ11. Each of the catalytic domains together with the cell binding domain were able to lyse isolated cell walls of *Staphylococcus simulans* 22, but with a reduced enzymatic activity. Each catalytic domain on its own did not show any activity, whereas both catalytic domains together without the cell wall binding domain had nearly full activity against isolated cell walls. However, only the full-length ϕ11 and none of the truncations showed lytic activity against whole heat-killed staphylococcal strains or biofilms. Sass & Bierbaum (2006) concluded that both catalytic domains have to be combined and that substrate recognition of the cell-wall binding domain is necessary for the full function of ϕ11 and its ability to cleave the cell wall of intact cells. It has also been shown for lysostaphin that the cell wall binding domain is essential for full lytic activity (Baba & Schneewind 1996). Furthermore, the study showed that a concentration of 20 µg/ml of full-length ϕ11 causes the lysis of the strains *S. aureus* NCTC8325, *S. aureus* Wood 46, *S. aureus* Newman, *S. epidermis* O-47 and *S. simulans* 22 with a lytic activity that

was comparable to highly purified lysostaphin (5 µg/ml). Moreover, Sass & Bierbaum (2006) showed that ϕ11 can eradicate *S. aureus* NCTC8325 biofilms with an efficiency nearly equivalent to lysostaphin, which was the first report of a staphylococcal endolysin eliminating biofilms. The ability to disrupt staphylococcal biofilms makes ϕ11 particular interesting as an antibacterial agent, since biofilms represent a major problem for the treatment and management of staphylococcal infections, especially given that the build up of biofilms on catheters and other long-term medical devices remains challenging (Donlan & Costerton 2002).

A second study by Donovan et al. (2006) analysed truncation mutants of ϕ11 and found that both ϕ11(1-194) (endopeptidase domain with parts of the amidase domain) and ϕ11(1-389) (endopeptidase and full amidase domain without the cell binding domain) had lytic activity against whole untreated *S. aureus* cells, but the authors also state that the truncations had less activity than full-length ϕ11. The major aim of this study was to investigate the potential of ϕ11 as a treatment against bovine mastitis. This infection of the mammary gland of dairy cows is a problem worldwide and is the number one reason for antibiotic use in the dairy industry (Donovan et al. 2006; Erskine et al. 2002). The development of a pathogen-specific antimastitis treatment could reduce the use of broad-range antibiotics and at the same time the risk of antibiotic resistance development. Donovan et al. (2006) demonstrated that ϕ11 is able to lyse live staphylococcal mastitis pathogens such as *S. aureus* and coagulase-negative staphylococci including *S. chronogenes, S. epidermis, S. hyicus, S. simulans, S. warneri and S. xylosus*. Together with the results of Sass & Bierbaum (2006), this shows that ϕ11 is effective against a broad range of staphylococcal species. Furthermore, the study showed that ϕ11 is active at a broad range of physiologically relevant pHs values (pH 5.5 – 8) including that of milk (pH 6.7) and that the endolysin is active at the calcium concentration of milk (3 mM). Both findings are important for the long-term goal of Donovan et al. to express ϕ11 in the mammary glands of transgenic cows to prevent the occurrence of mastitis.

David M. Donovan holds a patent on the “Specific lysis of staphylococcal pathogens by bacteriophage ϕ11 endolysin”, which was filed in July 2011 and published in January 2013 amongst others as US8361772 B2 and US20110318328 A1 patents. This patent covers the full-length endolysin as well as any ϕ11 truncations and the use as a treatment for any human and animal diseases caused by staphylococcal strains.

A short communication by Donovan et al. (2008) addresses the problem that two different gene sequences of the ϕ11 endolysin are available in the databases. The gene sequences differ only in three bases, but the changes result in 41 different amino acids due to a frame shift. The study used DNA sequence alignments and matrix-assisted desorption/ionization-time-of-flight (MALDI-TOF) mass spectroscopy to identify the correct sequence of the endolysin ϕ11 and found that the sequence determined by Iandolo et al. (2002) with the protein accession number NP_803306 and the nucleotide accession number NC_004615 is the correct sequence. This protein sequence of ϕ11 was used in this study and the corresponding gene sequence was codon-optimised for the *C. reinhardtii* chloroplast.

The endolysin ϕ11 is a promising candidate for the use as a novel antibacterial agent due to its efficiency against a variety of staphylococcal species including bovine mastitis pathogens and its ability to disrupt biofilms. *S. aureus* and other staphylococci species are major human and animal pathogens with a high percentage of antibiotic resistant strains including multi-drug resistances (1.3.2). As a treatment for bovine mastitis it would be possible to use ϕ11 in crude algal extracts as a topical treatment. The use of ϕ11 in a veterinary application would strongly facilitate the approval process compared to an application in human medicine. Nevertheless, *S. aureus* causes several skin infections in humans and a topical administration in human medicine would also be conceivable despite a protracted and more expensive approval process.

5.1.2 Aims and objectives

The aim of the experiments in this chapter was the synthesis of the endolysin ϕ11, a promising candidate as a novel antibacterial agent against staphylococcal human and animal pathogens, in the *C. reinhardtii* chloroplast. Subsequently, the aim was to analyse the antibacterial activity of *C. reinhardtii*-produced ϕ11 against *S. aureus* including strains with antibiotic resistance and to compare the activity to ϕ11 produced in *Escherichia coli.*

5.2 Results and discussion

5.2.1 Creation of transgenic lines of *C. reinhardtii* carrying the *ϕ11* gene in the plastome

A transgenic line of *C. reinhardtii* carrying a synthetic *ϕ11* gene in the plastome was created to study the synthesis of the ϕ11 protein in the algal chloroplast. The line uses as expression elements the *atpA* promoter/5'UTR and the *rbcL* 3'UTR, which are described in 3.2.1.2. The *ϕ11* gene contains the coding sequence for a C-terminal HA-tag (Figure 5.3). To enable a straightforward purification procedure for ϕ11 using commercially available Ni-NTA (nickel-nitrilotriacetic acid) columns, a second transgenic line was created carrying the *ϕ11* gene with the coding sequence for a C-terminal HA-tag followed by the sequence of a polyhistidine (His)-tag (Figure 5.3). The line carries the same expression cassette as TN72_*ϕ11-HA*. The HA-tag was included in addition to the His-tag to enable the detection of ϕ11 using anti-HA antibodies, which are more sensitive than antibodies against the His-tag. Finally, a line carrying the *pal* gene with coding sequences for both tags was created to test another purification strategy for Pal (Figure 5.3). The analysis of the transgene expression of both lines is discussed in this chapter.

All lines were created using the *C. reinhardtii* chloroplast transformation system that consists of the cell wall-less recipient strain TN72 and the expression vector pASapI. For a detailed description of the transformation system see 2.3.8 and 3.2.1.

5.2.1.1 Design and codon-optimisation of the synthetic *ϕ11* gene

The sequence of the ϕ11 protein was taken from the database UniProtKB/Swiss-Prot (Entry: Q8SDS7; Entry name: Q8SDS7_BPPHA; Protein name: Amidase; Protein accession number: NP_803306.2; Organism: Staphylococcus phage phi11 (Taxonomic identifier: 12360)). The protein ϕ11 is comprised of 481 amino acids and has a mass of 54,030 Da. The corresponding gene was codon-optimised for the *C.*

reinhardtii chloroplast to a Codon Adaption Index (CAI) of 0.8 with respect to the codon usage table from Nakamura et al. (2000) (http://www.kazusa.or.jp/codon) and synthesised by GENEART (Regensburg, Germany) with the addition of a 5' SapI and a 3' SphI site for subsequent cloning, and sequence for a C-terminal human influenza haemagglutinin (HA) epitope tag for detection. The created *ϕ11* gene has a length of 1,443 bp and including the HA-tag coding sequence and two stop codons (TAA) a length of 1,476 bp. The codon-optimised DNA sequence of the *ϕ11* gene is attached in the appendix. The HA-tagged ϕ11 protein has a predicted molecular mass of 55.1 kDa. In TN72_*ϕ11-HA-His* and TN72_*pal-HA-His* the genes of interest contain additionally the coding sequence for a polyhistidine-tag, which consist of six histidines residues. The resulting recombinant proteins have a mass of 56.0 and 36.4 kDa, respectively.

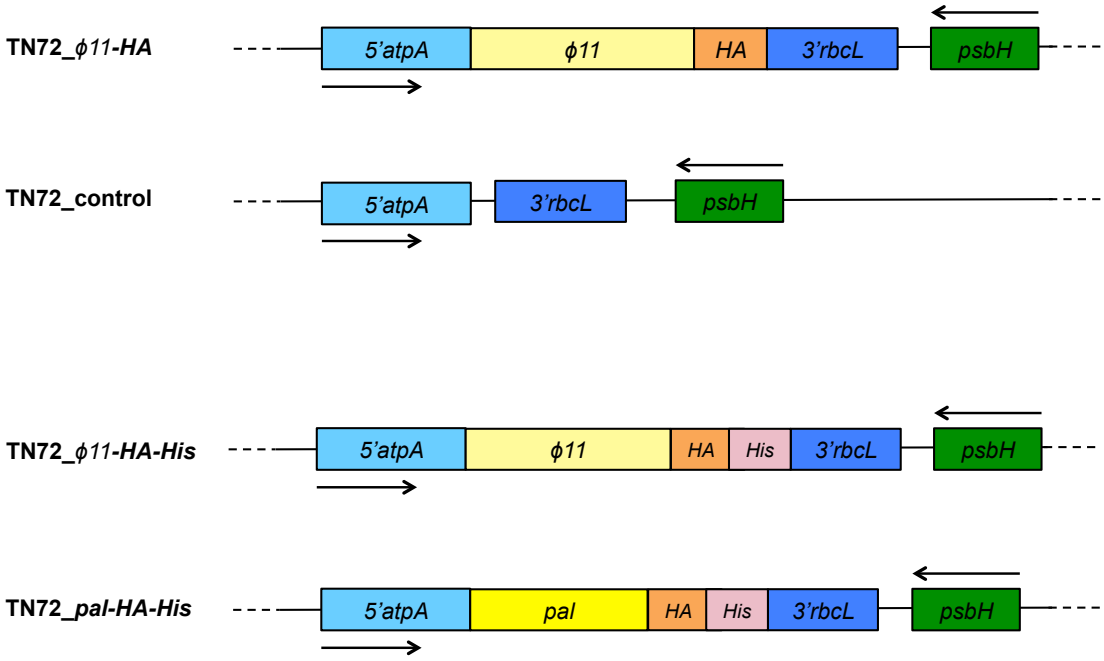

Figure 5.3: Strains of *C. reinhardtii* TN72_x analysed in this chapter
The diagram shows the differences in the gene of interest and tags of the *C. reinhardtii* TN72_x strains, which were created to study the expression of ϕ11 in the *C. reinhardtii* chloroplast or to facilitate the purification of ϕ11 and Pal. Endogenous chloroplast genes are indicated in green, expression elements in blue, the genes of interest in yellow and the tags in orange.

5.2.1.2 Creation of the transgenic lines

5.2.1.2.1 TN72_*ϕ11-HA*

For the creation of TN72_*ϕ11-HA* the expression vector pASapI was used (Economou et al. 2014). The *ϕ11-HA* gene was cloned from the GENEART vector pMK_*ϕ11-HA* into pASapI using the SapI and SphI restriction sites. The successful cloning of *ϕ11-HA* into pASapI was confirmed by sequencing. The resulting plasmid pASapI_*ϕ11-HA* was transformed into *C. reinhardtii* TN72 using the glass bead method. Colonies obtained from transformation were restreaked three times to achieve homoplasmicity. Insertion of *ϕ11-HA* into the correct location in the chloroplast genome and homoplasmicity were confirmed by PCR with the primers FLANK1, atpA.R and rbcL.Fn (Figure 5.4) and by sequencing between the primers atpA.F and rbcL.R. Of six transformants analysed by PCR, five contained the expression cassette with *ϕ11-HA* in the correct location. Figure 5.4 B shows transformant 1 and 2 after one round of restreaking in a heteroplasmic state and transformant 3 and 4 after three rounds of restreaking in a homoplasmic state.

5.2.1.2.2 TN72_*ϕ11-HA-His* and TN72_*pal-HA-His*

For the addition of the His-tag coding sequence, the *pal-HA and ϕ11-HA* genes were amplified in a PCR with primers that bind at both ends of the genes and contain the restriction sites SphI and SapI. The reverse primer used binds within the HA-tag sequence and contains the sequence for six histidines, which form the His-tag. The primers used for this PCR were Pal.F, ϕ11.F and for both genes Histag.R. Afterwards, the PCR products were digested with SphI and SapI and cloned into pASapI. Subsequently, the constructs were transformed into *C. reinhardtii* TN72 and the correct insertion of the genes was confirmed as described for TN72_ *ϕ11-HA* (5.2.1.2.1).

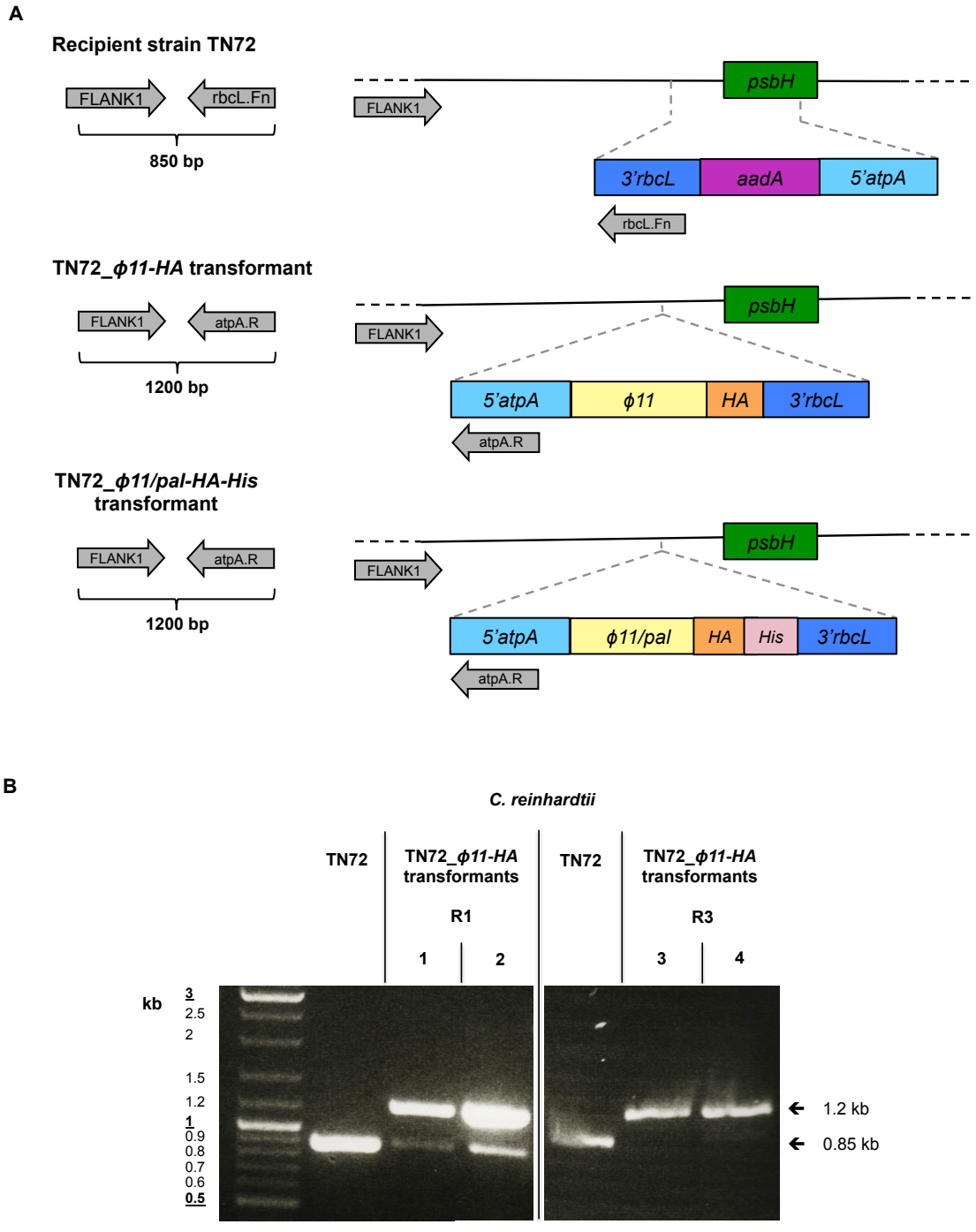

Figure 5.4: PCR screening for the successful transformation of the *C. reinhardtii* TN72 chloroplast

Schematic diagram showing the binding sites of the used set of primers and the expected fragment sizes for the recipient strain TN72 and successful TN72_*ϕ11-HA,* TN72_*ϕ11-HA-His* and TN72_*pal-HA-His* transformants (A). PCR screening for putative transformants with the recipient strain TN72 as control (B). The primer FLANK1 binds to the plastome outside of the insertion area. RbcL.Fn binds within the *aadA* cassette of the untransformed recipient strain TN72 and results together with FLANK1 in a product of 0.85 kb. The third primer atpA.R binds to the promoter of the expression cassette, which results together with FLANK1 in a product of 1.2 kb. Homoplasmic transformants show only a band at 1.2 kb. Heteroplasmic transformants show additionally a 0.85kb band. (A) Grey arrows = primers, blue boxes = expression elements, green boxes = plastome genes. (B) 1 = Transformant 1, R1/3 = First/third restreak.

Both TN72_*pal-HA-His* transformants analysed by PCR contained the expression cassette with *pal-HA-His* in the correct location and had achieved homoplasmicity (Figure 5.5). The PCR screening showed that of five TN72_*ϕ11-HA-His* transformants analysed, four had been successfully transformed and had reached homoplasmicity (Figure 5.5).

5.2.1.2.3 TN72_control

The corresponding control strain was created by transformation of the recipient strain TN72 with the corresponding transformation vector pASapI carrying an empty expression cassette with the *atpA* promoter/5'UTR and the *rbcL* 3'UTR to ensure the same genetic background (Figure 5.3) (Ninlayarn 2012).

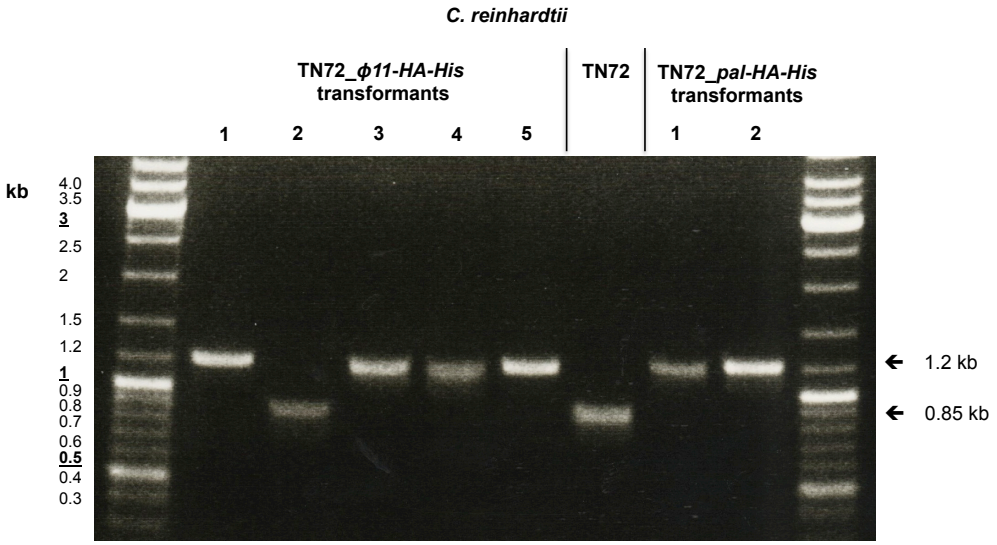

Figure 5.5: PCR screening for the successful transformation of the *C. reinhardtii* TN72 chloroplast with pASapI_*ϕ11-HA–His* and pASapI_*pal-HA–His*
In the PCR screening for putative TN72_*ϕ11-HA-His* and TN72_*pal-HA-His* transformants the primers FLANK1, atpA.R and rbcL.Fn were used. For binding regions of the primers see Figure 5.4 A. TN72 = Recipient strain; 1,2.. = Transformants; Expected band sizes are: TN72 = 0.85 kb; Homoplasmic transformant = 1.2 kb; Heteroplasmic transformant: 0.85 kb and 1.2 kb.

5.2.2 Expression of *ϕ11* in the *C. reinhardtii* chloroplast

5.2.2.1 Confirmation of *ϕ11* expression using anti-HA antibodies

The ϕ11 protein was synthesised with the addition of a C-terminal HA-tag to enable the detection of ϕ11 using commercially available anti-HA antibodies, which had been successfully used for the detection of Pal and Cpl-1 (this study, Taunt 2013).
The transformant lines were therefore analysed for the presence of HA-tagged ϕ11 protein, which has a predicted size of 55.1 kDa, by western blot analysis using anti-HA antibodies together with IRDye® secondary antibodies and the Odyssey® Infrared (IR) Imaging System. Alternatively, horseradishperoxidase-linked secondary (ECL) antibodies were used and the resulting chemiluminescence was detected with photographic film. Both detection systems showed a band at approximately 55 kDa for samples of TN72_ϕ11-HA that was not present in samples of the TN72_control strain (Figure 5.6 A, Figure 5.15). These results confirm the successful synthesis of ϕ11 in the chloroplast of *C. reinhardtii.*

The majority of western blot analyses with TN72_*ϕ11-HA* showed an additional band at approximately 38 kDa, which was not present in analyses of TN72_control (Figure 5.6 A). It is conceivable that the additional band is a degradation product of ϕ11, and has lost approximately the first 150 N-terminal amino acids due to proteolytic degradation at a specific cleavage site. This would mean that the truncation had resulted in the loss of the majority of the first catalytic domain, which consists of 180 amino acids (Figure 5.7). Another explanation could be that the truncated protein is a result of a cryptic ribosome-binding site within the *ϕ11* mRNA. The protein sequence of ϕ11 contains in the region of the truncation start a methionine and a translation start at this position would result in a protein with a mass of 38.9 kDa. This explanation would be therefore feasible as well. Figure 5.7 shows the protein sequence of ϕ11 with the potential methionine start codon highlighted in red and the three domains of ϕ11.

Transgenic lines that are created via the introduction of genes into the chloroplast genome by homologous recombination are genetically identical and are therefore expected to show identical expression levels for recombinant proteins. A western blot

analysis of two TN72_*ϕ11-HA* transformants harvested at the same growth stage showed similar ϕ11 protein levels for both transformants (Figure 5.6 B). This indicates that the proposed theory is right that genetically identical transformants have comparable recombinant protein production levels. Furthermore, it has been shown in a previous study that independent *C. reinhardtii* TN72_*cpl-1-HA* transformants produce similar levels of recombinant Cpl-1 protein (Taunt 2013). TN72_*ϕ11-HA* transformant 1 was chosen for further experiments. The synthesis of ϕ11 in TN72_*ϕ11-HA-His* is analysed together with the production of Pal in TN72_*pal-HA-His* in section 5.2.5.

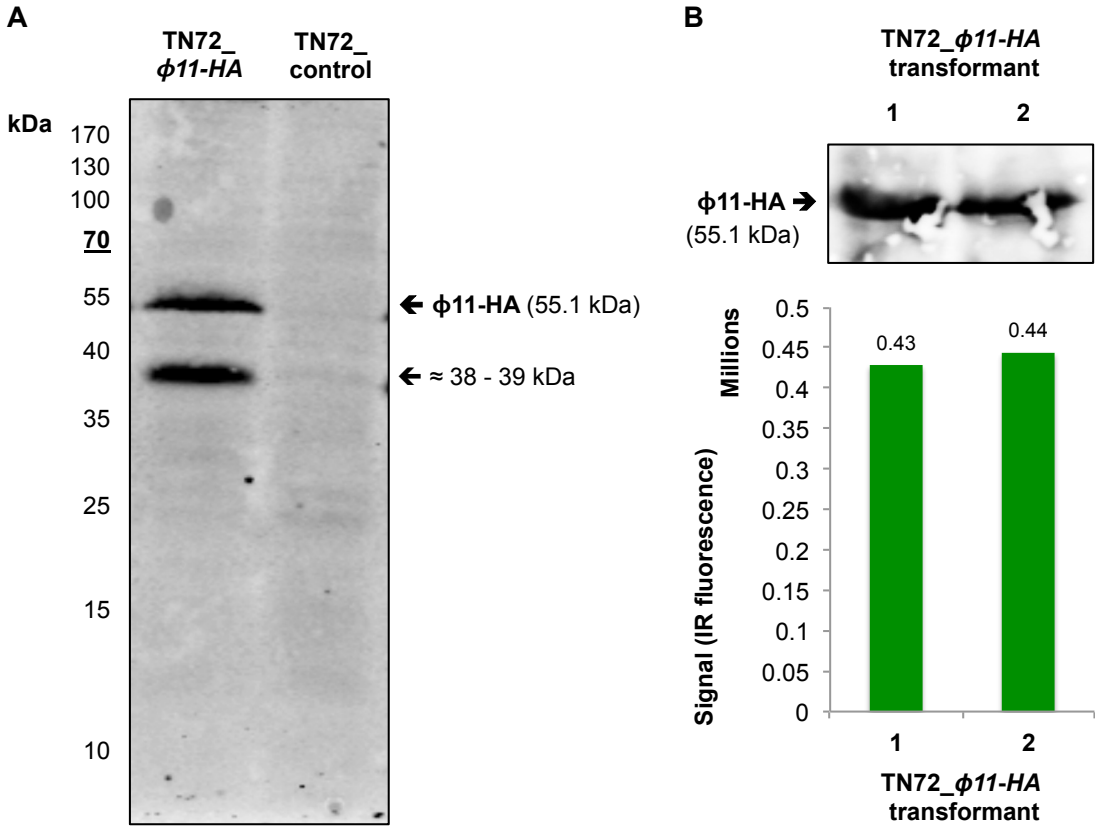

Figure 5.6: Western blot analysis of crude extract (A) and whole cell extract of two TN72_*ϕ11-HA* transformants showing the presence of HA-tagged ϕ11 protein
The western blot was performed with samples of TN72_ *ϕ11-HA* and anti-HA antibodies, IRDye® secondary antibodies and the Odyssey® Infrared Imaging System for detection. TN72_control was used as a negative control. The expected band size is 55.1 kDa. Protein sizes were determined using the PageRuler™ Prestained Protein ladder (Thermo Scientific).

Figure 5.7: Protein sequence of ϕ11 showing the potential alternative methionine start codon that would result in a 38.9 kDa protein and the three domains of ϕ11
The methionine highlighted in red could potentially function as an alternative translation start, which would be a possible explanation for the approximately 38 kDa ϕ11 truncation observed in western blot analyses with TN72_*ϕ11-HA*. The protein molecular mass was calculated using http://bioinformatics.org/sms/prot_mw.html. The HA-tag is highlighted in dark green. The first catalytic domain is indicated in light green, the second catalytic domain in yellow and the cell binding domain in light blue.

5.2.2.2 Expression of *ϕ11* in *Escherichia coli* DH5α

As mentioned already in chapter 3, *Escherichia coli* is widely used as an established expression system for the production of recombinant proteins and it was therefore of interest to compare also ϕ11 synthesised in *E. coli* to the *C. reinhardtii*-produced endolysin. It has been shown in 3.2.2.3 and previous studies that the expression cassette of pASapI results also in the expression of the gene of interest (GOI) in *Escherichia coli* DH5α (Szaub 2012; Taunt 2013). This allows an easy qualitative analysis of the synthesis of ϕ11 in *E. coli* compared to *C. reinhardti*. Furthermore, it enables a comparison of the antibacterial activity of ϕ11 produced in both systems.

The construct pASapI_*ϕ11-HA* was transformed into *E. coli* DH5α and a western blot analysis with anti-HA antibodies was performed using crude cell extracts. It was

possible to detect a strong band at approximately 55 kDa. However, the negative control with DH5α_control also showed a band at approximately the same size (Figure 5.8, Figure 3.10), though the band in the control samples was always found weaker than the band in the samples of DH5α_*ϕ11-HA* (Figure 5.8). Furthermore, the extract of DH5α_*ϕ11-HA* showed bacteriolytic activity against *Staphylococcus aureus* in turbidity reduction assays (TRAs), which is discussed in section 5.2.4. Taken together, this suggests that ϕ11 is synthesised in *E. coli* DH5α_*ϕ11-HA*. Additionally, the western blot analyses with DH5α_*ϕ11-HA* showed a band at approximately 38 – 39 kDa that was not present in the negative control (Figure 5.8). This indicates that the same truncation of ϕ11 occurs in *C. reinhardtii* and *E. coli* either by proteolytic activity or an alternative translation start site.

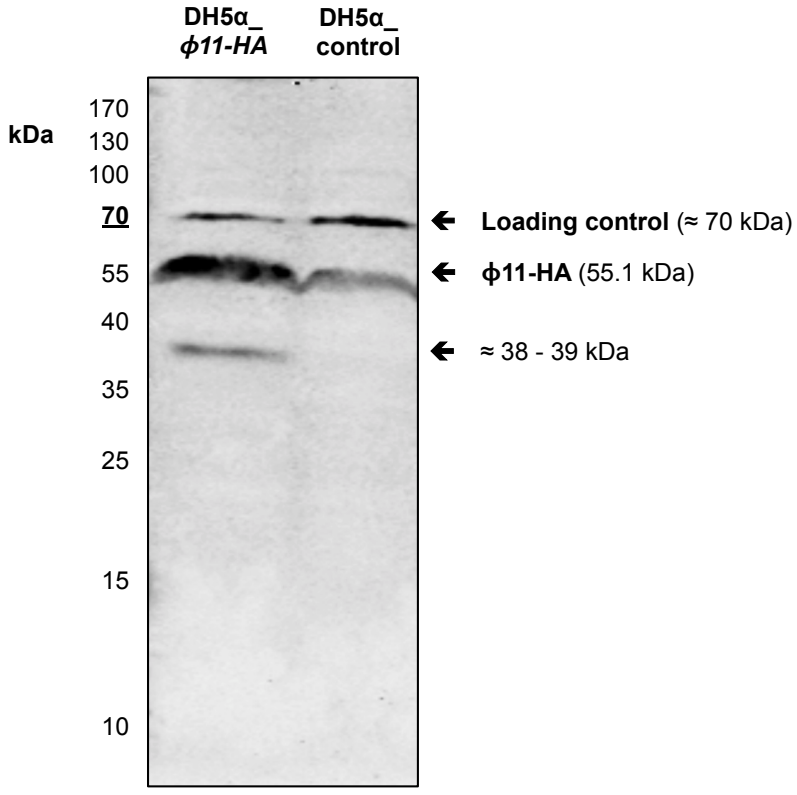

Figure 5.8: Western blot analysis with crude extracts of *Escherichia coli* DH5α_*ϕ11-HA* for the presence of HA-tagged ϕ11 protein
The western blot analysis was performed with 20 µl of crude extract prepared from *E. coli* overnight cultures that had been concentrated to 20 times of the culture volume and broken by passing the suspension through a French Pressure cell press. Anti-HA antibodies and IRDye® secondary antibodies and the Odyssey® Infrared Imaging System were used for detection. The expected band size is 55.1 kDa. Protein size was determined using the PageRuler™ Prestained Protein ladder (Thermo Scientific).

5.2.2.3 Yield of ϕ11 at different growth stages

As a next step the yield of recombinant ϕ11 protein in cells of TN72_*ϕ11-HA* was determined at different growth stages to analyse the expression and stability of the endolysin in the chloroplast. Additionally, it was of interest to further investigate the truncation of ϕ11 that had been observed in several western blot analyses.

For this experiment, TN72_*ϕ11-HA* was grown under standard conditions, the culture growth was recorded by measuring the OD_{750nm} and samples were taken at multiple time points during growth. After harvesting, the cell pellet was resuspended in a volume depending on the OD_{750nm} of the culture at the time of sampling to obtain the same cell density in every sample. Subsequently, the samples were analysed by western blot with anti-HA antibodies and the Odyssey® Infrared Imaging System was used for quantification.

This analysis showed that predominantly full-length ϕ11 was present in the cells until the mid-logarithmic phase, which explains the absence of the truncation in some western blot results. At the end of the logarithmic phase the amount of ϕ11 truncation increased. Similar amounts of truncation and full-length ϕ11, or even higher amounts of the truncation were detected at the end of the logarithmic phase and the beginning of the stationary phase. In contrast, the last sample, which was taken after the OD_{750nm} started to decrease, contained again a higher proportion of full-length ϕ11. Overall, the yield of recombinant ϕ11 per cell increased slightly during culture growth.

The metabolism of cells changes during the transition into the stationary phase to adapt to the changing conditions and to become more resistant to stress and nutrient limitation. The overall protein synthesis generally decreases, whereas the synthesis of proteases and peptidases increases (Navarro Llorens et al. 2010). The observation that more ϕ11 truncation is formed during the transition into the stationary phase compared to the logarithmic phase therefore supports the hypothesis that the truncation is formed by proteolytic activity.

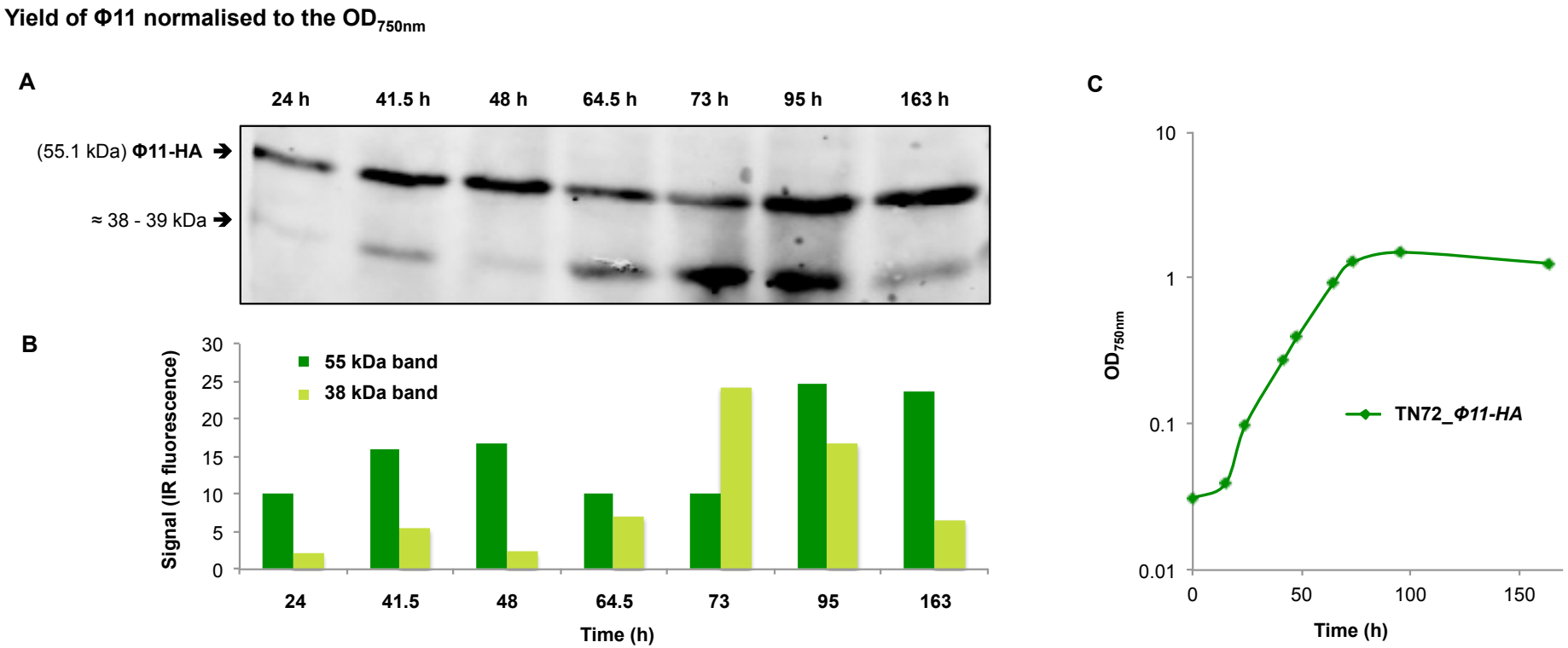

Figure 5.9: Yield of ϕ11 synthesis at different growth stages
Cultures of TN72_*ϕ11-HA* were grown under standard conditions and samples were taken at multiple time points during growth. After harvesting the samples were normalised to the OD_{750nm} at the time of sampling (cells were resuspended in 1 ml of buffer per OD_{750nm} of 2) and 20 µl of the samples were analysed in a western blot analysis with anti-HA antibodies, IRDye® secondary antibodies and the Odyssey® Infrared Imaging System for detection and quantification. A shows the western blot picture, B the Odyssey IR fluorescence signals of both bands and C the growth of the TN72_*ϕ11-HA* culture.

5.2.3 Production of ϕ11 protein preparations for activity assays

For the performance of assays analysing the antibacterial activity of ϕ11 against *S. aureus* it was necessary to break the *C. reinhardtii* cells and to recover ϕ11 without denaturing the endolysin. It has been already shown in 4.2.1 that the cell wall-less strain TN72 can be easily broken by freezing and thawing and that the majority of Pal can be recovered in active form and subsequently separated from the cell debris afterwards. Nevertheless, it was still important to analyse whether ϕ11 would behave in the same way.

TN72_*ϕ11-HA* cells were therefore broken by freezing and thawing for three cycles as described in 4.2.1. Subsequently, the amount of ϕ11 in the whole cell extracts and the supernatants after pelleting the cell debris by centrifugation was determined in western blot analyses. All samples were additionally treated with SDS and boiling to break leftover unbroken cells. These analyses showed that it was also possible to recover the majority of ϕ11 into the supernatant (= crude extract) after cell breakage by freezing and thawing (Figure 5.10 A). However, the supernatant contained about 23% less ϕ11 compared to the whole cell extract in the experiment shown in Figure 5.10 experiment. Similar or even higher losses were observed in different performances of the experiment.

The green pigment chlorophyll can interfere with the spectrophotometric-based turbidity reduction assay (TRA) when highly concentrated crude extract is used in the assay. For the performance of TRAs with highly concentrated crude extracts of TN72_*ϕ11-HA*, it was therefore desired to remove the chlorophyll. Ultracentrifugation is a useful first purification step for soluble proteins, which removes cell membranes and the majority of the chlorophyll. Furthermore, ultracentrifugation can be used to analyse the solubility of a recombinant protein (Shih et al. 2002; Gutmann et al. 2007). For that reason, crude extracts of TN72_*ϕ11-HA* prepared as described before were treated by ultracentrifugation (100,000 x *g*, 1h). Subsequently, the amount of ϕ11 in the crude extract before and the supernatant and pellet after ultracentrifugation were determined in western blot analyses.

The majority of full-length ϕ11 (71% in A, B; 76% in C, D of Figure 5.11) and nearly all of the 38 kDa ϕ11 truncation (90% in Figure 5.11 A, B) precipitated during ultracentrifugation. This suggests that a majority of full-length ϕ11 does not exist as a soluble protein in *C. reinhardtii* chloroplast and that especially the 38 kDa truncation is present as mainly insoluble protein. Furthermore, it demonstrates that ultracentrifugation cannot be used for the purification of ϕ11 without significant loss of the enzyme. The TRAs with *S. aureus* described in the next section were therefore mainly performed with TN72_*ϕ11-HA* crude extract despite the presence of the chlorophyll.

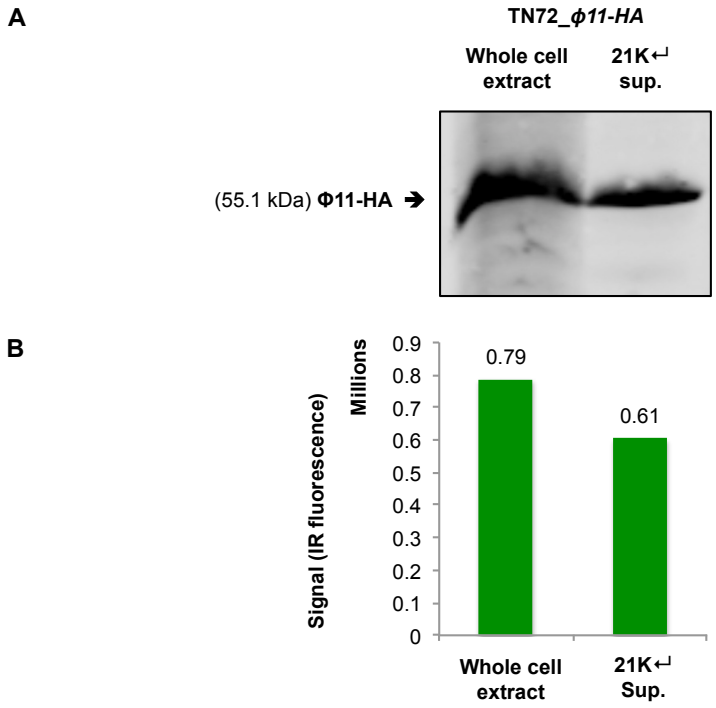

Figure 5.10: Western blot analysis showing the recovery of ϕ11 in the supernatant after cell breakage by freezing and thawing
TN72_*ϕ11-HA* cells were broken by freezing in liquid nitrogen, thawing at 30ºC and vortexing for 10 sec for three cycles, followed by centrifugation at 21,000 x *g* for 5 min. The presence of ϕ11 in the whole cell extracts before centrifugation and the 21K↵ supernatant (crude extract) was determined by western blot analysis with anti-HA antibodies, IRDye® secondary antibodies and the Odyssey® Infrared Imaging system was used for detection (A) and for quantification (B).

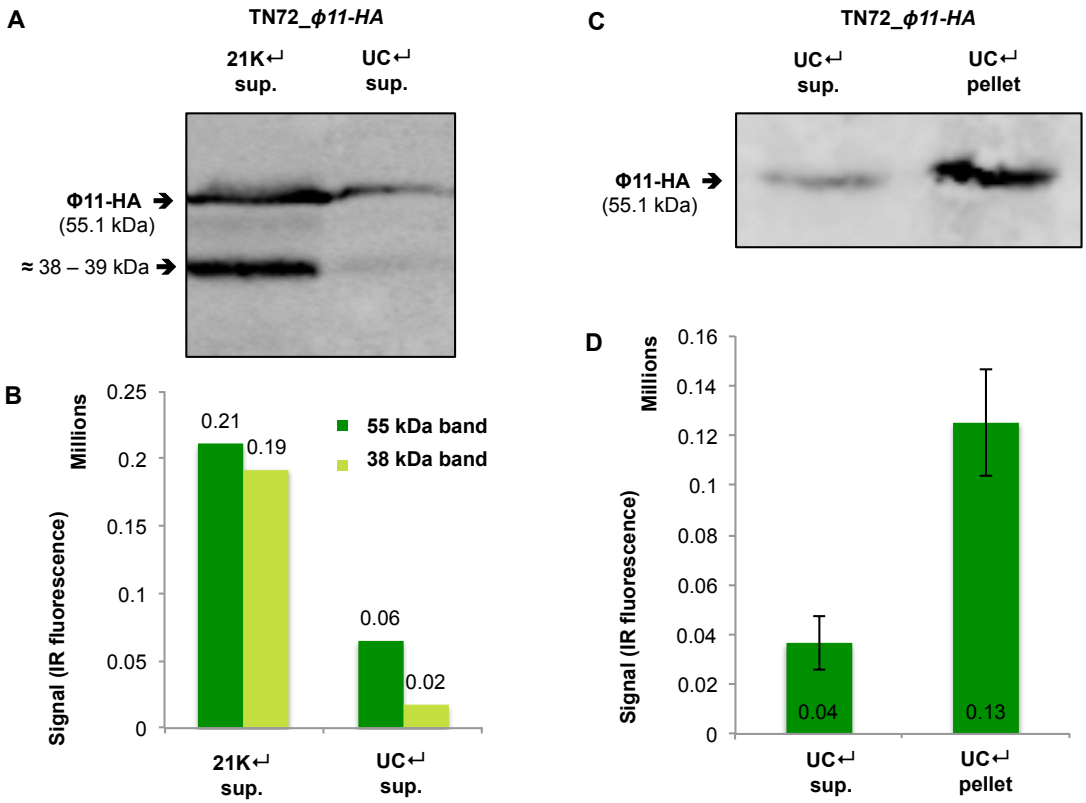

Figure 5.11: Western blot analysis showing the precipitation of ϕ11 during ultracentrifugation
TN72_*ϕ11-HA* cells were broken by freezing in liquid nitrogen, thawing at 30ºC and vortexing for 10 sec for three cycles, followed by centrifugation at 21,000 x *g* for 5 min. Ultracentrifugation (UC↵) was performed with the 21K↵ supernatant at 100,000 x *g* for 1 h. The presence of ϕ11 in the 21K↵ supernatant (crude extract), the UC↵ supernatant and UC↵ pellet was determined by western blot analysis with anti-HA antibodies, IRDye® secondary antibodies and the Odyssey® Infrared Imaging system was used for detection (A, C) and for quantification (B, D). The data presented in A+B and C+D are from two different performances of the experiment. The error bars in D show ± one standard deviation (n = 2).

5.2.4 Investigation of the antibacterial activity of *C. reinhardtii*- and *E. coli*-produced ϕ11 against *S. aureus*

As already mentioned in 4.2.2, it is of great importance to analyse the activity of a recombinant protein after its expression in a new system has been confirmed. Turbidity reduction assays (TRAs) had been used successfully to demonstrate the activity of the *C. reinhardtii*-produced endolysin Pal (4.2.2). Furthermore, previous studies by Sass & Bierbaum (2006) and Donovan et al. (2006) used TRAs with heat-killed and live staphylococcal cells to demonstrate the lytic activity of *E. coli*-produced ϕ11. Consequently, as a next step the antibacterial activity of ϕ11 produced in the *C. reinhardtii* chloroplast was analysed using TRAs with heat-killed *S. aureus* cells to investigate whether the endolysin has full enzymatic activity.

Cells of a *S. aureus* culture were harvested and resuspended in NaPi-buffer before the suspension was heated to 80°C for 10 min. Subsequently, crude algal extracts from either TN72_*ϕ11-HA* or TN72_control were added to the cell suspensions to start the assays and the change in OD_{600nm} was determined over a time course. In contrast to TRAs with *S. pneumoniae* cells, *S. aureus* cells did not show marked autolysis, since the OD_{600nm} hardly decreased without the addition of enzyme or in the control assays even over long periods of time. However, the TRAs performed with the TN72_*ϕ11-HA* crude extracts also did not show a decrease in OD_{600nm} compared to the control assays (Figure 5.12 A) and therefore showed no detectable lytic activity.

As a first attempt the ϕ11 concentration used in the assays was increased. This was done by enriching the ϕ11 concentration in the crude extracts using centrifugal concentrators (MWCO 30,000) or alternatively by an increase of the initial cell density of the whole cell extract before cell breakage. This resulted in a concentration of the chlorophyll and therefore strong green background of the assays. As already mentioned in 5.2.3, ultracentrifugation was investigated as a method to separate the chlorophyll from the extract with ϕ11, but was found to be unsuitable since the majority of ϕ11 moved into the pellet during the procedure together with the chlorophyll. Subsequently, lysostaphin was used as a positive control and to investigate whether the lysis of the *S. aureus* cells is still measurable as a decrease in

OD_{600nm} in the presence of high chlorophyll concentrations. Lysostaphin is a zinc endopeptidase, which is produced by *Staphylococcus staphylolyticus* and cleaves the polyglycine bridge of the peptidoglycan of *Staphylococcus aureus* (Cui et al. 2010). After addition of lysostaphin (20 µg/ml) to *S. aureus s*uspensions, which already contained crude algal extract, a fast decrease of the OD_{600nm} was measurable (Figure 5.12 A). This proves that the experimental design used is suitable to measure the enzymatic lysis of *S. aureus* cells and that the background caused by the green pigment chlorophyll does not interfere with the measurement. Nevertheless, higher concentrations of ϕ11 also did not result in a measurable decrease of the OD_{600nm} of the *S. aureus* suspensions. Furthermore, proteinase inhibitors were added to the crude extract before cell breakage to prevent inactivation of ϕ11 by proteinases in the algal extract, but this procedure also did not result in measurable lytic activity of the algal-produced ϕ11.

Moreover, experiments analysing the bactericidal activity of ϕ11 against *S. aureus* were performed. In spot tests, crude extracts of TN72*_ϕ11-HA* and TN72_control were spotted onto a lawn of *S. aureus* cells*,* which had been plated onto agar plates*.* After incubation overnight, the plates were analysed for inhibition zones in the area of the spots. Alternatively, the crude extracts were mixed with a suspension of *S. aureus* cells*,* and spotted in different dilutions onto agar plates. On the next day, the numbers of colony forming units (cfu) were determined and the cfu/ml calculated. However, none of these experiments confirmed the antibacterial activity of ϕ11 produced in *C. reinhardtii*.

To investigate whether the absence of observed activity is caused by insufficient concentrations of ϕ11 or whether the experimental design used is not suitable to measure the lytic activity of the endolysin, ϕ11 produced in *E. coli* was used as a positive control. *E. coli* DH5α*_ϕ11-HA* cells were broken using a French pressure cell press and the crude extract was analysed in TRAs with heat-killed *S. aureus* cells. In the TRAs with DH5α*_ϕ11-HA,* a marked decrease of the OD_{595nm} compared to the control was measurable (Figure 5.12 B), which proved the lytic activity of ϕ11 produced in DH5α*_ϕ11-HA*.

To compare ϕ11 produced in *C. reinhardtii* to the endolysin produced in *E. coli*, TRAs with different dilutions of TN72_*ϕ11-HA* and DH5α_*ϕ11-HA* crude extracts were performed. Subsequently, the amount of ϕ11 in the extracts was analysed and quantified in western blot analyses with anti-HA antibodies. These analyses showed that equivalent amounts of ϕ11 produced in *C. reinhardtii* had no measurable effect on *S. aureus* cells. In contrast, equal amounts of *E. coli*-produced ϕ11 caused a marked decrease in OD_{600nm} of *S. aureus* suspensions. Figure 5.12 shows two representative TRAs with *C. reinhardtii*- and *E. coli*-produced ϕ11 and the corresponding western blot analysing the concentration of ϕ11 in the extracts. The western blot shows that similar amounts of full-length Pal were present in the algal and the bacterial extract, which were used in the shown TRAs (Figure 5.12, first and last lane). It can be assumed that the ϕ11 concentration in the *E. coli* extract is even lower, since the non-specific band at the same size (which is also present in the negative control) most likely contributes to the IR fluorescence signal. The concentration of the ϕ11 truncation is even higher in the algal extract. Furthermore, one in two dilutions of the *E. coli* extract containing ϕ11 still had a measurable effect on *S. aureus* (Figure 5.13). These results suggest that the activity of ϕ11 in the *C. reinhardtii* crude extract is strongly reduced or completely abolished.

It was considered whether a substance or molecule within in the *C. reinhardtii* crude extract has an inhibitory effect on the activity of ϕ11. Therefore, crude extract of TN72_*ϕ11-HA* and DH5α_*ϕ11-HA* were mixed in a ratio of 1:1 and the lytic activity was analysed in a TRA. The mixture of both extracts caused a nearly identical decrease in OD_{595nm} as the same amount of DH5α_*ϕ11-HA* extract on its own (Figure 5.13). This indicates that the lytic activity of ϕ11 is not inhibited or destroyed by a substance contained in the crude extract of *C. reinhardtii*.

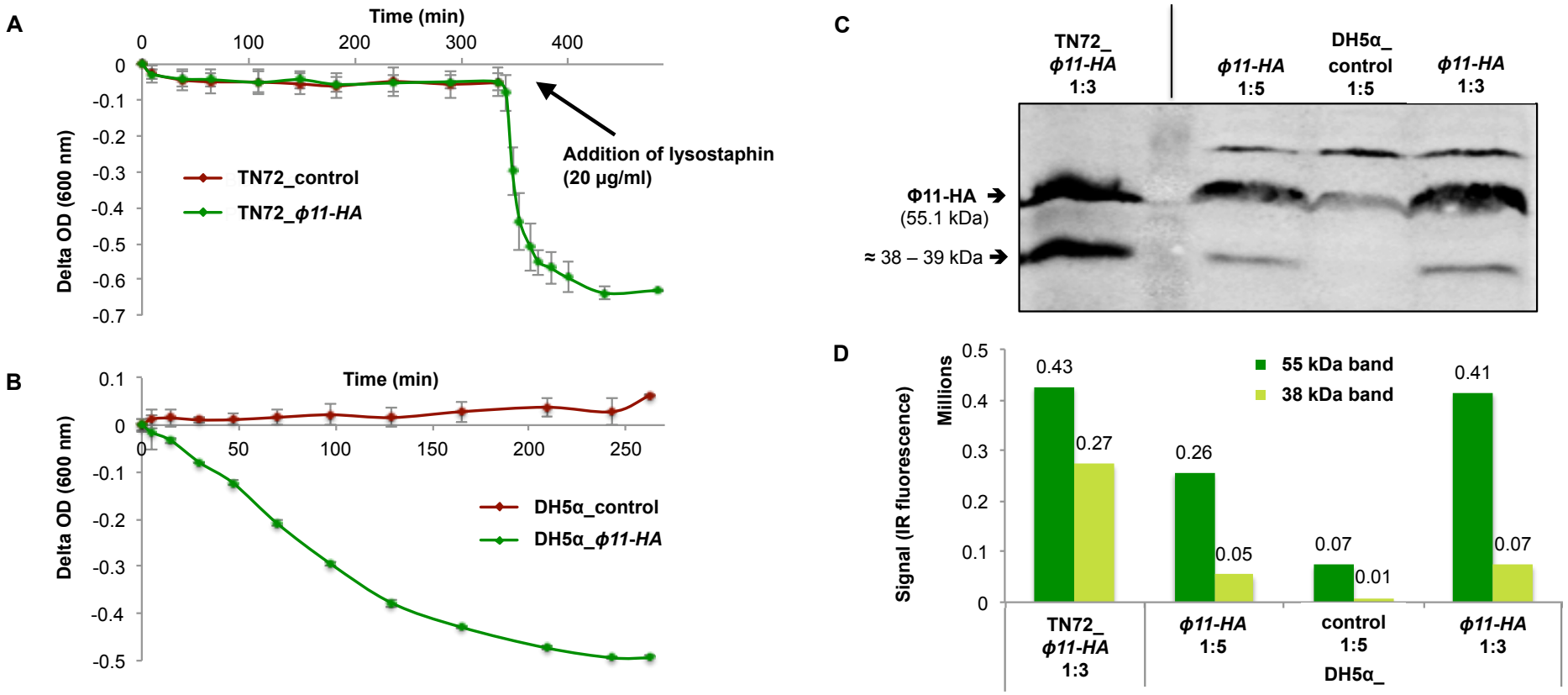

Figure 5.12: Turbidity reduction assays (A, B) and western blot analysis (C, D) showing the absence of lytic activity of *C. reinhardtii*-produced ϕ11 (A) and the lytic activity of *E. coli* DH5α-produced ϕ11 (B) against *Staphylococcus aureus*

The *S. aureus* cells were resuspended in NaPi-buffer to an optical density (OD_{595nm}) of 1.0. *E. coli* DH5α_*ϕ11-HA*, *C. reinhardtii* TN72_*ϕ11-HA* crude extract and the corresponding control extracts were added to the cell suspensions and the OD_{595nm} was measured over a time course at 37ºC. The extracts were analysed for HA-tagged ϕ11 protein in a western blot analysis with anti-HA antibodies, IRDye® secondary antibodies and the Odyssey® Infrared Imaging system, to compare the amount of ϕ11 in the different extracts. The error bars show ± one standard deviation (n = 3 (A), n = 2 (B)).

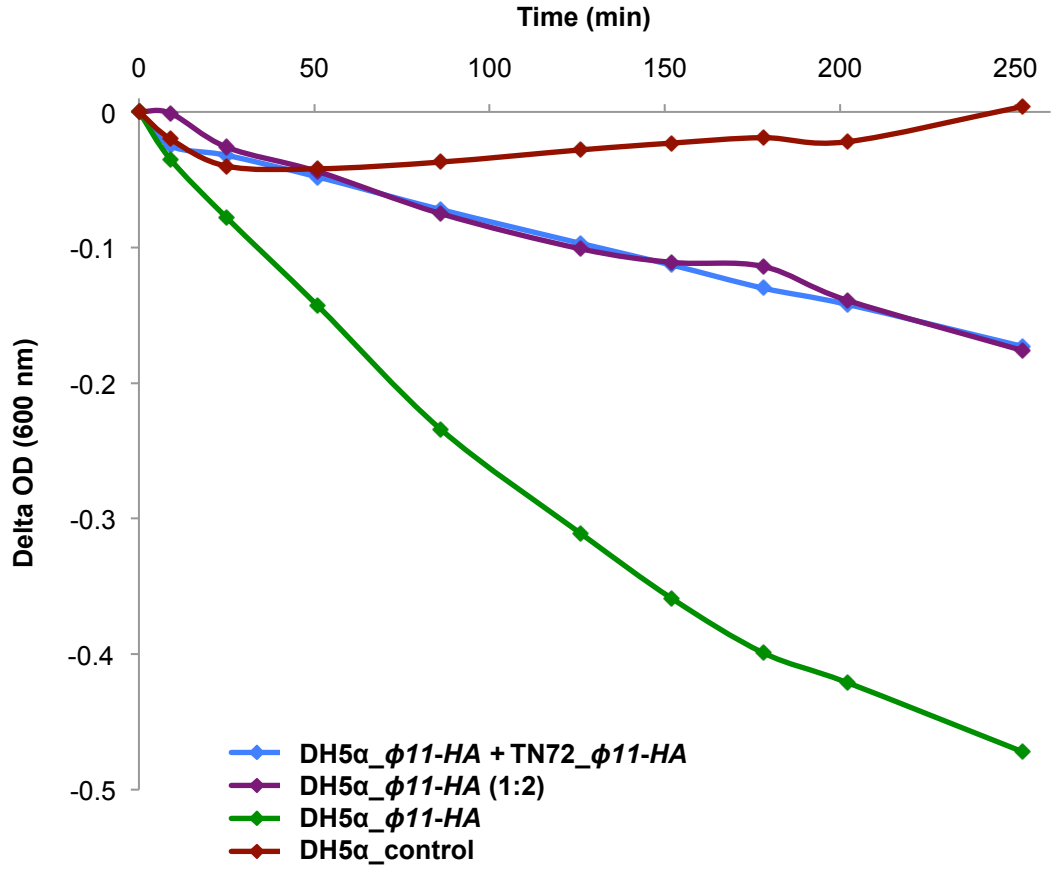

Figure 5.13: Turbidity reduction assay showing the lytic activity of *E. coli* DH5α_*ϕ11-HA* crude extract mixed with *C. reinhardtii* crude extract against *Staphylococcus aureus*
The *S. aureus* cells were resuspended in NaPi-buffer to an optical density (OD_{595nm}) of 0.9. *E. coli* DH5α_*ϕ11-HA* (undiluted and diluted 1:2), DH5α_*ϕ11-HA* mixed in a ratio of 1:1 with *C. reinhardtii* TN72_*ϕ11-HA* crude extract and the corresponding control extract were added to the cell suspension and the OD_{595nm} was measured over a time course at 37ºC.

Overall, the results indicate that *C. reinhardtii*-produced ϕ11 is not active or has a markedly lower activity compared to the same endolysin produced in *E. coli* and is therefore not fully active. It is conceivable that differences in the protein folding machinery of *E. coli* and the *C. reinhardtii* chloroplast are responsible for the differences in the lytic activity of both versions of ϕ11. Navarre et al. (1999) found a conserved cysteine residue using sequence alignments of the N-terminal endopeptidase domain of ϕ11 with the catalytic domains of the *S. aureus* specific endolysins Twort, ϕPVL, ϕ187 and α80. Furthermore, the study showed that ϕ11 is inhibited by *p*-hydroxymercuribenzoic acid, which is an organic mercurial that forms stable complexes with cysteine thiol residues, and concluded therefore that the conserved cysteine residues is important for the activity of the endopeptidase domain.

Differences in the reductant levels in both expression platforms could have an influence on the interactions of this cysteine residue, which could have resulted in a misfolding of ϕ11 in the *C. reinhardtii* chloroplast.

5.2.4.1 Antibacterial activity of ϕ11 against clinical isolates of *S. aureus*

Endolysins against Gram-positive bacteria are often highly specific and can even exhibit specificities for certain strains and serotypes within one species. It was observed in this study that the endolysin Pal lyses different strains of *S. pneumoniae* with varying rates. Furthermore, Rodríguez-Cerrato et al. (2007) reported minimal inhibitory concentrations for Pal varying from 32 to 256 µg/ml. Therefore the antibacterial activity of ϕ11 produced in *C. reinhardtii* was tested using another *S. aureus* strain to investigate whether the algal endolysin is able to lyse this strain with a measurable activity. It was of particular interest to analyse whether the produced endolysins have antibacterial activity against clinical isolates, including antibiotic-resistant strains, since effective killing of these strains would highlight the potential as a form of treatment when traditional antibiotics fail. Therefore two clinical isolates of *S. aureus* (provided by Bambos Charalambous from the Royal Free Hospital) were used for further tests. The strain ATCC 25923 is methicillin-sensitive clinical isolate of *S. aureus* (MSSA strain), whereas the strain ATCC 43300 is a MRSA isolate of *S. aureus* (methicillin-resistant *S. aureus)* with resistances against methicillin and oxacillin.

Spot tests and assays analysing a decrease in cfu (as described in 5.2.4) were performed with the *S. aureus* MSSA strain and crude extract of TN72_*ϕ11-HA* and the corresponding control extract, but none of the assays demonstrated any antibacterial activity of *C. reinhardtii*-produced ϕ11 against this *S. aureus* strain (not shown).

However, preliminary TRAs performed with crude extract of *E. coli* DH5α_*ϕ11-HA* showed a marked decrease in OD_{595nm} of suspensions of both *S. aureus* clinical

isolates. The assays were performed with wild type microalgal extract as control and need to be repeated with DH5α_control. Nevertheless, since DH5α_control did not cause any decrease in OD_{595nm} against the reference *S. aureus* strain and the OD did not decrease in any of the performed control assays, the results suggest that *E. coli*-produced ϕ11 has antibacterial activity against the two *S. aureus* clinical isolates, including a MRSA strain.

This is another demonstration that ϕ11 has great potential to be used as an antibacterial agent against human and animal staphylococcal pathogens and that it is worth undertaking further attempts to produce the endolysin in active form in *C. reinhardtii* or in other microalgae.

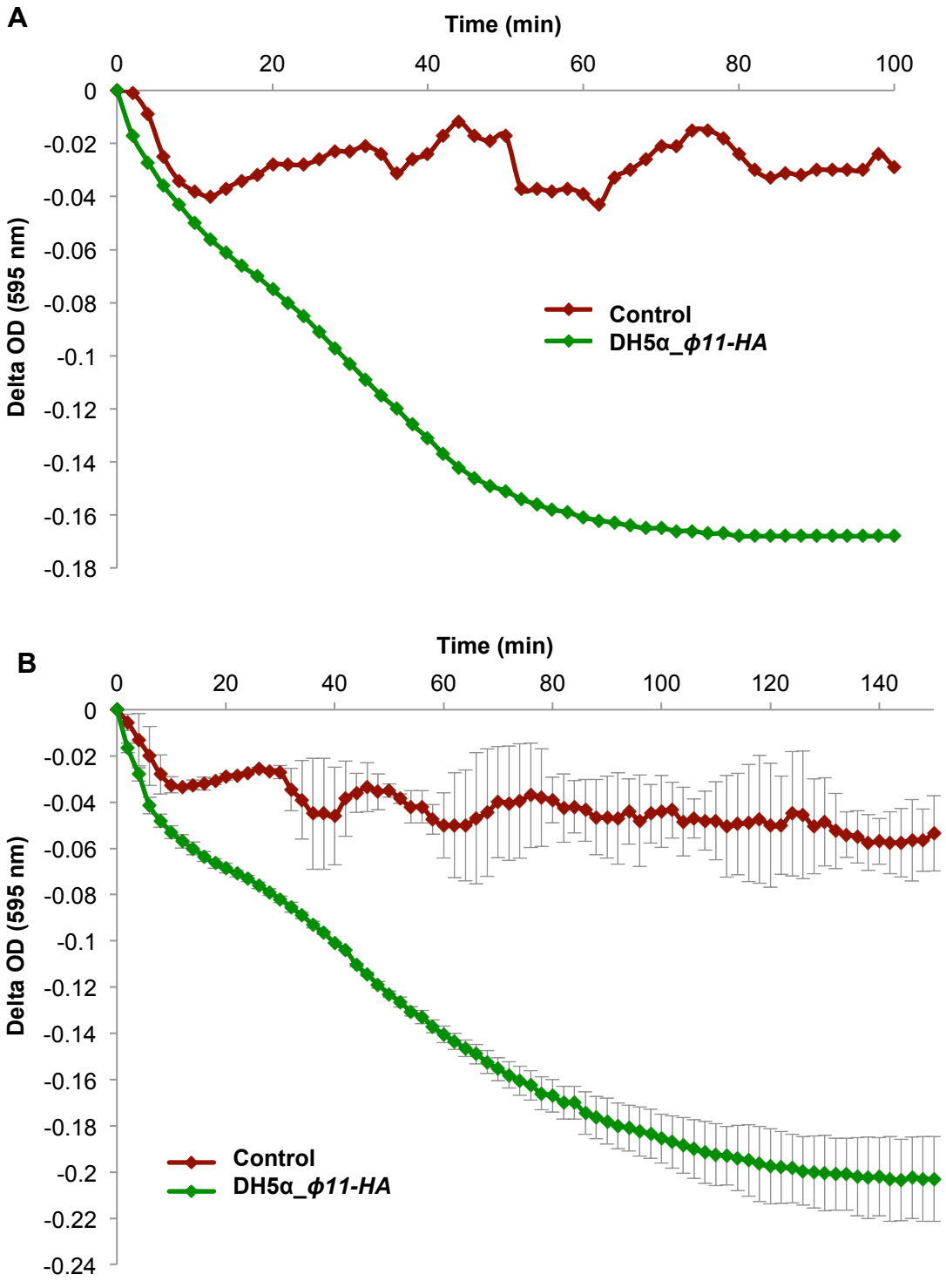

Figure 5.14: Turbidity reduction assays indicating the lytic activity of *E. coli* DH5α-produced ϕ11 against two clinical isolates of *Staphylococcus aureus*, a MSSA (A) and a MRSA strain (B)
The *S. aureus* strains were resuspended in NaPi-buffer to an optical density (OD_{595nm}) of 0.8. *E. coli* DH5α_*ϕ11-HA* crude extract was added to the cell suspensions and the OD_{595nm} was measured over a time course at 37ºC. The control is *Synechocystis* PCC6803 wild type crude extract. Clinical isolates: A = *Staphylococcus aureus* ATCC 25923, B = *Staphylococcus aureus* ATCC 43300. MSSA = Methicillin-sensitive *S. aureus,* MRSA = Methicillin-resistant *S. aureus.* The error bars in B show ± one standard deviation (n = 2).

5.2.5 The addition of a His-tag to ϕ11 and Pal interferes with the production of the recombinant proteins

The purification of *C. reinhardtii*-produced ϕ11 would enable the investigation of the antibacterial activity of the endolysin without the interference of other cell compounds in the alga that may inhibit the antibacterial activity of the endolysin. It would also allow a strong concentration of ϕ11 without the simultaneous concentration of the chlorophyll to investigate whether the antibacterial activity of *C. reinhardtii*-produced ϕ11 is reduced or completely abolished. Furthermore, it is possible in some cases to denature and subsequently correctly refold misfolded recombinant proteins *in vitro* after purification and restore the enzymatic activity (De Bernardez Clark 1998).

The addition of polyhistidine-tags (His-tags) to recombinant proteins is widely used for the purification of proteins using commercially available and inexpensive sepharose or agarose columns with nickel bound to iminodiacetic acid (Ni-IDA) or nitrilotriacetic acid (Ni-NTA). Previous studies used the addition of a His-tag for the purification of ϕ11 produced in *E. coli* (Donovan et al. 2006, Sass & Bierbaum 2007) and no purification protocol specific for ϕ11 without the use of tags has been developed so far.

Therefore the *C. reinhardtii* transgenic line TN72*_ϕ11-HA-His*, which carries the *ϕ11* gene attached to the sequence of a His-tag was created (5.2.1.2.2). The *ϕ11* gene is additionally attached to the sequence of a HA-tag, which is located in between the gene and the His-tag sequence (Figure 5.3). This was done to enable an easy detection of the recombinant protein in western blot analyses, since anti-HA antibodies are known to be more sensitive than anti-His antibodies. At the same time the transgenic line TN72*_pa1-HA-His*, which carries the *pal* gene with both tags in the same arrangement was created. This was done to evaluate another method for the purification of Pal in addition to the purification methods discussed in 4.2.4.

Whole cell extracts of TN72*_ϕ11-HA-His* and TN72*_pa1-HA-His* were analysed for the presence of HA- and His- tagged ϕ11 and Pal protein by western blot analysis

using anti-HA antibodies and horseradish peroxidase-linked secondary antibodies and the resulting chemiluminescence was detected with photographic film. In these analyses the strain TN72_control was used as a negative control and the strains TN72_*ϕ11-HA* and TN72_*pa1-HA* were used as positive controls. However, none of the performed western blot analyses showed bands that were not present in the negative control for any of the *TN72_ϕ11-HA-His* and *TN72_pal-HA-His* transformants, whereas samples of the positive controls with the same cell densities showed strong bands at the size of ϕ11-HA and Pal-HA (Figure 5.15)

Subsequently, the gene sequences of the TN72_*ϕ11-HA-His* and TN72_*pa1-HA-His* transformants were analysed by sequencing to investigate whether the absence of detectable recombinant protein can be explained by erroneous mutations. However, the analyses confirmed that the transgenic lines have the correct sequences.

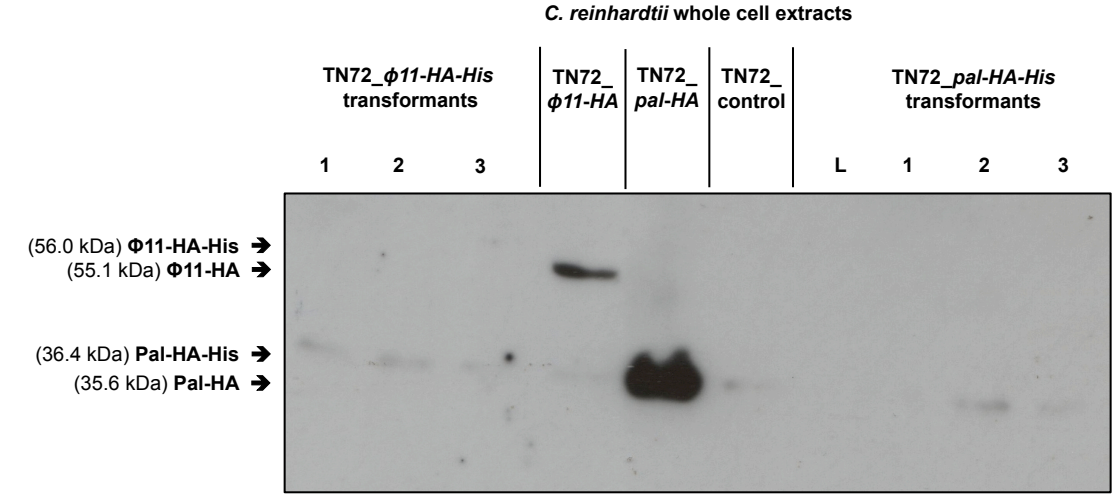

Figure 5.15: Western blot analysis with whole cell extract of TN72_*ϕ11-HA-His* and TN72_*pal-HA-His* transformants for the presence of HA- and His-tagged ϕ11 and Pal
The western blot was performed with samples of TN72_*ϕ11-HA,* TN72_pal-*HA* and TN72_control as controls and anti-HA antibodies, horseradish peroxidase-linked secondary (ECL) antibodies and the resulting chemiluminescence was detected with photographic film. The cultures were harvested at an OD_{750nm} of approximately 3 and normalised to the OD_{750nm} at the time of sampling (cells were resuspended in 1 ml of buffer per OD_{750nm} of 1). The expected band sizes are shown in the figure. Protein sizes were determined using the PageRuler^{TM} Prestained Protein ladder (Thermo Scientific), L = ladder.

These results indicate that the addition of six histidine residues to the C-terminal end of ϕ11 and Pal interferes with either the synthesis or the stability of the recombinant endolysins, which results in protein levels that are reduced below the detection limit of the method used in this study. It is conceivable that the attachment of six further amino acids in addition to the nine amino acids of the HA-tag prevents the correct folding of the proteins and that the misfolded endolysins are quickly degraded by the proteolytic machinery in the chloroplast.

5.3 Conclusion and future work

The study described in this chapter investigated the synthesis of the endolysin ϕ11, a potential candidate for use as a novel antibiotic against staphylococcal human and animal pathogens, in the *C. reinhardtii* chloroplast to evaluate the suitability of the microalga as a novel expression platform using another example.

Two lines of *C. reinhardtii* were created with a transgene encoded HA-tagged ϕ11 inserted in the plastome, in one case with the addition of a His-tag sequence. Subsequently the expression of *ϕ11* in the algal chloroplast was confirmed with anti-HA antibodies. Furthermore, the results suggested that genetically identical lines, created by homologous recombination in the chloroplast, produce comparable levels of recombinant protein.

The western blot analyses confirming the synthesis of ϕ11 protein in the *C. reinhardtii* chloroplast also showed the presence of an approximately 38 kDa truncation of ϕ11 missing the first 150 N-terminal amino acids. This truncation product was present in the majority of western blots performed with ϕ11 and its size did not vary between different analyses. The same truncation was also present when ϕ11 was produced using *Escherichia coli* DH5α. This is in contrast to the endolysin Pal, of which no truncations accumulate to detectable levels in the *C. reinhardtii* chloroplast, whereas in *E. coli* DH5α truncations of Pal accumulate to even higher levels than the full-length Pal. The ϕ11 sequence contains a methionine in the predicted start region of the truncation and a translational start at this AUG codon would result in a 38.9 kDa protein. It is therefore conceivable that this AUG functions as part of a cryptic internal translation initiation region. Another explanation would be that the truncation is formed by proteolytic degradation. The observation that more ϕ11 truncated protein compared to full-length protein is formed at the transition from exponential to stationary phase supports this theory, because the production of proteases increases in the stationary phase. Furthermore, the proteases in the cytoplasm have more time to cleave ϕ11. Analysis using the ExPASy PeptideCutter showed that most proteases are predicted to cleave ϕ11 multiple times and did not reveal an obvious candidate.

However, the amount of proteases in the database is very limited. Several proteases exist that have very specific cleavage sites consisting of sequence combinations of four and even more amino acids. It is conceivable that a protease with a specific cleavage site that appears only once in the sequence of ϕ11 and that exists in *E. coli* DH5α and the *C. reinhardtii* chloroplast is responsible for the ϕ11 truncation product. The vast majority of proteases in the chloroplast are homologues of bacterial proteases (Adam et al. 2006). It is therefore likely that homologue proteases are involved in the degradation of ϕ11 in both organisms. It would also be possible that the structure of ϕ11 allows easy access for proteases only in this region. Furthermore, it should be borne in mind that the western blot analysis with anti-HA antibodies shows only C-terminal degradation products that still contain the HA-tag. A potential experiment to investigate whether the truncation is caused by an alternative translation initiation at the mentioned methionine (rather than proteolytic activity) would be to change the ATG codon of the methionine to another codon by site-specific mutagenesis. Provided this change does not abolish the expression of *ϕ11* it would make it possible to confirm or exclude this theory.

As a next step the isolation of ϕ11 in an active form was investigated. It was shown that, like Pal, ϕ11 can be easily recovered after breakage of the cell wall-less strain TN72*_ϕ11-HA* by freezing and thawing. However, the results indicated that some parts of the protein precipitated during the subsequent centrifugation together with the cell debris. An even higher percentage of full-length ϕ11 and the vast majority of the ϕ11 truncation were found to be located in the pellet following ultracentrifugation. These results suggest that a high percentage of ϕ11 does not exist as soluble protein in the *C. reinhardtii* chloroplast and might exist as aggregates instead (Shih et al. 2002).

Subsequently, the antibacterial activity of ϕ11 produced in *C. reinhardtii* was analysed using TRAs, spot tests and assays analysing a decrease in cfu. None of these assays demonstrated any enzymatic activity for ϕ11 produced in *C. reinhardtii*. In contrast, TRAs using ϕ11 produced in *E. coli* DH5α showed marked bacteriolytic activity against *S. aureus*, whereas the same amount of ϕ11 produced in *C. reinhardtii* did not show any activity. These results suggest that *C. reinhardtii*-produced ϕ11 is

not active or has a significantly lower activity compared to the same endolysin produced in *E. coli*.

A likely explanation for the absence or reduced activity is that ϕ11 is not folded correctly in the chloroplast of *C. reinhardtii*, which might result in aggregates. The observation that a high percentage of ϕ11 precipitates during ultracentrifugation, which suggest that ϕ11 does not exist as soluble protein in the chloroplast, supports this theory. The misfolding of ϕ11 might be the result of differences in the protein folding machinery in the two organisms. Furthermore, Navarre et al. (1999) found a conserved cysteine residue and concluded that it is important for the activity of the endopeptidase domain. Since the formation of disulphide bonds is influenced by the reductant levels, unfavourable levels in the chloroplast stroma could have been therefore responsible for a misfolding of the ϕ11 protein. Navarre et al. (1999) and Donovan et al. (2006) added dithiothreitol (DTT) to the TRA buffer or the protein purification buffer, respectively. DDT reduces disulphide bonds and prevents in this way the formation of intramolecular and intermolecular disulphide bonds between cysteine residues of proteins, which can result in misfolding or aggregation. Sass & Bierbaum (2006) demonstrated the enzymatic activity of ϕ11 produced in *E. coli* without the addition of DDT. In this study the lytic activity of ϕ11 produced in DH5α was also shown without the addition of DDT. Nevertheless, the addition of DDT to the lysis buffer might preserve (or restore) the antibacterial activity of ϕ11 produced in *C. reinhardtii*.

The NCBI database predicts using sequence alignments that the *N*-acetylmuramoyl-*L*-alanine amidase domain, which belongs to the PGRP (peptidoglycan recognition protein) superfamily, contains three zinc binding residues. Another explanation for the absence of lytic activity could be therefore that the availability of the cofactor zinc was insufficient in the *C. reinhardtii* chloroplast. During this study an attempt was made to perform TRAs with the addition of zinc ions (50, 500, 1000 µM $ZnSO_4$, performed in 50 mM Tris-HCl buffer). However, the TRAs were hindered by precipitations in the presence of the zinc, which resulted in an increase of the OD_{750nm} that masked any lytic activity. However, the performance of TRAs in different buffer conditions might allow the experiment. Provided that a lack of zinc in the chloroplast

does not result in irreversible damage of the endolysin, the addition of zinc after cell breakage might result in the restoration of the lytic activity. Another option would be the cultivation of TN72_*ϕ11-HA* in the presence of higher zinc concentrations in the medium. In this study 2.5 µM $ZnSO_4$ were used for the cultivation, which is considered as zinc-replete growth for *C. reinhardtii*. The alga can tolerate up to 125 – 250 µM chelated (EDTA) zinc ions and it is therefore possible to increase the zinc concentration in the medium (Malasarn et al. 2013). However, excess zinc within the cell is toxic, since it can compete for binding sites with other metal cofactors. The intracellular zinc concentration in microalgae and other organisms is therefore regulated (Malasarn et al. 2013). Provided that an increase of the zinc concentration in the medium, despite the regulation mechanisms, has an influence on the availability of zinc inside the chloroplast, this cultivation method might result in the production of fully active ϕ11.

Another strategy to produce active ϕ11 in *C. reinhardtii* could be to grow the alga at a lower temperature. Shih et al. (2002) found that a number of proteins are soluble when the synthesising *E. coli* JM109 strain was grown at 20ºC, but not after cultivation at a temperature of 37ºC. The study concludes that a lower cultivation temperature and long induction periods facilitate correct protein folding. Furthermore, Pal and the human growth hormone show higher recombinant protein levels in the *C. reinhardtii* chloroplast during cultivation at 25ºC compared to 35ºC, which suggests an influence of temperature on the production of stable protein in the alga as well (R. Young, unpublished). It might therefore be conceivable that a cultivation of TN72_*ϕ11-HA* at an even lower temperature than 25ºC can facilitate the correct folding of ϕ11 and results in the production of active endolysin in the chloroplast.

It has been shown in 3.2.2.4 that the levels of recombinant Pal are three to ten times higher when produced under the control of the *psaA* exon 1 promoter/5'UTR compared to the *atpA* promoter/5'UTR. Further studies showed also higher recombinant protein levels for Cpl-1 and VFP under the control of the *psaA* exon 1 promoter/5'UTR in the *C. reinhardtii* chloroplast (Taunt 2013; Braun Galleani 2014). It was not attempted in this study to produce ϕ11 under the control of the *psaA* exon 1 promoter/5'UTR, because of the absence of any detectable antibacterial activity.

However, it is likely that an expression of *ϕ11* using this promoter would result also in higher levels of the endolysin. Provided that the activity of ϕ11 is reduced and not completely abolished, higher expression levels might make it possible to at least demonstrate the antibacterial activity against *S. aureus* and to further investigate what is reducing the activity.

Another observation during the experiments described in this chapter was that the addition of a His-tag comprised of six histidine residues at the C-terminal end of Pal and ϕ11 resulted in undetectable protein levels. A possible explanation is that the additional residues, together with the nine amino acids of the HA-tag, interfere with the correct folding of endolysins, which could result in rapid degradation. This suggests that the correct folding of recombinant proteins in the chloroplast can be easily disturbed. The aim of the addition of a His-tag to ϕ11 was to enable the purification of the endolysin to be able to analyse its antibacterial activity without the inference of any potential inhibitory substances or conditions present in the crude algal extract. Furthermore, it might be possible to denature and subsequently correctly refold misfolded ϕ11 *in vitro* after purification and so to restore the enzymatic activity (De Bernardez Clark 1998; Lilie et al. 1998). It would therefore be worthwhile to attempt the purification of ϕ11 using different methods. One option would be to try the addition of a Strep-tag or the addition of a His-tag without the HA-tag, which might not interfere with the production the endolysin. The HA-tagged ϕ11 could be purified using immunoprecipitation with monoclonal anti-HA agarose conjugate resin. Furthermore, untagged ϕ11 could be purified using fast protein liquid chromatography (FPLC).

As already mentioned in 4.2.2.2, the addition of N- or C-terminal tags can hamper the correct folding of proteins and reduce or eliminate in this way the activity of enzymes in some cases (C. Economou, unpublished; Rehm 2006). Nevertheless, this explanation is less likely, since HA-tagged ϕ11 produced in *E. coli* shows antibacterial activity. However, it is conceivable that in less favourable conditions the HA-tag hampers the folding, even it does not interfere with the activity when the protein is produced in *E. coli.*

Taken together, the results show that it is possible to synthesise the staphylococcal specific endolysin ϕ11 in the *C. reinhardtii* chloroplast. However, it was not possible so far to synthesize the enzyme in a fully active form. As discussed in this section there are still several strategies that can be tried to produce active ϕ11 in *C. reinhardtii*. It is too early to conclude that the *C. reinhardtii* chloroplast is not a suitable production platform for the endolysin ϕ11.

The great potential of ϕ11 as an antibacterial agent against human and animal staphylococcal pathogens has been demonstrated by Donovan et al. (2006) and Sass & Bierbaum (2006). Furthermore, it has been shown in this study that ϕ11 exhibits antibacterial activity against two clinical isolates of *S. aureus* including a MRSA strain. Microalgae are believed to have the potential to be a cost-efficient production platform (Gimpel et al. 2014; Rasala et al. 2010) and the availability of several microalgae with GRAS status is of great advantage. Furthermore, the occurrence of antibacterial properties, amongst others against *S. aureus*, of *C. reinhardtii* and other microalgae adds a very interesting argument for the use of microalgae as production platform for antimicrobial proteins and the use of crude algal extract for administration. A conceivable application for algal crude extract containing ϕ11 could be a topical treatment for mastitis, which is externally applied to the udder of infected dairy cows. The use of a crude extract from a GRAS organism would be highly desirable in this case. The use of ϕ11 in crude extract as a topical treatment for mastitis seems to be more realistic in the close future than the idea of Donovan et al. (2006) to express ϕ11 in the udder of transgenic cows for the production of milk for human consumption. Moreover, a variety of topical treatments for human skin infections is conceivable as well. It is therefore worth undertaking additional attempts to produce the endolysin in active form in *C. reinhardtii* or other microalgae, which is further investigated in the following chapter.

CHAPTER 6

Synthesis of bacteriophage endolysins in the cyanobacterium *Synechocystis* sp. PCC 6803

6 Synthesis of bacteriophage endolysins in the cyanobacterium *Synechocystis* sp. PCC 6803

6.1 Introduction

6.1.1 Limitations of the *C. reinhardtii* chloroplast as an expression platform

The results presented in chapter 3 and 4 strongly support the feasibility of the *C. reinhardtii* chloroplast as a platform for the synthesis of endolysins. Reliable expression of predominantly full-length Pal was achieved and the endolysin exhibited a high stability and full bacteriolytic and bactericidal activity against *S. pneumoniae*. Furthermore, Cpl-1, a second *S. pneumoniae* specific endolysin was successfully synthesised in active form in the *C. reinhardtii* chloroplast (Taunt 2013).

However, it has been shown in chapter 5 that the *staphylococci* specific endolysin ϕ11 was successfully synthesised in *C. reinhardtii*, but the endolysin was not active or had a markedly lower activity compared to *E. coli*-produced ϕ11. Another problem that was encountered was that the addition of a His-tag comprising of six histidines to the C-terminal end of already HA-tagged Pal and ϕ11 resulted in undetectable protein levels.

The study by Taunt (2013) attempted to produce two further endolysins in the *C. reinhardtii* chloroplast: the *S. aureus* specific endolysin Lys16 and the *P. acnes* specific endolysin Gp20. The expression of Gp20 was even attempted with two differently codon-optimised versions of the *gp20* gene and the expression of both proteins was attempted with two different promoters, and through translational fusions of these non-expressing endolysins to expressed proteins. Nevertheless, neither endolysin accumulated to detectable levels in the *C. reinhardtii* chloroplast. Table 6.1 shows a summary of the endolysins, whose expression in the *C. reinhardtii* chloroplast has been investigated in this study and the study by Taunt (2013).

Table 6.1: Summary of the endolysins, whose expression in the *C. reinhardtii* chloroplast has been investigated in this study and the study by Taunt (2013).
All proteins mentioned in this table carry a HA-tag. NA = not analysed.

Endolysin	Expression in the *C. reinhardtii* chloroplast	Activity	Study
Pal	Yes	Active	This study
Cpl-1	Yes	Active	Taunt 2013
ϕ11	Yes	Not detectable with applied methods	This study
ϕ11-His	Not detectable with applied methods	NA	This study
Pal-His	Not detectable with applied methods	NA	This study
Gp20	Not detectable with applied methods	NA	Taunt 2013
Lys16	Not detectable with applied methods	NA	Taunt 2013

These findings are in agreement with a study by Rasala et al. that found that out of seven human proteins they attempted to express in the *C. reinhardtii* chloroplast, three accumulated to detectable levels under the control of the *atpA* and *psbA* promoters, and a fourth one was only synthesised to detectable levels when fused to a well-expressed serum amyloid protein. The other three did not accumulate to any detectable level (Rasala et al. 2010).

The earliest studies on the production of recombinant therapeutic protein in the *C. reinhardtii* chloroplast were performed over a decade ago (Mayfield 2003) and several studies since then have demonstrated the production of a variety of proteins such as antibodies, hormones and vaccines (He et al. 2007; Dreesen et al. 2010; Rasala et al. 2010). However, *C. reinhardtii* is still a relatively new production platform for recombinant proteins compared to established platforms such as *E. coli* or the yeast *Saccharomyces cerevisiae*. Several investigations have already contributed to an improvement of the expression levels, including studies that investigated different promoters and UTRs as well as codon optimisation strategies (Purton et al. 2013; Michelet et al. 2011; Franklin et al. 2002). It is therefore likely that further research

will result in increased yields of recombinant protein in the *C. reinhardtii* chloroplast and will help to identify the reasons that lead to non-expression or inactivity of some proteins. Nevertheless, since several endolysins were not produced to detectable levels in *C. reinhardtii* or were found to be inactive, the use of an alternative microalgal protein production platform was considered.

6.1.2 Cyanobacteria as production platform for endolysins

Endolysins are naturally produced in bacteriophage-infected bacteria and have evolved over billions of years to be adapted to a prokaryotic environment. Therefore it can be assumed that these proteins have a high resistance against prokaryotic proteases, and that endolysins are adapted to the prokaryotic protein synthesis machinery and the conditions in the bacterial cytoplasm.

Cyanobacteria, also called blue-green algae, are prokaryotic microorganisms that carry out oxygenic photosynthesis and have similar advantages for recombinant protein production as the *C. reinhardtii* chloroplast. These eubacteria have minimal nutrient requirements and are capable of photoautotrophic or mixotrophic growth, and their cultivation is inexpensive. Furthermore, several species of cyanobacteria have GRAS status. Species such as *Arthrospira plantesis* and *Arthrospira maxima* (better known as Spirulina) as well as *Nostoc flagelliforme* and *Nostoc commune* are even used as food supplements for vitamins, minerals and β-carotene. Moreover, several studies identified antimicrobial compounds in cyanobacteria. Ishida et al. (2007) for example identified Kawaguchipeptin B, an antibacterial cyclic undecapeptide that was isolated from the cyanobacterium *Microcystis aeruginosa* (Ishida et al. 1997). Furthermore, two highly halogenated aromatic compounds, Ambigol A and B, were isolated from *Fischerella ambigua* and characterized by Falch et al. (1993). An application is therefore conceivable, in which crude cyanobacterial extracts are used that contain endolysins and have potentially additive antibacterial properties, as was described for *C. reinhardtii* extracts.

Cyanobacteria are classified as Gram-negative bacteria, but their peptidoglycan is thicker and has a higher degree of cross-linking than that of most Gram-negative bacteria (Hoiczyk and Hansel 2000). However, the peptide chains that crosslink the polysaccharide strands have the typical Gram-negative composition and differ therefore from the peptidoglycan of *S. pneumoniae*, *S. aureus* and other Gram-positive bacteria. These cell walls lack for example the glycine bridge, which contains the bond that is cleaved by the endopeptidase domain of ϕ11, suggesting that synthesis of ϕ11 in cyanobacteria would be feasible. Furthermore, the cytoplasmic membrane would present a barrier, in the absence of holins that prevents the endolysins from reaching the peptidoglycan. Finally, the endolysins investigated in this study are highly specific and have been successfully produced in the Gram-negative bacterium *E. coli*. It can be therefore assumed that these proteins can be synthesised in the cyanobacterial cytoplasm without causing major harm to the cell.

Cyanobacteria have been seldom considered as production platforms for recombinant proteins despite the fact that genetic engineering tools for the expression of foreign genes have been developed for several species (Zhou et al. 2014). In most cases the introduction of foreign genes is used for metabolic engineering and the creation of novel biosynthetic pathways. For example, Lan & Liao (2011) expressed a trans-enoyl-CoA reductase gene for the production of butanol in *Synechococcus elongatus* PCC 7942, whereas Guerrero et al. (2012) produced an ethylene-forming enzyme (EFE) in *Synechocystis* sp. PCC 6803 for the production of ethylene. Furthermore, applications in which the cyanobacterium can be used as the production and delivering system have been investigated. A study by Zang et al. (2007) produced *Paralichthys olivaceus* (flounder) growth hormone (fGH) in *Synechocystis* sp. PCC 6803. The group investigated also the effect of supplementing the feed of turbot (*Scophthalmus maximus* L.) with the transgenic *Synechocystis* cells producing fGH and found that it can be used as an efficient growth promoter without any observed side effects (Liu et al. 2007). These results indicated therefore that *Synechocystis* sp. PCC 6803 does not contain major amounts of endotoxins that harm turbot following oral administration.

Synechocystis sp. PCC 6803 is the cyanobacterial model organism and it was the first photosynthetic organisms whose genome was sequenced and annotated (Kaneko et al. 1996; Ikeuchi & Tabata 2001). The bacterium is naturally transformable by exogenous DNA and several tools for the genetic manipulation are already available (Ikeuchi & Tabata 2001). Furthermore, it has been shown that *Synechocystis* species have antibacterial activity against Gram-positive bacteria (Martins et al. 2008).

Synechocystis sp. PCC 6803 was therefore chosen to investigate the potential of cyanobacteria as a production platform for endolysins and other antibacterial proteins. The endolysin ϕ11, which did not show activity when produced in *C. reinhardtii*, and Pal as a positive control were used to analyse the endolysin synthesis in *Synechocystis.* Furthermore, Gp20, an endolysin from the study of Taunt (2013) was chosen to investigate the production of an endolysin in *Synechocystis* that did not accumulate to detectable levels in *C. reinhardtii*.

6.1.3 The *Propionibacterium acnes*-specific endolysin Gp20 from bacteriophage PA6

Farrar et al. (2007) were the first to sequence the genome of a bacteriophage that infects *Propionibacterium acnes*, a bacterium that is associated with inflammatory acnes vulgaris. The bacteriophage PA6 has a high genetically and morphologically similarity to several mycobacteriophages. Like Dp-1 and ϕ11, PA6 belongs to the family of the *Siphoviridae.* The genome of PA6 consists of double-stranded DNA and has a length of 29.7 kb. Farrar et al. (2007) showed that the bacteriophage could infect 32 different isolates of *P. acnes*, including clinical isolates with antibiotic resistances to erythromycin and clindamycin. In contrast, PA6 showed a high specificity for *P. acnes* and did not infect other bacteria that are common commensals in the human skin microflora such as *Propionibacterium granulosum*, *Propionibacterium avidum*, *Staphylococcus epidermis* or *Corynebacterium bovis*.

Farrar et al. (2007) identified 48 ORFs in the genome of PA6 and predicted that ORF20 encodes a putative *N*-acetyl-muramoyl-L-alanine amidase and defined the encoded protein as Gp20. Gp20 was found to have homology to the amidases of the mycobcteriophages PG1 and Che8 and a high similarity (67% identity for amino acids 2 to 145, N-terminal catalytic domain) to another *N*-acetyl-muramoyl-L-alanine amidase, which is an autolysin of *P. acnes*. Furthermore, the downstream ORF21 is predicted to encode the holin of the lytic system. The gene arrangement is typical for endolysin and holin genes in bacteriophage genomes.

The study by Taunt (2013) confirmed using sequence alignments and database analysis, the prediction that ORF20 encodes an amidase at the N-terminus and therefore the endolysin of PA6. At the time Taunt started the investigation of the production of Gp20 in *C. reinhardtii*, PA6 was the only *P. acnes* bacteriophage that had been sequenced so far. Since then, several further *P. acnes* specific bacteriophages have been sequenced and further putative endolysins have been described by Lood & Collin (2011) and Marinelli et al. (2012). Marinelli et al. (2012) found that the genome sequence of all 11 bacteriophages they analysed exhibit a remarkably high nucleotide identity of more than 85%. Furthermore, the study found that ORF20 encodes the endolysin in all analysed *P. acnes* bacteriophages and that the N-terminal domains of these endolysins are predicted to be *N*-acetyl-muramoyl-L-alanine amidases. The N-terminal domain and also the C-terminal domain, that is predicted to be responsible for cell binding, are highly conserved within different *P. acnes* bacteriophage endolysins and have sequence identities of 92 to 96%. Gp20 from phage PA6 can be therefore seen as a representative example for *P. acnes* bacteriophage endolysins in general. None of the mentioned studies has experimentally shown that the encoded putative endolysins are able to cleave peptidoglycan. A successful production followed by the demonstration of its lytic activity against *P. acnes* would therefore provide the experimental proof that ORF20 encodes for the endolysin in *P. acnes* bacteriophages. However, the patent US_2012_0195872_A1 describes a fusion of *gp20* from PA6 to an 18 amino acid long peptide sequence and showed the antimicrobial activity of the fusion protein against two strains *P. acnes*, which already indicates that *gp20* encodes for an endolysin.

6.1.4 Aims and objectives

The aim of the experiments in this chapter was the production in *Synechocystis* sp. PCC 6803 of several bacteriophage endolysins, including candidates that could not be produced as functional proteins in the *C. reinhardtii* chloroplast. Subsequently, the aim was to analyse the antibacterial activity of the produced endolysins against their target bacteria to investigate whether the proteins are functional. Overall, the aim was to investigate the suitability of the cyanobacterium *Synechocystis* sp. PCC 6803 as an alternative and novel production platform for endolysins and other therapeutic proteins.

6.2 Results and discussion

6.2.1 Creation of transgenic lines of *Synechocystis* sp. PCC 6803 for the synthesis of bacteriophage endolysins

Six different transgenic lines of *Synechocystis* sp. PCC 6803 carrying a synthetic endolysin gene in their genome were created to study the synthesis of endolysins in the cyanobacterium. The lines differ in regard to the promoters used for the expression of the genes and the endolysin genes they are carrying (Figure 6.1, Figure 6.2).

All lines were created using one of the two *Synechocystis* transformation vectors pLAH.AII and the pLAH.nrsB that were created by Lamya Al-Haj (2014) and the *Synechocystis* sp. PCC 6803 wild type strain as recipient strain. The vectors carrying a Tn903 kanamycin resistance cassette and successful transformants can be therefore selected for kanamycin resistance. Both vectors insert the genes of interest into the locus of the *psbAII* gene. The *psbAII* encodes together with *psbAI* and *psbAIII* the D1 subunit of the photosystem II (Vermaas 1998). It has been shown that a knockout of *psbAII* does not have an adverse effect on the growth of *Synechocystis* (Vermaas 1998; Al-Haj 2014).

6.2.1.1 Promoters and 5'/3' untranslated regions (UTR)

The vector pLAH.AII carries an expression cassette, which is flanked with upstream and downstream flanking regions of the *psbAII* gene that include the 5´UTR and 3´UTR of the *psbAII* gene and the *psbAII* promoter (see vector map in appendix). These elements allow the expression of the gene of interest and the insertion into the *psbAII* locus by homologous recombination. The expression cassette of pLAH.nrsB is also flanked with upstream and downstream regions of the *psbAII* gene, but these elements exclude the *psbAII* promoter (see vector map in appendix).

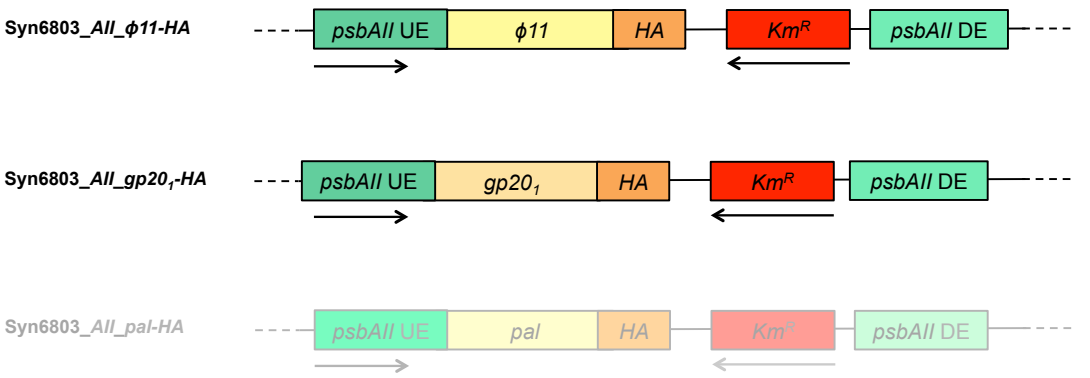

Figure 6.1: Strains of *Synechocystis* sp. PCC 6803 expressing the endolysin genes using the constitutive promoter of the *psbAII* gene
The diagram shows the *Synechocystis* sp. PCC 6803 strains that were created to study the expression of different endolysins in the cyanobacterium under the control of the *psbAII* promoter. Endogenous genes and expression elements are indicated in green, genes of interest in yellow, Tn903 kanamycin resistance cassette (Km^R) in red and the HA-tag in orange. The strain Syn6803*_AII_pal-HA* whose production was attempted and is discussed in 6.2.1.3.3 is shown in faint colours. UE = upstream element, DE = downstream element.

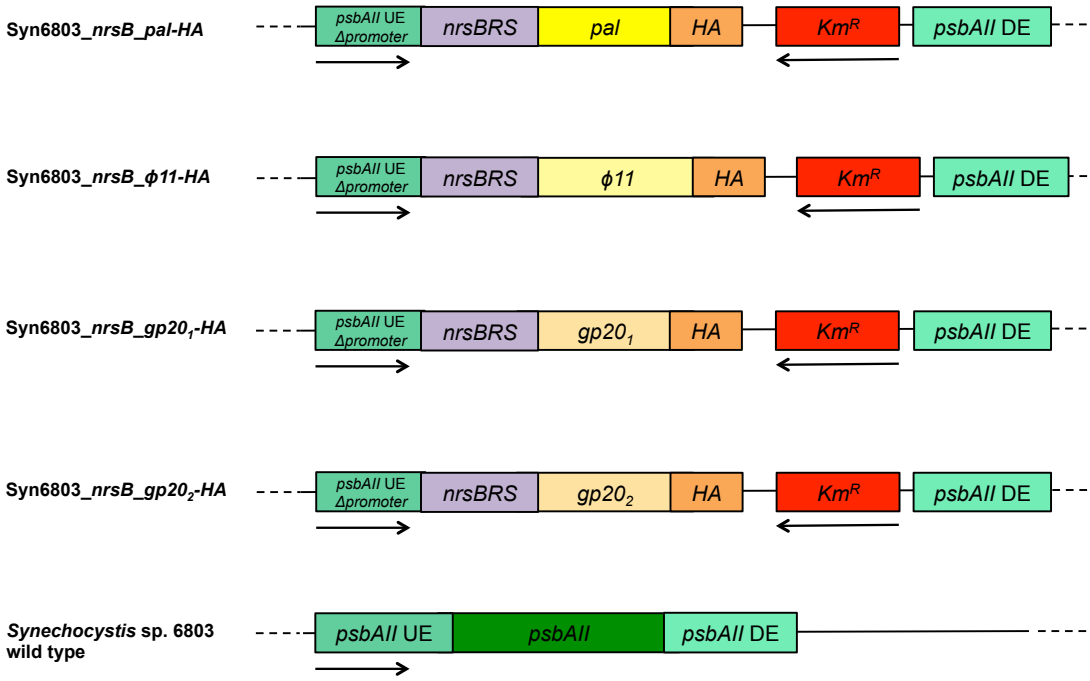

Figure 6.2: Strains of *Synechocystis* sp. PCC 6803 expressing the endolysin genes under the control the nickel-inducible promoter *nrsB* and the corresponding wild type strain
The diagram shows the *Synechocystis* sp. PCC 6803 strains that were created to study the expression of different endolysins in the cyanobacterium under the control of the *nrsB* promoter and its nickel regulatory elements *nrsRS*. The wild type strain was used as the recipient strain and as a negative control. Endogenous genes and expression elements are indicated in green, *nrsBRS* system in purple, genes of interest in yellow, Tn903 kanamycin resistance cassette (Km^R) in red and the HA-tag in orange. UE = upstream element, DE = downstream element.

The vector pLAH.nrsB lacks the *psbAII* promoter and carries instead the nickel inducible endogenous promoter from *nrsB* that is part of the *nrsBACD* operon. The four proteins encoded by *nrsBACD* are involved in the resistance of *Synechocystis* to nickel (Lopez-Maury et al. 2002). The *nrsB* promoter is controlled by a two-component transduction system that is involved in nickel sensing and induces the promoter in the presence of nickel (Lopez-Maury et al. 2002). The transduction system is encoded by the genes *nrsR* and *nrsS,* which are located upstream of *nrsBACD* operon in the opposite orientation. The expression vector pLAH.nrsB carries beside the promoter *nrsB* also *nrsR* and *nrsS.*

6.2.1.2 Design and codon-optimisation of the synthetic endolysin genes

The gene sequences that were originally codon-optimised for the *C. reinhardtii* chloroplast were used in this study for a first investigation of *Synechocystis* sp. PCC 6803 as a production platform for endolysins. An analysis of the codon usage tables from Nakamura et al. (2000) for both the *C. reinhardtii* chloroplast and *Synechocystis* sp. PCC 6803 shows that most codons that are used less frequently in *Synechocystis*, are less frequent in the *C. reinhardtii* chloroplast as well (Figure 6.3), which is not surprising given that the chloroplast evolved from a cyanobacterium. Overall, all codons are used in *Synechocystis* and the cyanobacterium shows less bias for particular codons for each amino acid, instead the codon usage is more evenly spread over the available codons for one amino acid compared to the *C. reinhardtii* chloroplast. The codons of the *pal* and *ϕ11* genes used in this study are therefore mainly codons that are frequent in *Synechocystis* sp. PCC 6803 and should be therefore suitable for expression in the cyanobacterium. One exception is the UCA codon, which is less frequently used for serine in *Synechocystis*, but it is the most often used codon for serine in the *C. reinhardtii* chloroplast. This codon is present 16 times in the *pal* gene and 13 times in the *ϕ11* gene (Appendix 1). However, it was found 5,029 times in the coding sequences of *Synechocystis* sp. PCC 6803 that were analysed for the codon usage table. It can be therefore assumed that the corresponding tRNA for UCA is present in sufficient amounts in the cyanobacterium. For

comparison, the most frequently used codons for serine in *Synechocystis*, UCC and AGU, were found 18,364 and 17,502 times within this set of genes, which is approximately 3.5 times as often. The designs of the *pal* and *ϕ11* genes are described in 3.2.1.1 and 5.2.1.1, respectively.

The *gp20₁* and *gp20₂* genes were obtained from Henry Taunt. The sequence of the Gp20 protein is available in the database UniProtKB/Swiss-Prot (Entry: A4K487; Entry name: A4K487_9CAUD; Protein name: Gp20, EC=3.5.1.28; Organism: Propionibacterium phage PA6 (Taxonomic identifier: 376758)). Gp20 is comprised of 286 amino acids and has a predicted mass of 31,237 Da. The *gp20₁* gene was codon-optimised for the *C. reinhardtii* chloroplast to a Codon Adaption Index (CAI) of 0.8 with respect to the codon usage table from Nakamura et al. (2000) (http://www.kazusa.or.jp/codon), whereas the *gp20₂* gene was designed using the CUO Moptomiser subroutine, which was developed by Henry Taunt and Khai Kong Jien. This program codon-optimises genes for the *C. reinhardtii* chloroplast not only in respect to the codon usage, but also takes into account codon-pairing and the usage of codons found in a subset of highly expressing *C. reinhardtii* chloroplast genes. The DNA sequences of the *gp20₁* and *gp20₂* gene are attached in the appendix. The previously mentioned UCA codon appears six times in *gp20₁* and 13 times in *gp20₂*.

Both *gp20* genes were synthesised by GENEART (Regensburg, Germany) with a C-terminal human influenza haemagglutinin (HA) epitope tag for detection. The created *gp20* genes have a length of 858 bp and including the HA-tag coding sequence and two stop codons (TAA) a length of 891 bp. The HA-tagged Gp20 protein has a molecular mass of 32.3 kDa.

***Synechocystis* sp. PCC 6803**

UUU 29.4(34201)	UCU 9.0(10445)	UAU 17.4(20257)	UGU 6.3(7322)
UUC 10.5(12206)	UCC 15.8(18364)	UAC 11.9(13849)	UGC 3.9(4482)
UUA 26.4(30619)	UCA 4.3(5029)	UAA 1.4(1607)	UGA 0.6(747)
UUG 28.9(33614)	UCG 4.1(4723)	UAG 1.1(1269)	UGG 15.5(17981)
CUU 10.2(11827)	CCU 10.0(11628)	CAU 11.7(13564)	CGU 10.3(12025)
CUC 13.9(16178)	CCC 24.5(28447)	CAC 7.2(8310)	CGC 12.2(14172)
CUA 14.0(16296)	CCA 8.1(9434)	CAA 34.0(39494)	CGA 5.4(6267)
CUG 20.0(23264)	CCG 8.3(9614)	CAG 21.2(24630)	CGG 13.4(15524)
AUU 40.0(46527)	ACU 13.9(16157)	AAU 25.7(29897)	AGU 15.1(17502)
AUC 17.8(20730)	ACC 26.0(30223)	AAC 15.0(17423)	AGC 10.3(11939)
AUA 4.9(5744)	ACA 7.0(8150)	AAA 30.1(34968)	AGA 4.6(5315)
AUG 19.3(22456)	ACG 7.8(9038)	AAG 12.8(14924)	AGG 4.8(5602)
GUU 16.8(19493)	GCU 20.0(23248)	GAU 32.5(37772)	GGU 19.8(23048)
GUC 11.2(12973)	GCC 37.5(43610)	GAC 17.8(20706)	GGC 22.3(25904)
GUA 10.5(12223)	GCA 10.9(12646)	GAA 44.7(51919)	GGA 12.9(15026)
GUG 28.0(32580)	GCG 15.2(17647)	GAG 16.1(18664)	GGG 17.6(20506)

***Chlamydomonas reinhardtii* chloroplast**

UUU 33.4(894)	UCU 17.0(455)	UAU 24.6(657)	UGU 7.6(203)
UUC 17.1(456)	UCC 2.8(74)	UAC 10.0(266)	UGC 1.5(39)
UUA 77.7(2078)	UCA 22.0(588)	UAA 2.9(78)	UGA 0.1(3)
UUG 4.3(114)	UCG 4.0(107)	UAG 0.4(12)	UGG 13.5(361)
CUU 14.3(383)	CCU 15.5(414)	CAU 10.1(270)	CGU 32.4(866)
CUC 1.0(28)	CCC 3.4(90)	CAC 8.8(235)	CGC 4.1(110)
CUA 6.4(170)	CCA 23.6(630)	CAA 38.4(1026)	CGA 3.4(90)
CUG 3.7(99)	CCG 2.4(63)	CAG 4.1(110)	CGG 0.5(14)
AUU 51.4(1374)	ACU 24.4(651)	AAU 42.1(1126)	AGU 16.0(428)
AUC 8.2(219)	ACC 5.1(135)	AAC 17.7(472)	AGC 5.4(144)
AUA 6.9(184)	ACA 32.4(865)	AAA 69.1(1847)	AGA 5.3(143)
AUG 22.3(596)	ACG 3.9(103)	AAG 6.2(167)	AGG 0.9(23)
GUU 29.3(783)	GCU 34.0(908)	GAU 25.3(676)	GGU 44.0(1177)
GUC 2.5(68)	GCC 5.9(159)	GAC 9.8(263)	GGC 6.4(172)
GUA 26.0(696)	GCA 20.7(554)	GAA 41.1(1098)	GGA 8.6(229)
GUG 5.6(149)	GCG 3.3(88)	GAG 5.7(152)	GGG 3.7(99)

Figure 6.3: Codon usage tables from Nakamura et al. (2000) for *Synechocystis* sp. PCC 6803 and the *C. reinhardtii* chloroplast
The tables show in the first row the codon triplet, in the second the frequency of the codon per thousand codons and in brackets the number of times the codon was found in the analysed coding sequences (CDS). In the *C. reinhardtii* chloroplast 93 CDS with 26,731 codons and in *Synechocystis* sp. PCC 6803 3623 CDS with 1,161,949 codons were analysed. Codons with a frequency of 5.0 and below are highlighted in red, stop codons in green. The tables were taken from http://www.kazusa.or.jp/codon.

6.2.1.3 Creation of the transgenic lines

6.2.1.3.1 **Syn6803_*AII_ϕ11-HA* and Syn6803_*AII_gp20$_1$-HA***

The vector pLAH.AII (Al-Haj 2014) was used for the creation of Syn6803_*AII_ϕ11-HA* and Syn6803_*AII_gp20$_1$-HA*. The expression cassette of pLAH.AII carries the restriction sites NdeI and BamHI for the insertion of the gene of interest.

The *ϕ11-HA* gene was amplified in a PCR reaction with the primers Syn6803ϕ11.F and Syn6803ϕ11.R, which bind at the ends of the gene and contain the restriction sites for AseI and BamHI, respectively. Since the *ϕ11* gene contains an NdeI site, an AseI site was attached to prevent cleavage of the *ϕ11* gene during subsequent cloning. The restriction of DNA by AseI results in the same overhang as the restriction by NdeI and the fragment can be therefore ligated with the pLAH.AII plasmid cut with NdeI. The *gp20$_1$-HA* gene was amplified in a PCR with the primers Syn6803gp20.F and Syn6803gp20$_1$.R, which bind at the ends of the gene and contain the restriction sites of AseI and BamHI respectively, since the *gp20* gene also contains an NdeI site. The PCR products were digested with AseI and BamHI followed by ligation with pLAH.AII, which was cut by NdeI and BamHI. Subsequently, the construct was transformed into *Synechocystis* sp. PCC 6803. The colonies obtained were restreaked two times to achieve homoplasmicity. The correct insertion of the genes into the genome of *Synechocystis* was confirmed by PCR analysis with the primers psbAII.F and psbAII.R (Figure 6.4) and by sequencing. The PCR screening showed that all analysed colonies had been successfully transformed (Figure 6.5).

6.2.1.3.2 **Syn6803_*nrsB_pal-HA*, Syn6803_*nrsB_ϕ11-HA*, Syn6803_*nrsB_gp20$_1$-HA* and Syn6803_*nrsB_gp20$_2$-HA***

The vector pLAH.nrsB (Al-Haj 2014) was used for the creation of Syn6803_*nrsB_pal-HA*, Syn6803_*nrsB_ϕ11-HA*, Syn6803_*nrsB_gp20$_1$-HA* and

Syn6803_*nrsB_gp20₂-HA*. The expression cassette of pLAH.nrsB carries also the restriction sites NdeI and BamHI for the insertion of the gene of interest.

The creation of the lines was performed as described in 6.2.1.3.1, except that the primers Syn6803pal.F and Syn6803pal.R, which contain the restriction sites NdeI and BamHI were used for the amplification of the *pal-HA* gene. For the amplification of *gp20₂-HA* the primers Syn6803gp20.F and Syn6803gp20₂.R were used. The successful transformation was confirmed as described in 6.2.1.3.1. The PCR screening confirmed once more that all analysed colonies had been successfully transformed (Figure 6.5).

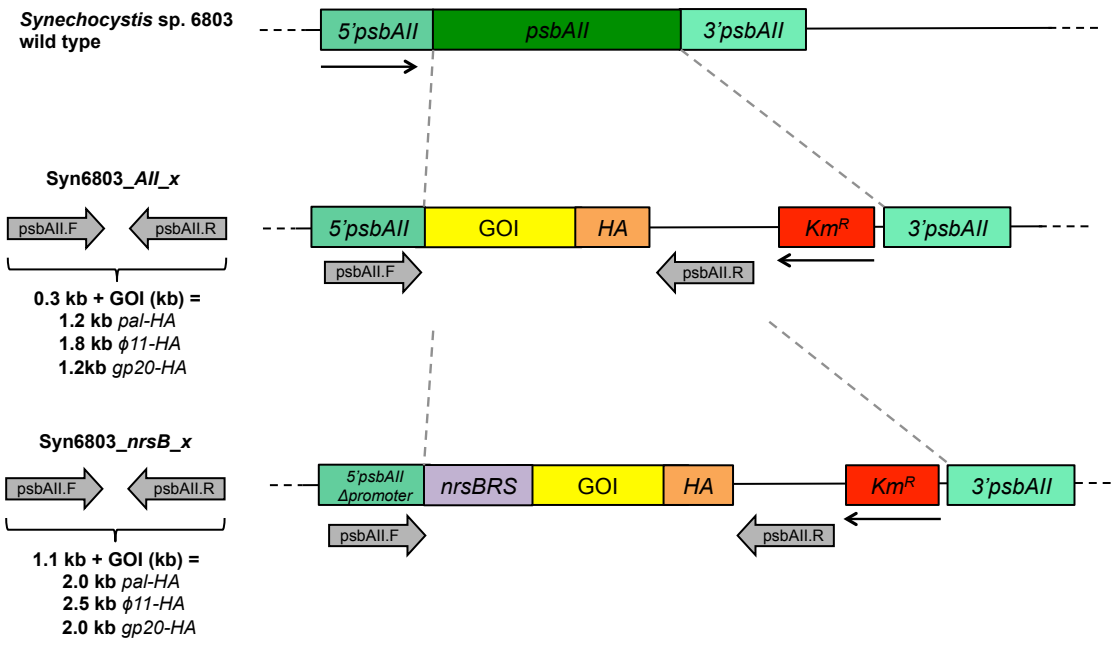

Figure 6.4: Schematic diagram showing the binding sites of the used sets of primers and the expected fragment sizes for the different transformants
The primer psbAII.F binds to the 5´UTR of psbAII, whereas psbAII.R binds just outside of the insertion site of the gene of interest. Together these primers result in fragments sizes of 0.3 kb + the size of the gene of interest (kb) for Syn6803_*AII_x* transformants and 1.1 kb kb + the size of the gene of interest (kb) for Syn6803_*nrsB_x* transformants. Primers are shown as grey arrows, endogenous genes and expression elements are indicated in green, *nrsBRS* system in purple, genes of interest in yellow, Tn903 kanamycin resistance cassette (Km^R) in red and the HA-tag in orange.

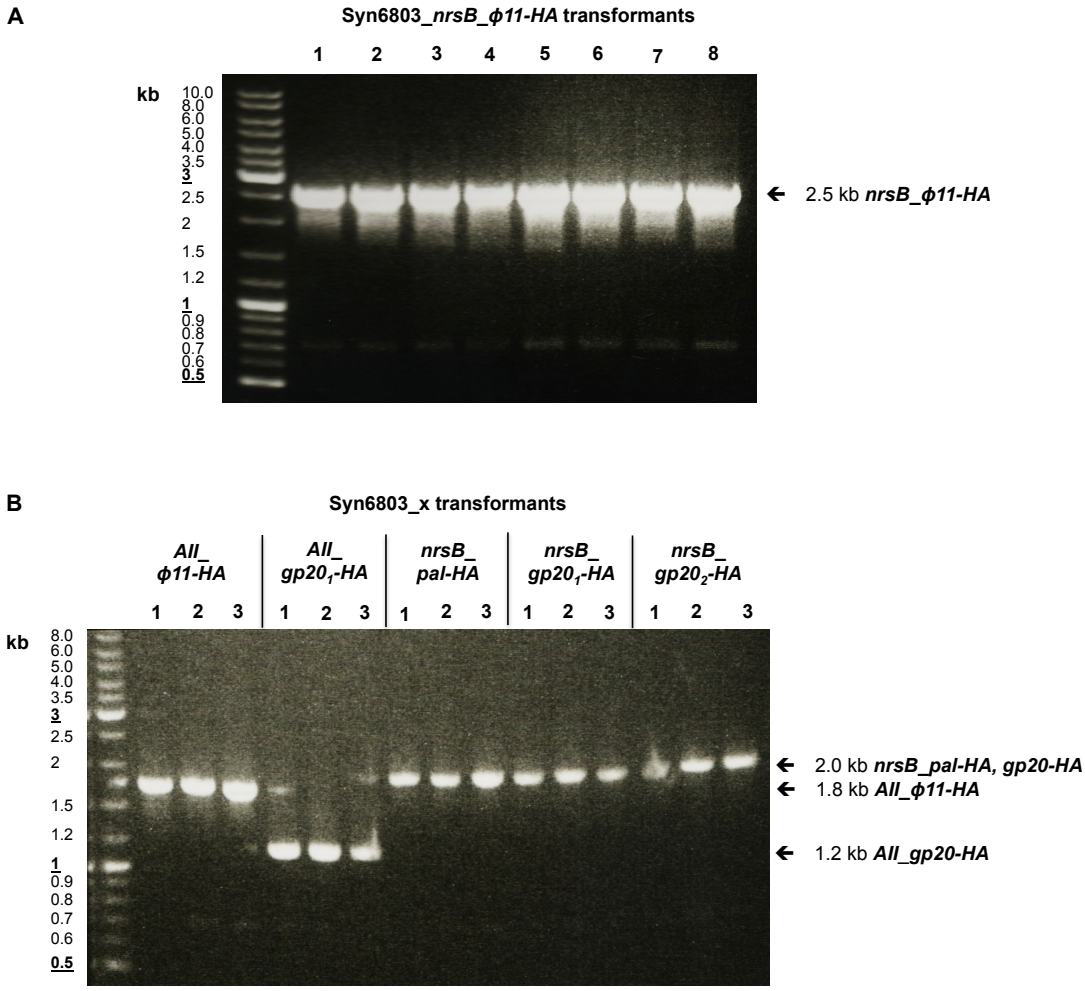

Figure 6.5: PCR screening for the successful transformation of *Synechocystis* sp. PCC 6803 with the expression vectors pLAH.AII and pLAH.nrsB
In the PCR screening for putative Syn6803_*AII_x* and Syn6803_*nrsB_x* transformants the primers psbAII.F and psbAII.R were used. For the binding sites of the primers see Figure 6.4. Expected band sizes are as follows: (A) Syn6803_*nrsB_ ϕ11-HA*: 2.5 kb; (B) Syn6803_*AII_gp20$_1$-HA*: 1.2 kb; Syn6803_*AII_ϕ11-HA*: 1.8 kb; Syn6803_*nrsB_pal-HA:* 2.0 kb; Syn6803_nrsB_ *gp20-HA*:2.0 kb.

6.2.1.3.3 The transformation plasmid pLAH.AII_*pal-HA* could not be produced in *Escherichia coli* DH5α

The *pal-HA* gene was amplified as described in 6.2.1.3.2, cut with NdeI and BamHI and subsequently ligated into pLAH.AII, which had been cut with the same restriction enzymes. Alternatively, the PCR product was first cloned into pJet before restriction digestion. The ligated plasmids pLAH.AII_*pal-HA* were then transformed into

competent *Escherichia coli* DH5α cells using the kanamycin resistance cassette as the selectable marker.

In total 15 ligations of *pal-HA* into pLAH.AII with different preparations and different concentrations of the insert and the vector followed by transformation into *E. coli* were performed, but none resulted in *E. coli* colonies carrying the desired plasmid. After transformation into *E. coli* DH5α either no colonies appeared or only very few colonies appeared, which contained the empty vector. In one case an *E. coli* colony appeared that carried pLAH.AII with only one half of the *pal* gene. In contrast, the *pal-HA* insert could be successfully cloned into the plasmid pLAH.nrsB, which carries a promoter that induces expression only in the presence of nickel. Furthermore, the genes of *ϕ11-HA and* $gp20_1$*-HA* were successfully cloned into the same preparations of the pLAH.AII plasmid. Therefore it can be excluded that the insert or the vector were unsuitable for ligation.

It has been shown in a previous study that the promoter and expression elements of the *psbAII* gene result in the expression of the gene of interest in *E. coli* DH5α using two different antibiotic resistance cassettes (*ble* (zeocin resistance) and *aadA* (spectinomycin resistance)) as well as *gfp* (Mackrow 2012). It can be therefore assumed that the endolysin genes are also expressed under the control of the *psbAII* promoter in *E. coli* DH5α. As mentioned already in 3.1.1, a study by Oey et al. reported that the genes of *pal* and *cpl-1* could not be cloned into a tobacco chloroplast expression vector in *E. coli* and concluded therefore that their chloroplast vectors reach production levels of Pal and Cpl-1, which become toxic to *E. coli* (Oey et al. 2009b). It is therefore conceivable that the transformation of *E. coli* DH5α with pLAH.AII_*pal-HA* results in a level of *pal* expression that becomes harmful for *E. coli.* All studies that produced Pal or Cpl-1 in *E. coli* used inducible promoter systems, which enables the production of moderately toxic proteins (Jado et al. 2003; Loeffler & Fischetti 2003).

Furthermore, the creation of pLAH.AII_$gp20_2$*-HA* in *E. coli* failed as well, whereas the $gp20_2$*-HA* gene could be cloned into pLAH.nrsB. Gp20 is predicted to have, like Pal, *N*-acetylmuramoyl-*L*-alanine amidase activity. In contrast, it was possible to

clone *ϕ11-HA* into pLAH.AII using *E. coli*. However, the D-alanyl-glycyl endopeptidase domain of ϕ11, which seems to be the more active domain, cleaves the peptidoglycan between the D-alanine of the peptide chain and the first glycine of the glycine bridge (Navarre et al. 1999). The peptidoglycan of the Gram-negative bacterium *E. coli* does not contain a glycine bridge. Sass & Bierbaum (2006) found that both catalytic domains have to be combined and that substrate recognition of the cell-wall binding domain is necessary for the full function of ϕ11 and the ability to cleave the cell wall of intact cells. It is therefore likely that ϕ11 cannot interact with the peptidoglycan of *E. coli*.

These results therefore support the conclusion of Oey et al. (2009b) that the endolysin Pal, when it is synthesised inside the cell in high concentrations is harmful for *E. coli.* This observation is surprising, since the endolysin Pal is described to be highly specific for *S. pneumoni*ae (Loeffler et al. 2001). However, it is conceivable that higher Pal concentrations inside the cell have a negative effect caused either by interaction with the peptidoglycan through the cleaving of specific bonds or binding to cell wall structures, or in a completely different unknown way.

In contrast, it has been shown in 3.2.3.1 that the production of Pal in the *C. reinhardtii* chloroplast does not have any negative impact on the growth of the alga. It should be therefore possible to produce the endolysin Pal in *C. reinhardtii* in continuous cultivation, which is likely not possible in *E. coli*. This would highlight an advantage of *C. reinhardtii* as an expression platform over the conventional platform *E. coli*.

6.2.2 Confirmation of the production of the endolysins in *Synechocystis* sp. PCC 6803

After the successful creation of the transgenic *Synechocystis* sp. PCC 6803 lines carrying the genes of three different endolysins under the control of two different promoters, the next stage was to analyse whether the endolysins were accumulating to detectable levels in the cyanobacterium. Of particular interest was the investigation of the *gp20* expression, where the gene product did not accumulate to detectable levels in the *C. reinhardtii* chloroplast (Taunt 2013).

6.2.2.1 Expression of *pal* in Syn6803_*nrsB_pal-HA*

To investigate the expression of *pal* in Syn6803_*nrsB_pal-HA,* the strain was grown under standard conditions to an OD_{750nm} of 0.5 before expression was induced with 6.4 µM of $NiCl_2$. Samples were taken before induction, as well as at four, seven and 24 hours after the start of the induction. Subsequently, the samples were equalised to the same concentration of cells and analysed for the presence of the Pal protein by western blot using antibodies against the HA-tag and the Odyssey® Infrared (IR) Imaging System.

The western blot analysis confirmed the successful production and accumulation of Pal in Syn6803_*nrsB_pal-HA* (Figure 6.6). Furthermore, the analysis showed that only trace amounts of Pal (about 160 times less compared to seven hours after induction) are detectable before induction proving that the *nrsB* promoter is tightly regulated in the absence of nickel (Figure 6.6, Figure 6.7). The analysis showed as well that Pal steadily accumulates in the *Synechocystis* cells following induction, since more Pal was present per cell after seven hours compared to four hours after induction. However, 24 hours after the induction by nickel the Pal levels per cell had dropped again (Figure 6.6). These results were confirmed in a repetition of the experiment with induction times of three, seven and 24 hours.

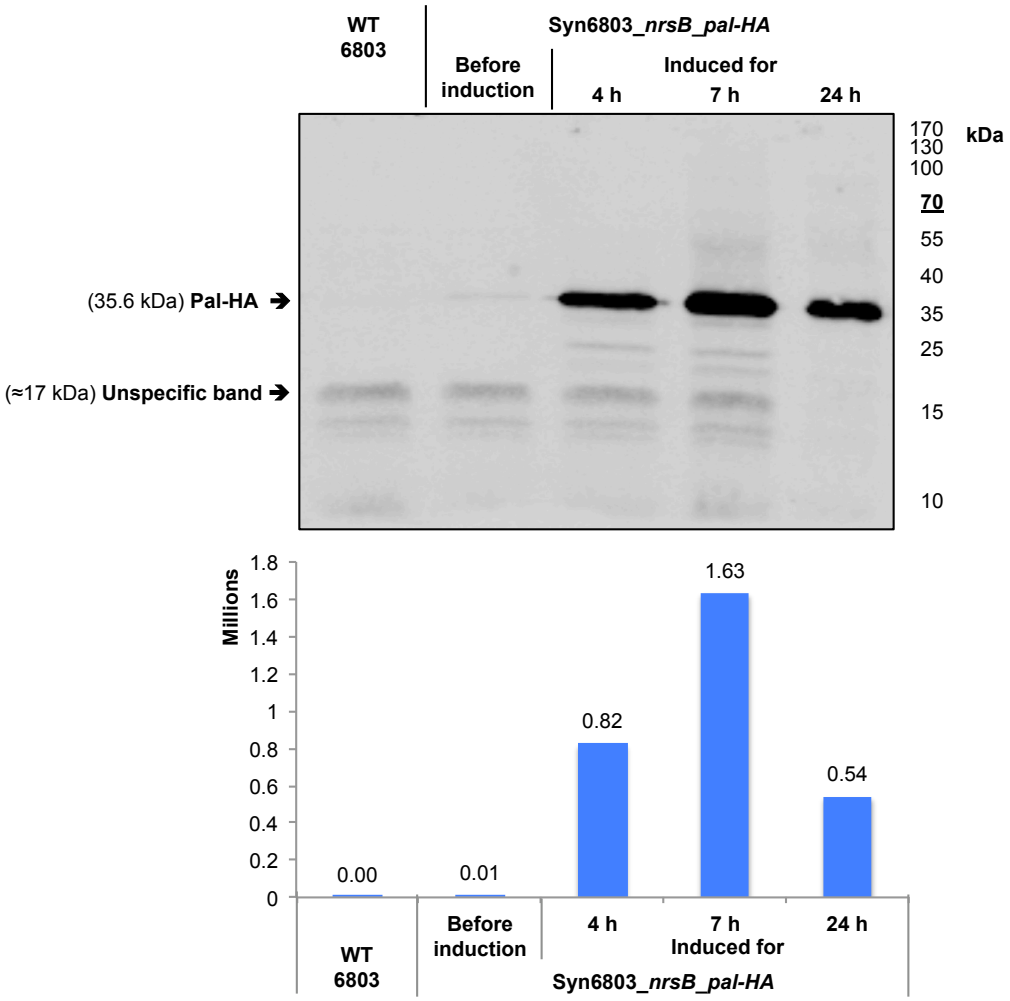

Figure 6.6: Western blot analysis of whole cell extracts of Syn6803_*nrsB_pal-HA* transformants showing the presence of HA-tagged Pal after induction for 0, 4, 7 and 24 h
The gene expression was induced with 6.4 µM of $NiCl_2$ and samples were taken at different time points before and after induction, normalised to the OD_{750nm} at the time of sampling (cells were resuspended in 1 ml of buffer per OD_{750nm} of 1) and 20 µl of each sample (= suspension of whole cells that were broken by the addition of SDS (2% w/v) and boiling) were analysed in a western blot with anti-HA antibodies, IRDye® secondary antibodies and the Odyssey® Infrared Imaging System for detection (A) and quantification (B). *Synechocystis* sp. PCC 6803 wild type was used as a negative control. The expected band size is 35.6 kDa. Protein sizes were determined using the PageRuler™ Prestained Protein ladder (Thermo Scientific).

6.2.2.2 Expression of ϕ11 in Syn6803_*nrsB_ϕ11-HA* and Syn6803_*AII_ϕ11-HA*

After the accumulation of Pal protein in the transgenic *Synechocystis* line had been confirmed, the two lines carrying the ϕ11 gene were analysed for HA-tagged protein. Syn6803_*nrsB_ϕ11-HA* was cultured and induced as described in 6.2.2.1 and samples were taken before induction, as well as three, five and 9.5 hours after the start of the

induction, since the amount of Pal protein in the transgenic *Synechocystis* line had already decreased 24 h after induction. Syn6803*_AII_ϕ11-HA,* which carries a constitutive promoter*,* was grown to an OD_{750nm} of 0.9 and subsequently harvested. All samples were analysed for the presence of the ϕ11 protein by western blot analysis with anti-HA antibodies and the Odyssey® Infrared (IR) Imaging System. Alternatively, horseradish peroxidase-linked secondary (ECL) antibodies were used and the resulting chemiluminescence was detected with photographic film. Both detection systems were used to confirm the successful accumulation of ϕ11 in Syn6803*_nrsB_ϕ11-HA* and the Odyssey® Infrared (IR) Imaging System to confirm the production of ϕ11 in Syn6803*_AII_ϕ11-HA.*

This analysis of the Syn6803*_nrsB_ϕ11-HA* samples showed again that the endolysin ϕ11 accumulated in the *Synechocystis* cells within the first hours after induction, since more ϕ11 was present per cell after five hours compared to three hours after induction. However, already 9.5 hours after the induction by nickel the amount of ϕ11 was lower than five hours after induction. A repeat of the experiment showed a decrease between six hours and 18 hours after induction. The study by Al-Haj (2014) showed as well that the highest concentration of α-farnesene synthase was achieved 7.5 hours after induction and found that nine hours after induction the yields had decreased and after 24 hours the enzyme was no longer detectable.

The results indicate therefore that the induction time that results in the highest endolysin yields is between five and seven hours when the induction is performed with 6.4 µM Ni^{2+}. However, the experiments need to be repeated and samples need to be taken at more time points to determine the exact induction time for the highest Pal and ϕ11 yields.

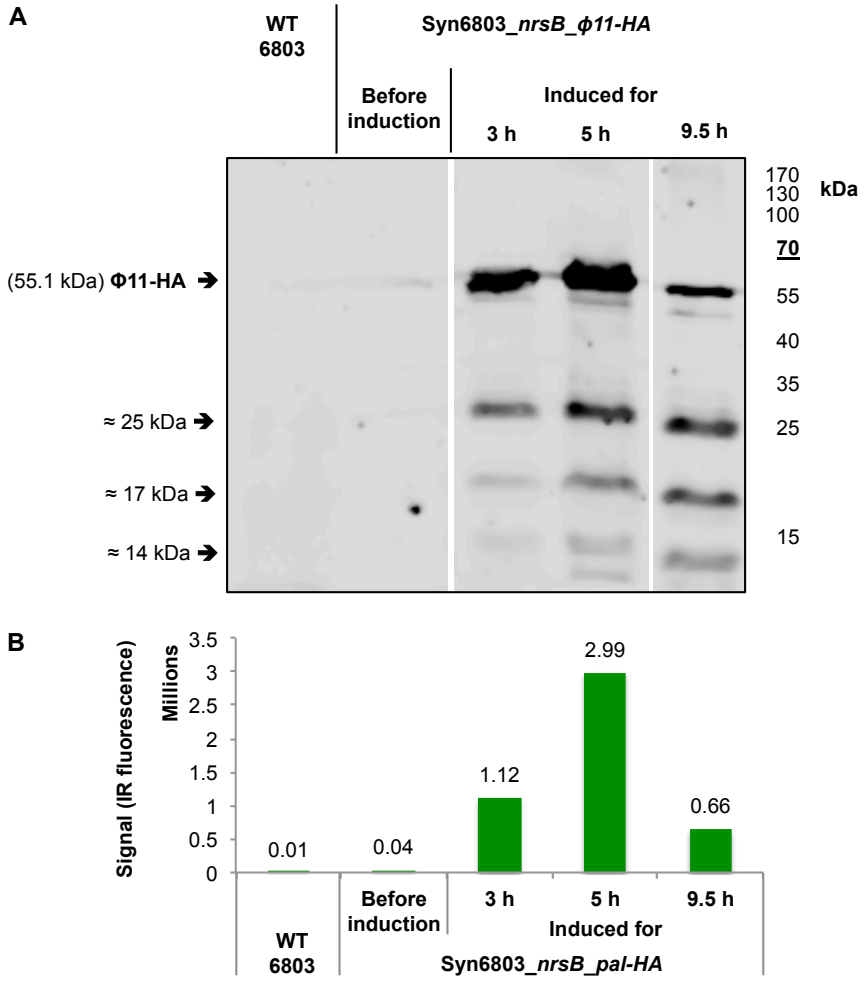

Figure 6.7: Western blot analysis of whole cell extracts of Syn6803_*nrsB_ϕ11-HA* transformants showing the presence of HA-tagged ϕ11 protein after induction for 0, 3, 5 and 9.5 h
The gene expression was induced with 6.4 µM of $NiCl_2$ and samples were taken at different time points before and after induction, normalised to the OD_{750nm} at the time of sampling (cells were resuspended in 1 ml of buffer per OD_{750nm} of 1) and 20 µl of each sample (= suspension of whole cells that were broken by the addition of SDS (2% w/v) and boiling) were analysed in a western blot with anti-HA antibodies, IRDye® secondary antibodies and the Odyssey® Infrared Imaging System for detection (A) and quantification (B). *Synechocystis* sp. PCC 6803 wild type was used as a negative control. The expected band size for full-length ϕ11 is 55.1 kDa. Protein sizes were determined using the PageRuler™ Prestained Protein ladder (Thermo Scientific). The black box indicates that all samples were analysed on the same gel and membrane and the white lines indicate that lanes were cut out between the samples for the preparation of the figure.

However, it was also observed during this study that the addition of nickel had a negative impact on the growth of *Synechocystis* including the wild type strain. The addition of 6.4 µM Ni^{2+} resulted, independent of the OD_{750nm} the culture had reached at the time of the addition, in a slowing down of the growth and a plateauing of the OD_{750nm} (not shown). These results indicate that the used nickel concentration used

has a negative effect on the growth and health of *Synechocystis* during longer induction periods, which then results in a decrease of the recombinant protein yield after induction for 9.5 hours or longer.

The concentration of 6.4 µM $NiCl_2$ was chosen in this study and the study by Al-Haj (2014), because a study that used the *nrsB* promoter for the expression of the reporter gene *luxAB* found that an induction with 6.4 µM Ni^{2+} results in the highest level of bioluminescence (Peca et al. 2008). The study created a whole-cell bioluminescent reporter that quantitatively responds to Ni^{2+} and other metal ions and showed that increasing concentrations of Ni^{2+} result in a dose dependent bioluminescence signal, but concentrations above 6.4 µM resulted in a reduced bioluminescence. These results suggest that higher concentrations of Ni^{2+} have a negative impact on either the activity or production of the luminescent protein or the health of the cells. However, the study performed the induction for only three hours. It is therefore conceivable that extending the induction time to 9.5 hours or more has a negative impact on *Synechocystis* cells already at a concentration of 6.4 µM.

Another study showed that *nrs* mRNA can be already detected after induction by 0.45 µM Ni^{2+} for one hour, but the mRNA levels were higher after induction with 17 µM Ni^{2+}. Higher concentrations of Ni^{2+} did not increase the mRNA levels any further (García-Domínguez et al. 2000). In contrast, the study by Al-Haj (2014) and a second study (Y. Lui, unpublished) did not observe a difference in recombinant protein yields after induction with Ni^{2+} concentrations between 0.8 and 6.4 µM.

It is therefore conceivable that an induction with lower Ni^{2+} concentrations results in the same rate of protein accumulation, but might have less impact on the health of the *Synechocystis* cells and enable an induction over a longer period, which might result in the accumulation of higher final yields of the endolysins. This might be therefore a strategy to maximise the yield of endolysin protein under the control of the *nrsBRS* system in *Synechocystis*.

Another observation during this analysis was that between three and six (depending on the overall intensity of the signal) additional bands were detectable in the samples

of the transgenic lines expressing ϕ11, which were not present in the wild type samples. This shows that multiple truncated protein products of ϕ11 are formed in *Synechocystis* sp. PCC 6803. The truncated ϕ11 products seen in each repeat of the analysis appeared to be the same size, but their relative intensities varied between experiments. In the western blot analysis shown in Figure 6.8, predominately full-length ϕ11 was detected. The truncation products are further discussed in 6.2.2.4.

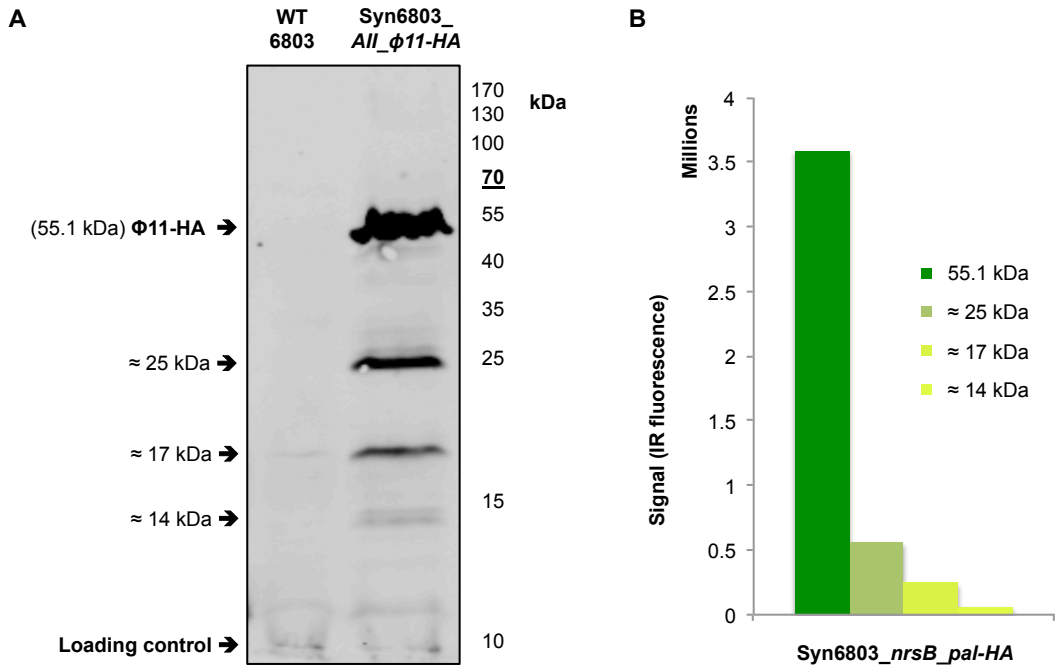

Figure 6.8: Western blot analysis of whole cell extracts of Syn6803_*All_ϕ11-HA* transformants showing the presence of HA-tagged ϕ11 protein
Samples were normalised to the OD_{750nm} at the time of sampling (cells were resuspended in 1 ml of buffer per OD_{750nm} of 1) and 20 µl of each sample (= suspension of whole cells that were broken by the addition of SDS (2% w/v) and boiling) were analysed in a western blot with anti-HA antibodies, IRDye® secondary antibodies and the Odyssey® Infrared Imaging System for detection (A) and quantification (B).*Synechocystis* sp. PCC 6803 wild type was used as a negative control. The expected band size for full-length ϕ11 is 55.1 kDa. Protein sizes were determined using the PageRuler™ Prestained Protein ladder (Thermo Scientific).

6.2.2.3 Expression of *gp20* in Syn6803_*nrsB_gp20$_1$-HA*, Syn6803_*nrsB_gp20$_2$-HA* and Syn6803_*AII_ gp20$_1$-HA*

As a next step it was of particular interest to investigate the production of the Gp20 endolysin in *Synechocystis*. Therefore the three transgenic lines carrying the *gp20* genes were analysed for HA-tagged protein in a western blot analysis. The strains were cultured as described in 6.2.2.1 and 6.2.2.2. The induction of Syn6803_*nrsB_gp20$_1$-HA* and Syn6803_*nrsB_gp20$_2$-HA* was performed at an OD_{750nm} of 0.8 and the cultures were harvested 5.5 hours after the start of the induction, whereas Syn6803_*AII_gp20$_1$-HA* was harvested at an OD_{750nm} of 0.9. After harvest the samples were concentrated 100 times.

Western blot analysis with anti-HA antibodies and the Odyssey® Infrared (IR) Imaging System, confirmed the successful production of the Gp20 protein in Syn6803_*nrsB_gp20$_1$-HA* (Figure 6.9, Figure 6.10), an endolysin that was not produced to detectable levels in either the *C. reinhardtii* chloroplast. Furthermore, the production of Gp20 on its own as a recombinant protein has not been described so far.

However, the analysis did not show any band in the sample of Syn6803_*AII_gp20$_1$-HA* and only a very weak band in the samples of Syn6803_*nrsB_gp20$_2$-HA* after the sample was analysed at two-fold concentration (Figure 6.9). Syn6803_*AII_gp20$_1$-HA* carries the same *gp20* gene as Syn6803_*nrsB_gp20$_1$-HA* and the *AII* promoter has been shown to work for the expression of ϕ11. It is therefore surprising that no Gp20 protein was detected in samples of Syn6803_*AII_gp20$_1$-HA*. One explanation would be that a mutation that prevents the expression appeared at some point during cloning or transformation. The correct sequence of *gp20* in the plasmid was confirmed by sequencing. However, the sequence of the expression elements was not fully analysed and could have therefore contained a mutation. As already discussed in 6.2.1.3.3 the cloning of the *pal* gene failed in *E. coli* despite several attempts and the fact that the insert could be cloned into the vector pLAH.nrsB with the inducible expression system, and the preparation of the pLAH.AII vector could be used for the successful cloning of *ϕ11*. Furthermore, the cloning of the *gp20$_2$* gene into pLAH.AII did not result in transformants. Since Oey et al. (2009b) describe a similar phenomenon when

creating expression vectors for the synthesis of Pal and Cpl-1 in tobacco, it is conceivable that the pLAH.AII vector results in protein production levels that are, in the case of certain endolysins, harmful for the cloning host. However, more experiments need to be performed to further investigate this hypothesis.

Furthermore, the western blot analysis suggested that the codon optimised version *gp20$_1$* results in higher expression levels than the *gp20$_2$* gene (Figure 6.9). The genes have a shared sequence identity of 85.7%. The *gp20$_1$* contains the UCA codon six times, which is less frequently used for serine in *Synechocystis*, whereas *gp20$_2$* contains it 13 times. This could be therefore an explanation for the lower protein levels. Though, the western blot analysis needs to be performed with a higher number of transformants and different induction times before it can be concluded that the gene sequence of *gp20$_1$* results in higher protein yields compared to *gp20$_2$*.

It is important to note that the levels of Gp20 produced in *Synechocystis* are significantly lower than the amounts of Pal and ϕ11 and that approximately ten–fold more concentrated samples were used compared to the western blot analysis showing the accumulation of Pal and ϕ11 in the previous sections. Figure 6.10 shows a comparison of samples from Syn6803*_nrsB_gp20$_1$-HA* with samples from Syn6803*_nrsB_pal-HA* and Syn6803*_nrsB_ϕ11-HA,* which were cultured, induced and prepared in the same way. This western blot analysis showed that under these conditions approximately 50 times more full-length ϕ11 and 60 times more Pal accumulated in *Synechocystis* using the same expression system. These results suggest, together with the fact that Gp20 could not be produced in the *C. reinhardtii* chloroplast or *Escherichia coli* DH5α, that either the synthesis of the protein is less efficient or that it is less stable than the endolysins Pal, Cpl-1 and ϕ11.

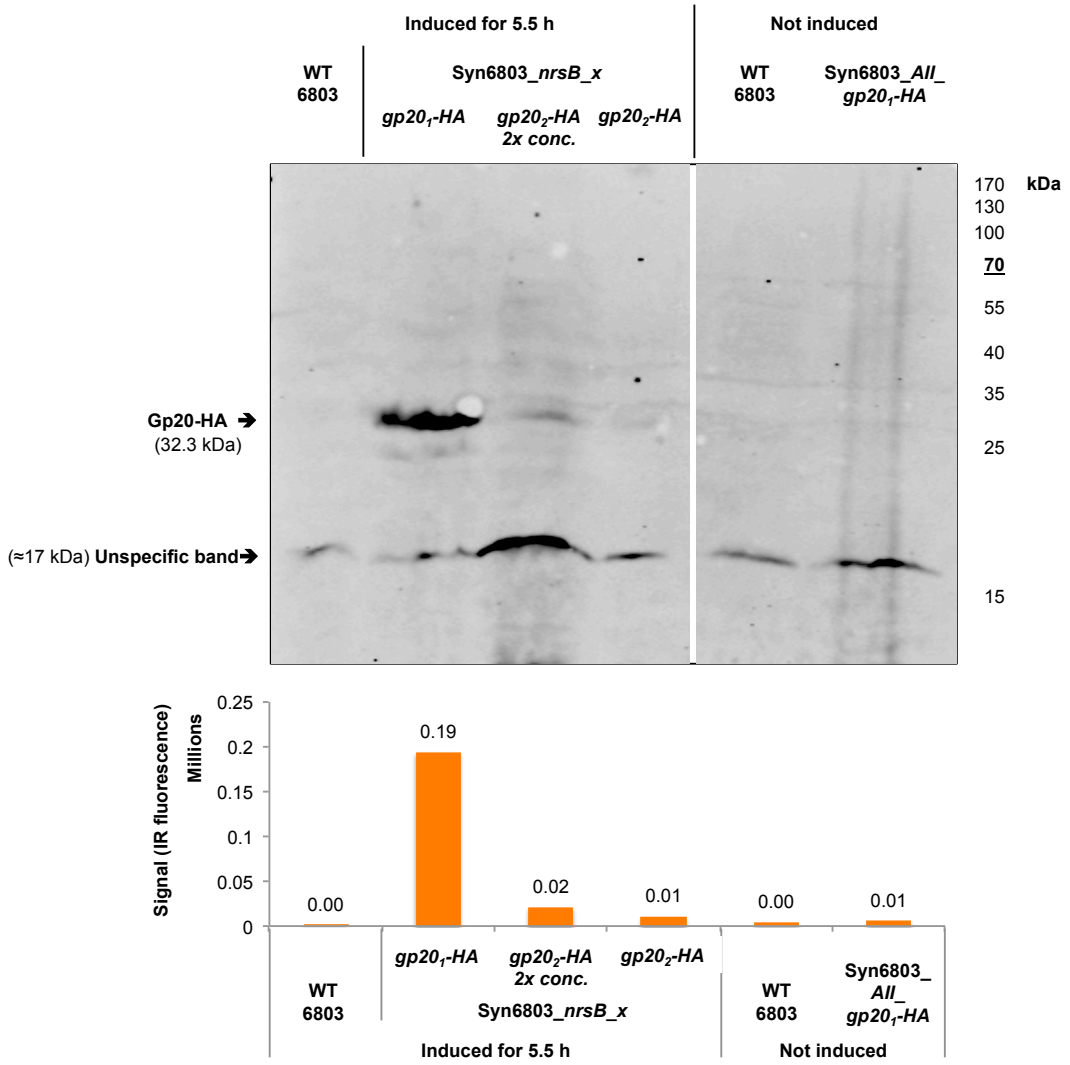

Figure 6.9: Western blot analysis of whole cell extracts of Syn6803_*nrsB_gp20₁*, Syn6803_*nrsB_gp20₂* and Syn6803_*AII_ gp20₁* transformants showing the presence or absence of HA-tagged Gp20 protein

The gene expression in Syn6803_*nrsB_gp20₁* and Syn6803_*nrsB_gp20₂* was induced with 6.4 µM of $NiCl_2$, samples were taken, concentrated to 100x the culture volume and 20 µl of each sample (= suspension of whole cells that were broken by the addition of SDS (2% w/v) and boiling) was analysed in a western blot with anti-HA antibodies, IRDye® secondary antibodies and the Odyssey® Infrared Imaging System for detection (A) and quantification (B). *Synechocystis* sp. PCC 6803 wild type (WT 6803) was used as a negative control. The expected band size for Gp20 is 32.3 kDa. Protein sizes were determined using the PageRuler™ prestained protein ladder (Thermo Scientific). The black box indicates that all samples were analysed on the same gel and membrane and the white line indicates that lanes were cut out between the samples for the preparation of the figure.

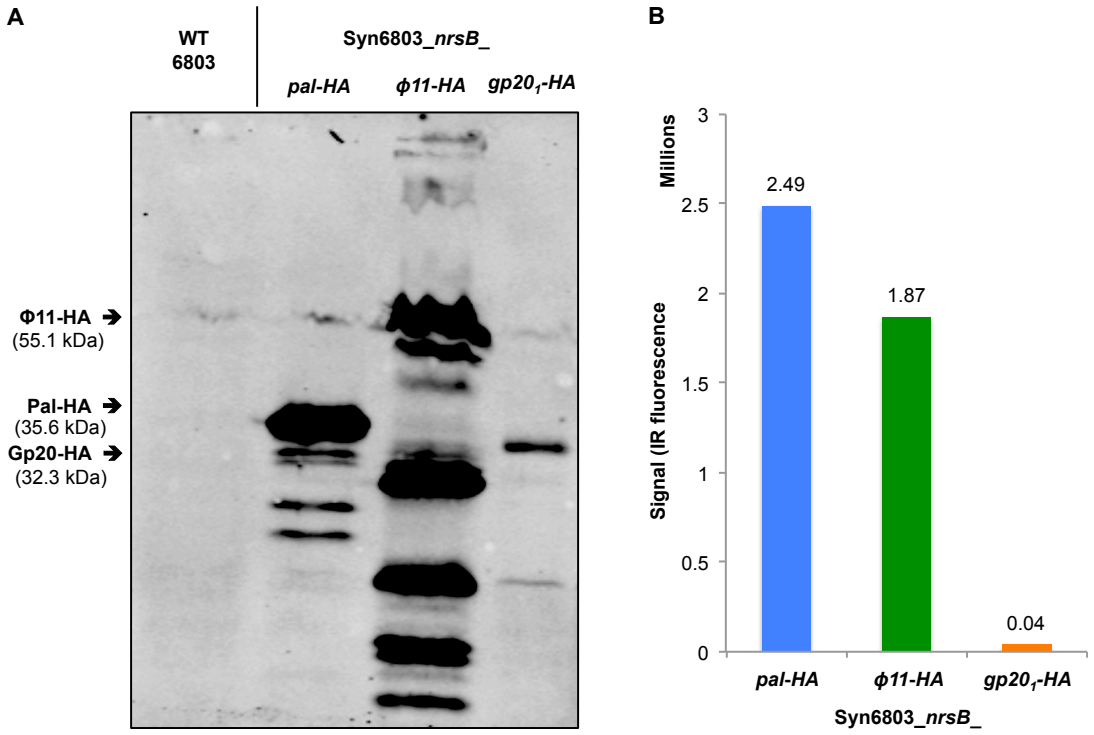

Figure 6.10: Western blot analysis of whole cell extracts of Syn6803_*nrsB_pal-HA*, Syn6803_*nrsB_ϕ11-HA* and Syn6803_*nrsB_gp20*$_1$ showing the relative amounts of Pal, ϕ11 and Gp20 protein

The gene expression was induced with 6.4 µM of $NiCl_2$ for 5.5 hours, harvested and concentrated to 100x the culture volume. The western blot analysis was performed with whole cell extract (= suspension of whole cells that were broken by the addition of SDS (2% w/v) and boiling) and anti-HA antibodies, IRDye® secondary antibodies and the Odyssey® Infrared Imaging System for detection (A) and quantification (B).

6.2.2.4 The occurrence of truncated protein products differs in the different expression platforms

A striking observation during this study was that the production of Pal and ϕ11 in three different organisms resulted in different but, for each organism and endolysin, characteristic patterns of truncated protein products (Figure 6.11). These bands of lower molecular weight appeared in the samples from the transgenic lines, but not in the corresponding controls. The production of one endolysin in the same organism always resulted in the same pattern, however the intensity and the proportion between the additional bands and the full-length proteins varied.

It has been already discussed in previous chapters how the truncated proteins might be formed. It was mentioned in chapter 5 that a possible explanation for the 38 kDa product of ϕ11, which is formed in *C. reinhardtii* and *E. coli*, could be an alternative translation start, since the protein sequence contains a methionine in this region. Another explanation would be that the products are formed by specific proteolytic activity. Table 6.2 gives an overview of all N-terminal truncated protein products that could be formed by a translation start at an alternative AUG codon. Interestingly, several sizes match the observed truncated protein products on the western blot analysis – for example, the two bands just under the full-length Pal in *Synechocystis* and *E. coli*, which could match the 29.17, 31.43, 33.09 or 34.05 kDa alternative translation start proteins. In contrast the two additional Pal bands in *Synechocystis* and in *E. coli* between 15 kDa and 25 kDa do not match any of the predicted protein sizes. The ϕ11 protein produced in *Synechocystis* on the other hand results in several lower molecular weight products that approximately match the 45.87, 38.89, 24.44, 14.75 and 10.76 predicted alternative translation start proteins. However the band around 17 kDa does not fit to any predicted sizes. It is difficult to predict the exact size of a protein using western blot analysis, since even in SDS-PAGEs proteins of the same size do not necessarily run with exactly the same mobility. Some proteins run therefore a bit slower or faster compared to the proteins of the ladder. Furthermore, in prokaryotes and in chloroplasts in some cases the alternative start codons GUG and UUG are used (Blattner et al. 1997). Pal does not contain either of these codons, but ϕ11 contains additionally eight GUG codons, which could function as potential alternative translation start sites. Another explanation for the additional bands that do not fit any predicted size could be a combination of alternative translation start sites and proteolytic activity.

However, taken the quantity of additional AUG codons in the *pal* and *ϕ11* genes, the fact that some of the lower molecular weight bands of Pal and ϕ11 match the predicted sizes of the alternative translation start proteins could be just a coincidence, and the characteristic pattern of truncated protein products is the result of different proteolytic activities in each of the three organisms.

Independent of the cause for the formation of the truncated protein products, it is noticeable that the production in the *C. reinhardtii* chloroplast does not result in detectable level of truncated Pal products unlike the production in *Synechocystis* or *E. coli* and therefore results in the highest proportion of full-length Pal. The synthesis of ϕ11 in both the *C. reinhardtii* chloroplast and in *E. coli* results in only one additional band, whereas multiple additional bands can be detected in *Synechocystis*. Taken together, these observations suggest either that the control of the true translational start is more tightly controlled in the *C. reinhardtii* chloroplast, compared to the two prokaryotic systems, or that the endolysins are less exposed to specific proteolytic activity in *C. reinhardtii*.

Table 6.2: Molecular weight of protein products that could be formed by alternative translation start sites
The molecular weight of the N-terminal truncated Pal and ϕ11 products resulting from a start at alternative AUG codons were calculated using: http://bioinformatics.org/sms/prot_mw.html.

Endolysin	**Molecular weight of alternative translation start protein products (kDa)**								
Pal	5.46	8.2	10.64	13.45	24.55	29.17	31.43	33.09	34.05
ϕ11	6.09	10.76	14.75	24.44	38.89	45.87			

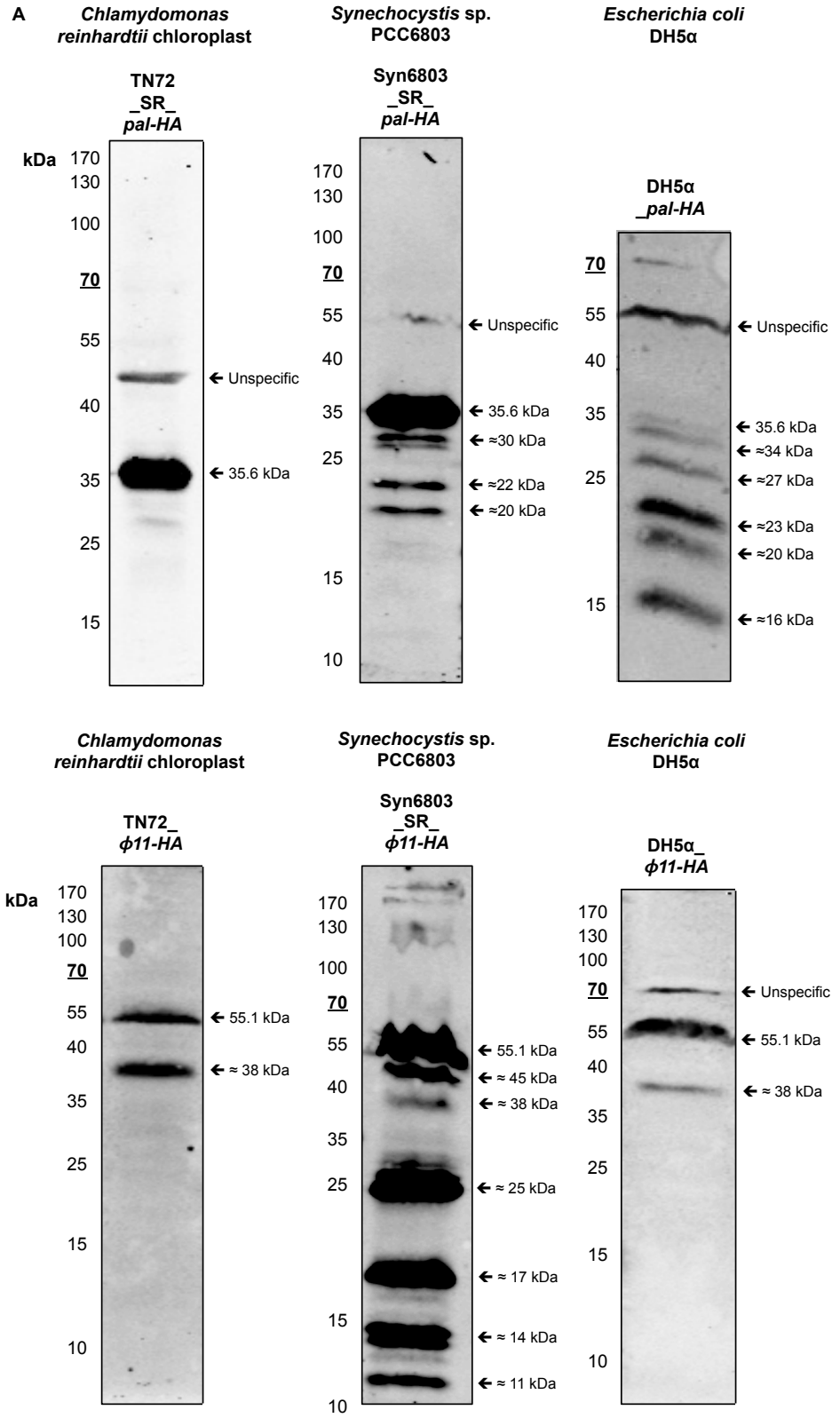

Figure 6.11: Western blot analyses showing the appearance of truncated Pal and ϕ11 protein products that were formed during production in three different systems
The western blot analysis was performed with whole cell extract (= suspension of whole cells that were broken by the addition of SDS (2% w/v) and boiling) and anti-HA antibodies, IRDye® secondary antibodies and the Odyssey® Infrared Imaging System.

6.2.2.5 Influence of endolysin synthesis on the growth of *Synechocystis* sp. PCC 6803

Beside the fact that the synthesis of a recombinant protein is generally a metabolic burden for a cell, it is conceivable that the production of endolysins could have a negative impact on *Synechocystis*, since the Gram-negative bacterium has a cell wall composed of the endolysin substrate peptidoglycan. Therefore, it was important to ensure that the production of the endolysins does not have any toxic effect on the cyanobacterium. This was analysed by following the growth of the transgenic line Syn6803*_AII_ϕ11-HA* in comparison to the wild type.

Syn6803*_AII_ϕ11-HA* and the *Synechocystis* sp. PCC 6803 wild type were grown under standard conditions in the Algem photobioreactor and the OD_{750nm} was automatically recorded every 30 min. The wild type was found to grow slightly faster than Syn6803*_AII_ϕ11-HA,* which had a slightly longer lag phase. However the growth rates of both strains were similar and the strains reached the same final OD_{750nm} (Figure 6.12). The results show therefore that the production of ϕ11 does not have any major impact on the growth of *Synechocystis*.

It was also of interest to analyse whether the production of the endolysin Pal has any negative impact on the growth of *Synechocystis*, especially since observations during this study and by Oey et al. (2009b) suggested a harmful effect against the Gram-negative bacterium *E. coli*. However, since a transgenic line was available only with the *pal* gene under the control of the *nrsB* promoter and the addition of Ni^{2+} on its own had already an impact on the growth of the cyanobacterium, it was not possible to evaluate the impact of the Pal production on *Synechocystis* using growth studies. The same was the case for Gp20, which was also only produced to detectable levels under the control of the *nrsB* promoter.

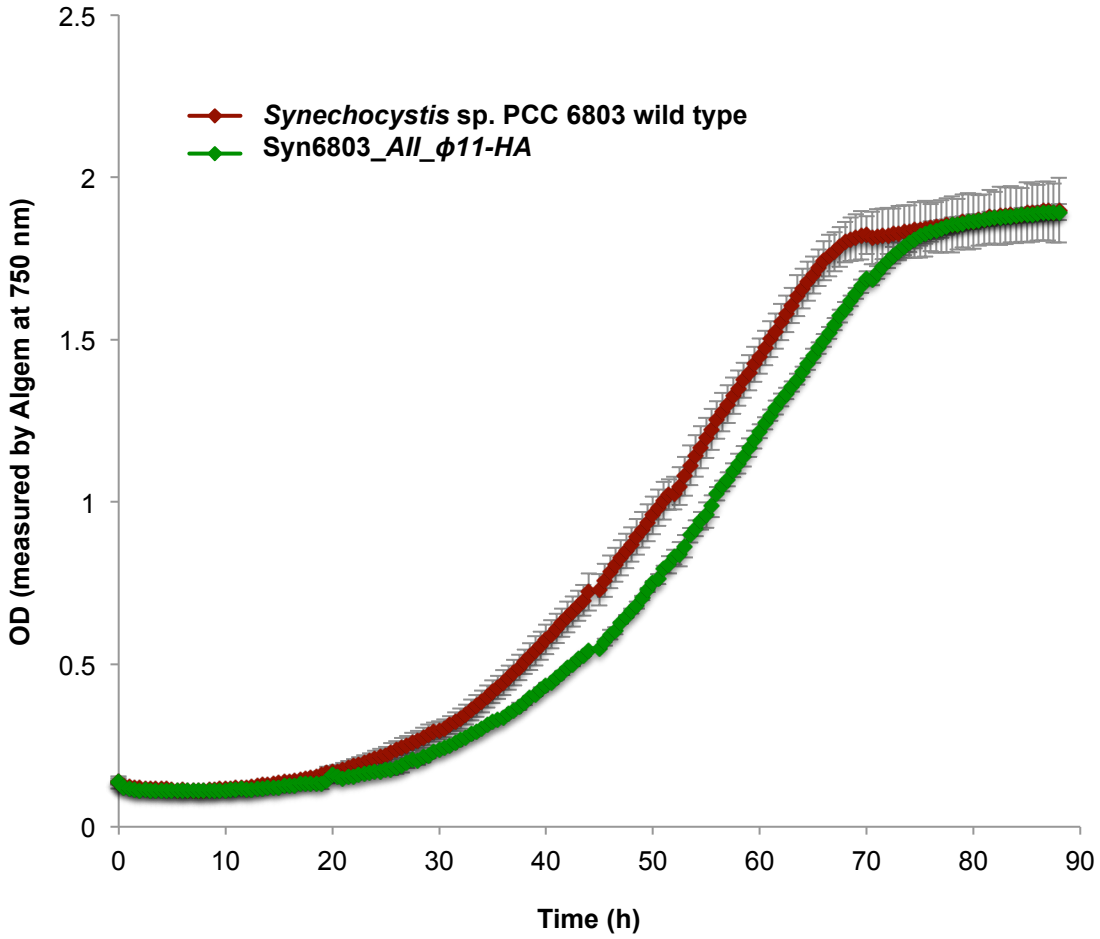

Figure 6.12: Growth of *Synechocystis* Syn6803_*AII_ϕ11-HA* in comparison to the *Synechocystis* sp. PCC6803 wild type

The strains were grown under continuous shaking at 120 rpm, at 30ºC and 200 µmol/m^2/s in BG11 medium in the Algem photobioreactor (Algenuity, Stewartby (UK)), the OD_{750nm} was automatically recorded every 0.5 h. The error bars show ± one standard deviation (n = 2).

6.2.3 Cell breakage of *Synechocystis* sp. PCC 6803 and production of endolysin protein preparations

In order to perform assays analysing the antibacterial activity of the three endolysins against the target bacteria, it was necessary to break the *Synechocystis* cells and to recover the endolysins without denaturing the proteins. Previous protocols have used vortexing in the presence of glass beads to break *Synechocystis* cells (Al´Haj 2014). This method was therefore used for cell breakage and it was evaluated whether the endolysins can be recovered and separated from the cell debris afterwards.

The three transgenic lines were broken by vortexing with glass beads (212 - 300 µm) for 2 min followed by 2 min on ice for five cycles. Subsequently the supernatant was separated from the cell debris by centrifugation (21,000 x *g* for 5 min). The whole cell extract before centrifugation and the supernatants (crude extract) were analysed by western blot analysis for the HA-tagged endolysins. All samples were additionally treated with SDS and boiling to break leftover unbroken cells.

These analyses showed that all three endolysins could be recovered into the supernatant after cell breakage using glass beads (Figure 6.13). However, the supernatants contained less protein compared to the whole cell extracts. Figure 6.13 shows a comparison of the whole cell extracts and the supernatants for Pal and Gp20. It is likely that the method does not result in the breakage of all cells, which then causes a loss of endolysin protein during centrifugation. Another explanation could be that a fraction of Pal and Gp20 is insoluble or aggregated and precipitates during centrifugation.

Nevertheless, vortexing in the presence of glass beads is an easy and quick method and it was possible to recover all three endolysins into the crude extract after cell breakage. Furthermore, the procedure can be easily performed under sterile conditions. This method was therefore used to break the *Synechocystis* cells for the performance of activity assays.

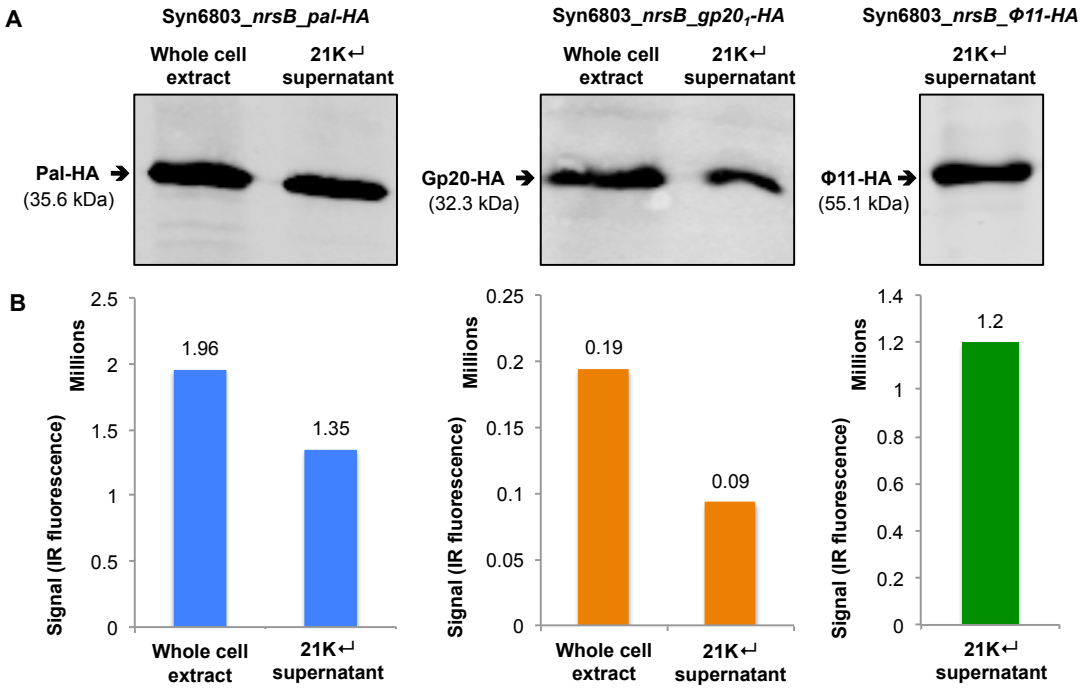

Figure 6.13: Western blot analysis showing the recovery of Pal, Gp20 and ϕ11 in the supernatant after cell breakage by vortexing in the presence of glass beads

The cells were broken by vortexing in the presence of glass beads (212 - 300 µm) for 2 min followed by 2 min on ice for five cycles, followed by centrifugation at 21,000 x *g* for 5 min. The presence of the endolysins in the whole cell extracts before centrifugation and the 21K↵ supernatant (crude extract) was determined by western blot analysis with anti-HA antibodies, IRDye® secondary antibodies and the Odyssey® Infrared Imaging system was used for detection (A) and for quantification (B).

6.2.4 Investigation of the antibacterial activity of *Synechocystis*-produced endolysins

It has been shown in 5.2.4 that ϕ11 produced in *C. reinhardtii* is not active or has a markedly lower activity compared to the same endolysin produced in *E. coli.* This demonstrates the importance of analysing the activity of recombinant proteins after expression in a new production system. Furthermore it was of interest to investigate whether ϕ11 produced in *Synechocystis* has detectable enzymatic activity and to analyse the antibacterial activity of Gp20. Turbidity reduction assays (TRAs) had been used successfully to demonstrate the activity of the *C. reinhardtii*-produced endolysin Pal (4.2.2) and *E. coli*-produced ϕ11 (5.2.4). Therefore as a next step the bacteriolytic activities of Pal, ϕ11 and Gp20 produced in *Synechocystis* were analysed using TRAs with cells of *S. pneumoniae*, *S. aureus* and *P. acnes*, respectively.

6.2.4.1 *Synechocystis*-produced Pal

TRAs were performed with crude extract of Syn6803*_nrsB_pal-HA* that had been prepared as described in 6.2.3. Cells of a *S. pneumoniae* culture were harvested and resuspended in NaPi-buffer before the addition of crude extracts from either the transgenic line producing Pal or the wild type. Subsequently, the OD was measured at 600 nm over a time course.

The TRAs were performed with *S. pneumoniae* cells from an overnight culture and had already reached the stationary phase, which caused an observable autolysis of the cells already in the control samples (4.2.2.1). However, all performances (three performances in duplicate) of the TRA showed a more rapid decrease of the OD_{600nm} in the presence of the cyanobacterial extract containing Pal compared to the wild type extract, confirming the lytic activity of *Synechocystis*-produced Pal against *S. pneumoniae.*

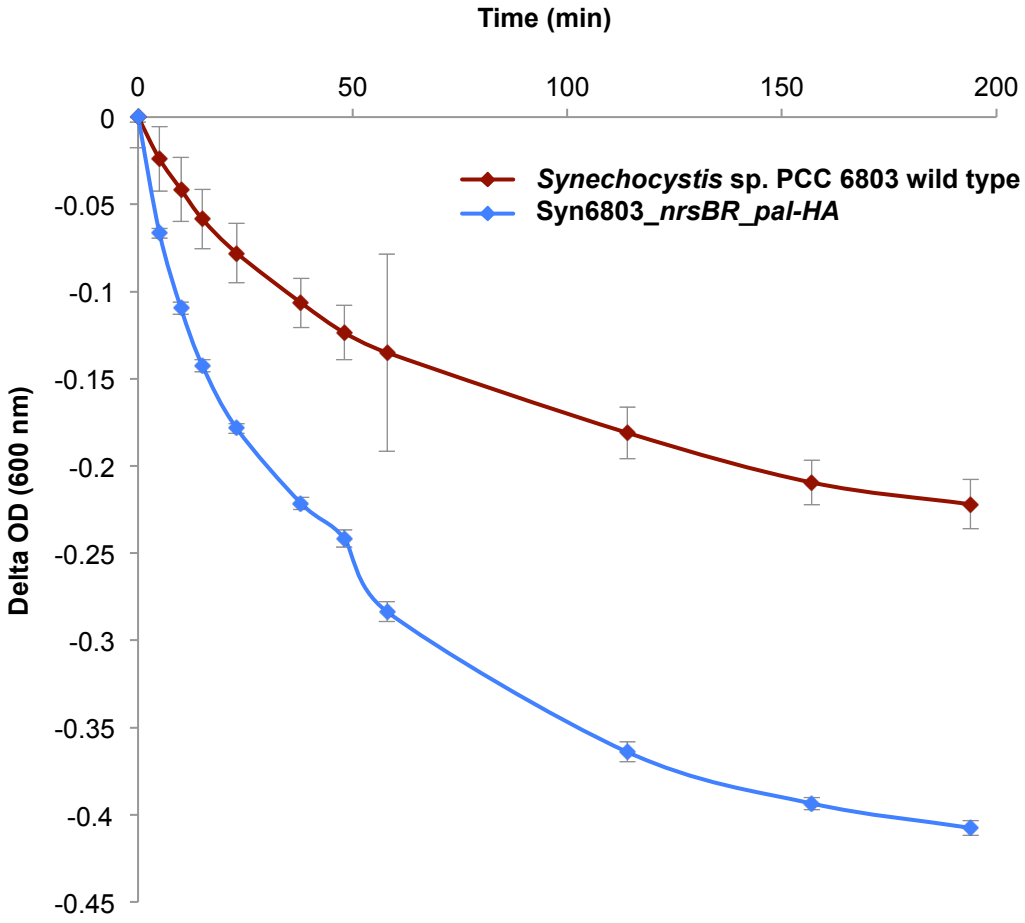

Figure 6.14: Turbidity reduction assay showing the lytic activity of Syn6803_*nrsB_pal-HA* crude extract against *Streptococcus pneumoniae*
The *S. pneumoniae* cells were resuspended in NaPi-buffer to an OD_{600nm} of 0.7. Crude extract of *Synechocystis* sp. PCC 6803 wild type was used as a negative control. The crude extracts were prepared from whole cell extract, the cells were harvested and resuspended in 1 ml of Na-Pi-buffer per OD_{750nm} of 0.5 and broken by vortexing in the presence of glass beads The Syn6803_*nrsB_pal-HA* and the control extract were added to the cell suspension and the OD_{600nm} was measured over a time course at room temperature. The error bars show ± one standard deviation (n = 2).

6.2.4.2 *Synechocystis*-produced ϕ11

As a next step, TRAs were performed to investigate the antibacterial activity of *Synechocystis*-produced ϕ11 against *S. aureus*. The TRAs were performed as described in 5.2.4 with heat inactivated *S. aureus* cells and crude extract of Syn6803_*AII_ϕ11-HA,* wild type extract as a negative control and extract of DH5α_*ϕ11*-HA as a positive control. These TRAs (two performances in duplicate) showed a clear decrease in OD_{595nm} of the *S. aureus* suspension after the addition of

Syn6803_*AII_ϕ11-HA* crude extract in comparison to the negative control, indicating that ϕ11 produced in *Synechocystis* has bacteriolytic activity against its target bacterium *Staphylococcus aureus* (Figure 6.15).

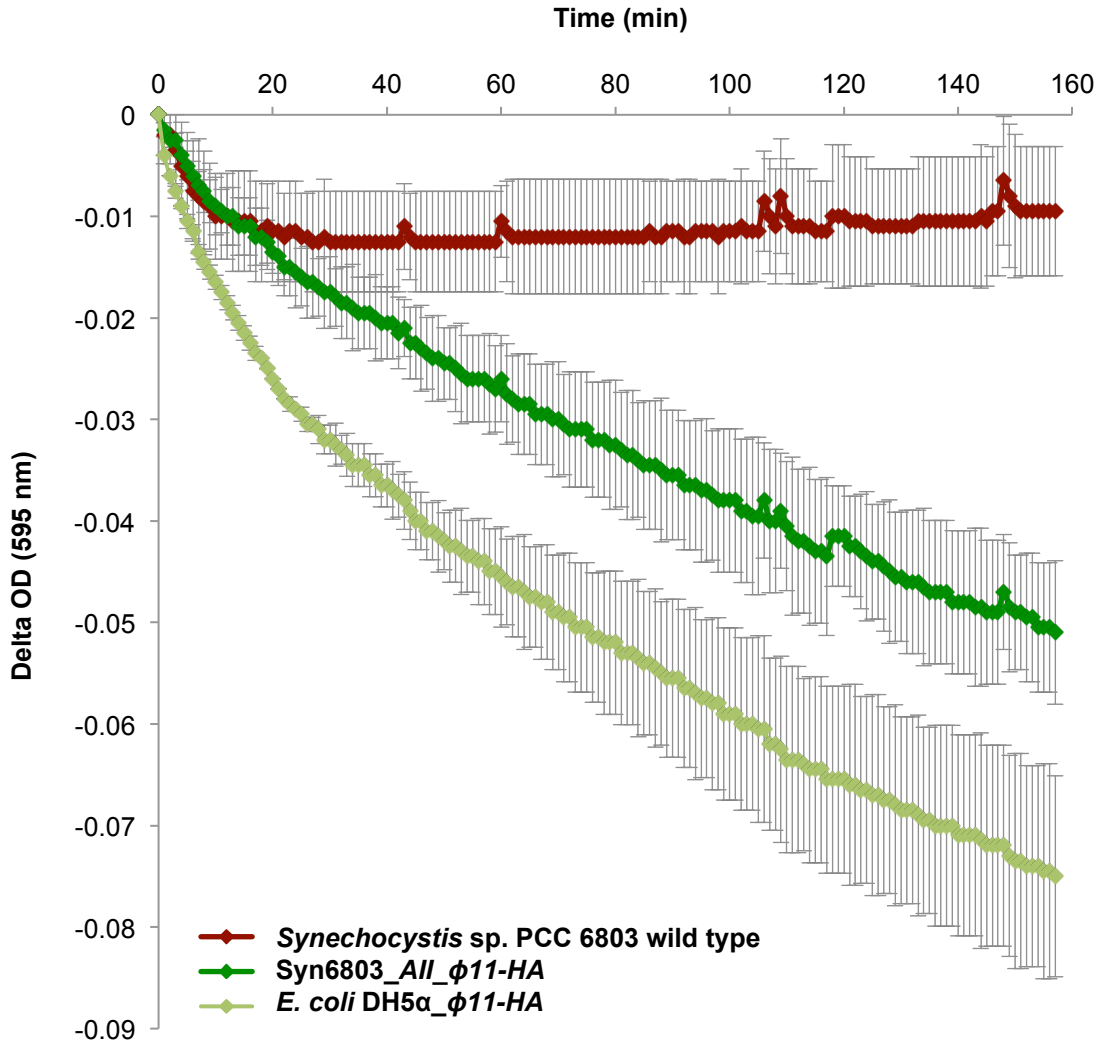

Figure 6.15: Turbidity reduction assay showing the lytic activity of Syn6803_*AII_ϕ11-HA* crude extract against *Staphylococcus aureus*
The *S. aureus* cells were resuspended in NaPi-buffer to an optical density (OD_{595nm}) of 0.4. Crude extracts of *E. coli* DH5α_*ϕ11-HA* and the *Synechocystis* sp. PCC 6803 wild type (WT) were used as a positive and negative control, respectively. The crude extracts were prepared from whole cell extract that was concentrated to 100x the culture volume and broken by vortexing in the presence of glass beads (*Synechocystis*) or using a French pressure cell press (*E.coli*). The extracts were added to the *S. pneumoniae* cell suspension and the OD_{595nm} was measured over a time course at 37ºC. The error bars show ± one standard deviation (n = 2).

The TRA in Figure 6.15 shows a faster decrease in OD_{595nm} for the positive control with DH5α*_ϕ11-HA*. However, a subsequent western blot analysis confirmed that the crude extract of Syn6803*_AII_ϕ11-HA* that was used for the assays contained less ϕ11 than the DH5α*_ϕ11-HA* extract (the IR fluorescence signal was approximately 40% lower). It can be therefore assumed that the slower lysis of the *S. aureus* cells by the *Synechocystis*-produced ϕ11 is due to lower concentrations of the endolysin and not due lower enzymatic activity. Nevertheless, the TRAs with crude extracts from both organisms need to be repeated to quantitatively analyse the enzymatic activities of ϕ11 produced in both systems.

Taken together, these results show that it is possible to produce ϕ11, a promising candidate for the use as an antibacterial agent against staphylococcal caused infections, in *Synechocystis* in active form. The results suggest that the enzymatic activity is comparable to *E. coli*-produced ϕ11, unlike ϕ11 produced in the *C. reinhardtii* chloroplast.

6.2.4.3 *Synechocystis*-produced Gp20

A study by Farrar et al. (2007) sequenced the genome of the bacteriophage PA6 that infects *Propionibacterium* acnes and predicted that ORF20 encodes an endolysin, given it has homology to the amidases of the mycobacteriophages PG1 and Che8 and a high similarity (67% identity for amino acids 2 to 145, N-terminal catalytic domain) to another *N*-acetyl-muramoyl-L-alanine amidase, which is an autolysin of *P. acnes*. Further studies found that other *P. acnes* phages have a high sequence similarity to PA6 and predicted as well that ORF20 encodes in all cases the endolysin, and predicted as well that it has most likely *N*-acetyl-muramoyl-L-alanine amidase activity. However, none of these studies produced Gp20 as a recombinant protein and confirmed experimentally that the protein cleaves the peptidoglycan of *P. acnes*. A demonstration of the lytic activity of *Synechocystis*-produced Gp20 would not only demonstrate that it can be produced as an active enzyme in the cyanobacterium, but would also show that Gp20 on its own has antibacterial activity against *P. acnes*.

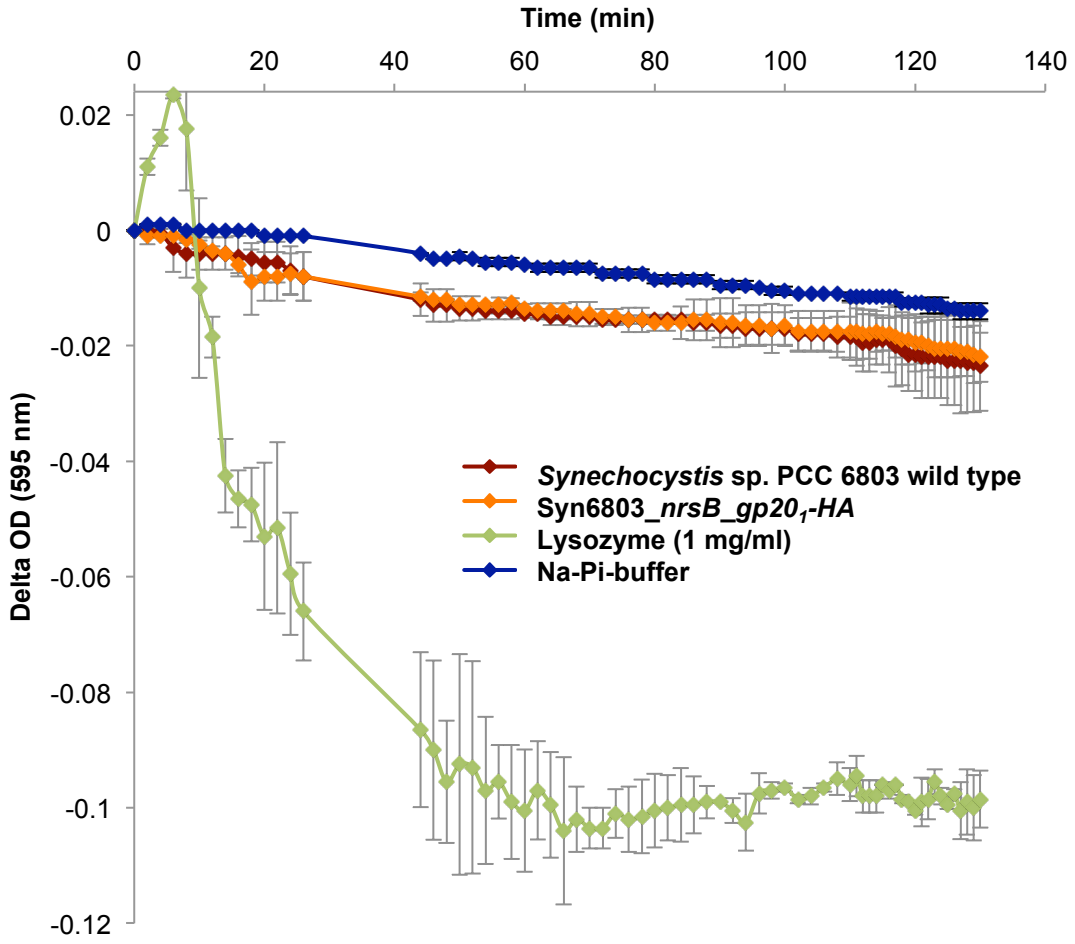

Figure 6.16: Turbidity reduction assay showing the absence of lytic activity of Syn6803_*nrsB_gp20$_1$-HA* crude extract against *Propionibacterium acnes*
The *P. acnes* cells were resuspended in NaPi-buffer to an optical density (OD_{595nm}) of 0.2. Crude extract of the *Synechocystis* sp. PCC 6803 wild type (WT) and Na-Pi-buffer were used as a negative control and lysozyme (1 mg/ml) as a positive control. The crude extracts of Syn6803_*nrsB_gp20$_1$-HA* and the WT were prepared from whole cell extract that was concentrated to 100x the culture volume and broken by vortexing in the presence of glass beads. The extracts were added to the *S. pneumoniae* cell suspension and the OD_{595nm} was measured over a time course at 37ºC. The error bars show ± one standard deviation (n = 2).

Therefore TRAs with a suspension of *P. acnes* cells and Syn6803_*nrsB_gp20$_1$-HA* crude extract as well as wild type extract and buffer as negative controls and lysozyme (1 mg/ml) as a positive control. However, the performed TRAs showed a decrease in the OD_{595nm} for the positive control, which proved that the lysis of *P. acnes* can be measured photometrically, but did not show a decrease in the presence of crude extract containing Gp20 (Figure 6.16).

It has been shown in figure 6.10 that the yield of Gp20 achieved after production in *Synechocystis* is a lot lower (50 – 60 times) than the Pal and ϕ11 yields. It is therefore likely that the amount used in the TRA is not sufficient to cause detectable lytic activity. It was therefore attempted to further concentrate the amount of Gp20 in the crude extracts. However, cyanobacteria contain phycobiliproteins, which have absorption maxima between 500 and 650 nm and therefore an intense blue colour. This interferes strongly with the TRAs, which are performed at 595 nm. Phycobiliproteins are water soluble, unlike chlorophyll, and it was therefore not possible to remove these proteins using ultracentrifugation. The protein-pigment complexes phycoerythrin and phycocyanin have masses of approximately 240 kDa, whereas allophycocyanin has a mass of 105 kDa. Therefore the removal was also attempted using centrifugal concentrator with a MWCO of 100,000. However, the proteins causing the intense "blue colour" were able to pass the membrane of the centrifugal concentrator, most likely because phycobilliproteins consist of several subunits, which easily fall apart outside the cell. So far it was therefore not possible to concentrate Gp20 enough to show its antibacterial activity in crude extract. However, further attempts should be made to gain the experimentally proof that it is an endolysin and to investigate whether it is produced in *Synechocystis* as an active enzyme. Gp20 can be seen as a potential candidate for an antibacterial treatment against acnes vulgaris and the production of Gp20 in a microalgae and the use of crude extract with the endolysin as a topical cosmetic treatment would be a commercially viable option.

6.3 Conclusion and future work

The study described in this chapter investigated the production of three endolysins, the *S. pneumoniae*-specific Pal, the *S. aureus*-specific ϕ11 and the *P. acnes*-specific Gp20, in *Synechocystis* sp. PCC 6803, in order to evaluate the cyanobacterium as an alternative production platform for endolysins.

For this purpose six transgenic lines of *Synechocystis* carrying one of three synthetic endolysin genes in their genome under the control of either the constitutive *psbAII* promoter or the nickel inducible promoter system *nrsBRS* were created to study the synthesis of the endolysins in the cyanobacterium.

One observation during the creation of the transgenic lines was that the cloning of the *pal* gene into the vector pLAH.AII that carries the constitutive expression system failed despite multiple attempts. As already mentioned, a study by Oey et. al. (2009b) described a similar observation. The study found that it was not possible to clone *pal* into a high expression tobacco vector and concluded that the Pal protein has a toxic effect on *E. coli* at higher expression rates (3.1). Figure 6.11 shows that the production of Pal in DH5α*_pal-HA* is possible, but results in hardly detectable levels of full-length Pal and mainly truncated protein products of Pal. This suggests that Pal is rapidly degraded in *E. coli*, and might be another hint that the protein is harmful to the bacterium. This makes it conceivable that the expression elements of pLAH.AII result in protein production levels that are, in the case of certain endolysins harmful for the cloning host. However, more experiments need to be performed to further investigate this hypothesis.

One possible approach could be to perform growth experiments with DH5α*_pal-HA,* DH5α_SR*_pal-HA* and the corresponding controls to investigate whether the expression levels of Pal under the control of the *atpA* and *psaA* exon 1 promoter, even if the levels do not completely kill *E. coli*, have a negative impact on the growth of the bacterium. Alternatively, growth studies with *E. coli* carrying the pLAH.nrsB*_pal-HA* plasmid with the addition of nickel could be performed to investigate whether this

results in Pal production levels that have a negative impact on the growth of *E. coli*. Another option would be to clone the endolysin genes into an inducible high expression system tailored to *E. coli* and subsequently to analyse whether, after induction, high expression rates of any of the endolysins have adverse effects on the bacterium.

To be able to transform *Synechocystis* with *pal* under the constitutive promoter *psbAII*, an attempt could be made to transform the ligated plasmid immediately into *Synechocystis*. Alternatively, transformation of *Synechocystis* with a PCR product consisting of the *pal* gene and 50 bp at each end of homologous regions can be performed as demonstrated in the study by Al-Haj (2014). Expression of *pal* and also *gp20* under the control of the *psbAII* promoter is of interest, since it allows a longer accumulation time for the endolysins and might result in higher recombinant protein yields. Furthermore, it would enable an investigation of whether *pal* or *gp20* expression have a negative impact on *Synechocystis* without the interference of nickel.

The experiments described in this chapter showed that all three endolysins accumulate in *Synechocystis* to detectable levels. This is especially of great interest in the case of Gp20, since this endolysin was not produced to detectable levels in either the *C. reinhardtii* chloroplast or *E. coli* DH5α and has not been produced as a recombinant protein before. However, the yields of Gp20 that accumulate in *Synechocystis* are significantly lower compared to the yields of Pal and ϕ11 protein. This indicates together with the fact that the protein could not be produced in the two other expression systems that the production of Gp20 is less efficient or the protein is more susceptible to degradation in comparison to the other two endolysins.

Several strategies could be tried to increase the yield of Gp20 as well as the yields of Pal and ϕ11 during production in *Synechocystis*. One possibility would be to codon-optimise the genes for *Synechocystis*. It was discussed in 6.2.1.2 that *Synechocystis* has less preferences for certain codons compared to the *C. reinhardtii* chloroplast and that the less frequently used codons are similar in both organisms. Furthermore, the successful expression of three genes in *Synechocystis* that were originally codon-optimised for the chloroplast of the alga suggests that the codon preferences of both

organisms are not extremely different. However, preliminary results suggested that the sequence of *gp20$_1$* results in higher production levels compared to the sequence of *gp20$_2$*, which indicates that the codons used do have an effect on the protein levels. Therefore it would be worthwhile to try different codon optimisation strategies to increase the recombinant protein production levels in *Synechocystis*, for example by either using the standard codon usage table of Nakamura et al (2000) or taking into account codon pairing preferences and the codon usage of highly expressed endogenous *Synechocystis* genes. Furthermore, the secondary structure of the mRNA transcript can have an influence on the translation efficiency and should be also consider for codon optimisation strategies. A further approach could be to take the predicted secondary structure of the protein into account. The introduction of rare codons, for example in the linker region, might slow down the translation at critical points and facilitates so the correct folding of the protein.

Beside the expression of Gp20 and Pal under the control of the constitutive promoter *psbAII*, a careful study of the optimal length of induction, as well as nickel concentration and the OD_{750nm} of the culture at the induction could help to increase the endolysin levels when produced under the control of the *nrsBSR* promoter system.

Another option to further increase the endolysin yields in *Synechocystis* would be to investigate the use of different promoters and expression elements. A recent study showed that by using the P_{cpc560} promoter for the expression of foreign genes, protein levels of up to 15% of total soluble protein can be achieved in *Synechocystis* sp. PCC 6803 (Zhou et al 2014). These levels are comparable to expression levels of recombinant proteins in *E. coli.* The promoter system P_{cpc560} regulates the expression of the *cpcB* gene and consists of two predicted promoters and 14 predicted transcription factor binding sites (TFBSs) and the study showed that the presence of multiple TFBSs is important to reach these high expression levels. It is likely that the expression of the endolysin genes using the P_{cpc560} promoter system would result in significantly higher expression levels. Furthermore, these result encourage the search for more strongly expressing promoter and expression elements that would increase the recombinant protein yields that can be gained in *Synechocystis* and other cyanobacteria and help to develop them into a viable alternative expression platform

compared to established bacterial expression systems. A possible tool for this could be the RBSDesigner, a software that helps to design synthetic ribosome binding sites and to predict endogenous expression elements that result in high translation efficiency (Na & Lee 2010). The results of this study suggest that the stability of Gp20 might be lower compared to the endolysins Pal and ϕ11, which would explain the lower protein yields using the same expression elements. An attempt to decrease the degradation of Gp20 and other recombinant proteins in *Synechocystis* could be to knock out specific proteases in *Synechocystis* as it has been done for other bacterial expression systems such as the knock out of the proteases *rpoH* and *degP* in *E. coli* (Meerman & Georgiou 1994).

For the performance of activity assays, it was necessary to break the *Synechocystis* cells and recover the endolysins without denaturing the protein. It was shown in this study that Pal, ϕ11 and Gp20 can be recovered and separated from the cell debris after the cells have been broken by vortexing in the presence of glass beads. However, this method resulted in up to 50% losses of the recombinant proteins. It would be therefore worthwhile to investigate other cell breakage methods such as using a cell disrupter, a French Pressure cell press or sonication to minimize the losses of endolysin proteins. Alternatively, the cells could be broken enzymatically or in a combination of mechanical and enzymatic breakage.

However, it was possible to show that Pal and ϕ11 are produced as functional proteins in *Synechocystis* and that both have antibacterial activity against their target bacteria *S. pneumoniae* and *S. aureus*, respectively. This is especially of interest in the case of ϕ11, which did not show any detectable antibacterial activity after the production in the *C. reinhardtii* chloroplast. The results suggest that the enzymatic activity of ϕ11 produced in *Synechocystis* is comparable to *E. coli*-produced ϕ11, but more quantitative studies need to be performed with both versions of ϕ11 to finally conclude this. As a next step it would be desirable to analyse the activity of *Synechocystis*–produced ϕ11 against clinical isolates of *S. aureus* and other staphylococcal species to further characterise the endolysin produced in the cyanobacterium. Furthermore, it would be of interest to perform assays demonstrating

the bactericidal activity of the endolysin against *S. aureus* by analysing a decrease in cfu after incubation in the presence of ϕ11.

So far it has not been possible to demonstrate the antibacterial activity of Gp20 against *P. acnes*. This was mainly hampered by the low accumulation levels of Gp20 in *Synechocystis*. An increase of the production using approaches as describe above would therefore most likely enable a straightforward demonstration of the enzymatic activity of the endolysin in crude cyanobacterial extracts. Another attempt would be to purify Gp20 using either a FPLC or by developing an ion exchange column protocol. Alternatively, the sequence for a His-tag or Strep-tag could be attached to the gene and commercial available columns could be used for the purification. In this way it would be possible to separate Gp20 from the phycobilliproteins that strongly interfere with the TRA and to concentrate the protein to levels that result in detectable activity. Another experiment that should be attempted is to mix crude extract containing Gp20 with *P. acnes* cells and analyse a decrease in cfu after incubation on agar plates. However, this experiment is complicated by the fact that the growth of *P. acnes* is very slow and results only in very faint lawns with hardly visible colonies on either Columbia blood or brain heart infusion medium agar plates.

Taken together, the experiments of this chapter demonstrated that *Synechocystis* can be used as an alternative expression platform for endolysins, since the successful production of three endolysins was achieved and the enzymatic activity was demonstrated for two of them. The results suggest that *Synechocystis* offers advantages for the production of certain endolysins over the *C. reinhardtii* chloroplast, since Gp20 that could not be produced in the *C. reinhardtii* chloroplast accumulated to detectable levels and ϕ11 was synthesized in active form, whereas *C. reinhardtii*-produced ϕ11 had no detectable enzymatic activity. To investigate whether *Synechocystis* or the *C. reinhardtii* chloroplast are advantageous for the production of Pal, quantifications of the protein yields and the enzymatic activities of the endolysin produced in *Synechocystis* need to be performed. Furthermore, it needs to be investigated whether the Pal production has any harmful effect on *Synechocystis*, which could prevent the continuous cultivation of the cyanobacterium for the production of this endolysin at industrial scale.

Overall, this study demonstrated as well that *Synechocystis* sp. PCC 6803, which has been seldom considered to-date purely for the production of recombinant proteins, is a viable alternative expression platform. Especially, since it has been shown recently that with the use of other promoter systems, such as P_{cpc560}, recombinant protein yields can be reached that are comparable to yields achieved in *E. coli* (Zhou et al. 2014). An interesting aspect of photosynthetic organisms such as cyanobacteria and eukaryotic microalgae as expression platforms over heterotrophic organisms is that these organisms can produce heterogeneous proteins purely from CO_2 and inorganic nutrients using sunlight. This offers the advantage that the cultivation of these organisms can help to decrease the carbon footprint caused by other steps during the production process of recombinant proteins.

CHAPTER 7
Final discussion & future prospects

7 Final discussion & future prospects

7.1 Summary of findings

The research presented in chapter 3 demonstrated the successful production of Pal, a bacteriophage endolysin with antibacterial activity against *Streptococcus pneumoniae*, in the *C. reinhardtii* chloroplast. It was shown that predominately full-length Pal accumulates in the microalga and experiments indicated that Pal accumulates as a stable protein in the chloroplast. The stability of Pal seems to be even further increased under dark conditions. Growth studies showed that the accumulation of Pal in the chloroplast does not interfere with the cultivation of the alga indicating that the endolysin does not have any negative impact on the viability of *C. reinhardtii*. Furthermore, this suggests that Pal production in *C. reinhardtii* could be performed using continuous cultivation systems. The accumulation of Pal was analysed under the control of two different promoters/5'UTR elements and at different growth stages before the yields of Pal protein were quantified using two HA-tagged standard proteins. These analyses suggested that approximately 10 mg Pal per litre of culture volume or 13 mg Pal per gram of cell dry weight can be achieved under the control of the *psaA* exon 1 promoter/5'UTR during mixotrophic cultivation. However, these results should be verified with purified Pal as a standard.

In chapter 4 the bacteriolytic activity of Pal was demonstrated using a reference strain and five clinical isolates of *S. pneumoniae,* which belong to five different serotypes and included one strain with resistance to penicillin and co-trimoxazole. Furthermore, the results indicated that the HA-tag does not have a major impact on the enzymatic activity of Pal and further analyses suggested that the endolysin has specificity for *S. pneumoniae*. As the next step different purification methods were investigated and Pal was purified in active form using a serial process of ultracentrifugation, DEAE cellulose with choline as specific eluent and ammonium sulphate precipitation. Subsequently, purified Pal was used to analyse the bactericidal activity against *S. pneumoniae*. These analyses suggested that the enzymatic activities of Pal and a second *S. pneumoniae*-specific endolysin, Cpl-1, are comparable to the activities of

the same endolysins produced in *E. coli*. Moreover, experiments presented in chapter 4 showed that crude extracts of *C. reinhardtii* have a growth inhibiting effect against *S. pneumoniae* and *S. pyogenes*. Further analyses indicated that the effect against *S. pneumoniae* is bactericidal rather than bacteriostatic. A literature research suggested that chlorophyll derivatives or fatty acids with antibacterial properties could be responsible for this endogenous antibacterial activity.

The experiments described in chapter 5 demonstrated the detectable accumulation of ϕ11, a *Staphylococcus aureus*-specific endolysin, in the *C. reinhardtii* chloroplast. However, to-date, it has not been possible to synthesize the enzyme in the chloroplast in a form that has detectable enzymatic activity against *S. aureus*. Possible reasons for the inactivity of the protein together with strategies that could be attempted to produce enzymatically active ϕ11 in the *C. reinhardtii* chloroplast are discussed in the chapter. Furthermore, it was shown that the addition of a His-tag sequence to the genes of *pal-HA* and *ϕ11-HA* results in non-detectable protein levels, which shows that the successful accumulation of recombinant protein in *C. reinhardtii* chloroplast can be easily disrupted through such seemingly minor alterations to the protein.

The results of chapter 5 together with findings from other studies that observed that certain proteins, including two endolysins did not accumulate to detectable levels in the *C. reinhardtii* chloroplast (Rasala et al. 2010; Taunt 2013) led to the investigation of *Synechocystis* sp. PCC 6803 as an alternative endolysin production platform. The experiments described in chapter 6 demonstrated the successful production of three different endolysins in *Synechocystis*, including the *Propionibacterium acnes*-specific endolysin Gp20, which did not accumulate to detectable levels in the *C. reinhardtii* chloroplast. Growth studies showed that the accumulation of ϕ11 inside the cell does not have a marked negative impact on the viability of *Synechocystis*. In addition, it was possible to demonstrate the enzymatic activity of *Synechocystis*-produced ϕ11 against *S. aureus*.

7.2 Evaluation of microalgae as a production platform for bacteriophage endolysins

Taken together, the results of this study show that it is possible to use the *C. reinhardtii* chloroplast for the production of active Pal endolysin. Furthermore, it has been previously shown that active Cpl-1 can also be produced in the chloroplast of the microalga (Taunt 2013). Moreover, it was shown in this study that the cyanobacterium *Synechocystis* can be used for the production of active Pal and ϕ11 and that the endolysin Gp20 accumulates to detectable levels, which suggests that the success rate for the accumulation of active endolysins could be higher in the prokaryote.

However, to establish the use of *C. reinhardtii*, *Synechocystis* or another microalga as commercially viable protein production platforms for endolysins, the production in these organism needs to be either cost-efficient or offer clear advantages over conventional production platforms such as yeast and bacterial systems, transgenic plants and mammalian cell cultures.

Recombinant protein production in yeast systems results usually in the glycosylation of the produced protein, which is not desired for endolysins that are naturally produced in bacteria and do not require glycosylation (Gellissen 2000). Mammalian cell cultures are the most expensive production platform and therefore mainly used for the production of complex mammalian proteins that cannot be produced in other systems (Dove 2002). It has been shown that endolysins can be produced in the tobacco chloroplast and that the proteins accumulate to levels of up to 70% of TSP (Oey et al. 2009a). Furthermore, the study by Dove (2002) suggests that transgenic plants for the production of recombinant proteins are the most cost-efficient platform. However, one big concern regarding the use of transgenic plants is the release of transgenes into the environment during open or semi-enclosed cultivation. In contrast, microalgae can be easily cultivated in closed containment to prevent the release of transgenic algae, but also to avoid contamination of the production system and the therapeutic protein. PBRs for the cultivation of transgenic plants, such as plant cell suspension cultures and temporary immersion bioreactors have been developed as

well, but have not reach the same scale as PBRs for microalgae. In addition, for the cultivation of microalgae outdoor PBRs can be used that can be build on wasteland (such as deserts or salt land) that is not fertile enough for the cultivation of crop plants.

Many bacterial production platforms contain endotoxins, for example the bacterium *Escherichia coli*, which makes it necessary to purify therapeutic proteins and significantly contributes to the production costs (Jonasson et al. 2002). In contrast, *C. reinhardtii* and several other microalgae such as *Chlorella* species have GRAS status, which could make protein purification steps dispensable in certain cases, for example, for topical or veterinary applications. It should be noted, however, that the transgenic DNA would need to be removed or degraded.

There are several bacterial systems, such as lactic acid and coryneform bacteria that also have GRAS status (Ferrer-Miralles & Villaverde 2013). A recent study showed that in *Lactococcus lactis,* which has been used in food production for hundreds of years and has GRAS status, yields of 2.5 g recombinant protein per litre of culture volume can be reached (Jørgensen et al. 2014). This is 250 times more than what was reached for the production of Pal in the *C. reinhardtii* chloroplast (10 mg Pal per litre of culture volume). However, the nutrient requirements of microalgae are simple and inexpensive, which is believed to reduce the costs for cultivation and potentially the production costs for recombinant proteins (Gimpel et al. 2014). However, the higher recombinant protein yields and higher cell densities that can be achieved in bacterial systems might compensate higher media or cultivation costs. To analyse whether the *C. reinhardtii* chloroplast as a recombinant protein production platform is competitive in comparison to equivalent bacterial or transgenic plant systems that offer similar advantages (e.g. GRAS status or containment), an accurate costing for the production of recombinant Pal in the *C. reinhardtii* chloroplast needs to be generated. This costing should take cultivation costs, as well as harvesting and downstream processing costs into account into, and compare the overall costs of the different production systems.

Should the use of microalgae not prove cost-efficient for the production of recombinant proteins in comparison to conventional systems, their use as production platforms could be justified by other clear advantages. It was shown in chapter 4 that *C. reinhardtii* crude extracts possess antibacterial activity against *S. pneumoniae* and *S. pyogenes*. It would therefore be highly desirable to perform studies that investigate what this substance could be and whether this activity has an additive antibacterial effect in combination with Pal, since an additive or even synergistic effect would be a clear advantage for using *C. reinhardtii* for the production of the endolysin and add another argument for the use of crude algal extracts.

Furthermore, observations during this study and the study by Oey et al. (2009b) suggest that high accumulation levels of the endolysin Pal inside bacterial cells might have a negative impact on the production host. This might be an even greater problem for the production of endolysins targeting Gram-negative bacteria, since these endolysins have often a broader spectrum and are not specific to the target bacterium (Schmelcher et al. 2012). The production of high levels of these endolysins might be therefore problematic in bacterial systems and the *C. reinhardtii* chloroplast, which has a prokaryotic origin but does not contain peptidoglycan, could be of great advantage.

However, to finally conclude whether *C. reinhardtii* or other microalgae as protein production platforms are competitive or have certain advantages in comparison to conventional systems, as mentioned above a commercial evaluation of the production costs needs to be generated and further experiments need to be performed.

7.3 Future prospects

7.3.1 The *C. reinhardtii* chloroplast as a production platform for endolysins specific to Gram-negative bacteria

The treatment of infections arising from multi-drug resistant Gram-negative bacteria is a major concern. The outer membrane of Gram-negative bacteria represents a barrier that several mainstream antibiotics cannot cross and the availability of antibiotics against Gram-negative bacteria is therefore more limited. The WHO report mentions five Gram-negative and only two Gram-positive bacteria, in their list of bacteria of international concern with a high rate of antibiotic resistance (WHO report 2014). The Gram-negative bacteria listed in the report are *E. coli*, *Klebsiella pneumoniae*, *Salmonella* and *Shigella* species, and *Neisseria gonorrhoeae*.

It has been mentioned in the last section that the *C. reinhardtii* chloroplast as a production platform might be advantageous for the production of endolysins specific to Gram-negative bacteria, since these endolysins are less specific and might have toxic effects on bacterial production systems containing peptidoglycan (Schmelcher et al. 2012). It was generally believed that endolysins could not be used as a treatment against Gram-negative bacteria, since the outer membrane represents a barrier for the enzymes. However, a few studies recently have demonstrated the successful application *in vitro* of endolysins against Gram-negative bacteria (Lai et al. 2011; Lukacik et al. 2012). Table 7.1 gives a summary of such studies. Lukacik et al. (2012) choose a very interesting approach by combining an endolysin with the FyuA binding domain of pesticin, which enables the endolysin to cross the outer membrane. Such approaches could be used to engineer further endolysins that can cross the outer membrane and are effective against Gram-negative bacteria. An interesting target bacterium would be *N. gonorrhoeae*, since the bacterium has developed many multi-drug resistant strains and most diseases caused by *N. gonorrhoeae* could be treated with topical or mucosal membrane applications.

The successful production in the *C. reinhardtii* chloroplast of an endolysin targeting Gram-negative bacteria that cannot be produced in bacterial systems would demonstrate a clear advantage of the eukaryotic microalga as a production system and would therefore make an interesting further study.

Table 7.1: Studies that demonstrated the efficacy of endolysins against Gram-negative bacteria

Endolysin phage	**Target bacteria**	**Strategies**	**Reference**
SPN9CC Phage SPN9CC	*Escherichia coli, Salmonella enterica*	+/- EDTA treatment	Lim et al. (2014)
LysAB2 Phage ΦAB2	*Acinetobacter baumannii Escherichia coli Citrobacter freundii Salmonella enterica*	Study speculates that the C-terminal domain enhances membrane permeability	Lai et al. (2011)
T4 lysozyme/pesticin hybrid	*Escherichia coli Yersinia pestis*	Hybrid of T4 lysozyme and FyuA binding domain of pesticin	Lukacik et al. (2012)
EL188 Phage EL	*Pseudomonas aeruginosa*	Tested different permeabilizer: EDTA most effective	Briers et al. (2011)

7.3.2 Further endolysin research

The use of endolysins as antibacterial agents is a relatively new, but immense field. It is estimated that, in total, 10^{31} bacteriophages exists globally, so there is a huge untapped resource of endolysins that could be investigated for their potential use as antimicrobials for a wide range of applications. Additionally, several research groups have started to create designer endolyins by removing cell wall binding domains, adding additional catalytic domains, or combining of domains from different endolysins. Several of these studies reported promising effects such as enhanced lytic activity or broader host ranges for the engineered endolysins (Schmelcher et al. 2012). Furthermore, it might be possible to improve certain endolyins by random mutagenesis or by site-directed mutagenesis of key residues as was already discussed

for the choline binding sites of Pal in 4.2.4.5.1. Overall, this opens a huge research field for the development of designer endolysins that are adapted to specific clinical needs.

It was discussed in the introduction that diagnostic methods need to be further improved before narrow-spectrum antibiotics can be used on an everyday basis. One approach would therefore be to combine different endolysins specific to those bacteria that are associated with the same disease, to decrease the diagnostic requirements before the application of narrow-spectrum endolysins. The skin disease impetigo, for example, is, in most cases, caused by either *S. aureus* or *S. pyogenes*. A combinational product consisting of different endolysins against both bacteria could be used to treat impetigo without having to determine which of the two pathogens is present, or needing to verify antibiotic susceptibility before administering treatment. Furthermore, the combination of endolysins targeting different bonds of the peptidoglycan might have a synergistic effect and might decrease the risk of resistance development.

7.3.3 The use of other microalgae as recombinant protein production systems

As already mentioned in 1.4.3, microalgae species other than *C. reinhardtii* or *Synechocystis* might offer advantages for the production of certain proteins. Higher growth rates and maximal cell densities, which can be reached, for example, by *Chlorella sorokiniana*, might result in faster production or in higher recombinant protein yields per litre of medium. Furthermore, the production of endolysins in microalgae with advantageous secondary metabolites would be an option as well. For example, an endolysin targeting a major fish pathogen could be synthesised in astaxanthin-producing *H. pluvialis* cells and the alga could be used to deliver the endolysin as the same time as the astaxanthin, as it has been previously suggested for vaccines (Gutiérrez et al. 2012).

REFERENCES

References

Adam, D., 2002. Global antibiotic resistance in Streptococcus pneumoniae. *Journal of Antimicrobial Chemotherapy*, 50(suppl 1), pp.1–5.

Adam, Z., Rudella, A. & van Wijk, K.J., 2006. Recent advances in the study of Clp, FtsH and other proteases located in chloroplasts. *Current Opinion in Plant Biology*, 9(3), pp.234–240.

Almaraz-Delgado, A.L. et al., 2014. Production of therapeutic proteins in the chloroplast of Chlamydomonas reinhardtii. *AMB Express*, 4, p.57.

Amaro, H.M., Guedes, A.C. & Malcata, F.X., 2011. Antimicrobial activities of microalgae: an invited review.

Antignac, A. & Tomasz, A., 2009. Reconstruction of the Phenotypes of Methicillin-Resistant Staphylococcus aureus by Replacement of the Staphylococcal Cassette Chromosome mec with a Plasmid-Borne Copy of Staphylococcus sciuri pbpD Gene. *Antimicrobial Agents and Chemotherapy*, 53(2), pp.435–441.

Arias, C.A. & Murray, B.E., 2009. Antibiotic-Resistant Bugs in the 21st Century — A Clinical Super-Challenge. *New England Journal of Medicine*, 360(5), pp.439–443.

Avery, O.T. & Cullen, G.E., 1920. Studies on the Enzymes of Pneumococcus I. Proteolytic Enzymes. *The Journal of Experimental Medicine*, 32(5), pp.547–569.

Baba, T. & Schneewind, O., 1996. Target cell specificity of a bacteriocin molecule: a C-terminal signal directs lysostaphin to the cell wall of Staphylococcus aureus. *The EMBO Journal*, 15(18), pp.4789–4797.

Barnes, D. et al., 2005. Contribution of 5′- and 3′-untranslated regions of plastid mRNAs to the expression of Chlamydomonas reinhardtii chloroplast genes. *Molecular Genetics and Genomics*, 274(6), pp.625–636.

Bateman, J.M. & Purton, S., 2000. Tools for chloroplast transformation in Chlamydomonas: expression vectors and a new dominant selectable marker. *Molecular and General Genetics MGG*, 263(3), pp.404–410.

Becker, B., Hoef-Emden, K. & Melkonian, M., 2008. Chlamydial genes shed light on the evolution of photoautotrophic eukaryotes. *BMC Evolutionary Biology*, 8(1), p.203.

Becker, S.C. et al., 2009. Differentially conserved staphylococcal SH3b_5 cell wall binding domains confer increased staphylolytic and streptolytic activity to a streptococcal prophage endolysin domain. *Gene*, 443(1–2), pp.32–41.

Becker, S.C., Foster-Frey, J. & Donovan, D.M., 2008. The phage K lytic enzyme LysK and lysostaphin act synergistically to kill MRSA. *FEMS microbiology letters*, 287(2), pp.185–191.

Benkendorff, K. et al., 2005. Free fatty acids and sterols in the benthic spawn of aquatic molluscs, and their associated antimicrobial properties. *Journal of Experimental Marine Biology and Ecology*, 316(1), pp.29–44.

Bergsson, G., Steingrímsson, Ó. & Thormar, H., 1999. In Vitro Susceptibilities of Neisseria gonorrhoeae to Fatty Acids and Monoglycerides. *Antimicrobial Agents and Chemotherapy*, 43(11), pp.2790–2792.

De Bernardez Clark, E., 1998. Refolding of recombinant proteins. *Current Opinion in Biotechnology*, 9(2), pp.157–163.

Berry, A.M. et al., 1989. Contribution of autolysin to virulence of Streptococcus pneumoniae. *Infection and Immunity*, 57(8), pp.2324–2330.

Bertani, G., 1951. STUDIES ON LYSOGENESIS I. *Journal of Bacteriology*, 62(3), pp.293–300.

Bishop, C., 2002. *An investigation of the small polypeptides of photosystem II*. PhD thesis. London: University College London.

Blaser, M., 2011. Antibiotic overuse: Stop the killing of beneficial bacteria. *Nature*, 476(7361), pp.393–394.

Blattner, F.R. et al., 1997. The Complete Genome Sequence of Escherichia coli K-12. *Science*, 277(5331), pp.1453–1462.

Bogaert, D., de Groot, R. & Hermans, P., 2004. Streptococcus pneumoniae colonisation: the key to pneumococcal disease. *The Lancet Infectious Diseases*, 4(3), pp.144–154.

Borysowski, J., Weber-Dąbrowska, B. & Górski, A., 2006. Bacteriophage Endolysins as a Novel Class of Antibacterial Agents. *Experimental Biology and Medicine*, 231(4), pp.366–377.

Boynton, J.E. et al., 1988. Chloroplast transformation in Chlamydomonas with high velocity microprojectiles. *Science*, 240(4858), pp.1534–1538.

Braun Galleani, S., 2014. PhD thesis. London: University College London.

Briers, Y., Lavigne, R., et al., 2007. A standardized approach for accurate quantification of murein hydrolase activity in high-throughput assays. *Journal of Biochemical and Biophysical Methods*, 70(3), pp.531–533.

Briers, Y., Volckaert, G., et al., 2007. Muralytic activity and modular structure of the endolysins of Pseudomonas aeruginosa bacteriophages φKZ and EL. *Molecular Microbiology*, 65(5), pp.1334–1344.

Briers, Y., Walmagh, M. & Lavigne, R., 2011. Use of bacteriophage endolysin EL188 and outer membrane permeabilizers against Pseudomonas aeruginosa. *Journal of Applied Microbiology*, 110(3), pp.778–785.

Brown, L.E., Sprecher, S.L. & Keller, L.R., 1991. Introduction of exogenous DNA into Chlamydomonas reinhardtii by electroporation. *Molecular and Cellular Biology*, 11(4), pp.2328–2332.

Burgess, R.R. & Jendrisak, J.J., 1975. Procedure for the rapid, large-scale purification of Escherichia coli DNA-dependent RNA polymerase involving polymin P precipitation and DNA-cellulose chromatography. *Biochemistry*, 14(21), pp.4634–4638.

Cannell, R.J.P., Owsianka, A.M. & Walker, J.M., 1988. Results of a large-scale screening programme to detect antibacterial activity from freshwater algae. *British Phycological Journal*, 23(1), pp.41–44.

Castenholz, R., 1988. Culturing Methods for Cyanobacteria. In *METHODS IN ENZYMOLOGY*.

Chen & Blaser, 2007. Inverse associations of helicobacter pylori with asthma and allergy. *Archives of Internal Medicine*, 167(8), pp.821–827.

Chen, F. & Johns, M.R., 1996a. Heterotrophic growth of Chlamydomonas reinhardtii on acetate in chemostat culture. *Process Biochemistry*, 31(6), pp.601–604.

Chen, F. & Johns, M.R., 1996b. High cell density culture of Chlamydomonas reinhardtii on acetate using fed-batch and hollow-fibre cell-recycle systems. *Bioresource Technology*, 55(2), pp.103–110.

Chen, F. & Johns, M.R., 1994. Substrate inhibition of Chlamydomonas reinhardtii by acetate in heterotrophic culture. *Process Biochemistry*, 29(4), pp.245–252.

Cheng, Q. et al., 2005. Removal of group B streptococci colonizing the vagina and oropharynx of mice with a bacteriophage lytic enzyme. *Antimicrobial Agents and Chemotherapy*, 49(1), pp.111–117.

Cheng, Q. & Fischetti, V.A., 2007. Mutagenesis of a bacteriophage lytic enzyme PlyGBS significantly increases its antibacterial activity against group B streptococci. *Applied Microbiology and Biotechnology*, 74(6), pp.1284–1291.

Cheng, X. et al., 1994. The structure of bacteriophage T7 lysozyme, a zinc amidase and an inhibitor of T7 RNA polymerase. *Proceedings of the National Academy of Sciences*, 91(9), pp.4034–4038.

Chisti, Y., 2013. Constraints to commercialization of algal fuels. *Journal of Biotechnology*, 167(3), pp.201–214.

Chow, K.-C. & Tung, W.L., 1999. Electrotransformation of Chlorella vulgaris. *Plant Cell Reports*, 18(9), pp.778–780.

Cui, F. et al., 2010. Extension of nasal anti-Staphylococcus aureus efficacy of lysostaphin by its incorporation into a chitosan-o/w cream. *Drug Delivery*, 17(8), pp.617–623.

Dawson, H.N., Burlingame, R. & Cannons, A.C., 1997. Stable Transformation of Chlorella: Rescue of Nitrate Reductase-Deficient Mutants with the Nitrate Reductase Gene. *Current Microbiology*, 35(6), pp.356–362.

Debuchy, R., Purton, S. & Rochaix, J.D., 1989. The argininosuccinate lyase gene of Chlamydomonas reinhardtii: an important tool for nuclear transformation and for correlating the genetic and molecular maps of the ARG7 locus. *The EMBO journal*, 8(10), pp.2803–2809.

Desbois, A.P., Mearns-Spragg, A. & Smith, V.J., 2009. A Fatty Acid from the Diatom Phaeodactylum tricornutum is Antibacterial Against Diverse Bacteria Including Multi-resistant Staphylococcus aureus (MRSA). *Marine Biotechnology*, 11(1), pp.45–52.

Desbois, A.P. & Smith, V.J., 2010. Antibacterial free fatty acids: activities, mechanisms of action and biotechnological potential. *Applied Microbiology and Biotechnology*, 85(6), pp.1629–1642.

Dexter, J. & Fu, P., 2009. Metabolic engineering of cyanobacteria for ethanol production. *Energy & Environmental Science*, 2(8), p.857.

Díaz, E. et al., 1996. The two-step lysis system of pneumococcal bacteriophage EJ-1 is functional in Gram-negative bacteria: triggering of the major pneumococcal autolysin in Escherichia coli. *Molecular Microbiology*, 19(4), pp.667–681.

Djurkovic, S., Loeffler, J.M. & Fischetti, V.A., 2005. Synergistic killing of Streptococcus pneumoniae with the bacteriophage lytic enzyme Cpl-1 and penicillin or gentamicin depends on the level of penicillin resistance. *Antimicrobial Agents and Chemotherapy*, 49(3), pp.1225–1228.

Doetsch, N.A. et al., 2001. Chloroplast transformation in Euglena gracilis: splicing of a group III twintron transcribed from a transgenic psbK operon. *Current Genetics*, 39(1), pp.49–60.

Domenech, M., García, E. & Moscoso, M., 2011. In Vitro Destruction of Streptococcus pneumoniae Biofilms with Bacterial and Phage Peptidoglycan Hydrolases. *Antimicrobial Agents and Chemotherapy*, 55(9), pp.4144–4148.

Donlan, R.M. & Costerton, J.W., 2002. Biofilms: Survival Mechanisms of Clinically Relevant Microorganisms. *Clinical Microbiology Reviews*, 15(2), pp.167–193.

Donovan, D.M. et al., 2008. Resolving the database sequence discrepancies for the Staphylococcus aureus bacteriophage ϕ 11 amidase. *Journal of Basic Microbiology*, 48(1), pp.48–52.

Donovan, D.M., Lardeo, M. & Foster-Frey, J., 2006. Lysis of staphylococcal mastitis pathogens by bacteriophage phi11 endolysin. *FEMS Microbiology Letters*, 265(1), pp.133–139.

Dove, A., 2002. Uncorking the biomanufacturing bottleneck. *Nature Biotechnology*, 20(8), pp.777–779.

Dreesen, I.A.J., Charpin-El Hamri, G. & Fussenegger, M., 2010. Heat-stable oral alga-based vaccine protects mice from Staphylococcus aureus infection. *Journal of Biotechnology*, 145(3), pp.273–280.

Dreesen, I.A.J., Hamri, G.C.-E. & Fussenegger, M., 2010. Heat-stable oral alga-based vaccine protects mice from Staphylococcus aureus infection. *Journal of Biotechnology*, 145(3), pp.273–280.

Eady, E. ann. et al., 1989. Erythromycin resistant propionibacteria in antibiotic treated acne patients: association with therapeutic failure. *British Journal of Dermatology*, 121(1), pp.51–57.

ECDC - Surveillance report, 2012. *ECDC - Surveillance report - Antimicrobial reistance surveillance in Europe*, The European Centre for Disease Prevention and Control (ECDC).

Economou, C. et al., 2014. A Simple, Low-Cost Method for Chloroplast Transformation of the Green Alga Chlamydomonas reinhardtii. In P. Maliga, ed. *Chloroplast Biotechnology*. Methods in Molecular Biology. Humana Press, pp. 401–411. Available at: http://link.springer.com/protocol/10.1007/978-1-62703-995-6_27 [Accessed August 11, 2014].

Elbreki, M. et al., 2014. Bacteriophages and Their Derivatives as Biotherapeutic Agents in Disease Prevention and Treatment. *Journal of Viruses*, 2014, p.e382539.

Entenza, J.M. et al., 2005. Therapeutic effects of bacteriophage Cpl-1 lysin against Streptococcus pneumoniae endocarditis in rats. *Antimicrobial Agents and Chemotherapy*, 49(11), pp.4789–4792.

Erskine, R.J. et al., 2002. Trends in Antibacterial Susceptibility of Mastitis Pathogens During a Seven-Year Period. *Journal of Dairy Science*, 85(5), pp.1111–1118.

Falch, B.S. et al., 1993. Ambigol A and B: new biologically active polychlorinated aromatic compounds from the terrestrial blue-green alga Fischerella ambigua. *The Journal of Organic Chemistry*, 58(24), pp.6570–6575.

Farrar, M.D. et al., 2007. Genome Sequence and Analysis of a Propionibacterium acnes Bacteriophage. *Journal of Bacteriology*, 189(11), pp.4161–4167.

Farrar, M.D. & Ingham, E., 2004. Acne: Inflammation. *Clinics in Dermatology*, 22(5), pp.380–384.

Fauci, A.S., 2001. Infectious Diseases: Considerations for the 21st Century. *Clinical Infectious Diseases*, 32(5), pp.675–685.

Feldlaufer, M.F. et al., 1993. Antimicrobial activity of fatty acids against Bacillus larvae, the causative agent of American foulbrood disease.

Fenton, M. et al., 2010. Recombinant bacteriophage lysins as antibacterials. *Bioengineered Bugs*, 1(1), pp.9–16.

Ferrer-Miralles, N. & Villaverde, A., 2013. Bacterial cell factories for recombinant protein production; expanding the catalogue. *Microbial Cell Factories*, 12, p.113.

Fischetti, V., 2008. Bacteriophage lysins as effective antibacterials. *Current Opinion in Microbiology*, 11(5), pp.393–400.

Fischetti, V.A., 2005. Bacteriophage lytic enzymes: novel anti-infectives. *Trends in Microbiology*, 13, pp.491–496.

Fowler, V.G. & Proctor, R.A., 2014. Where does a Staphylococcus aureus vaccine stand? *Clinical Microbiology and Infection*, 20, pp.66–75.

Franklin, S. et al., 2002. Development of a GFP reporter gene for Chlamydomonas reinhardtii chloroplast. *The Plant Journal*, 30(6), pp.733–744.

Franklin, S.E. & Mayfield, S.P., 2004. Prospects for molecular farming in the green alga Chlamydomonas. *Current Opinion in Plant Biology*, 7(2), pp.159–165.

Fuhrmann, M., Oertel, W. & Hegemann, P., 1999. A synthetic gene coding for the green fluorescent protein (GFP) is a versatile reporter in Chlamydomonas reinhardtii†. *The Plant Journal*, 19(3), pp.353–361.

Galbraith, H. et al., 1971. Antibacterial Activity of Long Chain Fatty Acids and the Reversal with Calcium, Magnesium, Ergocalciferol and Cholesterol. *Journal of Applied Bacteriology*, 34(4), pp.803–813.

García-Domínguez, M. et al., 2000. A Gene Cluster Involved in Metal Homeostasis in the Cyanobacterium Synechocystis sp. Strain PCC 6803. *Journal of Bacteriology*, 182(6), pp.1507–1514.

Garcia, P., Garcia, E., et al., 1983. A Phage-associated Murein Hydrolase in Streptococcus pneumoniae Infected with Bacteriophage Dp-1. *Journal of General Microbiology*, 129(2), pp.489–497.

Garcia, P., Lopez, R., et al., 1983. Mechanism Of Phage-Induced Lysis In Pneumococci. *Journal of General Microbiology*, 129(2), pp.479–487.

García, P., 1990. Modular organization of the lytic enzymes of Streptococcus pneumoniae and its bacteriophages. *Gene*, 86(1), pp.81–88.

Gellissen, G., 2000. Heterologous protein production in methylotrophic yeasts. *Applied Microbiology and Biotechnology*, 54(6), pp.741–750.

Geng, D. et al., 2003. Stable expression of hepatitis B surface antigen gene in Dunaliella salina (Chlorophyta). *Journal of Applied Phycology*, 15(6), pp.451–456.

Ghasemi, Y. et al., 2007. Antifungal and Antibacterial Activity of the Microalgae Collected from Paddy Fields of Iran: Characterization of Antimicrobial Activity of Chroococcus dispersus. Available at: http://agris.fao.org/agris-search/search.do?recordID=AV20120133973 [Accessed July 30, 2014].

Gimpel, J.A. et al., 2014. Production of recombinant proteins in microalgae at pilot greenhouse scale. *Biotechnology and Bioengineering*, p.n/a–n/a.

Giroud, C., Gerber, A. & Eichenberger, W., 1988. Lipids of Chlamydomonas reinhardtii. Analysis of Molecular Species and Intracellular Site(s) of Biosynthesis. *Plant and Cell Physiology*, 29(4), pp.587–595.

Grandgirard, D. et al., 2008. Phage lytic enzyme Cpl-1 for antibacterial therapy in experimental pneumococcal meningitis. *The Journal of Infectious Diseases*, 197(11), pp.1519–1522.

Gregory, J.A. et al., 2012. Algae-Produced Pfs25 Elicits Antibodies That Inhibit Malaria Transmission L. Hviid, ed. *PLoS ONE*, 7(5), p.e37179.

Gregory, J.A. et al., 2013. Alga-produced cholera toxin-Pfs25 fusion proteins as oral vaccines. *Applied and Environmental Microbiology*, 79(13), pp.3917–3925.

Guerrero, F. et al., 2012. Ethylene Synthesis and Regulated Expression of Recombinant Protein in Synechocystis sp. PCC 6803. *PLoS ONE*, 7(11), p.e50470.

Gutiérrez, C.L. et al., 2012. Chloroplast Genetic Tool for the Green Microalgae Haematococcus Pluvialis (chlorophyceae, Volvocales)1. *Journal of Phycology*, 48(4), pp.976–983.

Gutmann, D.A.P. et al., 2007. A high-throughput method for membrane protein solubility screening: The ultracentrifugation dispersity sedimentation assay. *Protein Science : A Publication of the Protein Society*, 16(7), pp.1422–1428.

Al-Haj, L.A., 2014. *Development of genetic engineering tools for the cyanobacterium Synechocystis PCC 6803 for advanced biofuel production*. PhD thesis. London: University College London.

Hanahan, D., 1983. Studies on transformation of Escherichia coli with plasmids. *Journal of Molecular Biology*, 166(4), pp.557–580.

Harris, E.H., 1989. *The Chlamydomonas Sourcebook*, San Diego: Academic Press.

Harris, E.H., 2009. *The Chlamydomonas Sourcebook - Volume 1 - Introduction to Chlamydomonas and Its Laboratory Use* Second Edition., Elsevier.

He, D.-M., Qian, K.-X., Shen, G.-F., Zhang, Z.-F., Li, Y.-N., et al., 2007. Recombination and expression of classical swine fever virus (CSFV) structural protein E2 gene in Chlamydomonas reinhardtii chroloplasts. *Colloids and Surfaces B-Biointerfaces*, 55(1), pp.26–30.

He, D.-M., Qian, K.-X., Shen, G.-F., Zhang, Z.-F., LI, Y.-N., et al., 2007. Recombination and expression of classical swine fever virus (CSFV) structural protein E2 gene in Chlamydomonas reinhardtii chroloplasts. *Colloids and Surfaces B: Biointerfaces*, 55(1), pp.26–30.

Hermoso, J.A. et al., 2003. Structural Basis for Selective Recognition of Pneumococcal Cell Wall by Modular Endolysin from Phage Cp-1. *Structure*, 11(10), pp.1239–1249.

Hoobert, J.K. & Blobel, G., 1969. Characterization of the chloroplastic and cytoplasmic ribosomes of Chlamydomonas reinhardi. *Journal of Molecular Biology*, 41(1), pp.121–138.

Huang, H.-H. et al., 2010. Design and characterization of molecular tools for a synthetic biology approach towards developing cyanobacterial biotechnology. *Nucleic acids research*, p.gkq164.

Huang, J. & Gogarten, J.P., 2007. Did an ancient chlamydial endosymbiosis facilitate the establishment of primary plastids? *Genome Biology*, 8(6), p.R99.

Hudson, I.R., 1994. The efficacy of intranasal mupirocin in the prevention of staphylococcal infections: a review of recent experience. *The Journal of Hospital Infection*, 27(2), pp.81–98.

Iandolo, J.J. et al., 2002. Comparative analysis of the genomes of the temperate bacteriophages φ11, φ12 and φ13 of Staphylococcus aureus 8325. *Gene*, 289(1–2), pp.109–118.

Ikeuchi, M. & Tabata, S., 2001. Synechocystis sp. PCC 6803 — a useful tool in the study of the genetics of cyanobacteria. *Photosynthesis Research*, 70(1), pp.73–83.

Infectious Diseases Society of America (IDSA), 2011. Combating Antimicrobial Resistance: Policy Recommendations to Save Lives. *Clinical Infectious Diseases*, 52(Supplement 5), pp.S397–S428.

Ishida, K. et al., 1997. Kawaguchipeptin B, an Antibacterial Cyclic Undecapeptide from the Cyanobacterium Microcystis aeruginosa. *Journal of Natural Products*, 60(7), pp.724–726.

Jado, I. et al., 2003. Phage lytic enzymes as therapy for antibiotic-resistant Streptococcus pneumoniae infection in a murine sepsis model. *Journal of Antimicrobial Chemotherapy*, 52(6), pp.967–973.

Jonasson, P. et al., 2002. Genetic design for facilitated production and recovery of recombinant proteins in Escherichia coli. *Biotechnology and Applied Biochemistry*, 35(2), pp.91–105.

Jørgensen, C.M., Vrang, A. & Madsen, S.M., 2014. Recombinant protein expression in Lactococcus lactis using the P170 expression system. *FEMS Microbiology Letters*, 351(2), pp.170–178.

Jørgensen, E.G., 1962. Antibiotic Substances from Cells and Culture Solutions of Unicellular Algae with Special Reference to some Chlorophyll Derivatives. *Physiologia Plantarum*, 15(3), pp.530–545.

Kabara, J.J. et al., 1972. Fatty Acids and Derivatives as Antimicrobial Agents. *Antimicrobial Agents and Chemotherapy*, 2(1), pp.23–28.

Kakikawa, M. et al., 2002. Molecular analysis of the lysis protein Lys encoded by Lactobacillus plantarum phage ϕg1e. *Gene*, 299(1–2), pp.227–234.

Kaneko, T. et al., 1996. Sequence Analysis of the Genome of the Unicellular Cyanobacterium Synechocystis sp. Strain PCC6803. II. Sequence Determination of the Entire Genome and Assignment of Potential Protein-coding Regions. *DNA Research*, 3(3), pp.109–136.

Kellam, S.J. & Walker, J.M., 1989. Antibacterial activity from marine microalgae in laboratory culture. *British Phycological Journal*, 24(2), pp.191–194.

Kindle, K.L., 1990. High-frequency nuclear transformation of Chlamydomonas reinhardtii. *Proceedings of the National Academy of Sciences of the United States of America*, 87(3), pp.1228–1232.

Koksharova, O.A. & Wolk, C.P., 2002. Genetic tools for cyanobacteria. *Applied Microbiology and Biotechnology*, 58(2), pp.123–137.

Korndörfer, I.P. et al., 2006. The Crystal Structure of the Bacteriophage PSA Endolysin Reveals a Unique Fold Responsible for Specific Recognition of Listeria Cell Walls. *Journal of Molecular Biology*, 364(4), pp.678–689.

Kumar, S.V. et al., 2004. Genetic transformation of the green alga—Chlamydomonas reinhardtii by Agrobacterium tumefaciens. *Plant Science*, 166(3), pp.731–738.

Laemmli, U.K., 1970. Cleavage of Structural Proteins during the Assembly of the Head of Bacteriophage T4. *Nature*, 227(5259), pp.680–685.

Lai, M.-J. et al., 2011. Antibacterial activity of Acinetobacter baumannii phage ϕAB2 endolysin (LysAB2) against both Gram-positive and Gram-negative bacteria. *Applied Microbiology and Biotechnology*, 90(2), pp.529–539.

Lan, E.I. & Liao, J.C., 2011. Metabolic engineering of cyanobacteria for 1-butanol production from carbon dioxide. *Metabolic Engineering*, 13(4), pp.353–363.

Lapidot, M. et al., 2002. Stable Chloroplast Transformation of the Unicellular Red AlgaPorphyridium Species. *Plant Physiology*, 129(1), pp.7–12.

Leu, S. et al., 1992. Complete DNA sequence of the Chlamydomonas reinhardtii chloroplast atpA gene. *Plant Molecular Biology*, 18(3), pp.613–616.

Levy & Marshall, B., 2004. Antibacterial resistance worldwide: causes, challenges and responses. *Nature Medicine*, 10, pp.S122–S129.

Levy, S.B., 2005. Antibiotic resistance—the problem intensifies. *Advanced Drug Delivery Reviews*, 57(10), pp.1446–1450.

Levy, S.B., 2002. *The Antibiotic Paradox: How the Misuse of Antibiotics Destroys Their Curative Powers*, Da Capo Press.

Liberton, M. et al., 2006. Ultrastructure of the membrane systems in the unicellular cyanobacterium Synechocystis sp. strain PCC 6803. *Protoplasma*, 227(2-4), pp.129–138.

Lilie, H., Schwarz, E. & Rudolph, R., 1998. Advances in refolding of proteins produced in E. coli. *Current Opinion in Biotechnology*, 9(5), pp.497–501.

Lim, J.-A. et al., 2014. Exogenous lytic activity of SPN9CC endolysin against gram-negative bacteria. , 24(6), pp.803–811.

Liu, S. et al., 2007. Effect of growth hormone transgenic Synechocystis on growth, feed efficiency, muscle composition, haematology and histology of turbot (Scophthalmus maximus L.). *Aquaculture Research*, 38(12), pp.1283–1292.

Loeffler, J.M., Djurkovic, S. & Fischetti, V.A., 2003. Phage lytic enzyme Cpl-1 as a novel antimicrobial for pneumococcal bacteremia. *Infection and Immunity*, 71(11), pp.6199–6204.

Loeffler, J.M. & Fischetti, V.A., 2003. Synergistic Lethal Effect of a Combination of Phage Lytic Enzymes with Different Activities on Penicillin-Sensitive and -Resistant Streptococcus pneumoniae Strains. *Antimicrobial Agents and Chemotherapy*, 47(1), pp.375–377.

Loeffler, J.M., Nelson, D. & Fischetti, V.A., 2001. Rapid Killing of Streptococcus pneumoniae with a Bacteriophage Cell Wall Hydrolase. *Science*, 294(5549), pp.2170–2172.

Loessner, M., 2005. Bacteriophage endolysins — current state of research and applications. *Current Opinion in Microbiology*, 8(4), pp.480–487.

Loessner, M.J., Wendlinger, G. & Scherer, S., 1995. Heterogeneous endolysins in Listeria monocytogenes bacteriophages: a new class of enzymes and evidence for conserved holin genes within the siphoviral lysis cassettes. *Molecular Microbiology*, 16(6), pp.1231–1241.

Lohman, T.M., Green, J.M. & Beyer, R.S., 1986. Large-scale overproduction and rapid purification of the Escherichia coli ssb gene product. Expression of the ssb gene under .lambda. PL control. *Biochemistry*, 25(1), pp.21–25.

Lood, R. & Collin, M., 2011. Characterization and genome sequencing of two Propionibacterium acnes phages displaying pseudolysogeny. *BMC Genomics*, 12(1), p.198.

Lopez-Maury, L. et al., 2002. A two-component signal transduction system involved in nickel sensing in the cyanobacterium Synechocystis sp. PCC 6803. *Molecular Microbiology*, 43(1), pp.247–256.

López, R. et al., 1977. Properties of "diplophage": a lipid-containing bacteriophage. *Journal of Virology*, 24(1), pp.201–210.

López, R. et al., 1992. Structural analysis and biological significance of the cell wall lytic enzymes of Streptococcus pneumoniae and its bacteriophage. *FEMS Microbiology Letters*, 100(1–3), pp.439–447.

López, R. et al., 1997. The Pneumococcal Cell Wall Degrading Enzymes: A Modular Design to Create New Lysins? *Microbial Drug Resistance*, 3(2), pp.199–211.

López, R., García, E. & García, P., 2004. Enzymes for anti-infective therapy: phage lysins. *Drug Discovery Today: Therapeutic Strategies*, 1(4), pp.469–474.

Lorian, V., 2005. *Antibiotics in Laboratory Medicine*, Lippincott Williams & Wilkins.

Low, L.Y. et al., 2011. Role of Net Charge on Catalytic Domain and Influence of Cell Wall Binding Domain on Bactericidal Activity, Specificity, and Host Range of Phage Lysins. *Journal of Biological Chemistry*, 286(39), pp.34391–34403.

Low, L.Y. et al., 2005. Structure and Lytic Activity of a Bacillus anthracis Prophage Endolysin. *Journal of Biological Chemistry*, 280(42), pp.35433–35439.

Lukacik, P. et al., 2012. Structural engineering of a phage lysin that targets Gram-negative pathogens. *Proceedings of the National Academy of Sciences*, 109(25), pp.9857–9862.

Mackrow, B., 2012. *Employing a Synthetic Biology "Parts-Based" approach to Algal Biotechnology*. MSc thesis. University College London.

Madigan, M., 2009. *Brock biology of microorganisms* 12th ed., San Francisco CA: Pearson/Benjamin Cummings.

Malasarn, D. et al., 2013. Zinc deficiency impacts CO2 assimilation and disrupts copper homeostasis in Chlamydomonas reinhardtii. *The Journal of Biological Chemistry*, 288(15), pp.10672–10683.

Manuell, A.L. et al., 2007. Robust expression of a bioactive mammalian protein in Chlamydomonas chloroplast. *Plant Biotechnology Journal*, 5(3), pp.402–412.

Manuell, A.L. et al., 2007. Robust expression of a bioactive mammalian protein in Chlamydomonas chloroplast. *Plant Biotechnology Journal*, 5(3), pp.402–412.

Marinelli, L.J. et al., 2012. Propionibacterium acnes Bacteriophages Display Limited Genetic Diversity and Broad Killing Activity against Bacterial Skin Isolates. *mBio*, 3(5), pp.e00279–12.

Martins, R.F. et al., 2008. Antimicrobial and Cytotoxic Assessment of Marine Cyanobacteria - Synechocystis and Synechococcus. *Marine Drugs*, 6(1), pp.1–11.

Maul, J.E. et al., 2002. The Chlamydomonas reinhardtii Plastid Chromosome Islands of Genes in a Sea of Repeats. *The Plant Cell Online*, 14(11), pp.2659–2679.

Mayfield, S.P., 2003. Expression and assembly of a fully active antibody in algae. *Proceedings of the National Academy of Sciences*, 100(2), pp.438–442.

Mayfield, S.P., Franklin, S.E. & Lerner, R.A., 2003. Expression and assembly of a fully active antibody in algae. *Proceedings of the National Academy of Sciences*, 100(2), pp.438–442.

Mazel, D., 2006. Integrons: agents of bacterial evolution. *Nature Reviews Microbiology*, 4(8), pp.608–620.

McCullers, J.A. et al., 2007. Novel strategy to prevent otitis media caused by colonizing Streptococcus pneumoniae. *PLoS pathogens*, 3(3), p.e28.

Meerman, H.J. & Georgiou, G., 1994. Construction and Characterization of a Set of E. coli Strains Deficient in All Known Loci Affecting the Proteolytic Stability of Secreted Recombinant Proteins. *Nature Biotechnology*, 12(11), pp.1107–1110.

Mellroth, P. et al., 2012. LytA, Major Autolysin of Streptococcus pneumoniae, Requires Access to Nascent Peptidoglycan. *Journal of Biological Chemistry*, 287(14), pp.11018–11029.

Merchant, S.S. et al., 2007. The Chlamydomonas genome reveals the evolution of key animal and plant functions. *Science (New York, N.Y.)*, 318(5848), pp.245–250.

Michelet, L. et al., 2011. Enhanced chloroplast transgene expression in a nuclear mutant of Chlamydomonas. *Plant Biotechnology Journal*, 9(5), pp.565–574.

Michoux, F. et al., 2011. Contained and high-level production of recombinant protein in plant chloroplasts using a temporary immersion bioreactor. *Plant Biotechnology Journal*, 9(5), pp.575–584.

Mullis, K. et al., 1992. Specific enzymatic amplification of DNA in vitro: the polymerase chain reaction. 1986. *Biotechnology (Reading, Mass.)*, 24, pp.17–27.

Nakamura, Y., Gojobori, T. & Ikemura, T., 2000. Codon usage tabulated from international DNA sequence databases: status for the year 2000. *Nucleic Acids Research*, 28(1), pp.292–292.

Navarre, W.W. et al., 1999. Multiple Enzymatic Activities of the Murein Hydrolase from Staphylococcal Phage phi 11. IDENTIFICATION OF A D-ALANYL-GLYCINE ENDOPEPTIDASE ACTIVITY. *Journal of Biological Chemistry*, 274(22), pp.15847–15856.

Navarro Llorens, J.M., Tormo, A. & Martínez-García, E., 2010. Stationary phase in gram-negative bacteria. *FEMS Microbiology Reviews*, 34(4), pp.476–495.

Nelson, D. et al., 2006. PlyC: A multimeric bacteriophage lysin. *Proceedings of the National Academy of Sciences*, 103(28), pp.10765–10770.

Nelson, D., Loomis, L. & Fischetti, V.A., 2001. Prevention and elimination of upper respiratory colonization of mice by group A streptococci by using a bacteriophage lytic enzyme. *Proceedings of the National Academy of Sciences of the United States of America*, 98(7), pp.4107–4112.

Neufeld, D.F., 1900. Ueber eine specifische bakteriolytische Wirkung der Galle. *Zeitschrift für Hygiene und Infektionskrankheiten*, 34(1), pp.454–464.

Nikaido, H., 1996. Multidrug efflux pumps of gram-negative bacteria. *Journal of Bacteriology*, 178(20), pp.5853–5859.

Ninlayarn, T., 2012. *Chloroplast genetic engineering in the microalga Chlamydomonas reinhardtii: Molecular tools and applications*. PhD thesis. London: Department of Structural & Molecular Biology, University College London.

O'Brien, K.L. et al., 2009. Burden of disease caused by Streptococcus pneumoniae in children younger than 5 years: global estimates. *The Lancet*, 374(9693), pp.893–902.

O'Brien, K.L. et al., 2001. Evaluation of a Medium (STGG) for Transport and Optimal Recovery of Streptococcus pneumoniae from Nasopharyngeal Secretions Collected during Field Studies. *Journal of Clinical Microbiology*, 39(3), pp.1021–1024.

Oey, M., Lohse, M., Kreikemeyer, B., et al., 2009. Exhaustion of the chloroplast protein synthesis capacity by massive expression of a highly stable protein antibiotic. *The Plant Journal*, 57(3), pp.436–445.

Oey, M., Lohse, M., Scharff, L.B., et al., 2009. Plastid production of protein antibiotics against pneumonia via a new strategy for high-level expression of antimicrobial proteins. *Proceedings of the National Academy of Sciences*, 106(16), pp.6579–6584.

O'Flaherty, S. et al., 2005. The Recombinant Phage Lysin LysK Has a Broad Spectrum of Lytic Activity against Clinically Relevant Staphylococci, Including Methicillin-Resistant Staphylococcus aureus. *Journal of Bacteriology*, 187(20), pp.7161–7164.

O'Flaherty, S., Ross, R.P. & Coffey, A., 2009. Bacteriophage and their lysins for elimination of infectious bacteria. *FEMS Microbiology Reviews*, 33(4), pp.801–819.

Ohta, S. et al., 1994. Anti methicillin-resistant Staphylococcus aureus (MRSA) activity by linolenic acid isolated from the marine microalga Chlorococcum HS-101. *Bulletin of Environmental Contamination and Toxicology*, 52(5), pp.673–680.

Parker, M.S., Mock, T. & Armbrust, E.V., 2008. Genomic insights into marine microalgae. *Annual Review of Genetics*, 42, pp.619–645.

Park, I.H. et al., 2007. Discovery of a New Capsular Serotype (6C) within Serogroup 6 of Streptococcus pneumoniae. *Journal of Clinical Microbiology*, 45(4), pp.1225–1233.

Payne, D.J. et al., 2007. Drugs for bad bugs: confronting the challenges of antibacterial discovery. *Nature Reviews. Drug Discovery*, 6(1), pp.29–40.

Peca, L. et al., 2008. Construction of bioluminescent cyanobacterial reporter strains for detection of nickel, cobalt and zinc. *FEMS Microbiology Letters*, 289(2), pp.258–264.

Potvin, G. & Zhang, Z., 2010. Strategies for high-level recombinant protein expression in transgenic microalgae: A review. *Biotechnology Advances*, 28(6), pp.910–918.

Preiss, S., Schrader, S. & Johanningmeier, U., 2001. Rapid, ATP-dependent degradation of a truncated D1 protein in the chloroplast. *European Journal of Biochemistry*, 268(16), pp.4562–4569.

Pritchard, D.G. et al., 2007. LambdaSa1 and LambdaSa2 Prophage Lysins of Streptococcus agalactiae. *Applied and Environmental Microbiology*, 73(22), pp.7150–7154.

Pritchard, D.G. et al., 2004. The bifunctional peptidoglycan lysin of Streptococcus agalactiae bacteriophage B30. *Microbiology*, 150(7), pp.2079–2087.

Purton, S. et al., 2013. Genetic engineering of algal chloroplasts: Progress and prospects. *Russian Journal of Plant Physiology*, 60(4), pp.491–499.

Randolph-Anderson, B.L. et al., 1993. Further characterization of the respiratory deficient dum-1 mutation of Chlamydomonas reinhardtii and its use as a recipient for mitochondrial transformation. *Molecular & general genetics: MGG*, 236(2-3), pp.235–244.

Rasala, B. et al., 2010. Production of therapeutic proteins in algae, analysis of expression of seven human proteins in the chloroplast of Chlamydomonas reinhardtii. *Plant Biotechnology Journal*, 8(6), pp.719–733.

Rasala, B.A. et al., 2011. Improved heterologous protein expression in the chloroplast of Chlamydomonas reinhardtii through promoter and 5′ untranslated region optimization. *Plant Biotechnology Journal*, 9(6), pp.674–683.

Rasala, B.A. et al., 2010. Production of therapeutic proteins in algae, analysis of expression of seven human proteins in the chloroplast of Chlamydomonas reinhardtii. *Plant biotechnology journal*, 8(6), pp.719–733.

Rasala, B.A. & Mayfield, S.P., 2011. The microalga *Chlamydomonas reinhardtii* as a platform for the production of human protein therapeutics. *Bioengineered Bugs*, 2(1), pp.50–54.

Rashel, M. et al., 2007. Efficient elimination of multidrug-resistant Staphylococcus aureus by cloned lysin derived from bacteriophage phi MR11. *The Journal of Infectious Diseases*, 196(8), pp.1237–1247.

Rehm, H., 2006. *Der Experimentator: Proteinbiochemie/Proteomics* 5th ed., Munich: Elsevier GmbH.

Resch, G., Moreillon, P. & Fischetti, V.A., 2011. A stable phage lysin (Cpl-1) dimer with increased antipneumococcal activity and decreased plasma clearance. *International Journal of Antimicrobial Agents*, 38(6), pp.516–521.

Rochaix, J., 1995. Chlamydomonas Reinhardtii As the Photosynthetic Yeast. *Annual Review of Genetics*, 29(1), pp.209–230.

Rodríguez-Cerrato, V. et al., 2007. In vitro interactions of LytA, the major pneumococcal autolysin, with two bacteriophage lytic enzymes (Cpl-1 and Pal), cefotaxime and moxifloxacin against antibiotic-susceptible and -resistant Streptococcus pneumoniae strains. *Journal of Antimicrobial Chemotherapy*, 60(5), pp.1159–1162.

Sager, R. & Granick, S., 1953. Nutritional Studies with Chlamydomonas Reinhardi. *Annals of the New York Academy of Sciences*, 56(5), pp.831–838.

Sanchez-Puelles, J.M. et al., 1992. Immobilization and single-step purification of fusion proteins using DEAE-cellulose. *European Journal of Biochemistry / FEBS*, 203(1-2), pp.153–159.

Santoyo, S. et al., 2009. Green processes based on the extraction with pressurized fluids to obtain potent antimicrobials from Haematococcus pluvialis microalgae. *LWT - Food Science and Technology*, 42(7), pp.1213–1218.

Sanz, J.M., Díaz, E. & García, J.L., 1992. Studies on the structure and function of the N-terminal domain of the pneumococcal murein hydrolases. *Molecular Microbiology*, 6(7), pp.921–931.

Sanz, J.M., Lopez, R. & Garcia, J.L., 1988. Structural requirements of choline derivatives for "conversion" of pneumococcal amidase A new single-step procedure for purification of this autolysin. *FEBS Letters*, 232(2), pp.308–312.

São-José, C. et al., 2000. The N-Terminal Region of the Oenococcus oeniBacteriophage fOg44 Lysin Behaves as a Bona Fide Signal Peptide inEscherichia coli and as a cis-Inhibitory Element, Preventing Lytic Activity on Oenococcal Cells. *Journal of Bacteriology*, 182(20), pp.5823–5831.

Sass, P. & Bierbaum, G., 2006. Lytic Activity of Recombinant Bacteriophage 11 and 12 Endolysins on Whole Cells and Biofilms of Staphylococcus aureus. *Applied and Environmental Microbiology*, 73(1), pp.347–352.

Scheer, H., 2012. Chlorophyll breakdown in aquatic ecosystems. *Proceedings of the National Academy of Sciences*, 109(43), pp.17311–17312.

Schindler, C.A. & Schuhardt, V.T., 1964. LYSOSTAPHIN: A NEW BACTERIOLYTIC AGENT FOR THE STAPHYLOCOCCUS. *Proceedings of the National Academy of Sciences of the United States of America*, 51(3), pp.414–421.

Schmelcher, M., Donovan, D.M. & Loessner, M.J., 2012. Bacteriophage endolysins as novel antimicrobials. *Future Microbiology*, 7(10), pp.1147–1171.

Schmelcher, M., Waldherr, F. & Loessner, M.J., 2011. Listeria bacteriophage peptidoglycan hydrolases feature high thermoresistance and reveal increased activity after divalent metal cation substitution. *Applied Microbiology and Biotechnology*. Available at: http://www.springerlink.com/index/10.1007/s00253-011-3372-6 [Accessed November 17, 2011].

Schuch, R., Nelson, D. & Fischetti, V.A., 2002. A bacteriolytic agent that detects and kills Bacillus anthracis. *Nature*, 418(6900), pp.884–889.

Sheehan, M.M. et al., 1997. The lytic enzyme of the pneumococcal phage Dp-1: a chimeric lysin of intergeneric origin. *Molecular Microbiology*, 25(04), pp.717–725.

Shih, Y.-P. et al., 2002. High-throughput screening of soluble recombinant proteins. *Protein Science : A Publication of the Protein Society*, 11(7), pp.1714–1719.

Silver, L.L., 2011. Challenges of Antibacterial Discovery. *Clinical Microbiology Reviews*, 24(1), pp.71–109.

Smith, L.W., 1955. The Present Status of Topical Chlorophyll Therapy.

Smith, V.J., Desbois, A.P. & Dyrynda, E.A., 2010. Conventional and Unconventional Antimicrobials from Fish, Marine Invertebrates and Micro-algae. *Marine Drugs*, 8(4), pp.1213–1262.

Specht, E., Miyake-Stoner, S. & Mayfield, S., 2010. Micro-algae come of age as a platform for recombinant protein production. *Biotechnology Letters*, 32(10), pp.1373–1383.

Spellberg, B. et al., 2008. The Epidemic of Antibiotic-Resistant Infections: A Call to Action for the Medical Community from the Infectious Diseases Society of America. *Clinical Infectious Diseases*, 46(2), pp.155–164.

Sun, M. et al., 2003. Foot-and-mouth disease virus VP1 protein fused with cholera toxin B subunit expressed in Chlamydomonas reinhardtii chloroplast. *Biotechnology Letters*, 25(13), pp.1087–1092.

Surzycki et al., 2009. Factors effecting expression of vaccines in microalgae. *Biologicals*, 37(3), pp.133–138.

Szaub, J., 2012. *Genetic Engineering of Green Microalgae for the Production of Biofuel and High Value Products*. PhD thesis. London: University College London.

Taunt, H.N., 2013. *The Synthesis of Novel Antibacterial Proteins in the Chlamydomonas reinhardtii Chloroplast*. PhD thesis. London: University College London.

Teresa, M., Petersen, S. & Prakash, G., 2012. UV Light Effects on Proteins: From Photochemistry to Nanomedicine. In S. Saha, ed. *Molecular Photochemistry - Various Aspects*. InTech. Available at: http://www.intechopen.com/books/molecular-photochemistry-various-aspects/uv-light-effects-on-proteins-from-photochemistry-to-nanomedicine [Accessed March 12, 2015].

Terpe, K., 2003. Overview of tag protein fusions: from molecular and biochemical fundamentals to commercial systems. *Applied Microbiology and Biotechnology*, 60(5), pp.523–533.

Thomson, T.M. et al., 2011. Scaffold number in yeast signaling system sets tradeoff between system output and dynamic range. *Proceedings of the National Academy of Sciences*, 108(50), pp.20265–20270.

Tran, M. et al., 2013. Production of unique immunotoxin cancer therapeutics in algal chloroplasts. *Proceedings of the National Academy of Sciences*, 110(1), pp.E15–E22.

Vahrenholz, C. et al., 1993. Mitochondrial DNA of Chlamydomonas reinhardtii: the structure of the ends of the linear 15.8-kb genome suggests mechanisms for DNA replication. *Current Genetics*, 24(3), pp.241–247.

Varea, J. et al., 2004. Structural and Thermodynamic Characterization of Pal, a Phage Natural Chimeric Lysin Active against Pneumococci. *Journal of Biological Chemistry*, 279(42), pp.43697–43707.

Vermaas, W., 1996. Molecular genetics of the cyanobacteriumSynechocystis sp. PCC 6803: Principles and possible biotechnology applications. *Journal of Applied Phycology*, 8(4-5), pp.263–273.

Vermaas, W.F.J., 1998. [20] Gene modifications and mutation mapping to study the function of photosystem II. In Lee McIntosh, ed. *Methods in Enzymology*. Photosynthesis: Molecular Biology of Energy Capture. Academic Press, pp. 293–310. Available at: http://www.sciencedirect.com/science/article/pii/S0076687998970227 [Accessed September 23, 2014].

Visweswaran, G.R.R., Dijkstra, B.W. & Kok, J., 2011. Murein and pseudomurein cell wall binding domains of bacteria and archaea—a comparative view. *Applied Microbiology and Biotechnology*, 92(5), pp.921–928.

Vonlanthen, S., 2013. *Analysis and manipulation of storage lipids in microalgae*. PhD thesis. Unversity College London.

Wang, X. et al., 2008. A novel expression platform for the production of diabetes-associated autoantigen human glutamic acid decarboxylase (hGAD65). *BMC biotechnology*, 8, p.87.

Wang, Y.V. et al., 2007. Quantitative analyses reveal the importance of regulated Hdmx degradation for P53 activation. *Proceedings of the National Academy of Sciences*, 104(30), pp.12365–12370.

Werner, R. & Mergenhagen, D., 1998. Mating Type Determination of Chlamydomonas reinhardtii by PCR. *Plant Molecular Biology Reporter*, 16(4), pp.295–299.

WHO report, 2014. WHO | Antimicrobial resistance: global report on surveillance 2014. *WHO*. Available at: http://www.who.int/drugresistance/documents/surveillancereport/en/ [Accessed October 6, 2014].

WHO report, 2004. WHO | The world health report 2004 - changing history. *WHO*. Available at: http://www.who.int/whr/2004/en/ [Accessed February 4, 2014].

Williams, J., 1988. Construction of Specific Mutations in Photosystem II Photosynthetic Reaction Center by Genetic Engineering Methods in Synechocystis 6803. In *Methods in Enzymology*. Molecular Genetics. Academic Press.

Witzenrath, M. et al., 2009. Systemic use of the endolysin Cpl-1 rescues mice with fatal pneumococcal pneumonia. *Critical Care Medicine*, 37(2), pp.642–649.

Wright, G.D., 2012. Antibiotics: A New Hope. *Chemistry & Biology*, 19(1), pp.3–10.

Yang, Z. et al., 2006. Expression of human soluble TRAIL in Chlamydomonas reinhardtii chloroplast. *Chinese Science Bulletin*, 51(14), pp.1703–1709.

Yoong, P. et al., 2006. PlyPH, a Bacteriolytic Enzyme with a Broad pH Range of Activity and Lytic Action against Bacillus anthracis. *Journal of Bacteriology*, 188(7), pp.2711–2714.

Young, R.E.B. & Purton, S., 2014. Cytosine deaminase as a negative selectable marker for the microalgal chloroplast: a strategy for the isolation of nuclear mutations that affect chloroplast gene expression. *The Plant Journal*, 80(5), pp.915–925.

Young, R., Wang, I.-N. & Roof, W.D., 2000. Phages will out: strategies of host cell lysis. *Trends in Microbiology*, 8(3), pp.120–128.

Zang, X.-N. et al., 2007. Transformation and expression of Paralichthys olivaceus growth hormone cDNA in Synechocystis sp. PCC6803. *Aquaculture*, 266(1–4), pp.63–69.

Zhou, J. et al., 2014. Discovery of a super-strong promoter enables efficient production of heterologous proteins in cyanobacteria. *Scientific Reports*, 4. Available at: http://www.nature.com/srep/2014/140328/srep04500/full/srep04500.html?WT.ec_id=SREP-631-20140401 [Accessed September 22, 2014].

Zimmer, M. et al., 2003. Genome and proteome of Listeria monocytogenes phage PSA: an unusual case for programmed + 1 translational frameshifting in structural protein synthesis. *Molecular Microbiology*, 50(1), pp.303–317.

APPENDIX A

Appendix A1: Gene sequences

Sequence of *pal i*ncluding HA-tag (921 bp)

ATGGGTGTTGATATTGAAAAAGGTGTTGCTTGGATGCAAGCTCGTAAAGGTCGTGTTTCATATTCAATG
GATTTCCGTGATGGTCCAGATTCATACGATTGTTCATCATCAATGTACTACGCTTTACGTTCAGCTGGT
GCTTCATCAGCTGGTTGGGCTGTTAATACAGAATATATGCACGCTTGGTTAATTGAAAACGGTTACGAA
TTAATTTCAGAAAACGCTCCATGGGATGCTAAACGTGGTGATATTTTCATTTGGGGTCGTAAAGGTGCT
TCTGCTGGTGCTGGAGGTCATACAGGTATGTTTATTGATTCAGATAACATTATTCACTGTAACTACGCT
TACGATGGTATTTCAGTTAATGATCACGATGAACGTTGGTATTATGCTGGTCAACCATATTACTACGTT
TACCGTTTAACAAACGCTAATGCTCAACCTGCTGAAAAAAAATTAGGTTGGCAAAAAGATGCTACAGGT
TTTTGGTATGCTCGTGCTAATGGTACATACCCAAAAGATGAATTTGAATACATTGAAGAAAACAAATCA
TGGTTCTACTTCGATGATCAAGGTTACATGTTAGCTGAAAAATGGTTAAAACACACAGATGGTAACTGG
TATTGGTTCGATCGTGATGGTTATATGGCTACATCATGGAAACGTATTGGTGAATCTTGGTACTATTTC
AACCGTGATGGTTCAATGGTTACAGGTTGGATTAAATACTACGATAACTGGTACTACTGTGATGCTACA
AACGGTGATATGAAATCAAACGCTTTCATTCGTTATAATGATGGTTGGTACTTATTATTACCAGATGGT
CGTTTAGCTGATAAACCACAATTCACAGTTGAACCTGATGGTTTAATTACAGCTAAAGTTTACCCATAC
GATGTTCCAGATTACGCTTAATAA

Frequency of each codon triplet in the *pal* gene sequence

UUU	9.8(	3)	UCU	6.5(	2)	UAU	32.6(	10)	UGU	9.8(	3)
UUC	26.1(	8)	UCC	0.0(	0)	UAC	71.7(	22)	UGC	0.0(	0)
UUA	39.1(	12)	UCA	52.1(	16)	UAA	6.5(	2)	UGA	0.0(	0)
UUG	0.0(	0)	UCG	0.0(	0)	UAG	0.0(	0)	UGG	55.4(	17)
CUU	0.0(	0)	CCU	6.5(	2)	CAU	3.3(	1)	CGU	45.6(	14)
CUC	0.0(	0)	CCC	0.0(	0)	CAC	13.0(	4)	CGC	0.0(	0)
CUA	0.0(	0)	CCA	26.1(	8)	CAA	19.5(	6)	CGA	0.0(	0)
CUG	0.0(	0)	CCG	0.0(	0)	CAG	0.0(	0)	CGG	0.0(	0)
AUU	45.6(	14)	ACU	0.0(	0)	AAU	16.3(	5)	AGU	0.0(	0)
AUC	0.0(	0)	ACC	0.0(	0)	AAC	35.8(	11)	AGC	0.0(	0)
AUA	0.0(	0)	ACA	35.8(	11)	AAA	52.1(	16)	AGA	0.0(	0)
AUG	32.6(	10)	ACG	0.0(	0)	AAG	0.0(	0)	AGG	0.0(	0)
GUU	32.6(	10)	GCU	91.2(	28)	GAU	94.5(	29)	GGU	91.2(	28)
GUC	0.0(	0)	GCC	0.0(	0)	GAC	0.0(	0)	GGC	0.0(	0)
GUA	0.0(	0)	GCA	0.0(	0)	GAA	45.6(	14)	GGA	3.3(	1)
GUG	0.0(	0)	GCG	0.0(	0)	GAG	0.0(	0)	GGG	0.0(	0)

Sequence of *ϕ11* including HA-tag (1,476 bp)

ATGCAAGCTAAATTAACAAAAAACGAATTTATTGAATGGTTAAAAACATCTGAAGGTAAACAATTCAAC
GTAGATTTATGGTACGGTTTCCAATGTTTCGATTATGCTAACGCTGGTTGGAAAGTGTTATTCGGTTTA
CTTTTAAAAGGTTTAGGTGCTAAAGACATTCCATTCGCTAACAATTTCGACGGTTTAGCTACAGTTTAC
CAAAACACACCAGATTTTTTAGCTCAACCAGGTGATATGGTTGTTTTCGGTTCTAATTATGGTGCTGGT
TATGGTCATGTTGCTTGGGTTATTGAAGCTACATTAGACTACATTATTGTGTACGAACAAAACTGGTTA
GGTGGTGGTTGGACAGATGGTATTGAACAACCAGGATGGGGTTGGGAAAAAGTTACACGTCGTCAACAT
GCTTACGATTTCCCAATGTGGTTCATTCGTCCAAACTTCAAATCAGAAACAGCTCCACGTTCAGTTCAA
TCACCAACACAAGCTCCAAAAAAAGAAACTGCTAAACCACAACCAAAAGCTGTGGAGCTTAAAATCATT
AAAGACGTGGTAAAAGGATACGACTTACCTAAACGTGGTAGCAATCCAAAAGGTATTGTTATTCACAAC
GACGCTGGTAGTAAAGGTGCTACAGCTGAAGCTTATCGTAATGGTTTAGTTAACGCTCCATTATCTCGT
TTAGAAGCTGGTATTGCTCACTCATATGTTTCAGGTAATACAGTTTGGCAAGCTTTAGACGAATCACAA
GTTGGTTGGCACACAGCTAATCAAATTGGAAACAAATACTACTACGGAATTGAAGTGTGTCAATCAATG
GGTGCTGACAACGCTACATTCTTAAAAAACGAACAAGCTACATTCCAAGAATGTGCTCGTTTACTTAAA
AAATGGGGTTTACCAGCTAACCGTAACACTATTCGTTTACACAACGAATTTACAAGCACATCATGTCCA
CACCGTTCATCAGTTTTACATACAGGTTTTGATCCAGTGACACGTGGATTATTACCAGAAGATAAAAGA
CTTCAACTTAAAGACTACTTCATTAAACAAATTCGTGCTTACATGGACGGTAAAATTCCAGTTGCTACA
GTATCAAACGAATCATCAGCTAGCAGCAACACAGTTAAACCAGTAGCTTCTGCTTGGAAACGTAACAAA
TACGGTACATACTACATGGAAGAAAGCGCTCGTTTCACAAATGGTAACCAACCAATTACAGTTCGTAAA
GTGGGTCCATTCTTATCTTGTCCAGTGGGTTATCAATTCCAACCTGGTGGTTATTGTGACTACACTGAA
GTAATGTTACAAGATGGTCACGTTTGGGTAGGTTATACATGGGAAGGTCAACGTTACTACTTACCAATT
CGTACTTGGAATGGTTCTGCTCCACCAAACCAAATTTTAGGTGACTTATGGGGTGAAATTAGCTATCCA
TACGATGTTCCAGACTACGCTTAATAA

Frequency of each codon triplet in the *ϕ11* gene sequence

UUU	8.1(4)	UCU	12.2(6)	UAU	18.3(9)	UGU	12.2(6)
UUC	32.5(16)	UCC	0.0(0)	UAC	38.6(19)	UGC	0.0(0)
UUA	56.9(28)	UCA	26.4(13)	UAA	4.1(2)	UGA	0.0(0)
UUG	0.0(0)	UCG	0.0(0)	UAG	0.0(0)	UGG	34.6(17)
CUU	10.2(5)	CCU	4.1(2)	CAU	6.1(3)	CGU	36.6(18)
CUC	0.0(0)	CCC	0.0(0)	CAC	12.2(6)	CGC	0.0(0)
CUA	0.0(0)	CCA	54.9(27)	CAA	50.8(25)	CGA	0.0(0)
CUG	0.0(0)	CCG	0.0(0)	CAG	0.0(0)	CGG	0.0(0)
AUU	42.7(21)	ACU	8.1(4)	AAU	16.3(8)	AGU	2.0(1)
AUC	2.0(1)	ACC	0.0(0)	AAC	40.7(20)	AGC	12.2(6)
AUA	0.0(0)	ACA	48.8(24)	AAA	63.0(31)	AGA	2.0(1)
AUG	14.2(7)	ACG	0.0(0)	AAG	0.0(0)	AGG	0.0(0)
GUU	36.6(18)	GCU	75.2(37)	GAU	20.3(10)	GGU	83.3(41)
GUC	0.0(0)	GCC	0.0(0)	GAC	26.4(13)	GGC	0.0(0)
GUA	12.2(6)	GCA	0.0(0)	GAA	46.7(23)	GGA	10.2(5)
GUG	16.3(8)	GCG	0.0(0)	GAG	2.0(1)	GGG	0.0(0)

Sequence of *gp20$_1$* including HA-tag (891 bp)

ATGGTTCGTTATATTCCAGCTGCTCATCACTCAGCAGGTTCTAACAATCCTGTTAATCGTGTAGTAATT
CATGCAACATGTCCAGATGTAGGATTTCCTAGTGCTAGCCGTAAAGGTCGTGCTGTTTCAACTGCTAAT
TACTTCGCATCACCATCTAGTGGTGGTAGCGCTCACTATGTGTGTGACATTGGAGAAACAGTACAATGT
TTATCTGAAAGTACTATTGGATGGCACGCACCACCAAACCCTCATTCATTAGGTATTGAAATTTGTGCT
GATGGTGGTTCTCATGCTAGCTTTCGTGTGCCTGGTCACGCATATACACGTGAACAATGGTTAGATCCA
CAAGTTTGGCCAGCTGTTGAACGTGCTGCAGTATTATGTCGTCGTTTATGTGACAAATACAATGTACCT
AAACGTAAATTATCAGCTGCTGACTTAAAAGCAGGTCGTCGTGGTGTTTGTGGTCATGTTGATGTAACT
GACGCTTGGCACCAAAGCGATCATGATGATCCAGGACCATGGTTTCCTTGGGACAAATTCATGGCTGTT
GTAAACGGTGGTAGCGGTGACAGCGGAGAATTAACAGTTGCAGATGTAAAAGCTTTACACGATCAAATT
AAACAATTATCAGCACAATTAACTGGTAGCGTGAACAAATTACATCACGATGTTGGTGTTGTACAAGTG
CAAAACGGTGACTTAGGAAAACGTGTAGACGCTTTAAGCTGGGTGAAAAATCCAGTGACTGGAAAATTA
TGGCGTACAAAAGATGCTTTATGGTCTGTTTGGTATTATGTATTAGAATGTCGTAGCCGTTTAGATCGT
TTAGAAAGCGCTGTAAATGACTTAAAAAAATACCCATATGATGTACCTGACTATGCTTAATAA

Frequency of each codon triplet in the *gp20$_1$* gene sequence

UUU 10.1(3)	UCU 16.8(5)	UAU 23.6(7)	UGU 26.9(8)
UUC 6.7(2)	UCC 0.0(0)	UAC 10.1(3)	UGC 0.0(0)
UUA 67.3(20)	UCA 20.2(6)	UAA 6.7(2)	UGA 0.0(0)
UUG 0.0(0)	UCG 0.0(0)	UAG 0.0(0)	UGG 33.7(10)
CUU 0.0(0)	CCU 23.6(7)	CAU 23.6(7)	CGU 57.2(17)
CUC 0.0(0)	CCC 0.0(0)	CAC 23.6(7)	CGC 0.0(0)
CUA 0.0(0)	CCA 37.0(11)	CAA 30.3(9)	CGA 0.0(0)
CUG 0.0(0)	CCG 0.0(0)	CAG 0.0(0)	CGG 0.0(0)
AUU 23.6(7)	ACU 16.8(5)	AAU 20.2(6)	AGU 10.1(3)
AUC 0.0(0)	ACC 0.0(0)	AAC 16.8(5)	AGC 33.7(10)
AUA 0.0(0)	ACA 16.8(5)	AAA 50.5(15)	AGA 0.0(0)
AUG 6.7(2)	ACG 0.0(0)	AAG 0.0(0)	AGG 0.0(0)
GUU 40.4(12)	GCU 64.0(19)	GAU 43.8(13)	GGU 57.2(17)
GUC 0.0(0)	GCC 0.0(0)	GAC 33.7(10)	GGC 0.0(0)
GUA 47.1(14)	GCA 30.3(9)	GAA 26.9(8)	GGA 23.6(7)
GUG 20.2(6)	GCG 0.0(0)	GAG 0.0(0)	GGG 0.0(0)

Sequence of *gp20₂* including HA-tag (891 bp)

ATGGTTCGTTATATTCCAGCTGCTCACCACTCTGCTGGTTCAAACAACCCAGTTAACCGTGTAGTTATT
CACGCTACTTGTCCAGATGTTGGTTTCCCTTCTGCTTCACGTAAAGGTCGTGCTGTTTCTACTGCTAAC
TACTTTGCTTCTCCATCTTCTGGTGGTTCAGCTCACTACGTATGTGACATCGGTGAAACAGTACAATGT
TTATCAGAATCAACTATTGGTTGGCACGCTCCACCAAACCCACACTCTTTAGGTATTGAAATTTGTGCT
GATGGTGGTTCACACGCTTCTTTCCGTGTTCCAGGTCACGCTTACACACGTGAACAATGGTTAGATCCA
CAAGTTTGGCCTGCTGTTGAACGTGCTGCTGTTTTATGTCGTCGTTTATGTGACAAATACAACGTTCCA
AAACGTAAATTATCAGCTGCTGATTTAAAAGCTGGTCGTCGTGGTGTTTGTGGTCACGTAGACGTAACT
GATGCTTGGCACCAATCTGATCACGACGACCCAGGTCCATGGTTCCCTTGGGATAAATTCATGGCTGTT
GTAAACGGTGGTTCAGGTGATTCTGGTGAATTAACAGTAGCTGATGTTAAAGCTTTACACGACCAAATT
AAACAATTATCAGCTCAATTAACAGGTTCAGTAAACAAATTACACCACGACGTAGGTGTTGTACAAGTA
CAAAACGGTGATTTAGGTAAACGTGTAGATGCTTTATCTTGGGTTAAAAACCCAGTTACAGGTAAATTA
TGGCGTACTAAAGATGCTTTATGGTCAGTATGGTACTACGTTTTAGAATGTCGTTCACGTTTAGACCGT
TTAGAATCAGCTGTAAACGATTTAAAAAAATACCCATACGATGTTCCAGATTACGCTTAATAA

Frequency of each codon triplet in the *gp20₂* gene sequence

UUU 3.4(1)	UCU 37.0(11)	UAU 3.4(1)	UGU 26.9(8)
UUC 13.5(4)	UCC 0.0(0)	UAC 30.3(9)	UGC 0.0(0)
UUA 67.3(20)	UCA 43.8(13)	UAA 6.7(2)	UGA 0.0(0)
UUG 0.0(0)	UCG 0.0(0)	UAG 0.0(0)	UGG 33.7(10)
CUU 0.0(0)	CCU 10.1(3)	CAU 0.0(0)	CGU 57.2(17)
CUC 0.0(0)	CCC 0.0(0)	CAC 47.1(14)	CGC 0.0(0)
CUA 0.0(0)	CCA 50.5(15)	CAA 30.3(9)	CGA 0.0(0)
CUG 0.0(0)	CCG 0.0(0)	CAG 0.0(0)	CGG 0.0(0)
AUU 20.2(6)	ACU 16.8(5)	AAU 0.0(0)	AGU 0.0(0)
AUC 3.4(1)	ACC 0.0(0)	AAC 37.0(11)	AGC 0.0(0)
AUA 0.0(0)	ACA 16.8(5)	AAA 50.5(15)	AGA 0.0(0)
AUG 6.7(2)	ACG 0.0(0)	AAG 0.0(0)	AGG 0.0(0)
GUU 60.6(18)	GCU 94.3(28)	GAU 50.5(15)	GGU 80.8(24)
GUC 0.0(0)	GCC 0.0(0)	GAC 26.9(8)	GGC 0.0(0)
GUA 47.1(14)	GCA 0.0(0)	GAA 26.9(8)	GGA 0.0(0)
GUG 0.0(0)	GCG 0.0(0)	GAG 0.0(0)	GGG 0.0(0)

Appendix A2: Vectors used in this study

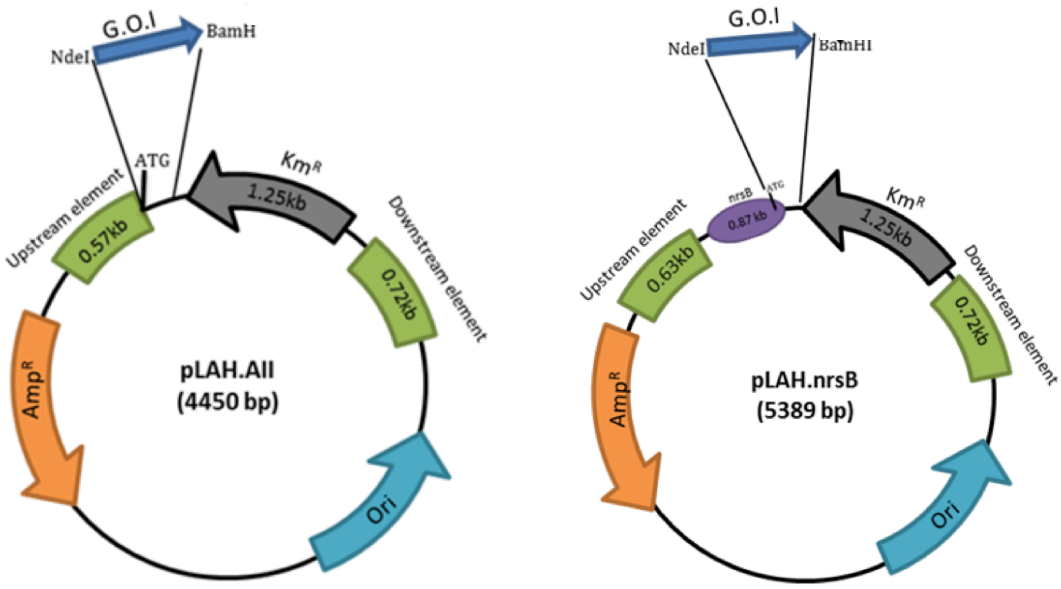

Figure 1: Vector maps of the plasmids pLAH.AII and pLAH.nrsB used for the transformation of *Synechocystis* sp. PCC 6803
The transformation vectors were created by Lamya Al'Haj. Reproduced from Al-Haj (2014).

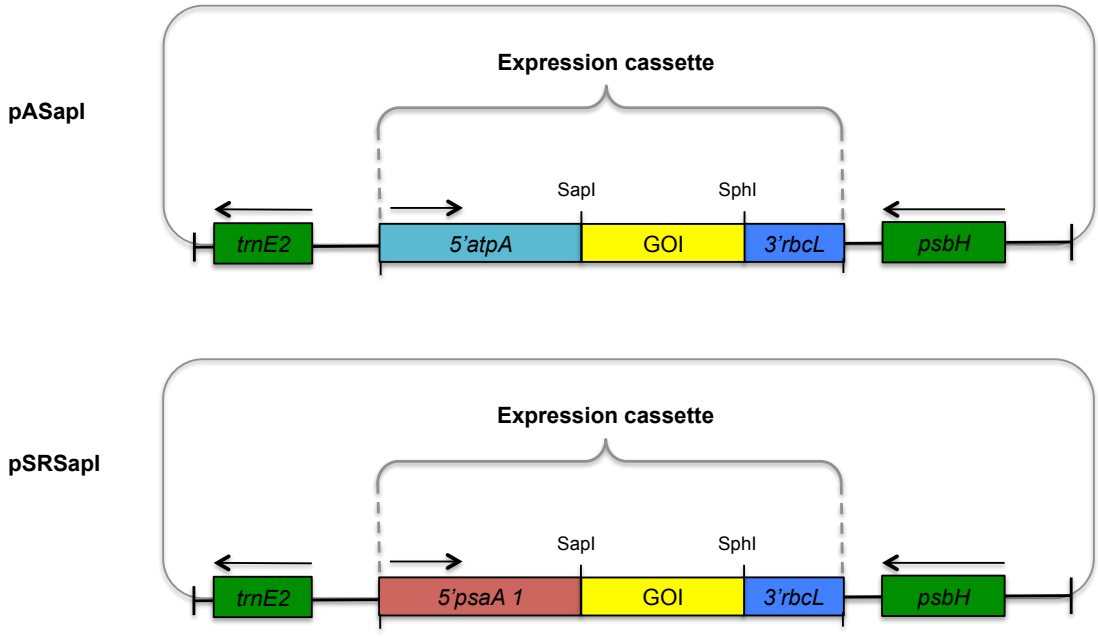

Figure 2: Vector maps of the plasmids pASapI and pSRSapI used for the transformation of *Chlamydomonas reinhardtii*
The transformation vector pASapI was created by Economou et al. (2014) and pSRSapI by (Young & Purton 2014).

APPENDIX B

Chapter 8 – Commercial evaluation of *Chlamydomonas reinhardtii* as a production platform for bacteriophage endolysins

8 COMMERCIAL EVALUATION OF *CHLAMYDOMONAS REINHARDTII* AS A PRODUCTION PLATFORM FOR BACTERIOPHAGE ENDOLYSINS 339

Table of figures

Table of tables

8 Commercial evaluation of *Chlamydomonas reinhardtii* as a production platform for bacteriophage endolysins

8.1 Introduction

The aim of the above-presented PhD thesis was to investigate the suitability of microalgae as a novel production platform for recombinant bacteriophage endolysins, a class of promising antibacterial proteins (for an introduction to endolysins, the rationale of this study and details of the microalga used, see chapter 1). During this study, it was shown that the two platforms used, the chloroplast of the eukaryotic green microalga *Chlamydomonas reinhardtii* and the cyanobacterium *Synechocystis* sp. PCC6803, are able to produce certain endolysins in an active form.

Microalgae have emerged in the last ten years as an alternative production platform and are believed to offer several advantages over conventional systems (1.4 and 7.2), including the potential to lower the costs of recombinant protein production due to low cost cultivation requirements (Gimpel et al. 2014). However, the maximal cell densities of microalgae cultivated in bioreactor systems and the yields of recombinant proteins from microalgae are often considerably lower compared to conventional systems with comparable advantages (7.2) (Jørgensen et al. 2014; Oey et al. 2009). Together this could outweigh lower cultivation costs and result overall in higher production costs per mg of recombinant protein. To further evaluate microalgae as a production platform for bacteriophage endolysins, it is therefore important to attempt a cost analysis for the cultivation and harvesting of the transgenic algae strains. This can be then used to further investigate whether the production of recombinant endolysins in microalgae is competitive in comparison to bacterial or transgenic plant systems that offer similar advantages.

Since the synthesis of the *S. pneumoniae*-specific endolysin Pal in the *C. reinhardtii* chloroplast showed the most promising results and had been most investigated during the research for this PhD thesis, it was used as a model to estimate the costs for the production of endolysins in microalgae.

8.1.1 Aims and objects of this study

The objective of this study is to investigate the feasibility of microalgae as a production platform for recombinant bacteriophage endolysins and other antimicrobial proteins from a financial perspective by using production of the *S. pneumoniae*-specific endolysin Pal in the chloroplast of *C. reinhardtii* as the model system. With this aim, the following studies were performed:

- Designing of a model facility for the cultivation of *C. reinhardtii* and production of the endolysin Pal

- Calculation of the costs for the production of Pal in *C. reinhardtii,*

- Comparison the costs of recombinant protein production in *C. reinhardtii* to conventional expression platforms with similar advantages

- Summary of the current market for antibiotics, particularly in endolysins, and the patent landscape

8.2 Methods

8.2.1 Algal strains and quantification of recombinant endolysin production

During this study, several transgenic lines of *C. reinhardtii* were created that produce the *S. pneumoniae*-specific endolysin Pal (chapter 3) in their chloroplast. Furthermore, it was shown that *C. reinhardtii*-produced Pal has specific antimicrobial activity against *S. pneumoniae* including clinical isolates with antibiotic resistances (4.2.2). Subsequently, the production of Pal was analysed under two different promoter systems and at different growth stages to optimise the yield of recombinant protein (3.2.2.4 and 3.2.3.2). Furthermore, the yield of Pal produced in the *C. reinhardtii* chloroplast was quantified using two standard proteins and the Odyssey® Infrared Imaging System. The quantification was performed at two growth stages that yield the highest amount of Pal per cell and per culture volume, respectively (3.2.4) (Table 8.1).

Table 8.1: Quantification of Pal at two different growth stages using CARHSP1 and a multiple tag fusion protein as standards
Cultures of TN72_SR_*pal-HA* were grown under standard conditions to an OD_{750nm} of 2 and 3.8; the cells were broken by the addition of SDS (2% w/v) and boiling. Dilution series of CARHSP1 or the multiple tag fusion protein were analysed together with two dilutions of TN72_SR_*pal-HA* whole cell extract on the same gel and membrane in western blot analyses with anti-HA antibodies and IRDye® secondary antibodies. Standard curves of quantities of the standard protein against the IR fluorescence signal of the Odyssey® Infrared Imaging System were used for the quantification of Pal, taking the lower molecular weight of Pal into account. The standard deviations (±) are stated (n = x).

Standard protein	OD_{750nm} of culture	Pal (mg) / L culture volume	Pal (mg) / g of cell dry weight
CARSHP1 as standard	**2**	6.5 ± 0.8 (n = 4)	12.6 ± 0.7
	3.8	9.6 ± 1.6 (n = 4)	NA
Multiple tag fusion protein as standard	**2**	7.2 ± 0.8 (n = 4)	14.0 ± 0.7
	3.8	10.6 ± 5.0 (n = 4)	NA

8.2.2 Modelling of large-scale cultivation system

The company Supreme Biotechnologies Ltd, which partly funded this study, cultivates *Haematococcus pluvialis* for the production of astaxanthin in Nelson, New Zealand. The cultivation of *H. pluvialis* for the production of astaxanthin is performed in two stages. In the first stage (the green phase), *H. pluvialis* is cultivated as continuous culture under optimal growth conditions. In the second phase (the red phase), the cultures are transferred to a batch cultivation and grown under high light and with limited nutrients to induce the formation of cysts with a high astaxanthin content. The culturing requirements of *C. reinhardtii* are comparable to the *H. pluvialis* green phase cultivation (similar nutrient, CO_2, mixing and temperature requirements). The green phase cultivation of *H. pluvialis* can be therefore used as a model for the cultivation of *C. reinhardtii.* Supreme Biotechnologies Ltd produces astaxanthin as a dietary supplement for human consumption. *H. pluvialis* is therefore grown in closed containment and under tightly controlled conditions in an indoor facility, which would also be required for the production of endolysins for human use in *C. reinhardtii*.

Supreme Biotechnologies Ltd uses a “hanging bag” system (Figure 8.1) for the cultivation of *H. pluvialis* in the green and red phases. This system consists of single independent 40-litre bags, which are connected to nutrient drippers and transfer lines for the continuous cultivation in the green phase, as well as CO_2/air lines. The cultivation conditions can be first tested in single bags and subsequently easily scaled up to high numbers of bags. The cell-wall deficient *C. reinhardtii* strains producing Pal were successfully cultivated in single bags under conditions comparable to the ones in the facility of Supreme Biotechnologies Ltd during this study (Figure 8.3). This cultivation system is therefore used as a model system for the large-scale cultivation of *C. reinhardtii* producing Pal. Supreme Biotechnologies Ltd has provided a figure for their production costs in the green phase.

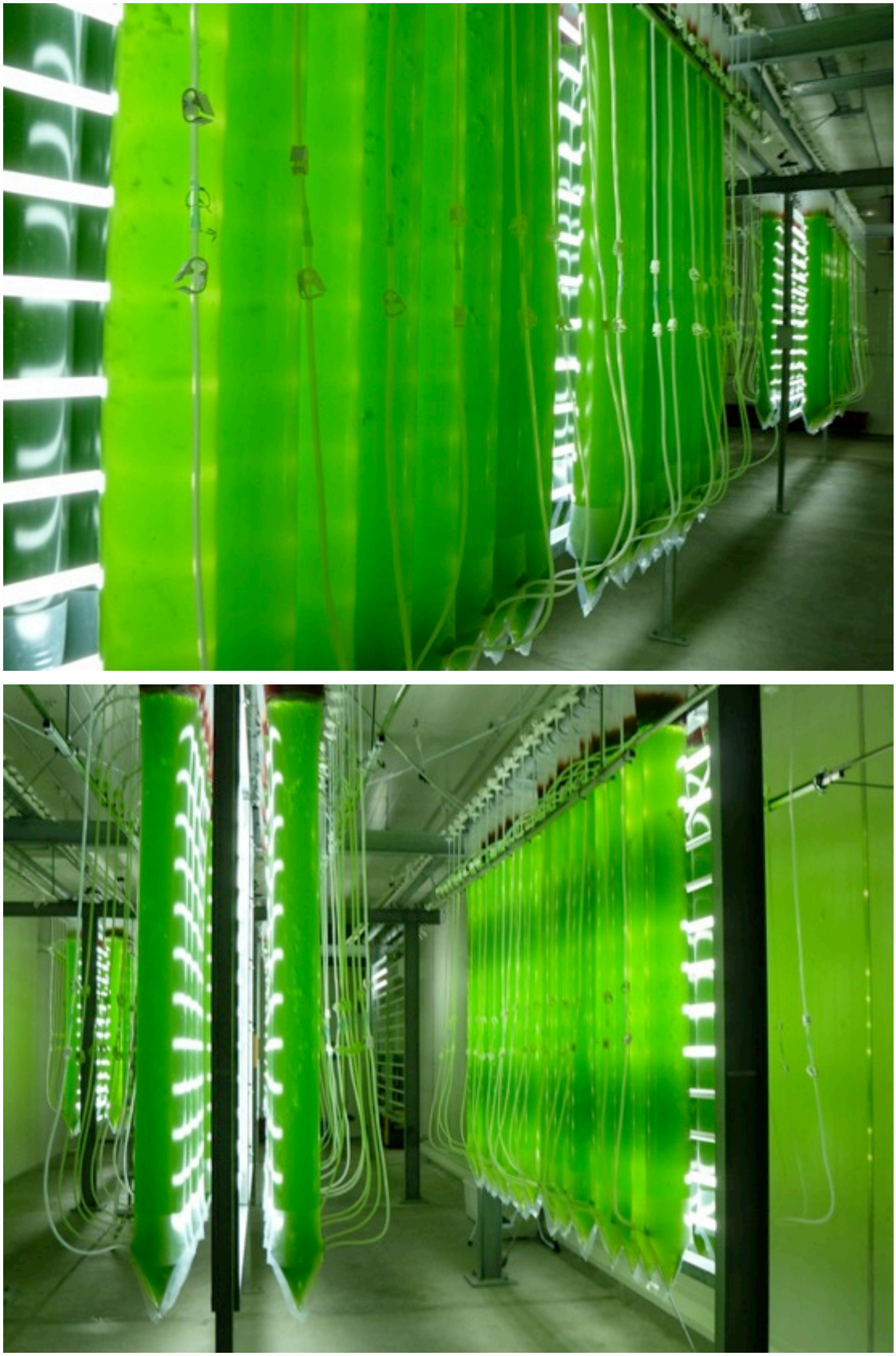

Figure 8.1: Green phase cultivation of *Haematococcus pluvialis* in the "hanging bag" system at Supreme Biotechnologies Ltd in Nelson, New Zealand.

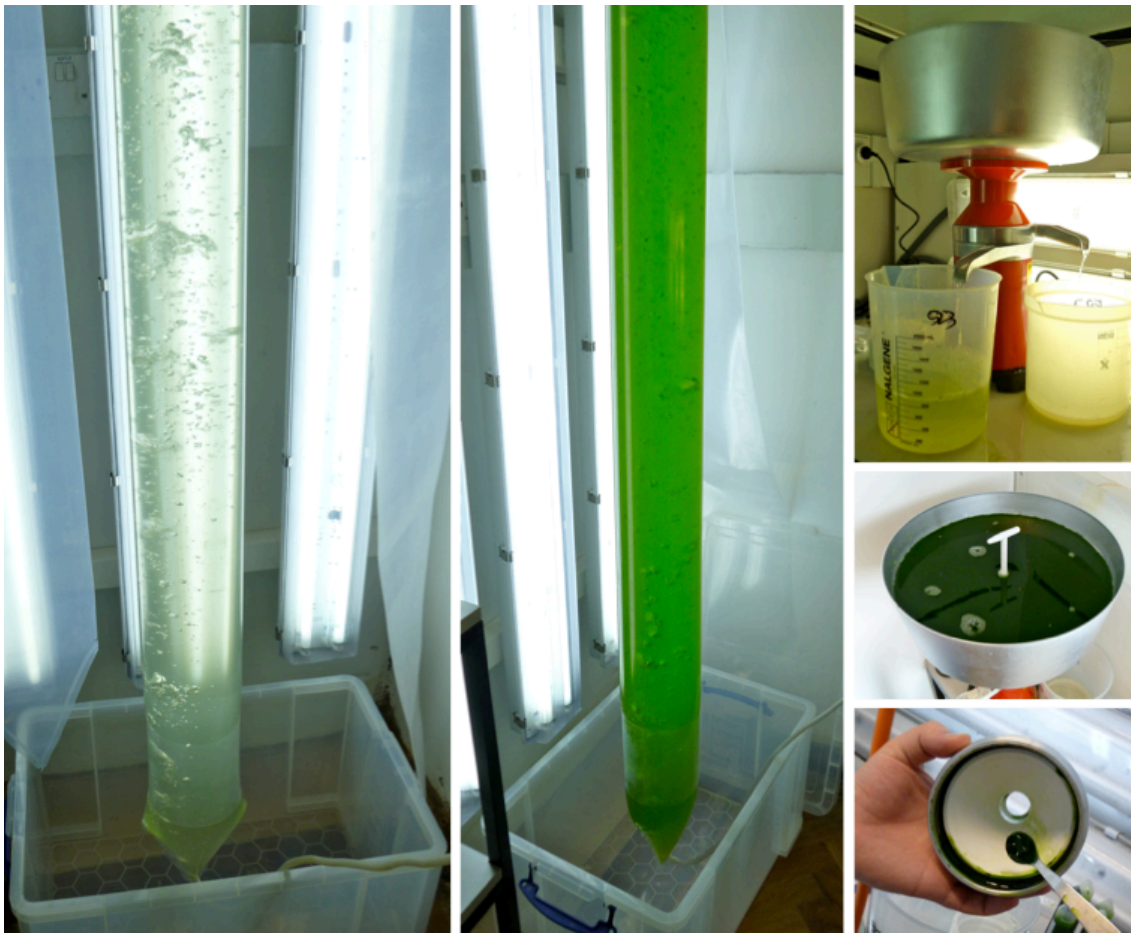

Figure 8.2: Cultivation (left) of *C. reinhardtii* TN72_*pal* at the University College London (UCL) (UK) using the "hanging bag system" of Supreme Biotechnologies Ltd, and harvesting of the cells at UCL (right)

8.2.3 Process of recombinant protein production in microalgae

The first step of the process is the cultivation of the transgenic microalga strain in the above described "hanging bag system". This process requires water (previously sterilized by filtration/ozonisation), as well as nutrients, CO_2 and power for lighting, pumping and temperature control. The next step is the harvesting, which requires an input of power and creates wastewater. The last step involves breakage of the cells and the recovery of an algal crude extract containing the recombinant protein. This requires additional energy input. The remaining algal biomass could be used for further applications, such as animal feed or for energy generation by anaerobic digestion (Figure 8.3).

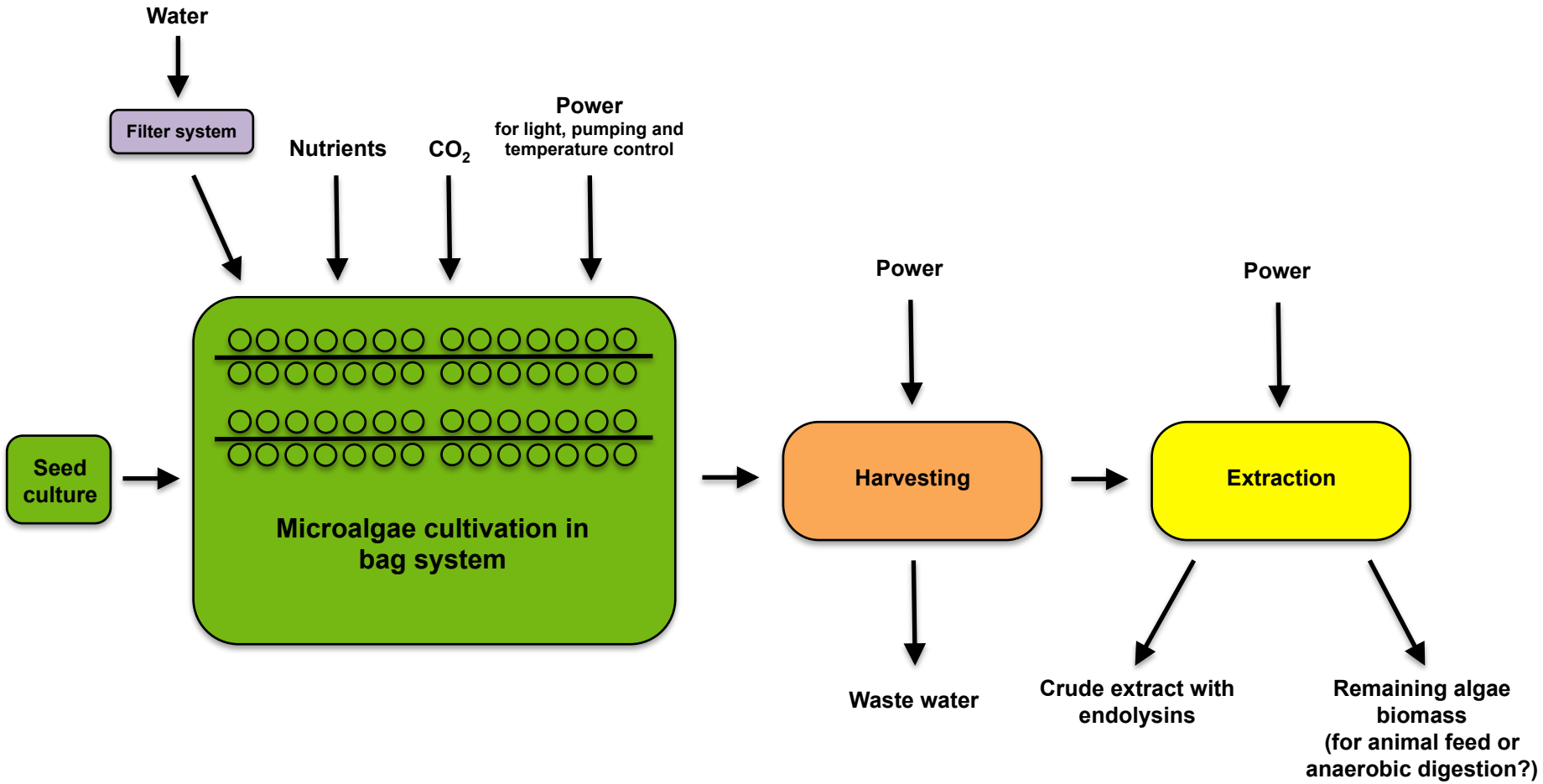

Figure 8.3: Process diagram for the production of recombinant proteins in microalgae

8.2.4 Cost evaluation

The cost evaluation was calculated based on figures for the cost of the green phase cultivation of *H. pluvialis* at the astaxanthin production facility of Supreme Biotechnologies Ltd; a study by Acién et al. (2012) that describes the operation of a 30 m^3 facility for the cultivation of *Scenedesmus almeriensis* in Almería (Spain), as well as further literature evaluating commercially the production of biodiesel in microalgae. The total capital is a combination of construction costs as well as operational and maintenance costs.

8.2.5 Market and patent landscape analysis

The analysis of the market and patent landscape was mainly performed using the patent database www.lens.org, and general internet searches.

8.3 Results

8.3.1.1 Modelling a facility for the cultivation of *C. reinhardtii* and the production of Pal: defining the scenario

The facility is assumed to be located in New Zealand, to have a size of 300 m^2 and to use the "hanging bag" system described in 8.2.2 for the cultivation of *C. reinhardtii* (Figure 8.4). The cultivation operates under steady state conditions in continuous flow with a total culture volume of 19,680 litres, which corresponds to 492 40-litre bags (Table 8.2). In the facility, the bags are attached in rows of 7 to both sides of a metal frame system, which contains the light systems, consisting of 12 horizontal fluorescent light tubes (58W, 152.4 cm) (Figure 8.1, Figure 8.4). The cultivation operates on 350 days per year with a 5-day shutdown every four months for cleaning and maintenance. The growth bags are single-use, whereas the silicone tubing is reused after cleaning and autoclaving. The facility includes a small laboratory for quality control and preparation of starter cultures.

The water for the preparation of the culture medium is sterilized by filtration/ozonisation, before nutrients and water are mixed using a medium preparation unit (Acién et al. 2012). The bags are connected to CO_2/air lines, which enable a constant bubbling of the bags for mixing of the culture and CO_2 supply. Culture medium is continuously pumped into the bags and the outflow containing cells flows automatically into harvest tanks. The microalgae biomass is harvested by centrifugation, since this method is not disruptive even to fragile cells and has a very high harvesting efficiency of more than 95% (Leite et al. 2013; Rawat et al. 2013). This is especially important, since the *C. reinhardtii* strains are cell-wall deficient and broken cells can easily release the soluble endolysin proteins into the culture medium. Harvesting by centrifugation is performed during the day with a continuous decanter (solid-liquid centrifugation unit) from Flotweg (Germany) at 9500 rpm, which results in a sludge with a 15% dry matter content (Acién et al. 2012). Subsequently, the sludge is frozen in a freezer room at -20ºC to prevent degradation of the endolysins.

The advantage of the cell-wall deficient *C. reinhardtii* strains is that the cells can be easily broken by simple mechanical methods (4.2.1). The freezing process (-20ºC) already breaks a high percentage of the cells and can be easily completed by mild and simple methods. Subsequently, a crude extract containing Pal can be obtained by centrifugation (21,000 x g, 5 min). *C. reinhardtii* is classified as a GRAS organism (Generally Recognized as Safe), which means this organism is even safe for human consumption. Crude extract containing an endolysin could be therefore used for certain applications, such as topical or non-medical applications, without expensive purification steps. However, the transgenic nature of the organism might necessitate for certain applications the removal or destruction of the DNA component. Alternatively, *C. reinhardtii*-produced Pal can be purified using DEAE cellulose with choline as specific eluent and ammonium sulphate precipitation (4.2.4).

The costs of the production process in this study are only analysed up to the harvesting and freezing step to simplify the analysis and to make the costing easier comparable to other production platforms, since extraction/purification costs vary depending on the protein and intended application.

Table 8.2: Main parameters defining the process and comparison of the growth parameters for *C. reinhardtii* and *H. pluvialis*

Parameter	Value	Source/Comment
Number of bags	492	Volume per bag: 40 litres
Total culture volume (litres)	19,680	Calculated from the outflow and daily renewal rate
Operation time (days/annum)	350	Every 4 months 5 days shut down for cleaning/renewal
Operation time (cultivation) (h/day)	24	
	H. pluvialis	
Cells per ml	150,000	Supreme Biotechnologies Ltd
Litres per minute (outflow)	4.1	Supreme Biotechnologies Ltd
Litres per month (outflow)	179,580	Supreme Biotechnologies Ltd
Litres per day (outflow)	5,904	Supreme Biotechnologies Ltd
Cells per month	26,937,000,000,000	Supreme Biotechnologies Ltd
Daily renewal rate	30%	Fábregas et al. (2001)
Growth rate	0.023 h^{-1}	Katsuda et al. (2004)
	0.024 h^{-1}	García-Malea et al. (2005)
	C. reinhardtii	
Growth rate	0.064 – 0.10 h^{-1}	Determined in this study for the *C. reinhardtii* strains producing Pal at 200 µmol m^{-2} s^{-1}, approximately 3.5 times higher than *H. pluvialis*
Litres per minute (outflow)	12.3	Assumption: Higher growth rate results in at least three times higher outflow
Litres per month (outflow)	538,740	
Litres per day (outflow)	17,712	
Daily renewal rate	90%	

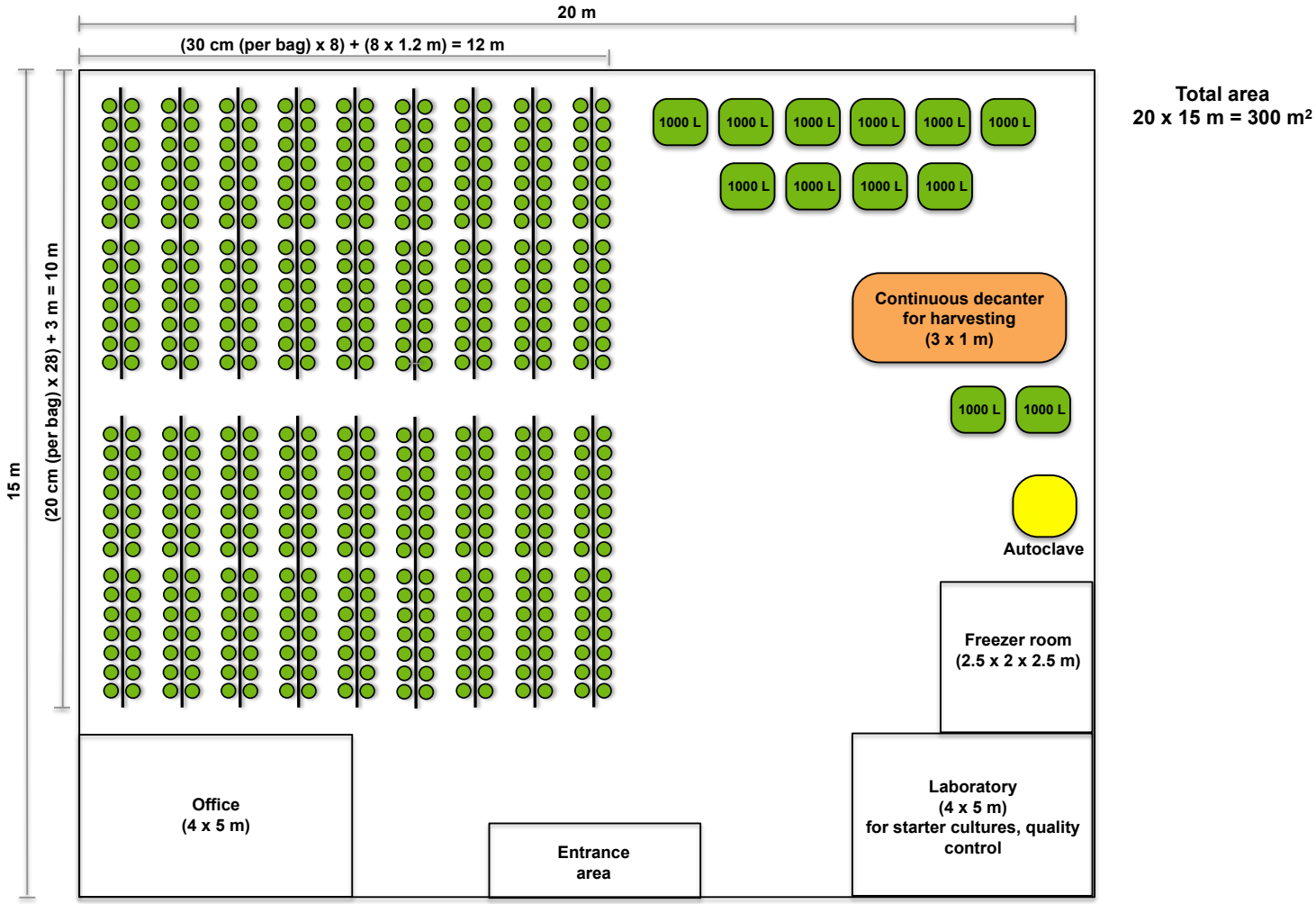

Figure 8.4: Model facility for the cultivation of *Chlamydomonas reinhardtii* for the production of recombinant endolysins
Green circles represent the "hanging bag" cultivation system, green squares harvest storage tanks.

8.3.2 Costing for the production of the endolysin Pal in *C. reinhardtii*

8.3.2.1 Capital costs

The total capital costs consist of the costs for construction and installation of the metal frame system and the major equipment, as well as a yearly lease for the premises (Tables 8.3 and 8.4). The costs of the facility are based on a lifespan of ten years. The depreciation for most items is therefore 10 years, except for items with a predicted shorter life span such as light tubes (15,000 h = 1.7 years) and silicone tubing (2 years). The costs for construction and installation, as well as contingency and insurance costs were estimated by multiplying the costs for major equipment by the corresponding Lang factors, which were taken from Acién et al. (2012) and Richmond (2008). The construction costs consist of onsite installation costs including piping and electrical installations, as well as labour costs. The estimated construction/installation time would be approximately six months.

Table 8.3: Summary of fixed capital estimated for the study analysed

Item		NZ$	Source/comments
Total costs for major equipment (MEC)		160,834	See table 8.4
Total costs for construction and installation		157,618	See table 8.4
Depreciation (per annum) in NZ$		**33,851**	10 years, unless otherwise stated
Contingency	0.08 x depreciation	2,708	Acién et al. (2012), Richmond (2008)
Insurance	0.006 x depreciation	203	Acién et al. (2012), Richmond (2008)
Purchase tax	0.15 (NZ $)	5,078	www.newzealandnow.govt.nz
Premises (300 m^2 in Nelson, New Zealand)	Lease/year (NZ$)	28,000	Colliers International New Zealand - Commercial Real Estate Agency - http://www.colliers.co.nz
Total fix capital per annum (NZ$)		**69,840**	
Total fix capital per month (NZ$)		**5,820**	

Table 8.4: Detailed fixed capital costs estimated for the study analysed

	Item	Units (max. capacity per unit)	Costs (NZ$)		Depreciation (DEP)	Source
			Per item	Total		
Major equipment for	Metal frame work	m^3 (18 x 8.75 m^3 = 158 m^3)	97.50	15,400	10	www.alibaba.com
- Cultivation	Fluorescent light tubes	432 (= 12 x 4 x 9)	4.20	1,814	1.7 (15,000 h)	www.lampshoponline.com
	Silicone tubing	1000 m	2.80	2,800	2	www.polymax.co.uk
	Air conditioning	For 300 m^2	1,120	1,120	10	www.alibaba.com
	Medium preparation unit	1 (4 m^3/h)	8,400	8,400	10	Acién et al. (2012)
	Water sterilization unit	1 (2 m^3/h)	21,000	21,000	10	Acién et al. (2012)
	CO_2 supply unit	1 (4 kg/h)	700	700	10	Acién et al. (2012)
	Autoclave	250 litres	20,000	20,000	10	www.fisher.co.uk
	Lab equipment	Microscope, shaker	4,200	4,200	10	www.fisher.co.uk
- Harvesting	Continuous decanter	1 (4 m^3/h)	63,000	63,000	10	Acién et al. (2012)
	Harvest/medium pumps	3 (2 m^3/h)	1,400	4,200	10	Acién et al. (2012)
	Harvest storage tanks	14 (1 m^3/h)	700	9,800	10	Acién et al. (2012)
- Cell breakage/storage	Freezer room	1 (2.5 x 2 x 2.5 m)	8,400	8,400	10	www.coldnet.co.uk
	Total costs for major equipment (MEC) (NZ$)			**160,834**		

	Item	Lang factor (x MEC)	Total (NZ$)	DEP	Source
Construction/	Installation costs	0.2	32,167	10	Acién et al. (2012)
installation costs	Instrumentation and control	0.15	24,125	10	Acién et al. (2012), Richmond (2008)
	Piping	0.2	32,167	10	Acién et al. (2012)
	Electrical	0.1	16,083	10	Acién et al. (2012), Richmond (2008)
	Engineering and supervision	0.3	48,250	10	Acién et al. (2012), Richmond (2008)
	Contractor's fee	0.03	4,825	10	Acién et al. (2012)
	Total costs for construction and installation (NZ$)		**157,618**		

Table 8.5: Direct monthly production/operational costs estimated for the case study analysed. Power costs are: 1 kWh is 0.1 NZ$ (http://www.electricityinfo.co.nz/)

	Item	*H. pluvialis* Costs (NZ$)	*C. reinhardtii* Costs (NZ$)	Comments	Source
Cultivation	Power	705	2,040	*C. reinhardtii*: Higher light intensity	Supreme Biotechnologies Ltd
	Water/wastewater	538	1,614	*C. reinhardtii*: 3 x higher flow rate	Supreme Biotechnologies Ltd
	Bags	37	37	-	Supreme Biotechnologies Ltd
	Nutrients	2,168	6,504	*C. reinhardtii*: 3 x higher flow rate	Supreme Biotechnologies Ltd
	Incidentals	100	100	-	Supreme Biotechnologies Ltd
	Filters	150	150	-	Supreme Biotechnologies Ltd
	CO_2	345	345	-	Supreme Biotechnologies Ltd
Harvest	Power (Continuous decanter, pumps)		114	Usage: 5h/day, 7.5 kWh	Acién et al. 2012
Storage	Power (freezer room)		109	Usage: 24h/day, 1.5 kWh	www.mellcon.com
Labour	Wages (4 Shifts)		12,480	2 shifts for cultivation and 2 shifts for harvesting (6,240 each)	Supreme Biotechnologies Ltd
	Supervision (0.2 labour)		2,496		Acién et al. 2012
	Payroll charges (0.25 labour + supervision)		3,120		Acién et al. 2012
Others	Maintenance (0.04 x MEC)		724	0.04 x 18,089 (depreciation MEC)	Acién et al. 2012
	Contingency (0.05 x production costs)		1,492	0.05 x 29,833	Acién et al. 2012
	Tax (0.15)		4,699	0.15 x 31,324	www.newzealandnow.govt.nz
Total raw materials (nutrients, CO_2) and consumables			7,136		
Total utilities (water, power)			3,877		
Total labour and others			25,010		
Total monthly production costs (NZ$)			**36,023**		

8.3.2.2 Production/operational costs

The production/operational costs are estimated based on the costs for the cultivation of *H. pluvialis* in the green phase at the facility of Supreme Biotechnologies assuming a three-fold higher flow rate, since *C. reinhardtii* has a higher growth rate than *H. pluvialis* (Table 8.2). This results in three times higher costs for water/waste water and nutrients. The optimal light intensity for the cultivation of *C. reinhardtii* (200 µmol m^{-2} s^{-1}) is higher compared to *H. pluvialis* (50 µmol m^{-2} s^{-1} (Harker et al. 1996)), which results in higher power costs for lighting (58W x 432 x 24h/day = 601 kWh/day x 30.4 days = 18,280 kWh/month x 0.1 NZ$ = 1828) + (30% of NZ$ 704 for other power costs) = NZ$ 2040). Furthermore, the production/operational costs include labour costs, comprising supervision and payroll charges, as well as maintenance and contingency. For details see table 8.5.

8.3.2.3 Total costs for the production of Pal produced in *C. reinhardtii*

The total fixed capital costs per month and the monthly production/operational costs were added, and divided by the amount of Pal that can be produced in the described facility per month (amount of Pal produced in the transgenic *C. reinhardtii* strain during exponential phase x total culture outflow per month) taking the annual operation time and harvesting efficiency into account. This resulted in estimated production costs of 13 NZ$ per gram of Pal, which are approximately 10 US$ per gram of recombinant Pal protein (Table 8.6).

It needs to be mentioned that these calculations strongly rely on the determination of the amount of Pal that is produced in the transgenic lines. This quantification was performed with two different standard proteins, which gave comparable results, during this study (3.2.4 and 8.1.2). However, to confirm the result, the quantification ideally needs to be repeated with purified Pal as the standard, to exclude protein-specific differences.

Table 8.6: Estimated total costs per g of Pal produced in *C. reinhardtii*

Total fix capital per month		5,820
Total production costs per month		36,023
Total monthly costs (NZ$)		**41,843**
Litres per month (outflow)		538,740
- Reduction due to	Operation time (350 days/year)	517,190
	Harvesting efficiency (90%)	465,471
Pal (mg) / litre culture volume in the exponential phase		6.9
Pal (mg) per month		3,211,752
Costs (NZ$) per mg Pal		0.013
Costs (NZ$) per g Pal		**13.03**
Costs (US$) per g Pal		**9.89**

This calculation represents a first attempt to estimate the costs for the production of endolysins in the green microalga *C. reinhardtii*. Subsequently, it may be possible to further optimise the production system to decrease the production costs. Janssen et al. (1999) and Janssen et al. (2000), for example, describe growth rates of up to $\mu = 0.16/h^{-1}$, which is more than double the growth rate that was used for this calculation. Optimisation of the light and mixing conditions in the cultivation system might therefore improve growth rates and subsequently decrease the production costs. Labour costs represent, as in many production processes, a major part of the costs (approximately 50%). Further automation of the process would therefore most likely reduce labour costs and resulting production costs. Furthermore, the remaining algae biomass could be separately sold, for example as lifestock feed or as substrate for the anaerobic digestion for the production of biogas, which would further reduce the production costs and reduce waste material. Moreover, a scale-up of the production facility would likely result in a reduction of the production costs per gram. On the other hand, it needs to be borne in mind that values such as the required work force, the monthly productivity and installation costs represents estimates and discrepancy could result in much higher production costs in reality.

8.3.3 Market and patent landscape

8.3.3.1 The market for antibiotics and antibacterial agents

The antibiotic market had a total value of US$42 billion globally in 2009 (Hamad 2010). It has an annual growth of around 4% and represents 5% of the global pharmaceutical market (Hamad 2010). As mentioned earlier, the development of new antibiotics has declined in recent decades, mainly owing to the lower profitability of antibiotics compared to other drugs (1.1). Nevertheless, the resulting decline in the approval of new antibiotics and the increase in resistant bacteria has now caused a pressing need for the development of new antibiotics, as emphasized by several institutions and experts such as the British Society for Antimicrobial Chemotherapy (BSAC), the World Health Organization (WHO), the Infectious Disease Society of America (IDSA) and the Chief Medical Officer for England, Professor Dame Sally Davies (1.1). New proposed strategies for the economic feasible research and development of new antibiotics involve collaborations between academia and pharmaceutical companies, combined with public funding (So et al. 2011).

Currently, the recommendation in many countries is to use antibiotics only when really necessary to limit the spread of resistances. However, the development of more specific antibiotics, which have less impact on the commensal bacterial flora (a reservoir for antibiotic resistance genes) and are more robust to resistance development, could make it safe again to use antibiotics for minor infections and as long-term treatment for recurring infections (1.1.2).

Furthermore there are significant markets for antibacterials in livestock farming (e.g. staphylococcal mastitis), agriculture (treatment of plant pathogens) and the conservation of food. As mentioned earlier, there is a potential application for the endolysin Gp20 in a cosmetic product for the treatment of acne vulgaris, which has a market that generates revenue of nearly $3 billion annually (1.3.3). These markets are more easily accessible and require less investment then the pharmaceutical market, which requires major investment for clinical trials.

8.3.4 The current market and patent landscape for bacteriophage endolysins

Bacteriophage endolysins are promising novel antibacterial agents due to their high specificity for the target bacteria, which enables the efficient elimination of the causative agent of an infection without affecting the beneficial commensal flora (1.2.3). Furthermore, the development of resistance against endolysins is very rare, because these enzymes evolved to target molecules in the cell wall that are essential for bacterial viability (1.2.4.1). Endolysins have been extensively investigated *in vitro* and several pre-clinical trials with a variety of endolysins specific to Gram-positive human pathogens showed a significant decrease of the bacterial loads and an increase of the survival rates of infected animals after treatment with endolysins (1.2.4, Table 1.1). In recent years, several companies have started to perform clinical trials, to file patents and to sign licencing deals to bring endolysins as novel antibiotics to market.

In November 2014, the Dutch company MICREOS (Bilthoven, Netherlands) was the first (and is still the only) company to sell products for human use that contain an endolysin. The company sells the pharmaceutical Staphefekt^{TM} for the topical treatment of *Staphylococcus aureus* infections. Furthermore, the product range comprises the series Gladskin with creams and gels for the treatment of acne, eczema, rosacea and skin irritations, which often have an *S. aureus* infection component. Furthermore, the US company GangaGen (Palo Alto, CA, USA) is working on the development of an *S. aureus*-specific human treatment based on the effect of an endolysin. Their product StaphTAME, containing the endolysin P128, is currently being evaluated as a treatment for the nasal decolonisation of *S. aureus* in a Phase 2 clinical trial. Whereas, the UK-based company Sarum Biosciences (Salisbury, UK) is working on the development of a bacteriophage endolysin technology for the treatment and the diagnosis of *Clostridium difficile* infections.

The Lysando AG (Triesenberg, Liechtenstein) holds several patents that relate to fusion proteins of endolysins and additional peptide sequences (which are often added for the extraction and purification of commercially produced proteins) and covers with these patents a wide range of endolysins against Gram-positive as well as Gram-

negative bacteria and a variety of commercial applications. In August 2014, the company licenced the rights for its inventions as Artilysin® technology to Boehringer Ingelheim Vetmedica (a devision of Boehringer Ingelheim GmbH, Ingelheim, Germany), which is the 6th largest animal health company in the world.

As well as applications in the treatment of human and animal infections, endolysins can be used for a variety of other applications, such as the control of bacterial contamination in food, feed and cosmetic products, as well as the abolishment of bacterial pathogens in crop plants. Several endolysins are also suitable for the eradication of biofilms on food processing equipment and medical devices, as well as surfaces in hospitals, surgeries and food producing factories. Furthermore, endolysins can be applied for the diagnosis of diseases and the detection of food spoilage.

The company BioMérieux (Craponne, France) that markets clinical diagnostic products, as well as environmental and industrial microbial monitoring services and products, holds several patents relating to endolysins for the diagnosis and eradication of the bacterium *Listeria* (a common cause of food spoilage and poisoning). Furthermore, the company holds patents that relate to the use of the cell wall binding domains of endolysins for the diagnosis, detection and removal of a wide range of Gram-positive bacteria. Another example is the company DSM (Heerlen, Netherlands) that produces food, beverage and dietary supplements, including enzymes for the preservation of food, and holds several patents relating to endolysins for the control of *Listeria* contamination in food products.

Taken together, this shows that there is a growing commercial interest in endolysins for medical as well as non-medical applications. And as for other recombinant protein therapeutics and agents, there is the need for a safe, reliable and commercially viable host organism for their production. Microalgal production platforms have not yet been exploited for the production of endolysins, and there are no patents relating to the production of non-mammalian recombinant proteins in *C. reinhardtii*, which could restrict the utilisation of this system.

Table 8.7: Summary of patents relating to endolysin inventions
(Source: www.lens.org)

Patent title	Patent holder	Patent number
Method Of Reducing Biofilms	Lysando Holding Ag	WO 2011/134998 A8 Patent Application
Antimicrobial Agents	Lysando Holding Ag	US 8906365 B2 Granted patent
Antimicrobial Agents	Lysando Holding Ag	WO 2010/149795 A1 Patent application
Endolysin Obpgplys	Lysando Holding Ag	US 8846865 B2 Granted patent
New Endolysin Obpgplys	Lysando Holding Ag	WO 2011/023702 A1 Patent application
Composition For Use In Mycobacteria Therapy	Lysando Holding Ag	WO 2014/001572 A1 Patent application
New Endolysin Plyp40	BioMérieux Sa	EP 2321409 B1 Granted patent
Modified Endolysin Ply511	BioMérieux Sa	WO 2009/138475 A1 Patent application
Method and Means For Concentrating, Removing, And Detection of Gram-positive Bacteria	BioMérieux Sa	EP 2121765 B1 Granted patent
Method and Means For Enrichment Removal And Detection of Listeria	BioMérieux Sa	US 8350005 B2 Granted patent
Endolysins For Controlling Listeria In Pasta Filata Cheese And Related Food Products	Dsm lp Assets Bv	WO 2012/159773 A1 Patent Application
Novel Listeria Bacteriophage P825 And Uses Thereof	Dsm lp Assets Bv	WO 2012/159774 A1 Patent Application
New Antimicrobial Compositions	Dsm lp Assets Bv	WO 2014/037589 A2 Patent Application
Polypeptide Mixes With Antibacterial Activity	Micreos Human Health B V	WO 2013/169104 A1 Patent Application
Polypeptide	Micreos Human Health B V	WO 2012/150858 A1 Patent Application
Combination Treatment For Atopic Dermatitis	Micreos Human Health B V	WO 2015/005787 A1 Patent Application
A Bacteriophage For Biocontrol Of Salmonella And IN The Manufacturing OR Processing Of Foods	Micreos Human Health B V	WO 2013/169102 A1 Patent Application

8.4 Discussion and conclusion

At the moment, the majority of recombinant proteins are commercially produced in mammalian cell cultures (mainly Chinese hamster ovary (CHO) cells) (45%), in yeast (15%) or in bacterial systems (40%) (Huang & McDonald 2009). Furthermore, a variety of other host expression systems have been brought to the market or are under development, including insect cells (baculovirus systems), transgenic plant cell cultures and whole plants, as well as transgenic mammal milk or chicken eggs (Huang & McDonald 2009; Dove 2002).

It has already been discussed in 1.4 and 7.2 that the *C. reinhardtii* chloroplast has the potential to offer advantages for the synthesis of endolysins over certain conventional recombinant protein production platforms, including the absence of glycosylation (which is unwanted for the production of these proteins that are naturally produced in a prokaryotic environment, and often happens in yeast systems or during nuclear expression in eukaryotic systems), the possibility to be grown in closed containment (in contrast to the open cultivation of transgenic plants) as well as the GRAS status, which means *C. reinhardtii* is free of toxins or infectious agents (in contrast to, for example the bacterial platform *Escherichia coli*), whose removal can result in high purification costs. However, there are other host systems that offer similar advantages, for example plant cell cultures or bacterial systems with GRAS status. Therefore it is desirable to be investigated whether microalgae would be competitive from a financial point of view.

The estimated production costs of US$ 10 per gram of the endolysin Pal produced in the *C. reinhardtii* chloroplast (without purification) are lower compared to estimates for the production of recombinant proteins in mammalian cell cultures. Dove (2002) and Hood et al. (2002) estimate raw material costs of US$100 – 600 per gram for the production of recombinant proteins in Chinese hamster ovary (CHO) cells. Farid (2007), Huang & McDonald (2009) and Boehm (2007) even describe production costs that range from US$ 300 to up to US$ 10,000 per gram of recombinant protein produced in mammalian cell cultures, due to expensive infrastructure and media

components, as well as the necessity of preventative measures against viral and oncogenic contamination.

However, the later figures include most likely purification costs. Evangelista et al. (1998) state that 88% of the costs for the production of recombinant β-Glucoronidase in transgenic corn are caused by protein extraction (40%) and purification (48%), which is about US$ 38 per gram with total production costs of US$ 42 per gram. The purification is done with DEAE resin, which can be used for the purification of Pal as well (4.2.4). Nfor et al. (2013) analysed different recombinant protein purification methods and state that purification by ion exchange chromatography (such as DEAE cellulose) produces costs of approximately US$ 8 per gram of product or in combination with other methods US$ 30. The purification of *C. reinhardtii*-produced Pal would therefore likely increase the overall production costs by two-fold or even up to ten-fold.

Furthermore, the capital investment costs for the installation of a facility for the cultivation of mammalian cell cultures are a lot higher than for the facility described here, that uses the relatively simple "hanging bag system". Farid (2007) describes capital investment costs of US$ 50 million for bioreactor capacities of 30,000 litres and up to US$ 600 million for total capacities of 200,000 litres.

However, other production platforms cause significantly less costs compared to mammalian cell cultures. Hood et al. (2002) estimates that the raw material production costs for recombinant proteins in transgenic plants is about US$ 0.1 to $1 per gram, and Dove (2002) describe production costs as low as US$ 0.05 per gram of recombinant protein. However, these figures are for the open cultivation of plants, which harbours the risk of gene flow to surrounding crop plants. Protein production in enclosed plant systems such as plant cell cultures costs US$ 50 – 100 per gram (Huang & McDonald 2009). The figures for the production costs of recombinant proteins per gram in bacterial systems range from US$ 1 (Hood et al. 2002) to US$ 20 – 100 (Huang & McDonald 2009). Other novel production platforms, which promise a reduction of the costs, are transgenic mammal milk and transgenic chicken eggs with estimated production costs of US$ 1 – 2 per gram of recombinant protein (Dove 2002;

Hood et al. 2002). However, these systems can contain agents such as viruses and prions, which might be able to infect humans, unlike algae or plants (Dove 2002). The use of yeast systems are described to cause production costs between US$ 20 and 100 per gram of recombinant protein, whereas the production in insect cell cultures is estimated at US$ 50 – 200 per gram of recombinant protein (Huang & McDonald 2009).

Overall, the stated costs for recombinant protein production in the same systems vary in the literature (see above), most likely due to protein-specific differences in production efficiencies and purification costs, as well as differences in the cultivation systems. Comparing the result of the here presented costing with the studies described above, the costs for the production of Pal in the *C. reinhardtii* chloroplast would most likely be lower compared to mammalian cell cultures (even with a ten-fold increase due to purification costs) and within the same range as several other systems (e.g. plant cell or insect cell cultures). Whilst for example, the production of Pal in openly cultivated transgenic plants would be most likely cheaper.

The calculation described here represents a first attempt to estimate the costs for the production of endolysins in the green microalga *C. reinhardtii.* The estimated costs of US$ 10 per gram of Pal produced in the *C. reinhardtii* chloroplast should be therefore verified by determining the amount of produced recombinant protein with purified Pal as a standard and ideally by running a pilot plant for the production of Pal in *C. reinhardtii*.

8.5 References

Acién, F.G. et al., 2012. Production cost of a real microalgae production plant and strategies to reduce it. *Biotechnology Advances*, 30(6), pp.1344–1353.

Boehm, R., 2007. Bioproduction of Therapeutic Proteins in the 21st Century and the Role of Plants and Plant Cells as Production Platforms. *Annals of the New York Academy of Sciences*, 1102(1), pp.121–134.

Dove, A., 2002. Uncorking the biomanufacturing bottleneck. *Nature Biotechnology*, 20(8), pp.777–779.

Evangelista, R.L. et al., 1998. Process and Economic Evaluation of the Extraction and Purification of Recombinant β-Glucuronidase from Transgenic Corn. *Biotechnology Progress*, 14(4), pp.607–614.

Fábregas, J. et al., 2001. Two-stage cultures for the production of Astaxanthin from *Haematococcus pluvialis*. *Journal of Biotechnology*, 89(1), pp.65–71.

Farid, S.S., 2007. Process economics of industrial monoclonal antibody manufacture. *Journal of Chromatography B*, 848(1), pp.8–18.

García-Malea, M.C. et al., 2005. Modelling of growth and accumulation of carotenoids in *Haematococcus pluvialis* as a function of irradiance and nutrients supply. *Biochemical Engineering Journal*, 26(2–3), pp.107–114.

Gimpel, J.A. et al., 2014. Production of recombinant proteins in microalgae at pilot greenhouse scale. *Biotechnology and Bioengineering*, p.n/a–n/a.

Hamad, B., 2010. The antibiotics market. *Nature Reviews Drug Discovery*, 9(9), pp.675–676.

Harker, M., Tsavalos, A.J. & Young, A.J., 1996. Autotrophic growth and carotenoid production of *Haematococcus pluvialis* in a 30 liter air-lift photobioreactor. *Journal of Fermentation and Bioengineering*, 82(2), pp.113–118.

Hood, E.E., Woodard, S.L. & Horn, M.E., 2002. Monoclonal antibody manufacturing in transgenic plants — myths and realities. *Current Opinion in Biotechnology*, 13(6), pp.630–635.

Huang, T.-K. & McDonald, K.A., 2009. Bioreactor engineering for recombinant protein production in plant cell suspension cultures. *Biochemical Engineering Journal*, 45(3), pp.168–184.

Janssen, M. et al., 2000. Efficiency of light utilization of *Chlamydomonas reinhardtii* under medium-duration light/dark cycles. *Journal of Biotechnology*, 78(2), pp.123–137.

Janssen, M. et al., 1999. Specific growth rate of *Chlamydomonas reinhardtii* and Chlorella sorokiniana under medium duration light/dark cycles: 13–87 s. *Journal of Biotechnology*, 70(1–3), pp.323–333.

Jørgensen, C.M., Vrang, A. & Madsen, S.M., 2014. Recombinant protein expression in *Lactococcus lactis* using the P170 expression system. *FEMS Microbiology Letters*, 351(2), pp.170–178.

Katsuda, T. et al., 2004. Astaxanthin production by *Haematococcus pluvialis* under illumination with LEDs. *Enzyme and Microbial Technology*, 35(1), pp.81–86.

Leite, G.B., Abdelaziz, A.E.M. & Hallenbeck, P.C., 2013. Algal biofuels: Challenges and opportunities. *Bioresource Technology*, 145, pp.134–141.

Nfor, B.K. et al., 2013. Model-based rational methodology for protein purification process synthesis. *Chemical Engineering Science*, 89, pp.185–195.

Oey, M. et al., 2009. Exhaustion of the chloroplast protein synthesis capacity by massive expression of a highly stable protein antibiotic. *The Plant Journal*, 57(3), pp.436–445.

Rawat, I. et al., 2013. Biodiesel from microalgae: A critical evaluation from laboratory to large scale production. *Applied Energy*, 103, pp.444–467.

Richmond, A., 2008. *Handbook of Microalgal Culture: Biotechnology and Applied Phycology*, John Wiley & Sons.

So, A.D. et al., 2011. Towards new business models for R&D for novel antibiotics. *Drug Resistance Updates*, 14(2), pp.88–94.